



# UFSAR Revision 30.0

 An AEP Company	<b>INDIANA MICHIGAN POWER</b> <b>D. C. COOK NUCLEAR PLANT</b> <b>UPDATED FINAL SAFETY ANALYSIS REPORT</b>	Revised: 29.0 Section: 14.3.1 Page: i of i
---	---	--

<b>14.3 REACTOR COOLANT SYSTEM PIPE RUPTURE (LOSS OF COOLANT ACCIDENT) .....</b>	<b>1</b>
<b>14.3.1 Large Break LOCA Analysis .....</b>	<b>1</b>
14.3.1.1 General.....	1
14.3.1.2 Method of Analysis .....	3
14.3.1.3 Analysis Assumptions .....	6
14.3.1.4 Design Basis Accident.....	6
14.3.1.5 Post LOCA Analyses.....	9
14.3.1.6 Post Analysis of Record Evaluations .....	10
14.3.1.6.1 LOTIC2 Error Resolution .....	11
14.3.1.6.2 Return to RCS Normal Operating Pressure / Normal Operating Temperature (NOP/NOT) Evaluation and Thermal Conductivity Degradation Error Resolution .....	11
14.3.1.6.3 Optimized ZIRLO™ Cladding .....	13
14.3.1.6.4 Revised Heat Transfer Multiplier Distributions.....	13
14.3.1.6.5 HOTSPOT Burst Strain Error Correction .....	13
14.3.1.6.6 Upflow Conversion (Reference 20).....	14
14.3.1.7 Conclusions .....	14
14.3.1.8 References for Section 14.3.1 .....	16

	<p>INDIANA MICHIGAN POWER D. C. COOK NUCLEAR PLANT UPDATED FINAL SAFETY ANALYSIS REPORT</p>	<p>Revised: 29.0 Section: 14.3.1 Page: 1 of 17</p>
---	---	--

## **14.3 REACTOR COOLANT SYSTEM PIPE RUPTURE (LOSS OF COOLANT ACCIDENT)**

### **14.3.1 Large Break LOCA Analysis**

#### **14.3.1.1 General**


A loss-of-coolant accident (LOCA) is the result of a pipe rupture of the RCS pressure boundary. For the analyses reported here, a major pipe break (large break) is defined as a rupture with a total cross-sectional area equal to or greater than 1.0 ft<sup>2</sup>. This event is considered an ANS Condition IV event, a limiting fault, in that it is not expected to occur during the lifetime of Cook Nuclear Plant Unit 1, but is postulated as a conservative design basis.

When the Final Acceptance Criteria (FAC) governing the loss-of-coolant accident (LOCA) for Light Water Reactors was issued in Appendix K of 10 CFR 50.46, both the Nuclear Regulatory Commission (NRC) and the industry recognized that the stipulations of Appendix K were highly conservative. That is, using the then accepted analysis methods, the performance of the Emergency Core Cooling System (ECCS) would be conservatively underestimated, resulting in predicted Peak Cladding Temperatures (PCTs) much higher than expected. At that time, however, the degree of conservatism in the analysis could not be quantified. As a result, the NRC began a large-scale confirmatory research program with the following objectives:

1. Identify, through separate effects and integral effects experiments, the degree of conservatism in those models permitted in the Appendix K rule. In this fashion, those areas in which a purposely prescriptive approach was used in the Appendix K rule could be quantified with additional data so that a less prescriptive future approach might be allowed.
2. Develop improved thermal-hydraulic computer codes and models so that more accurate and realistic accident analysis calculations could be performed. The purpose of this research was to develop an accurate predictive capability so that the uncertainties in the ECCS performance and the degree of conservatism with respect to the Appendix K limits could be quantified.

Since that time, the NRC and the nuclear industry have sponsored reactor safety research programs directed at meeting the above two objectives. The overall results have quantified the conservatism in the Appendix K rule for LOCA analyses and confirmed that some relaxation of the rule can be made without a loss in safety to the public. It was found that some plants were

## UFSAR Revision 30.0

 An AEP Company	<b>INDIANA MICHIGAN POWER</b> <b>D. C. COOK NUCLEAR PLANT</b> <b>UPDATED FINAL SAFETY ANALYSIS REPORT</b>	Revised: 29.0 Section: 14.3.1 Page: 2 of 17
---	---	---

being restricted in operating flexibility by the overly conservative Appendix K requirements. In recognition of the Appendix K conservatism that was being quantified by the research programs, the NRC adopted an interim approach for evaluation methods. This interim approach is described in SECY-83-472. The SECY-83-472 approach retained those features of Appendix K that were legal requirements, but permitted applicants to use best-estimate thermal-hydraulic models in their ECCS evaluation model. Thus, SECY-83-472 represented an important step in basing licensing decisions on realistic calculations, as opposed to those calculations prescribed by Appendix K.


In 1998, the NRC Staff amended the requirements of 10 CFR 50.46 and Appendix K, “ECCS Evaluation Models”, to permit the use of a realistic evaluation model to analyze the performance of the ECCS during a hypothetical LOCA. This decision was based on an improved understanding of LOCA thermal-hydraulic phenomena gained by extensive research programs. Under the amended rules, best-estimate thermal-hydraulic models may be used in place of models with Appendix K features. The rule change also requires, as part of the LOCA analysis, an assessment of the uncertainty of the best-estimate calculations. It further requires that this analysis uncertainty be included when comparing the results of the calculations to the prescribed acceptance criteria of 10 CFR 50.46. Further guidance for the use of best-estimate codes is provided in Regulatory Guide 1.157.

To demonstrate use of the revised ECCS rule, the NRC and its consultants developed a method called the Code Scaling, Applicability, and Uncertainty (CSAU) evaluation methodology (NUREG/CR-5249). This method outlined an approach for defining and qualifying a best-estimate thermal-hydraulic code and quantifying the uncertainties in a LOCA analysis.

A LOCA evaluation methodology for three- and four-loop Pressurized Water Reactor (PWR) plants based on the revised 10 CFR 50.46 rules was developed by Westinghouse with the support of EPRI and Consolidated Edison and has been approved by the NRC (WCAP-12945-P-A).

Westinghouse subsequently developed an alternative uncertainty methodology called ASTRUM, which stands for Automated Statistical Treatment of Uncertainty Method (WCAP-16009-P-A). This method is still based on the Code Qualification Document (CQD) methodology and follows the steps in the CSAU methodology (NUREG/CR-5249). However, the uncertainty analysis (Element 3 in the CSAU) is replaced by a technique based on order statistics. The ASTRUM methodology replaces the response surface technique with a statistical sampling method where the uncertainty parameters are simultaneously sampled for each case. The ASTRUM

## UFSAR Revision 30.0

 An AEP Company	<b>INDIANA MICHIGAN POWER</b> <b>D. C. COOK NUCLEAR PLANT</b> <b>UPDATED FINAL SAFETY ANALYSIS REPORT</b>	Revised: 29.0 Section: 14.3.1 Page: 3 of 17
---	---	---

methodology has received NRC approval for referencing in licensing applications in WCAP-16009-P-A.


The three 10 CFR 50.46 criteria (peak cladding temperature, maximum local oxidation, and core-wide oxidation) are satisfied by running a sufficient number of WCOBRA/TRAC calculations (sample size). In particular, the statistical theory predicts that 124 calculations are required to simultaneously bound the 95<sup>th</sup> percentile values of three parameters with a 95-percent confidence level.

This analysis is in accordance with the applicability limits and usage conditions defined in Section 13-3 of WCAP-16009-P-A, as applicable to the ASTRUM methodology. Section 13-3 of WCAP-16009-P-A was found to acceptably disposition each of the identified conditions and limitations related to WCOBRA/TRAC and the CQD uncertainty approach per Section 4.0 of the ASTRUM Final Safety Evaluation Report. Additionally, Westinghouse analyzed the D. C. Cook Unit 1 LBLOCA using a plant-specific adaptation of the ASTRUM methodology. The analysis was performed in compliance with all of the conditions and limitations identified in NRC Safety Evaluation approving ASTRUM (WCAP-16009-P-A). The plant-specific adaptation of ASTRUM better models the downcomer region by increasing the number of circumferential nodding stacks from four to twelve. This finer nodalization has been assessed against experimental data, as described in “WCOBRA/TRAC Validation with revised Downcomer Noding for D. C. Cook Unit 1 and 2”.

### **14.3.1.2 Method of Analysis**

The methods used in the application of WCOBRA/TRAC to the large break LOCA with ASTRUM are described in WCAP-12945-P-A and WCAP-16009-P-A. A detailed assessment of the computer code WCOBRA/TRAC was made through comparisons to experimental data. These assessments were used to develop quantitative estimates of the ability of the code to predict key physical phenomena in a PWR large break LOCA. Modeling of a PWR introduces additional uncertainties which are identified and quantified in the plant-specific analysis. WCOBRA/TRAC MOD7A was used for the execution of ASTRUM for D. C. Cook Unit 1 (WCAP-16009-P-A).

# UFSAR Revision 30.0

 An AEP Company	<b>INDIANA MICHIGAN POWER</b> <b>D. C. COOK NUCLEAR PLANT</b> <b>UPDATED FINAL SAFETY ANALYSIS REPORT</b>	Revised: 29.0 Section: 14.3.1 Page: 4 of 17
---	---	---

WCOBRA/TRAC combines two-fluid, three-field, multi-dimensional fluid equations used in the vessel with one-dimensional drift-flux equations used in the loops to allow a complete and detailed simulation of a PWR. This best-estimate computer code contains the following features:

1. Ability to model transient three-dimensional flows in different geometries inside the vessel
2. Ability to model thermal and mechanical non-equilibrium between phases
3. Ability to mechanistically represent interfacial heat, mass, and momentum transfer in different flow regimes
4. Ability to represent important reactor components such as fuel rods, steam generators, reactor coolant pumps, etc.

A typical calculation using WCOBRA/TRAC begins with the establishment of a steady-state, initial condition with all loops intact. The input parameters and initial conditions for this steady-state calculation are discussed in the next section.


Following the establishment of an acceptable steady-state condition, the transient calculation is initiated by introducing a break into one of the loops. The evolution of the transient through blowdown, refill, and reflood proceeds continuously, using the same computer code (WCOBRA/TRAC) and the same modeling assumptions. Containment pressure is modeled with the BREAK component using a time dependent pressure table. Containment pressure is calculated using the LOTIC2 code (WCAP-8354-P-A) and mass and energy releases from the WCOBRA/TRAC calculation.

The final step of the best-estimate methodology, in which all uncertainties of the LOCA parameters are accounted for to estimate a PCT, Local Maximum Oxidation (LMO), and Core-Wide Oxidation (CWO) at 95-percent probability (and 95-percent confidence level), is described in the following sections:

1. Plant Model Development:

In this step, a WCOBRA/TRAC model of the plant is developed. A high level of nodding detail is used in order to provide an accurate simulation of the transient. However, specific guidelines are followed to ensure that the model is consistent with models used in the code validation. This results in a high level of consistency among plant models, except for specific areas dictated by hardware

# UFSAR Revision 30.0

 An AEP Company	<p style="text-align: center;"><b>INDIANA MICHIGAN POWER</b> <b>D. C. COOK NUCLEAR PLANT</b> <b>UPDATED FINAL SAFETY ANALYSIS REPORT</b></p>	<p>Revised: 29.0 Section: 14.3.1 Page: 5 of 17</p>
---	--	--

differences, such as in the upper plenum of the reactor vessel or the ECCS injection configuration.

2. Determination of Plant Operating Conditions:


In this step, the expected or desired operating range of the plant to which the analysis applies is established. The parameters considered are based on a “key LOCA parameters” list that was developed as part of the methodology. A set of these parameters, at mostly nominal values, is chosen for input as initial conditions to the plant model. A transient is run utilizing these parameters and is known as the “initial transient”. Next, several confirmatory runs are made, which vary a subset of the key LOCA parameters over their expected operating range in one-at-a-time sensitivities. Because certain parameters are not included in the uncertainty analysis, these parameters are set at their bounding condition. This analysis is commonly referred to as the confirmatory analysis. The most limiting input conditions, based on these confirmatory runs, are then combined into the model that will represent the limiting state for the plant, which is the starting point for the assessment of uncertainties.

3. Assessment of Uncertainty:

The ASTRUM methodology is based on order statistics. The technical basis of the order statistics is described in Section 11 of WCAP-16009-P-A. The determination of the PCT uncertainty, LMO uncertainty, and CWO uncertainty relies on a statistical sampling technique. According to the statistical theory, 124 WCOBRA/TRAC calculations are necessary to assess against the three 10 CFR 50.46 criteria (PCT, LMO, CWO).

The uncertainty contributors are sampled randomly from their respective distributions for each of the WCOBRA/TRAC calculations. The list of uncertainty parameters, which are randomly sampled for each time in the cycle, break type (split or double-ended guillotine), and break size for the split break are also sampled as uncertainty contributors within the ASTRUM methodology.

Results from the 124 calculations are tallied by ranking the PCT from highest to lowest. A similar procedure is repeated for LMO and CWO. The highest rank of PCT, LMO, and CWO will bound 95 percent of their respective populations with 95-percent confidence level.

 <b>INDIANA MICHIGAN POWER</b> <b>D. C. COOK NUCLEAR PLANT</b> <b>UPDATED FINAL SAFETY ANALYSIS REPORT</b>	Revised: 29.0 Section: 14.3.1 Page: 6 of 17
---	---

#### 4. Plant Operating Range:

The plant operating range over which the uncertainty evaluation applies is defined. Depending on the results obtained in the above uncertainty evaluation, this range may be the desired range or may be narrower for some parameters to gain additional margin.

#### **14.3.1.3 Analysis Assumptions**

The expected PCT and its uncertainty developed are valid for a range of plant operating conditions. The range of variation of the operating parameters has been accounted for in the uncertainty evaluation. Table 14.3.1-1 summarizes the operating ranges for D. C. Cook Unit 1 as defined for the proposed operating conditions, which are supported by the Best-Estimate LBLOCA analysis. Tables 14.3.1-2, 14.3.1-3, and 14.3.1-7 summarize the LBLOCA containment data used for calculating containment pressure. If operation is maintained within these ranges, the LBLOCA results developed in this report are considered to be valid. Note that some of these parameters vary over their range during normal operation within a fuel cycle (e.g., accumulator temperature) and other parameters are typically fixed during normal operation within a fuel cycle (full-power Tav<sub>g</sub>).


#### **14.3.1.4 Design Basis Accident**

The D. C. Cook Unit 1 PCT/LMO/CWO-limiting transient is a cold leg split break (effective break area = 1.4465) which analyzes conditions that fall within those listed in Table 14.3.1-1. Traditionally, cold leg breaks have been limiting for large break LOCA. Analysis experience indicates that this break location most likely causes conditions that result in flow stagnation to occur in the core. Scoping studies with WCOBRA/TRAC have confirmed that the cold leg remains the limiting break location (WCAP-12945-P-A).

The large break LOCA transient can be divided into convenient time periods in which specific phenomena occur, such as various hot assembly heatup and cooldown transients. For a typical large break, the blowdown period can be divided into a Critical Heat Flux (CHF) phase, the upward core flow phase, and the downward core flow phase. These are followed by the refill, reflood, and long-term cooling periods. Specific important transient phenomena and heat transfer regimes are discussed below, with the transient results shown in Figures 14.3.1-1A through 14.3.1-1M. (The limiting case was chosen to show a conservative representation of the response to a large break LOCA.)



# UFSAR Revision 30.0

 An AEP Company	<p style="text-align: center;"><b>INDIANA MICHIGAN POWER</b> <b>D. C. COOK NUCLEAR PLANT</b> <b>UPDATED FINAL SAFETY ANALYSIS REPORT</b></p>	<p>Revised: 29.0 Section: 14.3.1 Page: 7 of 17</p>
---	--	--

1. Critical Heat Flux (CHF) Phase:

Immediately following the cold leg rupture, the break discharge rate is subcooled and high (Figures 14.3.1-1B and 14.3.1-1C). The regions of the RCS with the highest initial temperatures (core, upper plenum, upper head, and hot legs) begin to flash to steam, the core flow reverses and the fuel rods begin to undergo departure from nucleate boiling (DNB). The fuel cladding rapidly heats up (Figure 14.3.1-1A) while the core power shuts down due to voiding in the core. This phase is terminated when the water in the lower plenum and downcomer begins to flash (Figures 14.3.1-1G and 14.3.1-1M, respectively). The mixture swells and intact loop pumps, still rotating in single-phase liquid, push this two-phase mixture into the core.

2. Upward Core Flow Phase:


Heat transfer is improved as the two-phase mixture is pushed into the core. This phase may be enhanced if the pumps are not degraded, or if the break discharge rate is low due to saturated fluid conditions at the break. If pump degradation is high or the break flow is large, the cooling effect due to upward flow may not be significant. Figure 14.3.1-1D shows the void fraction for one intact loop pump and the broken loop pump. The figure shows that the intact loop remains in single-phase liquid flow for several seconds, resulting in enhanced upward core flow cooling. This phase ends as the lower plenum mass is depleted, the loop flow becomes two-phase, and the pump head degrades.

3. Downward Core Flow Phase:

The loop flow is pushed into the vessel by the intact loop pumps and decreases as the pump flow becomes two-phase. The break flow begins to dominate and pulls flow down through the core, up the downcomer to the broken loop cold leg, and out the break. While liquid and entrained liquid flow provide core cooling, the top of core vapor flow (Figure 14.3.1-1E) best illustrates this phase of core cooling. Once the system has depressurized to the accumulator pressure (Figure 14.3.1-1F), the accumulators begin to inject relatively cold borated water into the intact cold legs (Figures 14.3.1-1I). During this period, due to steam upflow in the downcomer, a portion of the injected ECCS water is calculated to be bypassed around the downcomer and out the break. As the system pressure continues to fall, the break flow, and consequently the downward core flow (i.e., reverse flow



## UFSAR Revision 30.0

 An AEP Company	<b>INDIANA MICHIGAN POWER</b> <b>D. C. COOK NUCLEAR PLANT</b> <b>UPDATED FINAL SAFETY ANALYSIS REPORT</b>	Revised: 29.0 Section: 14.3.1 Page: 8 of 17
---	---	---


in the fuel bundle region), is reduced. The core begins to heat up as the system pressure approaches the containment pressure and the vessel begins to fill with ECCS water (Figure 14.3.1-1L).

4. Refill Period:

As the refill period begins, the core begins a period of heatup and the vessel begins to fill with ECCS water (Figures 14.3.1-1I, 14.3.1-1J, and 14.3.1-1K). This period is characterized by a rapid increase in cladding temperatures at all elevations due to the lack of liquid and steam flow in the core region. This period continues until the lower plenum is filled and the bottom of the core begins to reflood and entrainment begins.

5. Reflood Period:

During the early reflood phase, the accumulators begin to empty and nitrogen enters the system. This forces water into the core, which then boils, causing system re-pressurization, and the lower core region begins to quench (Figure 14.3.1-1L). During this time, core cooling may increase due to vapor generation and liquid entrainment. During the reflood period, the core flow and temperatures are oscillatory as relatively cold water periodically rewets and quenches the hot fuel cladding, which generates steam and causes system re-pressurization. The steam and entrained water must pass through the vessel upper plenum, the hot legs, the steam generators, and the reactor coolant pumps before it is vented out of the break. This flow path resistance is overcome by the downcomer water elevation head, which provides the gravity driven reflood force. From the later stage of blowdown to the beginning of reflood, the accumulators rapidly discharge borated cooling water into the RCS, filling the lower plenum and contributing to the filling of the downcomer. The pumped ECCS water aids in the filling of the downcomer and subsequently supplies water to maintain a full downcomer and complete the reflood period. As the quench front progresses up the core, the PCT location moves higher into the top core region (Figure 14.3.1-1N). Please note that PCT location plot is based on the core noding (approximately one node for every 1.8" of core elevation). As the vessel continues to fill (Figure 14.3.1-1H), the PCT location is cooled and the early reflood period is terminated.

 An AEP Company	<p style="text-align: center;"><b>INDIANA MICHIGAN POWER</b> <b>D. C. COOK NUCLEAR PLANT</b> <b>UPDATED FINAL SAFETY ANALYSIS REPORT</b></p>	<p>Revised: 29.0 Section: 14.3.1 Page: 9 of 17</p>
---	--	--


A second cladding heatup transient may occur due to excessive boiling in the downcomer. The mixing of ECCS water with hot water and steam from the core, in addition to the continued heat transfer from the vessel and its components, reduces the subcooling of ECCS water in the lower plenum and downcomer. The saturation temperature is dictated by the containment pressure. If the liquid temperature in the downcomer reaches saturation, subsequent heat transfer from the vessel and other structures will cause boiling and level swell in the downcomer (Figure 14.3.1-1M). The downcomer liquid will spill out of the broken cold leg and reduce the driving head, which can reduce the reflood rate, causing a late reflood heatup at the upper core elevations.

### **14.3.1.5 Post LOCA Analyses**

Continued operation of the ECCS pumps supplies water during long-term cooling. Core temperatures have been reduced to long-term steady state levels associated with the dissipation of residual heat generation. After the water level of the refueling water storage tank (RWST) reaches a minimum allowable value, coolant for long-term cooling of the core is obtained by switching to the cold recirculation phase of operation in which spilled borated water is drawn from the engineered safety features (ESF) recirculation sump by the low head safety injection (residual heat removal) pumps and returned to the RCS cold legs. The containment spray system continues to operate to further reduce containment pressure.

A maximum time of 7.5 hours after the initiation of the LOCA, the ECCS is realigned to supply water to the RCS hot legs in order to control the boric acid concentration in the reactor vessel. Long-term cooling includes long-term criticality control. Post-LOCA criticality control is assured by two separate calculations; during cold leg recirculation, and at the time ECCS-recirculation is realigned from cold leg injection to hot leg injection. Criticality control during cold leg recirculation is achieved by determining the RWST and accumulator concentration necessary to maintain subcriticality without credit for RCCA insertion. However, RCCA insertion credit has been assumed to provide negative reactivity at the time of hot leg switchover following a cold leg break when the potential exists for the core to be flushed with relatively boron-dilute liquid from the containment sump. Thus, the time following the LOCA that hot leg switchover must occur is based upon boron precipitation concerns, and not criticality control. Once hot leg injection has been established, the concentrated boron within the reactor vessel would be mixed with the containment sump liquid, thereby reducing the differences in the boron concentrations between the core and the containment sump. The necessary RWST and

## UFSAR Revision 30.0

 An AEP Company	<p style="text-align: center;"><b>INDIANA MICHIGAN POWER</b> <b>D. C. COOK NUCLEAR PLANT</b> <b>UPDATED FINAL SAFETY ANALYSIS REPORT</b></p>	<p>Revised: 29.0 Section: 14.3.1 Page: 10 of 17</p>
---	--	---

accumulator concentration is a function of each core design and is checked each cycle. The current Technical Specification value is 2400 ppm to 2600 ppm boron (Reference 10).

The credit for RCCA insertion for criticality control upon hot leg switchover is applicable for large cold leg breaks only, as supported by Reference 12 and approved by NRC, as documented in Reference 13. The mechanism for containment sump dilution, which causes the hot leg switchover recriticality concern, does not apply for a hot leg break, as the break flow maintains the containment sufficiently borated.


An evaluation has been performed to determine the effect of a 5-minute interruption in RHR flow during the switchover to sump recirculation on the LBLOCA analysis. This flow interruption will occur when the RHR pump is secured to re-align its suction from the RWST to the recirculation sump. Using a conservatively short estimate of RWST drain down time and a bounding scenario for the availability of pumped injection, it was shown (Reference 11) that the short-term peak clad temperature results are not challenged by a 5-minute interruption in RHR ECCS flow. Note that the centrifugal charging and safety injection pumps are assumed to continue providing borated water to the core during this 5-minute interruption.

Revised post LOCA long term cooling analyses were completed and documented in References 18 and 19. The new analyses were performed to optimize margin and bound both Unit 1 and Unit 2. The revised analyses results demonstrate that all acceptance criteria are met with the previously assumed operator action times.

### **14.3.1.6 Post Analysis of Record Evaluations**

In addition to the analyses presented in this section, evaluations and reanalyses may be performed as needed to address computer code errors and emergent issues, or to support plant changes. The issues or changes are evaluated, and the impact on the Peak Cladding Temperature (PCT) is determined. The resultant increase or decrease in PCT is applied to the analysis of record PCT. The PCT, including all penalties and benefits is presented in Table 14.3.1-6 for the large break LOCA. The current PCT is demonstrated to be less than the 10 CFR 50.46(b) requirement of 2200 °F.

In addition, 10 CFR 50.46 requires that licensees assess and report the effect of changes to or errors in the evaluation model used in the large break LOCA analysis. These reports constitute addenda to the analysis of record provided in the UFSAR until the overall changes become significant as defined by 10 CFR 50.46. If the assessed changes or errors in the evaluation

 <p><b>INDIANA MICHIGAN POWER</b> <small>An AEP Company</small></p>	<p><b>INDIANA MICHIGAN POWER</b> <b>D. C. COOK NUCLEAR PLANT</b> <b>UPDATED FINAL SAFETY ANALYSIS REPORT</b></p>	<p>Revised: 29.0 Section: 14.3.1 Page: 11 of 17</p>
--	--	---

model results in significant changes in calculated PCT, a scheduled for formal reanalysis or other action as needed to show compliance will be addressed in the report to the NRC.

Finally, the criteria of 10 CFR 50.46 requires that holders and users of the evaluation models establish a number of definitions and processes for assessing changes in the models or their use. Westinghouse, in consultation with the PWR Owner's Group (PWROG), has developed an approach for compliance with the reporting requirements. This approach is documented in WCAP-13451, Westinghouse Methodology for Implementation of 10 CFR 50.46 Reporting. D. C. Cook provides the NRC with annual and 30-day reports, as applicable, for the D. C. Cook Unit 1 Power Station. D. C. Cook intends to provide future reports required by 10 CFR 50.46 consistent with the approach described in WCAP-13451.


#### **14.3.1.6.1 LOTIC2 Error Resolution**

The LOTIC2 containment calculations (Figures 14.3.1-3 and 14.3.1-4) were identified to have improperly modeled safety injection (SI) spilled mass and energy releases in the containment backpressure calculation (Reference 17). Correction of the error causes the LOTIC2 predicted containment backpressure to decrease, which is in the non-conservative direction for Large-Break LOCA analyses. The effect is fully offset by increasing the minimum Containment Spray (CTS) temperature from 45°F (Table 14.3.1-2) to 65°F, which is conservative relative to the minimum CTS design temperature of 70°F. With the revised CTS temperature, the containment pressure used in the Best-Estimate LBLOCA was confirmed to be conservatively low, leading to a PCT impact of 0°F (Reference 17). The PCT, including all penalties and benefits is presented in Table 14.3.1-6 for the large break LOCA. The current PCT is demonstrated to be less than the 10 CFR 50.46(b) requirement of 2200°F.

#### **14.3.1.6.2 Return to RCS Normal Operating Pressure / Normal Operating Temperature (NOP/NOT) Evaluation and Thermal Conductivity Degradation Error Resolution**

The Return to RCS NOP/NOT evaluation implements a return to normal operating pressure (2250 psia) and normal operating temperature (571°F  $T_{AVG}$ ). The LBLOCA Return to RCS NOP/NOT evaluation also considers fuel thermal conductivity degradation (TCD), which is a physical phenomenon that reduces the ability of the fuel pellet to transfer heat as burnup increases. Because of the reduced ability to transfer heat out of the pellet, TCD results in higher initial steady state fuel temperatures than would otherwise be expected. The impacts of the Return to RCS NOP/NOT design input changes and the effects of TCD were evaluated on the AOR LBLOCA PCT; it was found that the Unit 1 PCT increased by 404°F. In order to show


# UFSAR Revision 30.0

	<b>INDIANA MICHIGAN POWER</b> <b>D. C. COOK NUCLEAR PLANT</b> <b>UPDATED FINAL SAFETY ANALYSIS REPORT</b>	Revised: 29.0 Section: 14.3.1 Page: 12 of 17
---	---	--

compliance with the 10 CFR 50.46(b)(1) criterion of  $PCT < 2200^{\circ}\text{F}$ , it was necessary to credit conservatism in the analysis and offsetting design inputs. This was done by modifying the input parameters documented in Tables 14.3.1-1 and 14.3.1-2 in the following ways:

- Peak hot rod enthalpy rise hot channel factor ( $F_{\Delta H}$ ) ( $\leq 1.53$ )
- Peak heat flux hot channel factor ( $F_Q$ ) ( $\leq 2.09$ )
- Peaking factor burndown (Reduce both  $F_Q$  and  $F_{\Delta H}$  peaking factors as a function of burnup)
- Hot assembly radial peaking factor ( $\overline{P}_{HA}$ ) ( $\leq 1.53/1.04$ )
- Hot assembly heat flux hot channel factor ( $F_{QHA}$ ) ( $\leq 2.09/1.04$ )
- $T_{AVG}$  ( $571^{\circ}\text{F}$  at hot full power)
- Pressurizer pressure (2250 psia at hot full power)
- Pressurizer level (at hot full power) (49.9% of span at full load  $T_{AVG}$  of  $571^{\circ}\text{F}$ )
- Accumulator temperature ( $70^{\circ}\text{F} \leq T_{ACC} \leq 100^{\circ}\text{F}$ )
- Minimum safety injection flow (increased HHSI and RHR flow based on BE LBLOCA representative minimum RWST level and containment spilling assumption)
- Safety injection temperature ( $70^{\circ}\text{F} \leq T_{SI} \leq 100^{\circ}\text{F}$ )
- Safety injection delay time (17 seconds with offsite power and 28 seconds with LOOP)
- Containment modeling; increased assumed containment backpressure to recapture margins while still assuring a conservatively low backpressure. See Figures 14.3.1-3a, 14.3.1-4a, 14.3.1-5a, 14.3.1-6a, 14.3.1-7a, 14.3.1-8a and 14.3.1-9a. The following updates were applied:
  - Containment spray initiation delay (sprays effective 244 seconds following event initiation)
  - Deck Fan initiation delay (fan flow effective 270 seconds following event initiation)
  - Maximum containment spray flow rate (3600 gpm / pump)

## UFSAR Revision 30.0

 An AEP Company	<b>INDIANA MICHIGAN POWER</b> <b>D. C. COOK NUCLEAR PLANT</b> <b>UPDATED FINAL SAFETY ANALYSIS REPORT</b>	Revised: 29.0 Section: 14.3.1 Page: 13 of 17
---	---	--

- Updated mass and energy releases into containment

The benefits from crediting the conservatisms listed above are reflected in transient Figures 14.3.1-1Aa thru 14.3.1-1Na and resulted in a decrease in PCT of 489°F, as noted in Table 14.3.1-6.

### **14.3.1.6.3 Optimized ZIRLO™ Cladding**

Beginning with Unit 1 Cycle 25, **Optimized ZIRLO™** cladding is being used in feed fuel assemblies. **Optimized ZIRLO™** cladding has been evaluated and found to be acceptable with respect to the analysis described in Section 14.3.1.


### **14.3.1.6.4 Revised Heat Transfer Multiplier Distributions**

Errors were discovered in the heat transfer multiplier distributions, including errors in the grid locations specified in the WCOBRA/TRAC models for the G2 Refill and G2 Reflood tests, and errors in processing test data used to develop the reflood heat transfer multiplier distribution. Therefore, the blow-down heat-up, blowdown cooling, refill, and reflood heat transfer multiplier distributions were redeveloped. For the reflood heat transfer multiplier development, the evaluation time windows for each set of test experimental data and each test simulation were separately defined based on the time at which the test or simulation exhibited dispersed flow film boiling heat transfer conditions characteristic of the reflood time period. The revised heat transfer multiplier distributions have been evaluated for impact and found to have a 91 °F benefit for the PCT under NOP/NOT conditions, as noted in Table 14.3.1-6.

### **14.3.1.6.5 HOTSPOT Burst Strain Error Correction**

An error in the application of the burst strain was discovered in HOTSPOT. The outer radius of the cladding, after burst occurs, should be calculated based on the burst strain, and the inner radius of the cladding should be calculated based on the outer radius. In HOTSPOT, the burst strain is applied to the calculation of the cladding inner radius. The cladding outer radius is then calculated based on the inner radius. As such, the burst strain is incorrectly applied to the inner radius rather than the outer radius, which impacts the resulting cladding geometry at the burst elevation after burst occurs. Correction of the erroneous calculation results in thinner cladding at the burst node and more fuel relocating into the burst node, leading to an increase in the PCT at the burst node. The penalty was evaluated to have a PCT impact of 85 °F as noted in Table 14.3.1-6.

# UFSAR Revision 30.0

 An AEP Company	<p style="text-align: center;"><b>INDIANA MICHIGAN POWER</b> <b>D. C. COOK NUCLEAR PLANT</b> <b>UPDATED FINAL SAFETY ANALYSIS REPORT</b></p>	<p>Revised: 29.0 Section: 14.3.1 Page: 14 of 17</p>
---	--	---

## **14.3.1.6.6 Upflow Conversion (Reference 20)**

The upflow conversion program implements a field modification of the reactor vessel lower internals assembly to reduce the potential of fuel rod failures due to baffle joint jetting. This modification changes the flow paths during normal operation as well as accident scenarios and represents a change to the Best-Estimate LBLOCA licensing basis. The upflow conversion evaluation considers the new plant configuration, the upflow conversion design input changes, the return to RCS NOP/NOT evaluation and the effect of TCD over the life of the fuel. Relative to the original NOP/NOT and TCD evaluation (Section 14.3.1.6.2), the offsetting input margins that were updated are maintained. The upflow conversion estimate of effect on the PCT is determined based on the difference between parametric run sets. HOTSPOT executions are performed for each WCOBRA/TRAC case to consider the effect of local uncertainties for both integral fuel burnable absorber (IFBA) and non-IFBA fuel. The upflow conversion has been determined to be a 14°F penalty for the PCT, as noted in Table 14.3.1-6.


## **14.3.1.7 Conclusions**

It must be demonstrated that there is a high level of probability that the limits set forth in 10 CFR 50.46 are met. The demonstration that these limits are met is as follows:

- (b)(1) The limiting PCT corresponds to a bounding estimate of the 95<sup>th</sup> percentile PCT at the 95-percent confidence level. Since the resulting PCT for the limiting case is 2128°F, including consideration of the adjusted ECCS flow rates as described below, the analysis confirms that 10 CFR 50.46 acceptance criterion (b)(1), i.e., “Peak Cladding Temperature less than 2200°F, is demonstrated. The results are shown in Table 14.3.1-5.
- (b)(2) The maximum cladding oxidation corresponds to a bounding estimate of the 95<sup>th</sup> percentile LMO at the 95-percent confidence level. The resulting LMO for the limiting case, including consideration of the adjusted ECCS flow rates as described below, is 11.1 percent. The analysis confirms that 10 CFR 50.46 acceptance criterion (b)(2), i.e., “Local Maximum Oxidation of the cladding less than 17 percent of the total cladding thickness before oxidation”, is demonstrated. The results are shown in Table 14.3.1-5.
- (b)(3) The limiting core-wide oxidation corresponds to a bounding estimate of the 95<sup>th</sup> percentile CWO at the 95-percent confidence level. The limiting Hot Assembly Rod (HAR) total maximum oxidation is 0.40 percent, including consideration of the adjusted ECCS flow rates as described below. A detailed CWO calculation



## UFSAR Revision 30.0


 <b>INDIANA MICHIGAN POWER</b> <small>An AEP Company</small>	<b>INDIANA MICHIGAN POWER D. C. COOK NUCLEAR PLANT UPDATED FINAL SAFETY ANALYSIS REPORT</b>	Revised: 29.0 Section: 14.3.1 Page: 15 of 17
--	---	--

takes advantage of the core power census that includes many lower power assemblies. Because there is significant margin to the regulatory limit, the CWO value can be conservatively chosen as that calculated for the limiting HAR. A detailed CWO calculation is therefore not needed because the outcome will always be less than 0.12 percent. Since the resulting CWO is 0.40 percent, the analysis confirms that 10 CFR 50.46 acceptance criterion (b)(3), i.e., “Core-Wide Oxidation less than 1 percent of the metal in the cladding cylinders surrounding the fuel, excluding the cladding surrounding the plenum volume”, is demonstrated. The results are shown in Table 14.3.1-5.

- (b)(4) 10 CFR 50.46 acceptance criterion (b)(4) requires that the calculated changes in core geometry are such that the core remains amenable to cooling. This criterion has historically been satisfied by adherence to criteria (b)(1) and (b)(2), and by assuring that fuel deformation due to combined LOCA and seismic loads is specifically addressed. It has been demonstrated that the PCT and maximum cladding oxidation limits remain in effect for Best-Estimate LOCA applications. The approved methodology (WCAP-12945-P-A) specifies that effects of LOCA and seismic loads on core geometry do not need to be considered unless grid crushing extends beyond the 44 assemblies in the low-power channel. This situation has not been calculated to occur for D. C. Cook Unit 1. Therefore, acceptance criterion (b)(4) is satisfied.
- (b)(5) 10 CFR 50.46 acceptance criterion (b)(5) requires that long-term core cooling be provided following the successful initial operation of the ECCS. Long-term cooling is dependent on the demonstration of continued delivery of cooling water to the core. The manual actions that are currently in place to maintain long-term cooling remain unchanged with the application of the ASTRUM methodology (WCAP-16009-P-A).

As part of the response to the NRC request for additional information (see Reference 15), an evaluation of adjusted ECCS flow rates was included that resulted in a change to the PCT. The results of the Unit 1 design basis LBLOCA analysis, including the evaluation of adjusted ECCS flows, are presented in Table 14.3.1-5. Detailed analysis of record information for the Unit 1 LBLOCA is found in the analysis of record as presented in Reference 16. Unit 1 continues to satisfy the acceptance criteria of 10 CFR 50.46.

## UFSAR Revision 30.0


 An AEP Company	<b>INDIANA MICHIGAN POWER</b> <b>D. C. COOK NUCLEAR PLANT</b> <b>UPDATED FINAL SAFETY ANALYSIS REPORT</b>	Revised: 29.0 Section: 14.3.1 Page: 16 of 17
---	---	--

Based on the ASTRUM Analysis results (Table 14.3.1-5), and the applicable penalties and benefits (Table 14.3.1-6), it is concluded that D. C. Cook Unit 1 continues to maintain a margin of safety to the limits prescribed by 10 CFR 50.46. A time sequence of events for the limiting case is given in Table 14.3.1-8.

### **14.3.1.8 References for Section 14.3.1**

1. “Acceptance Criteria for Emergency Core Cooling Systems for Light Water Cooled Nuclear Power Reactors”, 10 CFR 50.46 and Appendix K of 10 CFR 50. Federal Register, Volume 39, Number 3, January 4, 1974.
2. SECY-83-472, Information Report from W.J. Dircks to the Commissioners, “Emergency Core Cooling System Analysis Methods”, November 17, 1983.
3. Regulatory Guide 1.157, Best-Estimate Calculations of Emergency Core Cooling System Performance, USNRC, May 1989.
4. NUREG/CR-5249, Qualifying Reactor Safety Margins: Application of Code Scaling Applicability and Uncertainty (CSAU) Evaluation Methodology to a Large Break Loss-of-Coolant-Accident, B. Boyack, et. al., 1989.
5. Bajorek, S.M., et. al., 1998, “Code Qualification Document for Best-Estimate LOCA Analysis”, WCAP-12945-P-A, Volume 1, Revision 2 and Volumes 2 through 5, Revision 1.
6. WCAP-16009-P-A, “Realistic Large Break LOCA Evaluation Methodology Using the Automated Statistical Treatment of Uncertainty Method (ASTRUM),” (Westinghouse Proprietary), in conjunction with Licensing Amendment Request “WCOBRA/TRAC Validation with revised Downcomer Noding for D. C. Cook Unit 1 and 2,” November 2007.
7. WCAP-8355, Supplement 1, May 1975, WCAP-8354 (Proprietary), “Long-Term Ice Condenser Containment LOTIC Code Supplement 1,” July 1974.
8. WCAP-13451, “Westinghouse Methodology for Implementation of 10 CFR 50.46 Reporting”, October 1992.
9. NRC Safety Evaluation Report for Amendment 306 to DPR 58, “Donald C. Cook Nuclear Plant, Unit 1 -Issuance of Amendment To Renewed Facility Operating License Regarding Use of The Westinghouse ASTRUM Large Break Loss-of-


## UFSAR Revision 30.0

 An AEP Company	<b>INDIANA MICHIGAN POWER</b> <b>D. C. COOK NUCLEAR PLANT</b> <b>UPDATED FINAL SAFETY ANALYSIS REPORT</b>	Revised: 29.0 Section: 14.3.1 Page: 17 of 17
---	---	--


Coolant Accident Analysis Methodology (TAC NO. MD7556)", October 17, 2008.

10. Attachment 13 to letter, M. P. Alexich, IMECo, to H. R. Denton, NRC, March 26, 1987, AEP: NRC: 0916W.
11. "Donald C. Cook Nuclear Plant Units 1 and 2, Modifications to the Containment Systems, Westinghouse Safety Evaluation, (SECL 99-076, Revision 3)", WCAP-15302, September, 1999 (Westinghouse Non-Proprietary Class 3)
12. Barsic, J. A., et al., "Control Rod Insertion Following a Cold Leg LBLOCA, D. C. Cook, Units 1 and 2, "WCAP-15245 (Proprietary) and WCAP-15246 (Non-proprietary), 1999.
13. Stang, J. F. (NRC), Letter to R. P. Powers (I&M) "Issuance of Amendments – Donald C. Cook Nuclear Plant, Units 1 and 2 (TAC Nos. MA6473 and MA6474), dated December 23, 1999.
14. Letter AEP:NRC:7565-01, Donald C. Cook Nuclear Plant Unit 1, Docket No. 50-315, License Amendment Request Regarding Large Break Loss-of-Coolant Accident Analysis Methodology, December 27, 2007.
15. Letter AEP-NRC-2008-10, Donald C. Cook Nuclear Plant Unit 1, Response to Request for Additional Information Regarding Reanalysis of Large Break Loss-of-Coolant Accident (TAC No. MD7556), July 14, 2008.
16. Letter AEP-NRC-2009-54, Donald C. Cook Nuclear Plant Unit 1 and 2 Annual Report of Loss-of-Coolant Accident Evaluation Model Changes, August 28, 2009.
17. Westinghouse Project Letter NF-AE-11-102, "Evaluation of the LOTIC2 Safety Injection Spill Mass and Energy Error (IR# 10-218-M021)," dated August 23, 2011.
18. Westinghouse Letter AEP-10-121, "Post LOCA Reanalysis Project (Phase IIIB) – Post LOCA Long Term Cooling Reanalysis", dated August 31, 2010.
19. Westinghouse Letter NF-AE-11-68, Revision 1, "Post LOCA Boron Precipitation Licensing Report and CAW-11-3188 Transmittal", dated June 13, 2011
20. Good, B. F., "Reactor Internals Upflow Conversion Program Engineering Report for Donald C. Cook Nuclear Generating Station Unit 1," WCAP-18346-P Rev. 0, November 2018.

# UFSAR Revision 30.0

 An <b>AEP</b> Company	<b>INDIANA MICHIGAN POWER</b> <b>D. C. COOK NUCLEAR PLANT</b> <b>UPDATED FINAL SAFETY ANALYSIS REPORT</b>	Revised: 29.0 Section: 14.3.2 Page: i of i
--	---	--

<b>14.3 REACTOR COOLANT SYSTEM PIPE RUPTURE (LOSS OF COOLANT ACCIDENT) .....</b>	<b>1</b>
<b>14.3.2 Loss of Reactor Coolant from Small Ruptured Pipes or from Cracks in Large Pipes Which Actuates the Emergency Core Cooling System .....</b>	<b>1</b>
14.3.2.1 Identification of Causes and Accident Description .....	1
14.3.2.2 Analysis of Effects and Consequences .....	2
14.3.2.2.1 Method of Analysis .....	2
14.3.2.2.2 Small Break LOCA Analysis Using NOTRUMP .....	2
<i>Description of Inputs and Initial Conditions.....</i>	<i>3</i>
14.3.2.3 Results .....	4
14.3.2.3.1 Limiting Break Results.....	4
14.3.2.3.2 Additional Break Cases .....	5
14.3.2.4 Conclusions.....	5
14.3.2.4.1 Additional Evaluations.....	6
14.3.2.4.1.1 <i>Optimized ZIRLO™ Cladding .....</i>	<i>6</i>
14.3.2.4.1.2 <i>Supplemental Calculations to Support the Upflow Conversion (Reference 11) .....</i>	<i>6</i>
14.3.2.5 References for Section 14.3.2.....	8

 An AEP Company	<p>INDIANA MICHIGAN POWER D. C. COOK NUCLEAR PLANT UPDATED FINAL SAFETY ANALYSIS REPORT</p>	<p>Revised: 29.0 Section: 14.3.2 Page: 1 of 8</p>
---	---	---

## **14.3 REACTOR COOLANT SYSTEM PIPE RUPTURE (LOSS OF COOLANT ACCIDENT)**

### **14.3.2 Loss of Reactor Coolant from Small Ruptured Pipes or from Cracks in Large Pipes Which Actuates the Emergency Core Cooling System**

#### **14.3.2.1 Identification of Causes and Accident Description**


A loss-of-coolant accident (LOCA) is defined as a rupture of the reactor coolant system (RCS) piping or of any line connected to the system up to the first closed valve. Ruptures of small cross section will cause loss of the coolant at a rate that can be accommodated by the charging pumps that would maintain an operational water level in the pressurizer permitting the operator to execute an orderly shutdown.

Should a larger break occur, depressurization of the reactor coolant system causes fluid to flow to the reactor coolant system from the pressurizer resulting in a pressure and level decrease in the pressurizer. Reactor trip occurs when the pressurizer low-pressure trip setpoint is reached. The consequences of the accident are limited in two ways:

1. Reactor trip and borated water injection complement void formation in causing rapid reduction of nuclear power to a residual level corresponding to the delayed fission and fission product decay.
2. Injection of borated water ensures sufficient flooding of the core to prevent excessive cladding temperatures.

Before the break occurs, the plant is in an equilibrium condition, i.e., the heat generated in the core is being removed via the secondary system. During blowdown, heat from fission product decay, hot internals and the vessel continues to be transferred to the reactor coolant system. The heat transfer between the reactor coolant system and the secondary system may be in either direction depending on the relative temperatures. In the case of continued heat addition to the secondary, system pressure increases and steam dumping may occur. The safety injection signal stops normal feedwater flow by closing the main feedwater line isolation valves. Emergency feedwater flow via the Auxiliary Feedwater (AFW) pumps is initiated on the reactor trip signal. The secondary flow aids in the reduction of reactor coolant system pressure. When the RCS depressurizes to the accumulator gas cover pressure, the accumulators begin to inject water into

# UFSAR Revision 30.0

 An AEP Company	<p style="text-align: center;"><b>INDIANA MICHIGAN POWER</b> <b>D. C. COOK NUCLEAR PLANT</b> <b>UPDATED FINAL SAFETY ANALYSIS REPORT</b></p>	<p>Revised: 29.0 Section: 14.3.2 Page: 2 of 8</p>
---	--	---

the reactor coolant loops. The reactor coolant pumps are assumed to be tripped at the initiation of the accident and effects of pump coastdown are included in the blowdown analyses.

## **14.3.2.2 Analysis of Effects and Consequences**

### **14.3.2.2.1 Method of Analysis**


For small breaks (less than 1.0 ft<sup>2</sup>), the NOTRUMP (References 7, 8, and 10) digital computer code is employed to calculate the transient depressurization of the reactor coolant system as well as to describe the mass and enthalpy of the flow through the break.

#### **14.3.2.2.2 Small Break LOCA Analysis Using NOTRUMP**

The NOTRUMP and small break specific version of LOCTA-IV (References 7, 8 and 10) computer codes are used in the analysis of loss-of-coolant accidents due to small breaks in the RCS. The NOTRUMP computer code is a one-dimensional general network code incorporating a number of advanced features. Among these are the calculations of thermal non-equilibrium in all fluid volumes, flow regime-dependent drift flux calculations with counter-current flooding limitations, mixture level tracking logic in multiple-stacked fluid nodes, and regime-dependent heat transfer correlations. The NOTRUMP small break LOCA emergency core cooling system (ECCS) evaluation model (NOTRUMP-EM) was developed to determine the RCS response to design basis small break LOCAs, and to address NRC concerns expressed in NUREG-0611 (Reference 4). The NOTRUMP-EM was modified in Reference 10 to incorporate modeling of safety injection in the broken loop and the COSI condensation model.

The reactor coolant system model is nodalized into volumes interconnected by flow paths. The NOTRUMP code includes an option to utilize the N-loop model, which explicitly models one broken loop and each of three intact loops. A standard analysis would normally use the lumped loop model with one broken loop and one intact loop representing three intact loops. The N-loop model is used here primarily to model asymmetric safety injection. Transient behavior of the system is determined from the governing conservation equations of mass, energy, and momentum. The multi-node capability of the program enables explicit, detailed spatial representation of various system components which, among other capabilities, enables a proper calculation of the behavior of the loop seal during a loss-of-coolant accident. The reactor core is represented as heated control volumes with associated phase separation models to permit transient mixture height calculations. Detailed descriptions of the NOTRUMP code and the evaluation model are provided in References 7, 8 and 10.

## UFSAR Revision 30.0

 An AEP Company	<p style="text-align: center;"><b>INDIANA MICHIGAN POWER</b> <b>D. C. COOK NUCLEAR PLANT</b> <b>UPDATED FINAL SAFETY ANALYSIS REPORT</b></p>	<p>Revised: 29.0 Section: 14.3.2 Page: 3 of 8</p>
---	--	---

Fuel rod heat-up calculations are performed with the LOCTA-IV (Reference 2) code using the NOTRUMP calculated core pressure, core inlet enthalpy, fuel rod power history, core exit steam flow rate and mixture heights as boundary conditions.

### **Description of Inputs and Initial Conditions**


Figure 14.3.2-5 depicts the hot rod axial power shape used to perform the small break analysis. This shape was chosen because it represents a distribution with power concentrated in the upper regions of the core. Such a distribution is limiting for small break LOCAs because it minimizes coolant level swell, while maximizing vapor superheating and fuel rod heat generation at the uncovered elevations. The small break LOCA analysis assumes the core continues to operate at full rated power until the control rods are completely inserted.

Safety injection systems consist of gas pressurized accumulator tanks and pumped injection systems. Minimum emergency core cooling system availability is assumed for the analysis from one Charging (CHG) pump, one High Head Safety Injection (HHSI) pump, and one residual heat removal (RHR) pump. Assumed pumped safety injection characteristics as a function of RCS pressure used as boundary conditions in the analysis are shown in Figures 14.3.2-1 through -4 and in Tables 14.3.2-4 through -7. For the break sizes less than 8.75 inches the broken loop safety injection flow is assumed to spill to RCS pressure. For the 8.75-inch break case, the broken loop safety injection flow from the RHR and HHSI pumps are assumed to spill to the containment backpressure of 0 psig and the broken loop safety injection flow from the CHG pump is assumed to spill to RCS pressure. Safety injection is delayed 54 seconds after the occurrence of the injection signal to conservatively account for diesel generator startup and emergency power bus loading in case of a loss of offsite power coincident with an accident. During switchover from ECCS injection phase to ECCS recirculation phase the RHR flow is realigned to the sump, and as a result, an interruption in RHR flow for up to 5 minutes may occur. The analysis accounts for the RHR delay for break cases in which the RCS depressurizes to the RHR cut-in pressure. Note that modeling the HHSI cross-tie valve closed during the ECCS injection phase supports operation with the HHSI cross-tie valve open or closed during the ECCS injection phase.

The analysis supports operation for a nominal full-power vessel average temperature range of 553.7°F to 575.4°F (with +5.1°F/-4.1°F uncertainty) and nominal pressurizer pressure of 2100 psia and 2250 psia (with ±67 psi uncertainty). A list of input assumptions used in the analysis is provided in Table 14.3.2-1.



## UFSAR Revision 30.0

 An AEP Company	<p style="text-align: center;"><b>INDIANA MICHIGAN POWER</b> <b>D. C. COOK NUCLEAR PLANT</b> <b>UPDATED FINAL SAFETY ANALYSIS REPORT</b></p>	<p>Revised: 29.0 Section: 14.3.2 Page: 4 of 8</p>
---	--	---

### **14.3.2.3 Results**

Generic analyses using NOTRUMP (References 7 and 8) were performed and are presented in WCAP-11145-P-A (Reference 9). Those results demonstrate that in a comparison of cold leg, hot leg and pump suction leg break locations, the cold leg break location is limiting. To ensure that the worst possible small break size has been identified, calculations were performed using the NOTRUMP-EM for a spectrum of small breaks (1.5-, 2-, 2.5-, 2.75-, 3-, 3.25-, 3.5-, 3.75-, 4- and 6-inch equivalent diameter cold leg breaks) and includes an 8.75-inch equivalent diameter accumulator line break. The results of the small break LOCA analysis are summarized in Table 14.3.2-3, while the key transient event times are listed in Table 14.3.2-2. The limiting break was found to be a 3.25-inch diameter cold leg break. The maximum fuel cladding temperature attained during the transient was 1725°F.


#### **14.3.2.3.1 Limiting Break Results**

Figures 14.3.2-6 through -14 show the following for the limiting 3.25-inch break transient, respectively:

- Reactor Coolant System Pressure
- Core Mixture Level
- Clad Temperature at Peak Clad Temperature Elevation
- Vapor Mass Flow Rate Out of Top of Core
- Clad Surface Heat Transfer Coefficient at Peak Clad Temperature Elevation
- Fluid Temperature at Peak Clad Temperature Elevation
- Total Break Flow and Safety Injection Flow
- Total Reactor Coolant System Mass
- Top of Core Vapor Temperature

During the initial period of the small break, normal upward flow is maintained through the core and core heat is adequately removed. At the low heat generation rates following reactor trip, the fuel rods continue to be well cooled as long as the core is covered by a two-phase mixture level. Core uncover begins during the injection phase of the transient at 780 seconds (Figure 14.3.2-7). From the clad temperature transient for the 3.25-inch break calculation shown in Figure

## UFSAR Revision 30.0

 An AEP Company	<p style="text-align: center;"><b>INDIANA MICHIGAN POWER</b> <b>D. C. COOK NUCLEAR PLANT</b> <b>UPDATED FINAL SAFETY ANALYSIS REPORT</b></p>	<p>Revised: 29.0 Section: 14.3.2 Page: 5 of 8</p>
---	--	---

14.3.2-8, it is seen that the peak clad temperatures occurs near the time at which the core is most deeply uncovered when the top of the core is steam cooled. This time is also accompanied by the highest vapor superheating above the mixture level. From Figure 14.3.2-7 and Table 14.3.2-2 it can be seen that the core mixture level has completely recovered at 3840 seconds and continues to increase until the end of the calculated transient time. A comparison of the total break flow and safety injection flow (Figure 14.3.2-12) shows that at the time the transient was terminated the safety injection flow being delivered to the RCS exceeded the mass flow rate out the break.

### **14.3.2.3.2 Additional Break Cases**

Summaries of the transient responses for the non-limiting break cases (1.5-, 2-, 2.5-, 2.75-, 3-, 3.5-, 3.75-, 4-, 6- and 8.75 inches) are shown in Figures 14.3.2-15 through -52. The 1.5- and 8.75-inch breaks showed no core uncover; therefore, fuel rod heat-up calculations were not performed for these cases. The plots for each of the additional non-limiting break cases include:

- Reactor Coolant System Pressure
- Core Mixture Level
- Top of Core Vapor Temperature
- Clad Temperature at Peak Clad Temperature Elevation (Note no PCT plots provided for the 1.5- and 8.75- inch cases)


The fuel rod heat-up results for each of the additional breaks considered, as seen in Table 14.3.2-3, are less than the limiting 3.25-inch break case.

### **14.3.2.4 Conclusions**

The small break LOCA analysis considered a spectrum of cold leg breaks of 1.5-, 2-, 2.5-, 2.75-, 3-, 3.25-, 3.5-, 3.75-, 4-, 6- and 8.75-inch diameters. The analysis resulted in the limiting PCT of 1725°F for the 3.25-inch break and a maximum local transient oxidation of 3.61% calculated at the limiting time-in-life of 11,500 MWD/MTU for the 3.25-inch break. The analysis is applicable to core power levels up to and including 3304 MWt (plus 0.34% uncertainty) and modeling the HHSI cross-tie valve closed during the ECCS injection phase supports operation with the HHSI cross-tie valve open or closed during the ECCS injection phase.

The analysis presented herein shows that the accumulator and SI subsystems of the ECCS, together with the heat removal capability of the steam generators, provide sufficient core heat removal capability to maintain the calculated PCT for small break LOCA below the required limit of 10 CFR 50.46 (Reference 1). Furthermore, the analysis shows that the local cladding

# UFSAR Revision 30.0

 An AEP Company	<b>INDIANA MICHIGAN POWER</b> <b>D. C. COOK NUCLEAR PLANT</b> <b>UPDATED FINAL SAFETY ANALYSIS REPORT</b>	Revised: 29.0 Section: 14.3.2 Page: 6 of 8
---	---	--

oxidation and core wide average oxidation, including consideration of pre-existing and post-LOCA oxidation, are less than the 10 CFR 50.46 (Reference 1) limits. Note that the core wide average oxidation results illustrate that the total hydrogen generation is less than 1%.

Table 14.3.2-3 provides the summary of the results for the small break LOCA analysis including PCT, maximum local transient oxidation and total hydrogen generation.

### **14.3.2.4.1 Additional Evaluations**

#### **14.3.2.4.1.1 Optimized ZIRLO™ Cladding**

Beginning with Unit 1 Cycle 25, **Optimized ZIRLO™** cladding is being used in feed fuel assemblies. **Optimized ZIRLO™** cladding has been evaluated and found to be acceptable with respect to the analysis described in Section 14.3.2.


#### **14.3.2.4.1.2 Supplemental Calculations to Support the Upflow Conversion (Reference 11)**

SBLOCA calculations using the NOTRUMP-EM (described in Section 14.3.2.2.2) were performed to determine the effect of converting the barrel/baffle region from a downflow configuration to an upflow configuration. In order to assess the impact of implementing the Upflow Conversion, calculations were performed for a partial break spectrum to ensure the limiting results were captured. The key transient event times are listed in Table 14.3.2-2a, while the results of the evaluation are summarized in Tables 14.3.2-3a and 14.3.2-3b. A shift in limiting break size occurred, with the 3.0-inch break becoming limiting for the upflow configuration. In addition to a shift in limiting break size, the PCT has shifted from beginning of life to 8500 MWD/MTU. A burnup-dependent hot assembly average power factor ( $P_{HA}$ ) curve, presented in Table 14.3.2-1a, was credited to demonstrate compliance with the 10 CFR 50.46(b) acceptance criteria for maximum local oxidation for all times in life. The Upflow conversion has been determined to be a +107°F penalty for the PCT as noted in Table 14.3.2-8. The maximum fuel cladding temperature reached during the transient was 1831.4°F.

Plots of the following parameters are shown in Figures 14.3.2-53 through 14.3.2-56 for the limiting 3.0-inch break transient.


- Reactor Coolant System Pressure
- Core Mixture Level
- Top of Core Vapor Temperature
- Cladding Temperature at PCT Elevation

## UFSAR Revision 30.0

 An <b>AEP</b> Company	<b>INDIANA MICHIGAN POWER</b> <b>D. C. COOK NUCLEAR PLANT</b> <b>UPDATED FINAL SAFETY ANALYSIS REPORT</b>	Revised: 29.0 Section: 14.3.2 Page: 7 of 8
--	---	--


The results of the Upflow Conversion Calculations show that the requirements of 10 CFR 50.46(b) continue to be satisfied: total oxidation is less than 17%, core wide oxidation is less than 1%, and peak cladding temperature is less than 2200°F.

## UFSAR Revision 30.0


 <b>INDIANA MICHIGAN POWER</b> An AEP Company	<b>INDIANA MICHIGAN POWER</b> <b>D. C. COOK NUCLEAR PLANT</b> <b>UPDATED FINAL SAFETY ANALYSIS REPORT</b>	Revised: 29.0 Section: 14.3.2 Page: 8 of 8
---	---	--

### **14.3.2.5 References for Section 14.3.2**

1. "Acceptance Criteria for Emergency Core Cooling Systems for Light-Water Nuclear Power Reactors," 10 CFR 50.46, August 2007 and "ECCS Evaluation Models," Appendix K of 10 CFR 50, June 2000.
2. Bordelon, F. M., et al., "LOCTA-IV Program: Loss-of-Coolant Transient Analysis," WCAP-8301 (Proprietary), June 1974.
3. Not Used.
4. "Generic Evaluation of Feedwater Transients and Small Break Loss-of-Coolant Accidents in Westinghouse-Designed Operating Plants," NUREG-0611, January 1980.
5. Not Used.
6. Not Used.
7. Meyer, P. E., "NOTRUMP - A Nodal Transient Small Break and General Network Code," WCAP-10079-P-A (Proprietary), August 1985.
8. Lee, N., et al, "Westinghouse Small Break ECCS Evaluation Model Using the NOTRUMP Code," WCAP-10054-P-A (Proprietary), August 1985.
9. Rupprecht, S. D., et al, "Westinghouse Small Break LOCA ECCS Evaluation Model Generic Study with the NOTRUMP Code," WCAP-11145-P-A (Proprietary), October 1986.
10. Thompson, C. M. et al., "Addendum to the Westinghouse Small Break ECCS Evaluation Model Using the NOTRUMP Code: Safety Injection into the Broken Loop and COSI Condensation Model," WCAP-10054-P-A, Addendum 2, Revision 1 (Proprietary), July 1997.
11. Good, B. F., "Reactor Internals Upflow Conversion Program Engineering Report for Donald C. Cook Nuclear Generating Station Unit 1," WCAP-18346-P Rev. 0, November 2018.

 An AEP Company	INDIANA MICHIGAN POWER D. C. COOK NUCLEAR PLANT UPDATED FINAL SAFETY ANALYSIS REPORT	Revised: 26.0 Section: 14.3.3 Page: i of i
---	--	--

<b>14.3 REACTOR COOLANT SYSTEM PIPE RUPTURE (LOSS OF COOLANT ACCIDENT) .....</b>	<b>1</b>
<b>14.3.3 Core and Internals Integrity Analysis .....</b>	<b>1</b>
14.3.3.1 Input Assumptions and Results for LOCA Hydraulic Forcing Function Evaluation .....	1
14.3.3.2 Blowdown Model .....	3
14.3.3.3 Methodology .....	3
14.3.3.4 Blowdown Evaluations - Conclusions for Rerating and Reduced Temperature .....	5
14.3.3.5 Seismic Evaluation - For Rerating and Temperature Reduction .....	5
14.3.3.6 Leak-Before-Break Confirmation for Changes Due to SG Replacement Activities .....	6
14.3.3.7 Asymmetric Loca Loads And Mechanistic Fracture Evaluation .....	7
<i>Effect of the Replacement Steam Generators on Unit 1 .....</i>	<i>7</i>
14.3.3.8 References for Section 14.3.3 .....	7

 An AEP Company	<p>INDIANA MICHIGAN POWER D. C. COOK NUCLEAR PLANT UPDATED FINAL SAFETY ANALYSIS REPORT</p>	<p>Revised: 26.0 Section: 14.3.3 Page: 1 of 8</p>
---	---	---

## **14.3 REACTOR COOLANT SYSTEM PIPE RUPTURE (LOSS OF COOLANT ACCIDENT)**

### **14.3.3 Core and Internals Integrity Analysis**

The accident analysis for 15x15 Upgrade fuel is presented in Section 3.5.1. All of this material is considered to complement additional material on core and intervals integrity analysis presented in earlier chapters of this updated safety analysis report.

The information presented below reflects the analyses that were performed to support the rerating and temperature reduction program for Donald C. Cook Nuclear Plant Units 1 and 2 (Reference 15). The following information reflects the most recent reactor vessel internals analyses.


#### **14.3.3.1 Input Assumptions and Results for LOCA Hydraulic Forcing Function Evaluation**

For the Cook Nuclear Plant units a mechanistic fracture evaluation (Reference 11) was performed which demonstrated that the analytical conditions and margins against crack extension satisfy the criteria established by the staff so that the potential for rupture is low so that breaks in the main reactor coolant piping up to and including a break equivalent in size to the rupture of the largest pipe need not be postulated as a design basis for defining structural loads on or within the reactor vessel and the rest of the RCS main loops. This evaluation, corresponding Unit 2 license amendment No. 76 (Reference 14) and the NRC's revision to GDC-4 allow the exemption of postulating pipe ruptures of the primary loop for the Cook Nuclear Plant Units 1 and 2 Reduced Temperature and Pressure and Rerating Programs. The original qualification for the reactor internals is based on a double-ended severance of a reactor coolant system pipe, (WCAP-7332-L). However, in order to verify that the forcing functions based on the revised operating parameters are bounded by those previously analyzed, the next most limiting branch line break was analyzed. This comparison established that the limiting branch line loads for the accumulator line rupture are less severe than the reactor pressure vessel inlet nozzle (RPVIN) double-ended rupture in the original analysis.

Subsequently, the NRC modified 10 CFR 50 General Design Criteria 4, and published in the Federal Register (Vol. 52, No. 207) on October 27, 1987 its final rule, "Modification of General Design Criteria 4 Requirements for Protection Against Dynamic Effects of Postulated Pipe Ruptures". This change to the rule allows use of leak before break (LBB) technology for



## UFSAR Revision 30.0

 An AEP Company	<b>INDIANA MICHIGAN POWER</b> <b>D. C. COOK NUCLEAR PLANT</b> <b>UPDATED FINAL SAFETY ANALYSIS REPORT</b>	Revised: 26.0 Section: 14.3.3 Page: 2 of 8
---	---	--


excluding from the design basis the dynamic effects of postulated ruptures in primary coolant loop piping in pressurized water reactors. Westinghouse prepared WCAP-15131 to account for the changes to GDC-4, the effects of thermal aging of primary pipe and Unit 1 and 2 replacement steam generators. The analysis concluded that the LBB criterion remains valid for the Unit 1 and 2 current loading conditions and as a result, dynamic effects of reactor coolant system primary loop postulated pipe breaks need not be considered in the structural design basis for Unit 2 uprating and for Units 1 and 2 replacement steam generators conditions (Reference 18). The Westinghouse analysis has been reviewed and accepted by the NRC for incorporation into the D.C. Cook license basis (Reference 17).

The Cook Nuclear Plant Units 1 and 2 Reduced Temperature and Pressure and Rerating LOCA hydraulic forces analysis considered a break in the largest branch line connecting to the Reactor Coolant System (RCS). In the case for the Cook Nuclear Plant units the most limiting line would be the 10-inch accumulator line. This break is considered to be most limiting based on break area and sensitivity studies which demonstrate that breaks in the cold leg produce greater peak loads than those postulated elsewhere in the RCS. In order to compare the results of the accumulator line break directly and permit the use of consistent methodologies another break of the reactor coolant loop piping was analyzed. This analysis assumed a one hundred square inch reactor pressure vessel inlet nozzle (RPVIN) break, which is greater in size than the accumulator line break and is located closer to the vessel and internals. The one-hundred square inch break size was determined to be the maximum size of a RPVIN break due to limiting displacement conditions such as pipe supports, pipe restraints, rigidity of the RCS piping, and physical barriers such as the reactor vessel cavity wall. One-hundred square inches is, therefore, the effective break opening of the reactor vessel inlet nozzle rupture. This break size was used to determine a base line data point to evaluate the sensitivity to other break sizes; it was not needed to determine the acceptability of the reactor vessel internals for a LOCA with leak-before-break acceptance criteria.

In addition to the postulated break location and area, the severity of the postulated pipe break with respect to the reactor vessel internals is a function of the decompression path through the reactor internals, the break opening time, and the operating conditions of the plant at the time of the break. The break opening time used in the analysis was a conservative one millisecond as mandated by the Nuclear Regulatory Commission (NRC) in their Topical Evaluation Report.

In order to provide a Cook Nuclear Plant specific analysis, the most limiting plant operating parameters proposed for a potential rerating for the Cook Nuclear Plant units (Table 14.3.3-1)

## UFSAR Revision 30.0

 An AEP Company	<b>INDIANA MICHIGAN POWER</b> <b>D. C. COOK NUCLEAR PLANT</b> <b>UPDATED FINAL SAFETY ANALYSIS REPORT</b>	Revised: 26.0 Section: 14.3.3 Page: 3 of 8
---	---	--

were incorporated into the analysis, and the internals geometry, specifically the barrel baffle region former configuration, was explicitly modeled. The forcing functions were then generated for the 100 square inch RPVIN break, to establish a base case with an area characteristic of a primary loop break with current Westinghouse methodology, and for the accumulator line break, in order to establish the sensitivity of the resultant forces. As the hydraulic loads decay very quickly, only the first 0.5 second of the blowdown transient is of interest. The effects of the LOCA hydraulic loads on the internals beyond 0.5 second are considered insignificant.

The parameters chosen as most limiting incorporate a conservatively high power level (3588 MWt per Table 14.3.3-1) with respect to Cook Nuclear Plant Unit 1, as well as the upper bound primary pressure (2250 psia) and the lower bound vessel inlet temperature for the Rerating Program (511.7°F), since these are the conditions that force the maximum mass flow through the break.


### **14.3.3.2 Blowdown Model**

The purpose of the hydraulic forces analysis is to generate the forcing functions and loads that occur on RCS components as a result of a postulated loss-of-coolant accident (LOCA). The hydraulic forcing functions and loads that occur as a result of a postulated loss-of-coolant accident are calculated through the use of the MULTIFLEX 1.0 evaluation model. The initial phase of this model makes use of the MULTIFLEX 1.0 (Reference 12) computer code to determine the transient pressures, mass velocities, and densities throughout the entire reactor coolant system (RCS) as a function of time. This is accomplished through the use of a detailed thermal-hydraulic model of the RCS. In the second phase of the analysis, the LATFORC and FORCE-2 codes (Appendices A and B of Reference 12) use the time-history values as computed by MULTIFLEX and calculate the LOCA hydraulic forces on the vessel, core-barrel and other internal components of interest. The following sections briefly describe these programs with additional details available in Reference 12.

### **14.3.3.3 Methodology**

The MULTIFLEX 1.0 computer code calculates the thermal-hydraulic transient within the entire primary coolant system. It considers sub-cooled, transition, and two-phase (saturated) blowdown regimes, employing the method of characteristics to solve the conservation laws, assuming one-dimensionality of flow and homogeneity of the liquid-vapor mixture. With its ability to treat multiple flow branches and a large number of nodes, MULTIFLEX has the required flexibility to represent various flow passages within the primary reactor coolant system. Basically, the RCS is divided into subregions in which the fluid flows along the longitudinal axes. Each subregion is

# UFSAR Revision 30.0

 An AEP Company	<b>INDIANA MICHIGAN POWER</b> <b>D. C. COOK NUCLEAR PLANT</b> <b>UPDATED FINAL SAFETY ANALYSIS REPORT</b>	Revised: 26.0 Section: 14.3.3 Page: 4 of 8
---	---	--


regarded as an equivalent pipe and a complex network of these equivalent pipes is then used to represent the entire primary RCS.

A coupled fluid-structure interaction is considered by accounting for the deflection of constraining boundaries, which are represented by separate spring-mass oscillator systems. For the analysis, the core support barrel is modeled as an equivalent beam (with the structural properties of the core barrel) in the plane parallel to the broken inlet nozzle. Horizontally, the barrel is divided into ten segments, with each segment consisting of three separate walls. Mass and stiffness matrices, obtained from independent modal analyses of the core barrel, are applied at each of ten mass point locations. Horizontal forces are then calculated by applying the spatial pressure variation to the wall area at each of the elevations representative on the ten mass points of the beam model. The resultant barrel motion is translated into an equivalent change in flow area in each downcomer annulus channel. At every time increment, the code iterates between the hydraulic and structural subroutines of the program at each location confined by a flexible wall.

The LATFORC computer code utilizes the MULTIFLEX generated field pressures, together with geometric vessel information (component radial and axial lengths), to determine the horizontal forces on the vessel wall, core barrel, and thermal shield. The LATFORC code represents the vessel region with a model that is consistent with the model used in the MULTIFLEX blowdown calculation. The downcomer annulus is subdivided into cylindrical segments, formed by dividing this region into circumferential and axial zones. The horizontal forces are resolved into x and y direction forces and added algebraically at each of the ten elevations. Note that the x-axis coincides with the axis of the broken loop's RPV inlet nozzle, and the positive direction is directed away from this nozzle.

The vertical hydraulic loads on the reactor vessel internals during blowdown are determined by the FORCE2 computer code utilizing a detailed geometric description of the vessel components, and the transient pressures and mass velocities computed by the MULTIFLEX code. Conservation of linear momentum forms the analytical basis for the derivation of the mathematical equations used in the FORCE2 code. In evaluating the vertical hydraulic loads on the reactor vessel internals, the following types of transient forces are considered:

- Pressure differential acting across the element.
- Flow stagnation on the element and unrecovered orifice losses across the element.
- Friction losses along the element.

 <p><b>INDIANA MICHIGAN POWER</b> <small>An AEP Company</small></p>	<p><b>INDIANA MICHIGAN POWER</b> <b>D. C. COOK NUCLEAR PLANT</b> <b>UPDATED FINAL SAFETY ANALYSIS REPORT</b></p>	<p>Revised: 26.0 Section: 14.3.3 Page: 5 of 8</p>
--	--	---

These three types of forces are summed together to give the total force on each element. Individual forces on elements are further combined, depending upon what particular reactor vessel internals component is being considered, to yield the resultant vertical hydraulic load on that component.

#### **14.3.3.4 Blowdown Evaluations - Conclusions for Rerating and Reduced Temperature**

In support of the Rerating Program, LOCA Hydraulic Forcing Functions were generated for the accumulator branch line break and a 100 square inch reactor pressure vessel inlet nozzle break. The results of this analysis are summarized in Reference 13. The 100 square inch reactor pressure vessel inlet nozzle (RPVIN) break analysis was performed to represent the original design conditions of the Cook units. The original design condition, as stated in WCAP-7332-L, was a double-ended pipe break, which is a much more severe case than the 100 square inch RPVIN break.

A comparison of LOCA hydraulic forcing function for the accumulator branch line break and the 100 square inch RPVIN break shows the RPVIN break to be limiting with respect to the peak total horizontal and vertical forces.

Therefore, an evaluation of the Cook reactor internals for LOCA loads resulting from the rerating is not needed since the original design condition loads (double-ended pipe break) bound the accumulator branch line break loads. The use of the accumulator branch line break loads was allowed by the leak-before-break exemption.

#### **14.3.3.5 Seismic Evaluation - For Rerating and Temperature Reduction**

The dynamic response for the Cook RPV system will remain essentially unchanged for the parameters of the rerating program. The frequency of the components is a function of:

$$f_n = F(E/\rho)^{1/2}$$


where

F is a constant that varies from component to component

E is the Modulus of Elasticity

Therefore, the new frequency of the components is:

# UFSAR Revision 30.0

 <p><b>INDIANA MICHIGAN POWER</b> <small>An AEP Company</small></p>	<p><b>INDIANA MICHIGAN POWER</b> <b>D. C. COOK NUCLEAR PLANT</b> <b>UPDATED FINAL SAFETY ANALYSIS REPORT</b></p>	<p>Revised: 26.0 Section: 14.3.3 Page: 6 of 8</p>
--	--	---

$$f_n^* = f_n \left( \frac{E^* / \rho^*}{E / \rho} \right)^{1/2} = f_n \left[ \left( \frac{E^* / \rho^*}{E / \rho} \right) \left( \frac{\rho}{\rho^*} \right) \right]^{1/2}$$

where

$$\rho = (\rho_{\text{metal}} + \rho_{\text{water}})$$

$\rho^*, f_n^*, E^* =$  at rerated conditions

Since the density of metal changes only slightly with temperature, the density change of the water is the only concern. It will be conservative to assume the metal density changes at the same rate as the water density with temperature.

The quantity of  $\left( \frac{\rho^*}{\rho} \right) \left( \frac{E}{E^*} \right)$  was calculated to be equal to (1/1.03),

now:

$$f_n^* = f_n \left( \frac{1}{1.03} \right)^{1/2} = .985 f_n$$


The frequency of the components will only decrease by approximately 1.5%. Therefore, the dynamic response of the Cook internals is essentially unchanged for the rerating conditions, and as a result the original seismic loads are still considered valid.

## **14.3.3.6 Leak-Before-Break Confirmation for Changes Due to SG Replacement Activities**

As part of the effort to support taking credit for RCCA insertion for criticality control at the time the ECCS is realigned from cold leg recirculation to hot leg recirculation (Section 14.3.1 for both Units 1 and 2 for further discussion), a reanalysis was submitted to the NRC to demonstrate the continued applicability of the leak-before-break (LBB) technology for the Cook units. The NRC staff independently assessed the compliance of the reactor coolant system with the LBB criteria established in NUREG-1061, Volume 3. The NRC staff concluded in Reference 17 that the analyses and additional information submitted were sufficient to demonstrate that LBB behavior would be expected following the installation of the replacement steam generators (SGs).

Evaluations have concluded that the LBB analyses remain acceptable for the period of extended operation as described in Chapter 15 of the UFSAR.

## UFSAR Revision 30.0

 An AEP Company	<b>INDIANA MICHIGAN POWER</b> <b>D. C. COOK NUCLEAR PLANT</b> <b>UPDATED FINAL SAFETY ANALYSIS REPORT</b>	Revised: 26.0 Section: 14.3.3 Page: 7 of 8
---	---	--

### **14.3.3.7 Asymmetric Loca Loads And Mechanistic Fracture Evaluation**

References (3) through (9), (11), and (14) describe work done by a Westinghouse Owners' Utility Group specifically formed to provide an analytical evaluation of the effects of certain postulated break loads on the reactor coolant system and internals as well as the NRC safety evaluations. For a discussion of the group's work and results see Section 14.3.3, Unit 2.

The response of the reactor core and vessel internals under excitation produced by a simultaneous complete severance of a reactor coolant pipe and seismic excitation for typical 4-loop plant internals has been determined. A detailed description of the analysis applicable to the Donald C. Cook Nuclear Power Plant design appears in WCAP-7332-L (Reference 2), Indian Point Unit No. 2 Reactor Internals Mechanical Analysis for Blowdown Excitation (Westinghouse Proprietary).


### **Effect of the Replacement Steam Generators on Unit 1**

A detailed evaluation or analysis of the effect of the RSG on the core and internals integrity analysis was not performed. However, since the RSG operating parameters (i.e., pressure, temperature, and flowrate), are similar, and it has been concluded that the existing LOCA analysis is applicable to the RSGs, there is no impact by the use of the RSGs on the material presented in this section.

### **14.3.3.8 References for Section 14.3.3**

1. Reference deleted.
2. WCAP-7332-L, "Indian Point Unit No. 2 Reactor Internals Mechanical Analysis for Blowdown Excitation," G. J. Bohm, February 1970.
3. Letter from J. A. Tillinghast, Indiana & Michigan Power Co., to E. G. Case, NRC, dated March 8, 1978.
4. Letter from J. A. Tillinghast, Indiana & Michigan Power Co., to E. G. Case, NRC, dated May 15, 1978.
5. Letter from G. P. Maloney, Indiana & Michigan Power Co., to H. R. Denton, NRC, dated September 26, 1979, AEP:NRC:0137.
6. Letter from John E. Dolan, Indiana & Michigan Electric Co., to H. R. Denton, NRC, dated December 7, 1979, AEP:NRC:00137A.


# UFSAR Revision 30.0

 <b>INDIANA MICHIGAN POWER</b> An AEP Company	<b>INDIANA MICHIGAN POWER</b> <b>D. C. COOK NUCLEAR PLANT</b> <b>UPDATED FINAL SAFETY ANALYSIS REPORT</b>	Revised: 26.0 Section: 14.3.3 Page: 8 of 8
---	---	--


7. Letter from R. S. Hunter, Indiana & Michigan Electric Co., to H. R. Denton, NRC, dated February 15, 1980, AEP:NRC:00137B.
8. Letter from R. S. Hunter, Indiana & Michigan Electric Co., to H. R. Denton, NRC, dated October 8, 1980, AEP:NRC:0137C.
9. Letter from M. P. Alexich, Indiana & Michigan Electric Co., to H. R. Denton, NRC, dated September 10, 1984, AEP:NRC:0137D.
10. DC-D-3195-368-SC, Calculation of "Structural Analysis of Reactor Coolant Loop Piping for Replacement of Steam Generators on D.C. Cook Units 1 and 2" revision 0 (Westinghouse Calculation No. CN-SMT-99-75).
11. WCAP-9558, Rev. 2, May 1982, "Mechanistic Fracture Evaluation of Reactor Coolant Pipe Containing a Postulated Circumferential Through-Wall Crack".
12. Takeuchi, K., et al., MULTIFLEX, A Fortran-IV Computer Program for Analyzing Thermal Hydraulic Structure System Dynamics," WCAP-8708-P/A (Proprietary) and WCAP-8709-A (Non-Proprietary), September 1977.
13. 13 WCAP-11902, "Reduced Temperature and Pressure Operation for Donald C. Cook Nuclear Plant Unit 1 Licensing Report," October 1988.
14. NRC Unit 2 License Amendment No. 76 and associated SER, November 22, 1985.
15. WCAP-12135, "D. C. Cook Nuclear Plant Units 1 & 2, Rating Engineering Report," September 1989.
16. WCAP-12828, "Reactor Pressure Vessel & Internals System Evaluations for the D. C. Cook Unit 2 Vantage 5 Fuel Upgrade with IFMs," December 1990.
17. Stang, J. F. (NRC), Letter to R. P. Powers (I&M) "Issuance of Amendments – Donald C. Cook Nuclear Plant, Units 1 and 2 (TAC Nos. MA6473 and MA6474)," dated December 23, 1999.
18. Westinghouse WCAP-15131 revision 1 "Technical Justification for Eliminating Large Primary Loop Pipe Rupture as the Structural Design Basis for the D.C. Cook Units 1 and 2 Nuclear Power Plants" dated October 1999.



# UFSAR Revision 30.0

 An AEP Company	INDIANA MICHIGAN POWER D. C. COOK NUCLEAR PLANT UPDATED FINAL SAFETY ANALYSIS REPORT	Revised: 29.0 Section:14.3.4.1 Page: i of i
---	--	---

<b>14.3 REACTOR COOLANT SYSTEM PIPE RUPTURE (LOSS OF COOLANT ACCIDENT) .....</b>	<b>1</b>
<b>14.3.4 Containment Integrity Analysis .....</b>	<b>1</b>
14.3.4.1 Containment Structure .....	1
14.3.4.1.1 Design Basis .....	1
14.3.4.1.2 Design Features .....	2
14.3.4.1.3 Design Evaluation .....	3
14.3.4.1.3.1 Loss of Coolant Accident .....	3
14.3.4.1.3.1.1 Compression Ratio Analysis .....	3
14.3.4.1.3.1.1.a Introduction .....	3
14.3.4.1.3.1.1.b Air Compression Process Description .....	4
14.3.4.1.3.1.1.c Sensitivity to Blowdown Energy .....	7
14.3.4.1.3.1.1.d Effect of Blowdown Rate .....	8
14.3.4.1.3.1.1.e Effect of Steam Bypass .....	8
14.3.4.1.3.1.1.f Effect of Dead-Ended Volumes .....	10
14.3.4.1.3.1.2 Long Term Containment Pressure Analysis .....	11
14.3.4.1.3.1.3 Peak Containment Pressure Transient .....	12
14.3.4.1.3.1.4 Structural Heat Removal .....	16
14.3.4.1.3.1.5 Relevant Acceptance Criteria .....	16
14.3.4.1.3.1.6 Conclusions .....	17
14.3.4.1.3.2 Steam Line Break .....	17
14.3.4.1.3.2.1 Peak Containment Temperature Transients .....	17
14.3.4.1.3.2.2 Results .....	18
14.3.4.1.3.2.3 Sensitivity of the Results .....	19

 <b>INDIANA MICHIGAN POWER</b> <small>An AEP Company</small>	<b>INDIANA MICHIGAN POWER D. C. COOK NUCLEAR PLANT UPDATED FINAL SAFETY ANALYSIS REPORT</b>	Revised: 29.0 Section:14.3.4.1 Page: 1 of 20
--	---	--

## **14.3 REACTOR COOLANT SYSTEM PIPE RUPTURE (LOSS OF COOLANT ACCIDENT)**

### **14.3.4 Containment Integrity Analysis**

#### **14.3.4.1 Containment Structure**

##### **14.3.4.1.1 Design Basis**

The steel-lined, reinforced concrete containment structure, including foundations, access hatches, and penetrations is designed and constructed to maintain full containment integrity when subjected to accident temperatures and pressures, and the postulated earthquake conditions. Details of the Containment System are described in Chapter 5.

The containment design internal pressure is 12 psig. The effects of pipe rupture in the primary coolant system, up to and including a double-ended rupture of the largest pipe as well as a rupture of the main steam line, are considered in determining the peak accident pressure.

The internal structures of the containment vessel are also designed for subcompartment differential accident pressures. The accident pressures considered are due to the same postulated pipe ruptures as described for the containment vessel.


The other simultaneous loads in combination with the accident pressures, and the applicable load factors, are presented in detail in Chapter 5.

The functional design of the containment is based upon the following accident input source term assumptions and conditions:

1. The design basis accident blowdown mass and energy is put into the containment.
2. The hot metal energy is considered.
3. A reactor core power of 3317 MWt (100.34% of 3306 MWt – conservative compared to licensed power of 3304 MWt) is used for decay heat generation.
4. Minimum Engineering Safety Features performance is assumed based upon the limiting single failure criterion.

The ice condenser is designed to limit the containment pressure below the design pressure for all reactor coolant pipe break sizes up to and including a double-ended severance. Characterizing the performance of the ice condenser requires consideration of the rate of addition of mass and

# UFSAR Revision 30.0

 An AEP Company	<p style="text-align: center;"><b>INDIANA MICHIGAN POWER</b> <b>D. C. COOK NUCLEAR PLANT</b> <b>UPDATED FINAL SAFETY ANALYSIS REPORT</b></p>	<p>Revised: 29.0 Section: 14.3.4.1 Page: 2 of 20</p>
---	--	--

energy to the containment, as well as the total amounts of mass and energy added. Analyses have shown that the accident which produces the highest blowdown rate into the ice condenser containment results in the maximum containment pressure rise. That accident is the double-ended severance of a reactor coolant pipe.

Post-blowdown energy releases can also be accommodated without exceeding the containment design pressure.

### **14.3.4.1.2 Design Features**

The reactor containment is a reinforced concrete structure consisting of a vertical cylinder, a hemispherical dome and a flat base. The interior is divided into three volumes, a lower volume which houses the reactor and Reactor Coolant System, an intermediate volume housing the energy absorbing ice bed in which steam is condensed and an upper volume which accommodates the air displaced from the other two volumes during a design basis pipe break accident.


The type of containment used for Donald C. Cook Unit 1 was selected for the following reasons:

1. The Ice Condenser Containment can accept large amounts of energy and mass inputs and maintain low internal pressures and leakage rates. A particular advantage of the ice condenser is its passive design not requiring an actuation signal.
2. The Ice Condenser Containment combines the required integrity, compact size, and carefully considered advanced design desirable for a nuclear station.

Consideration is given to subcompartment differential pressure resulting from a design basis accident. If an accident were to occur due to a pipe rupture in one of these relative small volumes, the pressure would build up at a faster rate than in the containment, thus imposing a differential pressure across the wall of the structure. Section 14.3.4.2, "Containment Subcompartments", presents the subcompartment differential pressure analyses.

The Ice Condenser Containment, incorporating forced circulation of the containment atmosphere together with the containment spray system, ensures the functional capability of containment for as long as necessary following an accident. The peak pressure occurring as the result of the complete blowdown of the reactor coolant through any rupture of the Reactor Coolant System up to and including the hypothetical double-ended severance does not exceed the design pressure of the containment. The design pressure is also not exceeded during subsequent long term pressure transients.

# UFSAR Revision 30.0

 An AEP Company	<p>INDIANA MICHIGAN POWER D. C. COOK NUCLEAR PLANT UPDATED FINAL SAFETY ANALYSIS REPORT</p>	<p>Revised: 29.0 Section: 14.3.4.1 Page: 3 of 20</p>
---	---	--

## **14.3.4.1.3 Design Evaluation**

### **14.3.4.1.3.1 Loss of Coolant Accident**

The time history of conditions within an ice condenser containment during a postulated loss-of-coolant accident can be divided into two periods for calculational purposes:

1. The initial reactor coolant blowdown, which for the largest assumed pipe break occurs in approximately 30 seconds.
2. The post blowdown phase of the accident which begins following the blowdown and extends several hours after the start of the accident.

During the first few seconds of the blowdown period following a large rupture of the Reactor Coolant System, containment conditions are characterized by rapid pressure and temperature transients. To calculate these transients a detailed spatial and short time increment analysis is necessary. This analysis is performed with the TMD code with the calculation time of interest extending up to a few seconds following the accident initiation.

Physically, tests at the Waltz Mill ice condenser test facility have shown that the blowdown phase represents that period of time in which the lower compartment air, and a portion of the ice condenser air, are displaced and compressed into the upper compartment and the remainder of the ice condenser. The containment pressure at or near the end of blowdown is governed by this air compression process.

Containment pressure during the post blowdown phase of the accident is calculated with the LOTIC Code, which models the containment structural heat sinks and containment safeguards systems.


The paragraphs that follow describe key physical phenomena considered in the design pressure determination and the containment pressure response analysis. The methods of accounting for these phenomena in the analysis is also discussed.

#### **14.3.4.1.3.1.1 Compression Ratio Analysis**

##### **14.3.4.1.3.1.1.a Introduction**

Following the initial pressure peak from a double-ended cold leg break, blowdown continues and the pressure in the lower compartment again increases, reaching a peak at or before the end of blowdown. The pressure in the upper compartment continues to rise from beginning of blowdown and reaches a peak, which is approximately equal to the lower compartment pressure.

# UFSAR Revision 30.0

 <b>INDIANA MICHIGAN POWER</b> <small>An AEP Company</small>	<b>INDIANA MICHIGAN POWER D. C. COOK NUCLEAR PLANT UPDATED FINAL SAFETY ANALYSIS REPORT</b>	Revised: 29.0 Section:14.3.4.1 Page: 4 of 20
--	---	--

After blowdown is complete, the steam in the lower compartment continues to flow through the doors into the ice bed compartment and is condensed.

The primary factor in producing this upper containment pressure peak, and, therefore, in determining design pressure, is the displacement of air from the lower compartment into the upper compartment. The ice condenser quite effectively performs its function of condensing virtually all the steam that enters the ice beds. Essentially, the only source of steam entering the upper containment is from leakage through the drain holes and other leakage around crack openings in hatches in the operating deck, which separate the lower and upper portions of the containment building.

A method of analysis of the compression peak pressure was developed based on the results of full scale section tests. This method consists of the calculation of the air mass compression ratio, the polytropic exponent for the compression process, and the effect of steam bypass through the operating deck on this compression.

In the following sections, a discussion of the major parameters affecting the compression peak will be discussed. Specifically they are: air compression, steam bypass, blowdown rate, and blowdown energy.


### **14.3.4.1.3.1.1.b Air Compression Process Description**

The volumes of the various containment compartments determine directly the air volume compression ratio. This is basically the ratio of the total active containment air volume to the compressed air volume during blowdown. During blowdown, air is displaced from the lower compartment and compressed into the ice condenser beds and into the upper containment above the operating deck. It is this air compression process which primarily determines the peak in containment pressure following the initial blowdown release.

The actual Waltz Mill test compression ratios were found by performing air mass balances before the blowdown and at the time of the compression peak pressure, using the results of three full scale special section tests. These three tests were conducted with an energy input representative of the plant design.

In the calculation of the mass balance for the ice condenser, the compartment is divided into two subvolumes; one volume representing the flow channels and one volume representing the ice baskets. The flow channel volume is further divided into four subvolumes, and the partial air pressure and mass in each subvolume are found from thermocouple readings, assuming that the air is saturated with steam at the measured temperature. From these results, the average

## UFSAR Revision 30.0

 An AEP Company	<b>INDIANA MICHIGAN POWER</b> <b>D. C. COOK NUCLEAR PLANT</b> <b>UPDATED FINAL SAFETY ANALYSIS REPORT</b>	Revised: 29.0 Section: 14.3.4.1 Page: 5 of 20
---	---	---

temperature of the air in the ice condenser compartment is found, and the volume occupied by the air at the total condenser pressure is found from the equation of state as follows:

$$V_a = \frac{M_a R_a T_a}{P} \quad (1)$$

where:

- $V_a$  = Volume of ice condenser occupied by air (ft<sup>3</sup>).
- $M_a$  = Mass of air in ice condenser compartment (lb.).
- $T_a$  = Average temperature of air in ice condenser (°F).
- $P$  = Total ice condenser pressure (lb/ft<sup>2</sup>).

The partial pressure and mass of air in the lower compartment are found by averaging the temperatures indicated by the thermocouples during the test located in that compartment and assuming saturation conditions. For these three tests, it was found that the partial pressure, and hence the mass of air in the lower compartment, were zero at the time of the compression peak pressure.

The actual Waltz Mill test compression ratio is then found from the following:

$$C_r = \frac{V_1 + V_2 + V_3}{V_3 + V_a} \quad (2)$$

where:

- $V_1$  = Lower compartment volume (ft<sup>3</sup>).
- $V_2$  = Ice condenser compartment volume (ft<sup>3</sup>).
- $V_3$  = Upper compartment volume (ft<sup>3</sup>).


The polytropic exponent for these tests is then found from the measured compression pressure and the compression ratio calculated above. Also considered is the pressure increase that results from the leakage of steam through the deck into the upper compartment.

The compression peak pressure in the upper compartment for the tests for containment design is then given by:

$$P = P_o (C_r)^n + \Delta P_{\text{deck}} \quad (3)$$

where:

## UFSAR Revision 30.0

 An AEP Company	<b>INDIANA MICHIGAN POWER</b> <b>D. C. COOK NUCLEAR PLANT</b> <b>UPDATED FINAL SAFETY ANALYSIS REPORT</b>	Revised: 29.0 Section: 14.3.4.1 Page: 6 of 20
---	---	---

$P_o$	=	Initial pressure (psia).
$P$	=	Compression peak pressure (psia).
$C_r$	=	Volume compression ratio.
$n$	=	Polytropic exponent.
$\Delta P_{deck}$	=	Pressure increase caused by deck leakage (psi).

Using the method of calculation described above, the compression ratio was calculated for the three full scale section tests. From the results of the air mass balances, it was found that air occupied 0.645 of the ice condenser compartment volume at the time of peak compression, or

$$V_a = 0.645V_2 \quad (4)$$

The final compression volume includes the volume of the upper compartment as well as part of the volume of air in the ice condenser. The results of the full scale section tests (Figure 14.3.4-1) show a variation in steam partial pressure from 100% near the bottom of the ice condenser to essentially zero near the top. The thermocouples and pressure detectors confirm that at the time when the compression peak pressure is reached steam occupies less than half of the volume of the ice condenser. The analytical model used in defining the containment pressure peak uses the upper compartment volume 64.5 percent of the ice condenser air volume as the final volume. This 64.5 percent value was determined from appropriate test results.

The calculated volume compression ratios are shown in Figure 14.3.4-2, along with the compression peak pressures for these tests. The compression peak pressure is determined from the measured pressure, after accounting for the deck leakage contribution. From the results shown in Figure 14.3.4-2, the polytropic exponent for these tests is found to be 1.13.

For the long-term containment integrity analysis, the compression pressure is used to initialize the calculations.


The Donald C. Cook volume compression ratio, not accounting for the dead ended volume effect, is calculated using Equation 2 and using data from Table 14.3.4-1. The Table 14.3.4-1 containment compartment volume data have been adjusted, per the analysis methodology, to conservatively bias the analysis (References 35 & 36). Using the following volume information:

$V_1$	=	293,801 ft <sup>3</sup>
$V_2$	=	110,520 ft <sup>3</sup>
$V_3$	=	727,628 ft <sup>3</sup>

the compression ratio becomes:



## UFSAR Revision 30.0

 An AEP Company	<p style="text-align: center;"><b>INDIANA MICHIGAN POWER</b> <b>D. C. COOK NUCLEAR PLANT</b> <b>UPDATED FINAL SAFETY ANALYSIS REPORT</b></p>	<p>Revised: 29.0 Section: 14.3.4.1 Page: 7 of 20</p>
---	--	--

$$C_r = \frac{1,131,949}{727,628 + 0.645 * 110,520} = 1.42$$

The peak compression pressure, based on an initial containment pressure of 15.0 psia, is then given by Equation 3 as:

$$P_3 = 15.0 (1.42)^{1.13} + 0.4 = 22.64 \text{ psia or } 7.94 \text{ psig}$$

The peak compression pressure in the upper compartment for D.C. Cook Unit 1 design is 7.94 psig. This peak compression pressure includes a pressure increase of 0.4 psi from steam bypass. The nitrogen partial pressure from the accumulators is not included, since it is not added to the containment atmosphere until after the compression peak has passed. Accumulator nitrogen is considered in the long-term performance analysis of the containment pressure decay following blowdown, using the LOTIC code.

#### **14.3.4.1.3.1.1.c Sensitivity to Blowdown Energy.**

The sensitivity of the upper compartment compression pressure peak versus the amount of energy released is shown in Figure 14.3.4-3. This figure shows the magnitude of the peak compression pressure versus the amount of energy released in terms of percentage of reactor coolant system energy release. These data are based on test results wherein each of the tests were run at 110% and 200% of the initial blowdown rate equivalent to the maximum coolant pipe break flow.

These test results indicate the very large capacity of the ice condenser for additional amounts of energy with only a small effect on compression peak pressure. For example, during testing, 100% energy release gave a pressure of about 6.8 psig, while an increase up to 220% energy release gave an increase in peak pressure of only about 2 psi. It is also important to note that maldistribution of steam into different sections of the ice condenser would not cause even the small increase in peak pressure that is shown in Figure 14.3.4-3. For every section of the ice condenser that may receive more energy than that of the average section, other sections of the ice condenser would receive less energy than the average section. Thus, the compression pressure in the upper compartment would be indicated by the test performance based on 100% energy release rather than either the maximum energy release section or the minimum energy release section.

## UFSAR Revision 30.0


 An AEP Company	<p style="text-align: center;"><b>INDIANA MICHIGAN POWER</b> <b>D. C. COOK NUCLEAR PLANT</b> <b>UPDATED FINAL SAFETY ANALYSIS REPORT</b></p>	<p>Revised: 29.0 Section: 14.3.4.1 Page: 8 of 20</p>
---	--	--

Figure 14.3.4-4 gives some insight as to the very large capacity for energy absorption of the ice condenser as obtained from test results. Figure 14.3.4-4 is a plot of the amount of ice melted versus the amount of energy released based on test results at different energies and blowdown rates. These test results indicate that a 200% energy release melts only about 60% of the ice while 100% energy release melts only 30% of the ice. Thus, even for energy release considerably in excess of 200% there would still be a substantial amount of ice remaining in the ice condenser.

#### **14.3.4.1.3.1.1.d      Effect of Blowdown Rate**

Figure 14.3.4-5 shows the effect of blowdown rate upon the final compression pressure in the upper compartment. Figure 14.3.4-5 is based on the results of a series of tests, all with the plant design ice condenser configuration, but with the important difference that all of these tests were run with 185% of the Reactor Coolant System energy release quantity. There are two important effects to note from Figure 14.3.4-5. One, the magnitude of the compression peak pressure in the upper compartment is low (about 7.8 psig) for the reactor plant design blowdown rate; and two, even an increase in this rate up to 200% blowdown rate produces only a small increase in the magnitude of this peak pressure (about 1 psi).


#### **14.3.4.1.3.1.1.e      Effect of Steam Bypass**

The method of analysis used to obtain the maximum allowable deck leakage capacity as a function of the primary system break size is presented next. Two analyses were used to demonstrate the margin between the original design leakage value of 5 ft<sup>2</sup> and the maximum allowable. Considering the current design basis value of 7 sq. ft. for the deck leakage, the following discussion remains valid.

During the blowdown transient, steam and air will flow through the ice condenser doors and also through the deck bypass area into the upper compartment. For the containment the bypass area is composed of two parts, a known leakage area of 2.2 ft<sup>2</sup> with a geometric loss coefficient of 1.5 through the deck drainage holes location at the bottom of the refueling cavity, and an undefined deck leakage area with a conservatively small loss coefficient of 2.5. Leakage through the backdraft damper of the air return fans was determined to be 0.18 sq. ft./damper and was considered in the known leakage area. For the CEQ Fan Ventwell and Stairwell drains, the identified divider barrier bypass area is increased by approximately 0.16 ft<sup>2</sup> as a result of the removal of the check valve internals.

A resistance network similar to that used in TMD is used to represent 6 lower compartment volumes, each with a representative portion of the deck leakage and the lower inlet door flow

## UFSAR Revision 30.0

 An AEP Company	<p style="text-align: center;"><b>INDIANA MICHIGAN POWER</b> <b>D. C. COOK NUCLEAR PLANT</b> <b>UPDATED FINAL SAFETY ANALYSIS REPORT</b></p>	<p>Revised: 29.0 Section: 14.3.4.1 Page: 9 of 20</p>
---	--	--

resistance adjacent to the lower compartment element. The inlet door flow resistance and flow area are calculated for small breaks that would only partially open these doors.


The coolant blowdown rate as a function of time is used with this flow network to calculate the differential pressures on the lower inlet doors and across the operating deck. The resultant deck leakage rate and integrated steam leakage into the upper compartment are then calculated. The lower inlet doors are initially held shut by the cold head of air behind the doors (approximately 1/2 - 1 pound per square foot). The initial blowdown from a small break opens the doors and removes the cold head on the doors. With the door differential pressure removed the door position is slightly open. An additional pressure differential of one pound per square foot is then sufficient to fully open the doors. The nominal door opening characteristic are based on test results.

The first analysis conservatively assumed that flow through the postulated leakage paths is pure steam. During the actual blowdown transient, steam and air representative of the lower compartment mixture would leak through the holes; thus less steam would enter the upper compartment. If flow were considered to be a mixture of liquid and vapor, the total leakage mass would increase but the steam flow rate would decrease. The analysis also assumed that no condensing of the flow occurs due to structural heat sinks. The peak air compression in the upper compartment for the various break sizes is assumed with steam mass added to this value to obtain the total containment pressure. Air compression for the various break sizes is obtained from previous full scale section tests conducted at Waltz Mill.

The allowable leakage area for the following Reactor Coolant System break sizes was determined: DE, 0.6 DE, 3 ft<sup>2</sup>, 8 inch diameter, 6 inch diameter, 2.5 inch diameter, and 0.5 inch diameter. For break sizes 3 ft<sup>2</sup> and above a series of deck leakage sensitivity studies was made to establish the total steam leakage to the upper compartment over the blowdown transient. This steam was added to the air in the upper compartment to establish a peak pressure. Air and steam were assumed to be in thermal equilibrium, with the air partial pressure increased over the air compression value to account for heating effects. For these breaks, sprays were neglected. Reduction in compression ratio by return of air to the lower compartment was conservatively neglected. The results of this analysis are shown in Table 14.3.4-2. This analysis is confirmed by Waltz Mill tests conducted with various deck bypass leakages equivalent to over 50 ft<sup>2</sup> of deck leakage for the double ended blowdown rate.

For breaks 8 inches in diameter and smaller, the effect of containment sprays was included. The method used is as follows: For each time step of the blowdown the amount of steam leaking into

## UFSAR Revision 30.0

 An AEP Company	<p style="text-align: center;"><b>INDIANA MICHIGAN POWER</b> <b>D. C. COOK NUCLEAR PLANT</b> <b>UPDATED FINAL SAFETY ANALYSIS REPORT</b></p>	<p>Revised: 29.0 Section: 14.3.4.1 Page: 10 of 20</p>
---	--	---

the upper compartment was calculated to obtain the steam mass in the upper compartment. This steam was mixed with the air in the upper compartment, assuming thermal equilibrium with air. The air partial pressure was increased to account for air heating effects. After sprays were initiated, the pressure was calculated based on the rate of accumulation of steam in the upper compartment. Reduction in pressure due to operation of the air recirculation fans has been conservatively neglected.

This analysis was conducted for the 8 inch, 6 inch and 2-1/2 inch break sizes assuming two spray pumps were operating (4000 gpm at 80°F). As shown in Table 14.3.4-2, the 8 inch break is the limiting case for this range of break sizes although the 0.6 DE is the limiting case for the entire spectrum of break sizes. With one spray pump operating (2000 gpm at 80°F) the limiting case for the entire spectrum of break sizes is the 8 inch case and results in an allowable deck leakage area of approximately 35 ft<sup>2</sup>.

A second, more realistic, method was used to analyze this limiting case. This analysis assumed a 30 percent air, 70 percent steam mixture flowing through the deck leakage area. This is conservative considering the amount of air in the lower compartment during this portion of the transient. Operation of the deck fan would increase the air content of the lower compartment, thus increasing the allowable deck leakage area. Based on the LOTIC Code analysis a structural heat removal rate of over 8000 Btu/sec from the upper compartment is indicated. Therefore a steam condensation rate of 8 lbm/sec was used for the upper compartment. The results indicated that with one spray pump operating and a deck leakage area of 56 ft<sup>2</sup>, the peak containment pressure will be below design for the 8 inch case.


The 1/2 inch diameter break is not sufficient to open the ice condenser inlet doors. For this break, either the lower compartment or the upper compartment spray is sufficient to condense the break steam flow.

In conclusion, it is apparent that there is a substantial margin between the design deck leakage area and that, which can be tolerated without exceeding containment design pressure. This is true for both the original design deck leakage area of 5 sq. ft. and the current design deck leakage of 7 sq. ft.

### **14.3.4.1.3.1.1.f Effect of Dead-Ended Volumes**

In the preceding analysis of the containment compression ratio, it is conservatively assumed that only steam flows into the dead-ended volumes during the reactor coolant system blowdown. There are several dead-ended compartments in the plant containment design which are connected to the lower compartment. The dead-ended volumes considered in the containment integrity

## UFSAR Revision 30.0

 An AEP Company	<b>INDIANA MICHIGAN POWER</b> <b>D. C. COOK NUCLEAR PLANT</b> <b>UPDATED FINAL SAFETY ANALYSIS REPORT</b>	Revised: 29.0 Section:14.3.4.1 Page: 11 of 20
---	---	---

analysis are the instrumentation room and the pipe trench. Additional study has shown that the fan accumulator rooms would also act as dead-ended volumes. The storage of air in the dead-ended volumes has the effect of reducing the mass of air stored in the downstream volumes at the time of the compression peak pressure. Since including the dead-ended volumes reduces the calculated peak compression pressure, the results presented for the preceding analysis are conservative. It should be noted that the inclusion of the dead-ended volumes does not affect the magnitude of the second pressure peak, which occurs after the ice condenser has been exhausted, and after the dynamic effects of the blowdown have equalized throughout the containment. The second peak is controlling for plant design, therefore this discussion does not affect the available design margin.

The effect of the including the dead-ended volume was shown to decrease the final peak compression pressure by 0.2 psi. The magnitude of this effect was substantiated by a series of tests at Waltz Mill which were run at a mass compression ratio closely representative of the Cook plant design. Tests were run with and without a dead-ended volume equivalent to 155,000 ft<sup>3</sup> for the containment design. In these tests, the effect of the dead-ended volume was measured to be 0.5 psig, which is equivalent to a 0.32 psi decrease in final peak pressure per 100,000 ft<sup>3</sup> of dead-ended volume. At D.C. Cook, the dead-ended volume has been conservatively calculated to be 61,309 ft<sup>3</sup>.


### **14.3.4.1.3.1.2 Long Term Containment Pressure Analysis**

Early in the ice condenser development program it was recognized that there was a need for modeling of long term ice condenser containment performance. It was realized that the model would have to have capabilities comparable to those of the dry containment (COCO Code) model. These capabilities would permit the model to be used to solve problems of containment design and optimize the containment and safeguards systems. This has been accomplished in the development of the LOTIC Code. (Reference 1)

The model of the containment consists of five distinct control volumes, as follows: the upper compartment, the lower compartment, the portion of the ice bed from which the ice has melted, the portion of the ice bed containing unmelted ice, and the dead ended compartments. The ice condenser control volume with unmelted ice is further subdivided into six subcompartments to allow for maldistribution of break flow to the ice bed.

The conditions in these compartments are obtained as a function of time by the use of fundamental equations solved through numerical techniques. These equations are solved for three distinct phases in time. Each phase corresponds to a distinct physical characteristic of the

## UFSAR Revision 30.0

 An AEP Company	<p style="text-align: center;"><b>INDIANA MICHIGAN POWER</b> <b>D. C. COOK NUCLEAR PLANT</b> <b>UPDATED FINAL SAFETY ANALYSIS REPORT</b></p>	<p>Revised: 29.0 Section: 14.3.4.1 Page: 12 of 20</p>
---	--	---

problem. Each of these phases has a unique set of simplifying assumptions based on test results from the Waltz Mill ice condenser test facility. These phases are the blowdown period, the depressurization period, and the long term.

The most significant simplification of the problem is the assumption that the total pressure in the containment is uniform. This assumption is justified by the fact that after the initial blowdown of the Reactor Coolant System, the remaining mass and energy released from this system into the containment are small and very slowly changing. The resulting flow rates between the control volumes will also be relatively small. These small flow rates are unable to maintain significant pressure differences between the compartments.


In the control volumes, which are always assumed to be saturated, steam and air are assumed to be uniformly mixed and at the control volume temperature. The air is considered a perfect gas and the thermodynamic properties of steam are taken from the ASME steam tables.

### **14.3.4.1.3.1.3 Peak Containment Pressure Transient**

The following are the major input assumptions used in the LOTIC analysis for the limiting double-ended cold leg pipe rupture case with the steam generators considered as an active heat source for Donald C. Cook Unit 1 Containment:

1. Minimum safeguards are employed in all calculations, e.g., one of two spray pumps and one of two spray heat exchangers; one of two residual heat removal pumps and one of two residual heat removal heat exchangers with cross-tie valves open providing flow to the core; one of two safety injection pumps and one of two centrifugal charging pumps; and one of two air return fans.
2.  $2.2 \times 10^6$  pounds of ice initially in the ice condenser which is at 27°F. This temperature assumption maximizes the peak calculated pressure and corresponds to the 27°F Technical Specification limit.
3. The blowdown, reflood, and post reflood mass and energy releases described in Section 14.3.4.3 were used.
4. Blowdown and post blowdown ice condenser drain temperatures of 190°F and 130°F are used. (These numbers are based on Reference 2.)
5. Nitrogen from the accumulators in the amount of 4803 pounds is included in the calculations.


## UFSAR Revision 30.0

 <b>INDIANA MICHIGAN POWER</b> <small>An AEP Company</small>	<b>INDIANA MICHIGAN POWER D. C. COOK NUCLEAR PLANT UPDATED FINAL SAFETY ANALYSIS REPORT</b>	Revised: 29.0 Section:14.3.4.1 Page: 13 of 20
--	---	---

6. Essential service water temperature of 88.9°F is used for the spray heat exchanger and the component cooling heat exchanger.
7. The air return fan is effective 300 seconds accident initiation. This is conservative compared to the old value of 132 seconds.
8. No maldistribution of steam flow to the ice bed is assumed.
9. No ice condenser bypass is assumed. (This assumption depletes the ice in the shortest time and is thus conservative.)
10. The initial conditions in the containment are temperatures of 56°F in the upper, 60°F in the lower, 60°F in the dead ended and 27°F in the ice bed volumes. All volumes are at a pressure of 0.3 psig and 15 percent relative humidity, with the exception of the ice bed, which is at 100 percent relative humidity.
11. During the injection phase when the containment spray pumps are taking suction from the RWST, spray pump flow of 1960 gpm is used for the upper compartment and 706 gpm for the lower compartment. During the recirculation phase when the containment spray pumps are taking suction from the recirculation sump, containment spray flow to the upper compartment is 1960 gpm, containment spray flow to the lower compartment is 706 gpm.
12. Operators establish RHR spray no later than 70 minutes following the start of the accident, if the following conditions exist; 1) The Containment Spray System is in operation; 2) fewer than two (2) Containment Spray System (CTS) pumps are operating, and 3) the RHR system has been transferred to cold leg recirculation. The analysis uses the RHR spray flowrate of 1909 gpm.
13. Containment structural heat sink data are found in Table 14.3.4-4, and are assumed with conservatively low heat transfer coefficients, as listed in Table 14.3.4-5.
14. The operation of one containment spray heat exchanger ( $UA = 2.3 \times 10^6$  Btu/hr-°F) for containment cooling and the operation of one residual heat removal heat exchanger ( $UA = 2.2 \times 10^6$  Btu/hr-°F) for core cooling. The component cooling heat exchanger was modeled at  $3.433 \times 10^6$  Btu/hr-°F.
15. The air return fan returns air at a rate of 39,000 cfm from the upper to lower compartment.



## UFSAR Revision 30.0

 An AEP Company	<p style="text-align: center;"><b>INDIANA MICHIGAN POWER</b> <b>D. C. COOK NUCLEAR PLANT</b> <b>UPDATED FINAL SAFETY ANALYSIS REPORT</b></p>	<p>Revised: 29.0 Section: 14.3.4.1 Page: 14 of 20</p>
---	--	---

16. A containment sump volume of 72,000 ft<sup>3</sup> is used.
17. The refueling water storage tank is at a temperature of 105°F.
18. A core power of 3317 MWt (100.34% of 3306 MWt – conservative compared to licensed power of 3304 MWt) is used in the calculation (see section 14.3.4.1.1, item 3 of the accident input assumptions and conditions).
19. Credit is taken for cooling of the ECCS water from the RHR heat exchanger during the recirculation mode, starting with the time water is first drawn from the recirculation sump.
20. Essential service water flow to the containment spray heat exchanger was modeled as 2100 gpm. The essential service water flow to the component cooling heat exchanger was modeled as 5000 gpm.
21. The component cooling flow to the RHR heat exchanger was modeled as 5000 gpm.
22. The spurious operation of the upper containment ventilation heaters is included in the model as a 288 kW additional heat input.

With these assumptions, the heat removal capability of the containment is sufficient to absorb the energy releases and still keep the maximum calculated pressure well below design.

The following plots are provided:


- Figure 14.3.4-6, Containment pressure transient.
- Figure 14.3.4-7, Upper compartment temperature transients.
- Figure 14.3.4-8, Lower compartment temperature transients.
- Figure 14.3.4-9, Containment sump temperature transient.
- Figure 14.3.4-10, Ice melt transient.

In addition, Table 14.3.4-6 gives energy accountings at various points in the transient.

The analysis results show that the maximum calculated containment pressure is 10.10 psig, for the double-ended cold leg break minimum safeguards case. This pressure peak occurs at 10859 seconds, with ice bed meltout at 7713 seconds.

Non-condensable hydrogen gas is generated during the limiting design basis LOCA event (i.e. the double ended rupture of a cross-over leg), by several sources: hydrogen that is dissolved in

## UFSAR Revision 30.0

 An AEP Company	<p style="text-align: center;"><b>INDIANA MICHIGAN POWER</b> <b>D. C. COOK NUCLEAR PLANT</b> <b>UPDATED FINAL SAFETY ANALYSIS REPORT</b></p>	<p>Revised: 29.0 Section: 14.3.4.1 Page: 15 of 20</p>
---	--	---

the RCS, hydrogen generated by fuel clad oxidation, radiolysis in the core or by core material that has relocated to the containment sump, and hydrogen generated by corrosion of metal surfaces inside containment. The total hydrogen produced was calculated as a function of time, and the result used to calculate a partial pressure, which is then added to the peak containment pressure. The peak pressure was calculated to increase by 0.1 psig due to non-condensable hydrogen.

Following a LOCA event, the control room operators use the control air system to perform certain recovery and monitoring operations. Given the potential for in-leakage from this system into the containment, the partial pressure from this air must be considered in the peak pressure transient calculation. However, the timing of these remote manual recovery and monitoring operations is not explicitly modeled, so a time-dependent partial pressure transient has not been calculated. Instead, a portion of the containment pressure margin has been allotted to address this air. The control air system leakage will be limited by operator action, such that the effect on containment pressure will be less than 0.1 psi.


The ECCS pumps take suction from the RWST during the injection phase following a LOCA. As RWST volume is injected, the control room operator will transfer the ECCS pump suctions to the recirculation sump. During transfer to recirculation, the component cooling water flow to the RHR heat exchanger is increased. The evaluated impact of up to a 15-minute delay in the increase in CCW flow, during the transfer to recirculation, has an effect on the calculated containment peak pressure of less than 0.04 psi.

A failure of a flexible hose that connects the backup air supply bottles to the pressurizer power operated relief valves (PORVs) will discharge the contents of the air bottles to the containment. The partial pressure from this air must also be considered in the peak pressure transient calculation. The additional effect on containment pressure is calculated as 0.03 psi.

Chapter 5.5.3 describes the upper compartment ventilation units. Following a LOCA event, the spurious operation of the electric heaters in these units has been considered in the containment integrity analysis.

Therefore, when considering the calculated peak containment pressure for the design basis LOCA mass and energy release, including the contribution due to non-condensable hydrogen, control air system leakage, CCW flow during transfer to recirculation, and PORV backup air bottles, the total calculated peak containment pressure is 10.37 psig, which compares favorably to the containment design pressure of 12 psig.

## UFSAR Revision 30.0

 INDIANA MICHIGAN POWER An AEP Company	INDIANA MICHIGAN POWER D. C. COOK NUCLEAR PLANT UPDATED FINAL SAFETY ANALYSIS REPORT	Revised: 29.0 Section: 14.3.4.1 Page: 16 of 20
---	--	--

### **14.3.4.1.3.1.4 Structural Heat Removal**

Provision is made in the containment pressure analysis for heat storage in interior and exterior walls. Each wall is divided into a number of nodes. For each node, a conservation of energy equation expressed in finite difference form accounts for transient conduction into and out of the node and temperature rise of the node. Table 14.3.4-4 is a summary of the containment structural heat sinks used in the analysis. The material property data used are found in Table 14.3.4-5.

The heat transfer coefficient to the containment structures is based primarily on the work of Tagami. An explanation of the manner of application is given in Reference (4).


When applying the Tagami correlation, a conservative limit was placed on the lower compartment stagnant heat transfer coefficients. They were limited to 72 Btu/hr-ft<sup>2</sup>. This corresponds to a steam-air ratio of 1.4 according to the Tagami correlation. The imposition of this limitation is to restrict the use of the Tagami correlation within the test range of steam-air ratios where the correlation was derived.

### **14.3.4.1.3.1.5 Relevant Acceptance Criteria**

The LOCA mass and energy analysis has been performed in accordance with the criteria shown in the Standard Review Plan (SRP) section 6.2.1.3. In this analysis, the relevant requirements of General Design Criteria (GDC) 50 and 10 CFR Part 50 Appendix K have been included by confirmation that the calculated pressure is less than the design pressure, and because all available sources of energy have been included, which is more restrictive than the old GDC criteria, Appendix H of the original FSAR, to which the Donald C. Cook Plants are licensed. These sources include reactor power, decay heat, core stored energy, energy stored in the reactor vessel and internals, metal-water reaction energy, and stored energy in the secondary system.

Although the Donald C. Cook Nuclear Plant is not a Standard Review Plan plant, the containment integrity peak pressure analysis has been performed in accordance with the criteria shown in the SRP Section 6.2.1.1.b, for ice condenser containments. Conformance to GDC's 16, 38, and 50 is demonstrated by showing that the containment design pressure is not exceeded at any time in the transient. This analysis also demonstrates that the containment heat removal systems function to rapidly reduce the containment pressure and temperature in the event of a LOCA.

# UFSAR Revision 30.0

 <b>INDIANA MICHIGAN POWER</b> <small>An AEP Company</small>	<b>INDIANA MICHIGAN POWER D. C. COOK NUCLEAR PLANT UPDATED FINAL SAFETY ANALYSIS REPORT</b>	Revised: 29.0 Section: 14.3.4.1 Page: 17 of 20
--	---	--

## **14.3.4.1.3.1.6 Conclusions**

Based upon the information presented, taking into account modifications made to the containment and ECCS systems and related changes to the accident analysis input assumptions, it has been concluded that operation with the revised plant conditions and increased operating margins for the Donald C. Cook Nuclear Plant is acceptable. Operation with the RHR cross-tie valve open was modeled.

The peak containment pressure of 10.37 psig is below the design pressure 12.0 psig. Thus, the most limiting case has been considered, and has been demonstrated to yield acceptable results.

## **14.3.4.1.3.2 Steam Line Break**

Following a steam line break in the lower compartment of an ice condenser plant, two distinct analyses must be performed. The first analysis, the short term pressure analysis, has been performed with the TMD Code. The second analysis, the long term analysis, does not require the large number of nodes which the TMD analysis requires. The computer code which performs this analysis is the LOTIC (Reference 1) Code.


The LOTIC Code includes the capability to calculate the superheat conditions, and has the ability to begin calculations from time zero (References 6, 7, and 8). For all steam line breaks, no re-evaporation is assumed; however, convective heat transfer as detailed in Reference 7 is used. The version of the LOTIC Code that incorporates the above is the LOTIC3 Code (Reference 9). This code was used to perform the steam line break analyses and is the version which has been accepted for this use (References 10 and 11).

## **14.3.4.1.3.2.1 Peak Containment Temperature Transients**

The following are the major input assumptions used in the LOTIC3 steam break analysis:

1. Minimum safeguards are employed; e.g., one of two spray pumps and one of two air return fans.
2. The air return fan is effective 300 seconds after the high-1 containment pressure bistable signal is actuated.
3. A uniform distribution of steam flow into the ice bed is assumed.
4. The total initial ice mass is  $2.2 \times 10^6$  lbs.
5. The initial conditions in the containment are a temperature of 120°F in the lower and dead-ended volumes, a temperature of 57°F in the upper volume, and a temperature of 27°F in the ice condenser. All volumes are at a pressure of

## UFSAR Revision 30.0

 An AEP Company	<p style="text-align: center;"><b>INDIANA MICHIGAN POWER</b> <b>D. C. COOK NUCLEAR PLANT</b> <b>UPDATED FINAL SAFETY ANALYSIS REPORT</b></p>	<p>Revised: 29.0 Section: 14.3.4.1 Page: 18 of 20</p>
---	--	---

0.3 psig and a relative humidity of 15%, with the exception of the ice bed, which is at 100% relative humidity.


6. A spray pump flow of 1960 gpm is used in the upper compartment and 706 gpm in the lower compartment. The spray initiation time assumed was 315 sec. after reaching the high-high setpoint.
7. The refueling water storage tank temperature is assumed to be 105°F.
8. ESW is not assumed for the MSLB transient.
9. Containment structural heat sinks as presented in Table 14.3.4-4 were used.
10. The air return fan empties air at a rate of 39,000 cfm from the upper to the lower compartments.
11. The material property data given in Table 14.3.4-5 were used.
12. The mass and energy releases given in Tables 14.3.4-7 and 14.3.4-8 were used, reflecting limiting steam line breaks analyzed for the containment temperature response. Since these rates are considerably less than the RCS double-ended breaks, and their total integrated energy is not sufficient to cause ice bed meltout, the containment pressure transients generated for the previously presented double-ended pump suction RCS break is considerably more severe.
13. The heat transfer coefficients to the containment structures are based on the work of Tagami. An explanation of their manner of application is given in References 4, 6, and 7.
14. The spurious operation of the upper containment ventilation heaters is included in the model as a 288 kW additional heat input.

### **14.3.4.1.3.2.2 Results**

The results of the double-ended steam line break analysis are presented in Table 14.3.4-9. As indicated therein, peak containment temperature results for a number of the double-ended rupture steam line break cases are tightly grouped between 323.7°F and 324.5°F. A typical temperature transient is shown in Figure 14.3.4-11.

The results from the steam line split ruptures (or small breaks) are presented in Table 14.3.4-10. The worst case for these cases is a 0.865 ft<sup>2</sup> split break, occurring at a nominal NSSS power of 3327 MWt and with consideration for a full-power uncertainty of +0.34% and a main steam line

## UFSAR Revision 30.0

 An AEP Company	<p style="text-align: center;"><b>INDIANA MICHIGAN POWER</b> <b>D. C. COOK NUCLEAR PLANT</b> <b>UPDATED FINAL SAFETY ANALYSIS REPORT</b></p>	<p>Revised: 29.0 Section: 14.3.4.1 Page: 19 of 20</p>
---	--	---

isolation valve (MSIV) failure. A temperature transient of this case is presented in Figure 14.3.4-12.

Parametric studies have been performed as part of previous analyses, varying the ice mass between 2.0 and 2.45 million pounds. These previous ice mass parameter studies have shown that the maximum calculated containment temperatures is not sensitive (less than 1°F change) to ice mass over this range.

### **14.3.4.1.3.2.3 Sensitivity of the Results**

The previous section pertains to the steam line break analysis and its subsequent response in identifying the limiting small break. The following evaluation describes additional sensitivity studies of a generic nature, done for smaller breaks up to 0.942 ft<sup>2</sup> at 30% power.

The LOTIC-3 computer code was employed in the generic analysis (Reference 9). The LOTIC-3 computer code was found to be acceptable for the analysis of steam line breaks with the following restrictions (Reference 11):


- a. Mass and energy release rates are calculated with an approved model.
- b. Complete spectrum of breaks are analyzed.
- c. Convective heat flux calculations are performed for all break sizes.

A detailed comparison of the Cook Nuclear Plant characteristics with those of the generic plant can be found in Reference 13.

Figure 14.3.4-13 illustrates a comparison of small break cases, specifically 0.942 ft<sup>2</sup>, from Cook Nuclear Plant historical analyses with a similar break from the generic plant small break submittals. The figure shows that the elevated containment temperatures for Cook Nuclear Plant last for a shorter duration than predicted in the transient for the generic plant.

Further, the containment pressure High-2 setpoint, which provides the actuation signal for the containment spray and containment air recirculation fan systems was assumed to be 3.5 psig in the generic analysis. The Safety Analysis Limit (SAL) for the Cook Nuclear Plant High-1 and High 2 containment pressure setpoints are modeled to be 1.75 and 3.5 psig, respectively. In the Cook Nuclear Plant, the fans are started on High-1, and spray is started on High-2 containment pressure signals. Therefore, the actuation setpoint would have been reached sooner in the Cook Nuclear Plant compared to the generic plant, and therefore the containment transient would have been mitigated more rapidly.

## UFSAR Revision 30.0

 An AEP Company	<b>INDIANA MICHIGAN POWER</b> <b>D. C. COOK NUCLEAR PLANT</b> <b>UPDATED FINAL SAFETY ANALYSIS REPORT</b>	Revised: 29.0 Section:14.3.4.1 Page: 20 of 20
---	---	---

Therefore, a generic LOTIC3 spectrum of small breaks analysis is provided here for the Cook Nuclear Plant instead of plant specific analysis. The generic analysis provides the containment responses for a spectrum of small breaks at the 30% power level with assumed failure of the auxiliary feedwater runout protection system. The analyses studied a spectrum of breaks ranging in size from 0.1 ft<sup>2</sup> up to the break identified as the most severe small split break, 0.942 ft<sup>2</sup>. The lower bound break size was established in discussions held between the NRC staff and Westinghouse Electric Corporation.


This spectrum included breaks of 0.6, 0.35 and 0.10 ft<sup>2</sup>. Figures 14.3.4-14 and 14.3.4-15 provide the upper compartment temperature and lower compartment pressure transients. As Figure 14.3.4-16 shows, similar lower compartment temperature transients were calculated for the spectrum of breaks analyzed. However, the 0.6 ft<sup>2</sup> break resulted in a slightly higher maximum lower compartment temperature (see Table 14.3.4-11). When this transient was compared to the transient identified as the most severe small break at 30% power in the previous analysis, it was found to result in very similar peaks, with the difference being incidental to the results (See Figure 14.3.4-17).

In the generic analysis, spray and fan initiation are automatic after reaching the containment High-2 setpoint. Associated times are included in Table 14.3.4-11. As described above, these times are conservative in regard to the Cook Nuclear Plant, where the containment air recirculation fans are actuated by the High-1 containment pressure bistable signal. Tables 14.3.4-12 and 14.3.4-13 provide the mass and energy release rates for the transients analyzed. These results demonstrate the conservatism of the results previously discussed and also the somewhat insensitive nature of the ice condenser plant containment response to break size.


Table 14.3.4-14 further demonstrates the conservatism of the generic analysis discussed above. The actual plant specific analysis results for the smaller breaks would be similar to the Cook Nuclear Plant results in Figure 14.3.4-13. The temperature would peak, then sharply fall off when the sprays come on, and finally settle to a much lower temperature level for the remainder of the transient.



# UFSAR Revision 30.0

 An AEP Company	INDIANA MICHIGAN POWER D. C. COOK NUCLEAR PLANT UPDATED FINAL SAFETY ANALYSIS REPORT	Revised: 29.0 Section: 14.3.4.2 Page: i of i
---	--	--

<b>14.3 REACTOR COOLANT SYSTEM PIPE RUPTURE (LOSS OF COOLANT ACCIDENT)</b>	<b>1</b>
<b>14.3.4 Containment Integrity Analysis</b>	<b>1</b>
14.3.4.2 Containment Subcompartments	1
14.3.4.2.1 Design Basis	1
14.3.4.2.2 Design Features	1
14.3.4.2.3 Design Evaluation	2
14.3.4.2.3.1 Application to the Station Design	2
14.3.4.2.4 Steam Generator Enclosure Evaluation	4
14.3.4.2.5 Pressurizer Enclosure Evaluation	6
14.3.4.2.6 Fan Accumulator Room Evaluation	8
14.3.4.2.7 Loop Subcompartments Evaluation	10
14.3.4.2.7.1 Base Model Analysis	10
14.3.4.2.7.2 Current Analysis	11
Peak Differential Pressure	14
Peak Differential Pressure Between the Steam Generator Enclosure and the Ice Condenser	15
14.3.4.2.8 Reactor Cavity Evaluation	16
14.3.4.2.8.1 Upper Reactor Cavity	18
14.3.4.2.8.2 Lower Reactor Cavity	19
14.3.4.2.8.3 Reactor Vessel Annulus and Reactor Pipe Annulus	19
14.3.4.2.8.4 Reactor Vessel Nozzle Inspection Hatch Cover	20
14.3.4.2.9 Short Term Containment Analysis Conclusions	21

 An AEP Company	<p>INDIANA MICHIGAN POWER D. C. COOK NUCLEAR PLANT UPDATED FINAL SAFETY ANALYSIS REPORT</p>	<p>Revised: 29.0 Section: 14.3.4.2 Page: 1 of 21</p>
---	---	--

## **14.3 REACTOR COOLANT SYSTEM PIPE RUPTURE (LOSS OF COOLANT ACCIDENT)**

### **14.3.4 Containment Integrity Analysis**

#### **14.3.4.2 Containment Subcompartments**

The containment building sub compartments are the fully or partially enclosed volumes within the containment, which contain high-energy lines. These sub compartments are designed to limit the adverse effects of a postulated high-energy pipe rupture within them.

The short term mass and energy sub compartment analysis represents the initial seconds of the blowdown phase of the postulated rupture. The short-term analyses results are used in the design of the sub compartment walls in the ice condenser containment. The following results for short-term LOCA mass and energy releases and subsequent containment response has been validated for Unit 1 with the reactor internals converted to an upflow configuration.

##### **14.3.4.2.1 Design Basis**

Consideration is given in the design of the containment internal structures to localized pressure pulses that could occur following a postulated pipe break. If a pipe break accident were to occur due to a pipe rupture in these relatively small volumes, the pressure would build up at a rate faster than the overall containment, thus imposing a differential pressure across the walls of the structures.


These sub compartments include the steam generator enclosure, fan accumulator room, pressurizer enclosure, loop sub compartment and upper and lower reactor cavity. Each compartment is designed for the largest blowdown flow resulting from the severance of the largest connecting pipe within the enclosure or the blowdown flow into the enclosure from a break in an adjacent region.

The following sections summarize the design basis calculations.

##### **14.3.4.2.2 Design Features**

The basic performance of the Ice Condenser Reactor Containment System has been demonstrated for a wide range of conditions by the Waltz Mill Ice Condenser Test Program (Reference 2). These results have clearly shown the capability and reliability of the ice condenser concept to limit the containment pressure rise subsequent to a hypothetical loss-of-coolant accident.

To supplement this experimental proof of performance, a mathematical model has been developed to simulate the ice condenser pressure transients. This model, encoded as computer program TMD

 An <b>AEP</b> Company	<b>INDIANA MICHIGAN POWER</b> <b>D. C. COOK NUCLEAR PLANT</b> <b>UPDATED FINAL SAFETY ANALYSIS REPORT</b>	Revised: 29.0 Section: 14.3.4.2 Page: 2 of 21
--	---	---

(Transient Mass Distribution), provides a means for computing pressures, temperatures, heat transfer rates, and mass flow rates as a function of time and location throughout the containment. This model is used to compute pressure differences on various structures within the containment as well as the distribution of steam flow as the air is displaced from the lower compartment. Although the TMD Code can calculate the entire blowdown transient, the peak pressure differences on various structures occur within the first few seconds of the transient.

#### **14.3.4.2.3 Design Evaluation**

The mathematical modeling in TMD is similar to that of the SATAN blowdown code in that the analytical solution is developed by considering the conservation equations of mass, momentum, and energy and the equation of state, together with the control volume technique for simulating spatial variation. The governing equations for TMD are given in Reference (14).

The moisture entrainment modifications to the TMD Code are discussed in detail in Reference (14). These modifications comprise incorporating the additional entrainment effects into the momentum and energy equations.

As part of the review of the TMD Code, additional effects are considered. Changes to the analytical model required for these studies are described in Reference (14).


These studies consist of:

- a. Spatial acceleration effects in ice bed.
- b. Liquid entrainment in ice beds.
- c. Upper limit on sonic velocity.
- d. Variable ice bed loss coefficient.
- e. Variable door response.
- f. Wave propagation effects.

#### **14.3.4.2.3.1 Application to the Station Design**

The containment subcompartments include the steam generator enclosure, the pressurizer enclosure, the fan accumulator room, the loop subcompartment and the upper and lower reactor

# UFSAR Revision 30.0

 <b>INDIANA MICHIGAN POWER</b> <small>An AEP Company</small>	<b>INDIANA MICHIGAN POWER D. C. COOK NUCLEAR PLANT UPDATED FINAL SAFETY ANALYSIS REPORT</b>	Revised: 29.0 Section:14.3.4.2 Page: 3 of 21
--	---	--


cavity. Each of these containment subcompartments have been divided into nodes as shown on the following figures which represent the TMD nodalization model for each subcompartment.

- Figure 14.3.4-25 Steam Generator Enclosure
- Figure 14.3.4-27 Pressurizer Enclosure
- Figure 14.3.4-30 Fan Accumulator Room
- Figure 14.3.4-31 Loop Subcompartment
- Figure 14.3.4-34 Reactor Cavity

The TMD base model includes Nodes 1-45 as illustrated on Figures 14.3.4-18 through 14.3.4-21. The base model for the loop subcompartment, the steam generator enclosure and the pressurizer enclosure are identical. The fan accumulator room model is similar to the loop subcompartment model with one exception. In the loop subcompartment model, Node 27 represents one fan accumulator room. In the fan accumulator room model, the fan accumulator room is divided into five nodes based on the geometry of the subcompartment and internal equipment. These details are illustrated in Figures 14.3.4-28 and 14.3.4-29. The reactor cavity TMD model is significantly different than the 45 node TMD base model. The reactor cavity TMD model divides the reactor cavity area into 62 nodes, based on the geometry of the reactor cavity area. This basic geometry is shown on Figure 14.3.4-33. Figure 14.3.4-34 illustrates the complete nodalization network.

The division of the lower compartment into six volumes occurs at the points of greatest flow resistance, i.e., the four steam generators, pressurizer, and refueling cavity. Each of these lower compartment sections delivers flow through ice condenser lower inlet doors into a section behind the doors and below the ice bed. Each vertical section of the ice bed is, in turn, divided into nodes. The upper plenum between the top of the ice bed and the top deck doors is represented by another node. Thus, a total of thirty nodes (Nodes 7 through 24 and 34 through 45) are used to simulate the ice condenser. The nodes at the top of the ice bed between the ice bed and top deck doors deliver to Node 25, the upper compartment. Note that cross flow in the ice bed is not accounted for in the analysis; this yields the most conservative results for the particular calculations described herein. The upper reactor cavity (Node 33) is connected to the lower compartment volumes and provides cross flow for pressure equalization of the lower compartments. The less active compartments, called dead ended compartments (Nodes 26, 28, 29, 30 and 32), and the fan accumulator compartments (Nodes 27 and 31) outside the crane wall are pressurized by ventilation openings through the crane wall into the fan compartments.

## UFSAR Revision 30.0


 An AEP Company	<b>INDIANA MICHIGAN POWER</b> <b>D. C. COOK NUCLEAR PLANT</b> <b>UPDATED FINAL SAFETY ANALYSIS REPORT</b>	Revised: 29.0 Section: 14.3.4.2 Page: 4 of 21
---	---	---

For each node in the TMD network the volume (refer to Tables 14.3.4-21 through 14.3.4-25), initial pressure, and initial temperature conditions are specified. The ice condenser elements have additional inputs of mass of ice, heat transfer area, and condensate layer length. The required flow characteristics for each flow path between nodes are: loss coefficient ( $K$ ), friction factor ( $f$ ), inertia length ( $L_I$ ), hydraulic diameter ( $D_H$ ), minimum flow path area ( $A_T$ ), equivalent length ( $L_E$ ) and area ratios ( $A_T/A$ ). In the TMD analysis, the loss coefficient ( $K$ ) is used to calculate the pressure losses due to flow across equipment, projections, or sudden expansions and contractions. The  $fL_E/D_H$  term is used to calculate the frictional pressure loss.  $A_T$  is the minimum flow area for the path. The  $L_I/A_T$  term is used to account for inertia effects of the fluid in the momentum equation. The area ratios ( $A_T/A$ ) are used to account for compressibility effects of the fluid. In addition, the ice condenser loss coefficients have been based on the 1/4 scale tests representative of the current ice condenser geometry. The loss coefficient is based on removal of door port flow restrictors. To better represent short term transient effects, the opening characteristics of the lower, intermediate, and top deck ice condenser doors have also been modeled in the TMD Code. The TMD analysis evaluates a range of containment parameters for subcompartment peak pressure and differential pressures. These parameters include containment pressure, containment temperature, containment humidity, and ice condenser temperature. The bounding conditions are listed in each subcompartment evaluation that are described in the following sections.

### **14.3.4.2.4 Steam Generator Enclosure Evaluation**

Two breaks were analyzed for the steam generator enclosure, a main steam line break and a feedwater line break. The largest and most severe break possible in the steam generator enclosure is a double-ended break of the steam line. Based upon the high-energy line break analyses, this break can only occur in the enclosure at the terminal end at the nozzle (at the top of the enclosure). For the feedwater line break event, the break is postulated to occur at the side of the steam generator at the feedwater line inlet nozzle. The limiting mass and energy releases from these breaks are from the hot shutdown condition (no load). Refer to Section 14.3.4.4.1 for the initial conditions and assumptions used to determine the short-term mass and energy releases for the steam line and feedwater line breaks. The mass and energy release rates for the steam generator enclosure analysis are presented in Table 14.3.4-15 for both the main steam line break and the feedwater line break.

## UFSAR Revision 30.0

 An <b>AEP</b> Company	<b>INDIANA MICHIGAN POWER</b> <b>D. C. COOK NUCLEAR PLANT</b> <b>UPDATED FINAL SAFETY ANALYSIS REPORT</b>	Revised: 29.0 Section: 14.3.4.2 Page: 5 of 21
--	---	---

The range of initial containment conditions considered for the analyses are as follows:

- Temperature range of 60-185°F (Reference 45)
- Pressure range of 13.2-15.0 psia
- Humidity range of 15-100 percent
- Ice Condenser Temperature range of 10-30°F

The limiting values for containment temperature and pressure are given in Tables 14.3.4-33 and 14.3.4-34. For all cases, the limiting condition for humidity is at 15%. For the steam line break, the limiting ice condenser temperature is 30°F and for the feedwater line break the limiting values are presented in Table 14.3.4-34. In addition, the jet momentum from the steam blowdown from the main steam or feedwater line break within the steam generator enclosure would be large enough to blow the HVAC ductwork out the enclosures.


The steam generator enclosure TMD nodalization network is similar to the models for the pressurizer enclosure and the loop subcompartment for the first 45 nodes. Nodes 46-63 represent the steam generator enclosures. The nodalization network for the steam generator enclosures are illustrated in Figures 14.3.4-18 through 14.3.4-21 and Figures 14.3.4-24 and 14.3.4-25. Figure 14.3.4-18 illustrates the TMD model plan view at the equipment room elevation. Figure 14.3.4-19 provides the TMD model containment section view. Figure 14.3.4-20 is the plan view at the ice condenser compartments. Figure 14.3.4-21 contains the layout of the containment shell for the TMD model. Figures 14.3.4-22 and 14.3.4-23 show the details of the steam generator subcompartment used in the analysis. Figures 14.3.4-24 and 14.3.4-25 show the 18 node TMD steam generator enclosure model (9 nodes per enclosure) which was used in the analytical model.

This TMD model is designed to represent a steam generator pair as denoted in Figure 14.3.4-25 as Enclosure A and Enclosure B. The steam line break was postulated to occur in the steam generator enclosure in either Node 46 or 55. The feedwater line break was postulated to occur in the steam generator enclosure in either Node 54 or 63.

The TMD input flow path characteristics are based upon incompressible flow modeling. The TMD program adjusts the incompressible flow equations with the area ratios ( $A_T/A$ ) to account for compressible effects in the high subsonic flow regime. The TMD flow path input data for the steam generator enclosure is contained in Tables 14.3.4-26 and 14.3.4-27.

The steam generator enclosure free volumes and vent areas, which represent Enclosure A, and Enclosure B are given in Table 14.3.4-32. As shown in Table 14.3.4-32, the free volume and vent

## UFSAR Revision 30.0

 <b>INDIANA MICHIGAN POWER</b> <small>An AEP Company</small>	<b>INDIANA MICHIGAN POWER D. C. COOK NUCLEAR PLANT UPDATED FINAL SAFETY ANALYSIS REPORT</b>	Revised: 29.0 Section: 14.3.4.2 Page: 6 of 21
--	---	---

area for the steam generator pair is not identical. The vent area represents the minimum flow path area leaving the steam generator enclosure. The vent area for the steam generator enclosure (Enclosure A) is determined by summing the minimum flow path areas from Nodes 46-47, 48, 49, 50, 55, 47-56, 48-57, 47-51, 48-52, 49-53 and 50-54. The vent area for Enclosure B is determined in a similar fashion.

The maximum calculated differential pressure between the steam generator enclosure and the upper compartment due to a postulated steam line break is 42.77 psid (Reference 45). The maximum calculated differential pressure between the steam generator enclosure and the upper compartment due to a postulated feedwater line break is 16.29 psid. A complete summary of the peak differential pressures across the structures and the steam generator vessel are shown in Table 14.3.4-33 for the steam line break and Table 14.3.4-34 for the feedwater line break. Figures 14.3.4-35 through 14.3.4-52 present the differential pressure time histories for the steam line break. The Steam Line Break (SLB) Figures are for information only, and have not been updated to reflect results of Reference 45, and should not be used as input in other analyses. Figures 14.3.4-53 through 14.3.4-70 present the differential time histories for the feedwater line break.

It should be noted that the analyses discussed above are only for short term pressure peaks and are not applicable to long term type analyses. The dynamic analysis of the affected structures and of the steam generator vessel supports has shown that the effects of the short duration peak pressures will not result in consequences that will adversely affect the public health and safety.


### **14.3.4.2.5 Pressurizer Enclosure Evaluation**

The largest break possible in the pressurizer enclosure, a double-ended break of the spray line from the reactor coolant system, is postulated to occur at the top of the enclosure. The spray line break mass and energy releases are presented in Table 14.3.4-16. The RCS data utilized for the analysis is as follows:

- |                                      |               |
|--------------------------------------|---------------|
| • NSSS Power (MWt)                   | 3600          |
| • RCS Pressure (psia)                | 2250          |
| • Core Average Temperature (°F)      | 549.9 - 584.9 |
| • Vessel Outlet Temperature (°F)     | 582.2 - 615.2 |
| • Vessel/Core Inlet Temperature (°F) | 511.7 - 547.6 |



## UFSAR Revision 30.0

 An <b>AEP</b> Company	<b>INDIANA MICHIGAN POWER</b> <b>D. C. COOK NUCLEAR PLANT</b> <b>UPDATED FINAL SAFETY ANALYSIS REPORT</b>	Revised: 29.0 Section: 14.3.4.2 Page: 7 of 21
--	---	---

Measurement uncertainties of +67 psi for system pressure and  $\pm 5.1^{\circ}\text{F}$  for temperature are applied to the RCS data. The spray line mass and energy releases were determined utilizing the following bounding RCS initial conditions:

- Vessel/Core Inlet Temperature of  $506.6^{\circ}\text{F}$
- RCS Pressure of 2317 psia

The range of initial containment conditions bounded by the TMD analysis for the pressurizer enclosure includes the following:


- Temperature range of  $60\text{-}171^{\circ}\text{F}$
- Pressure range of 13.2-15.0 psia
- Humidity range of 15-100 percent
- Ice Condenser Temperature range of  $10\text{-}30^{\circ}\text{F}$

The low pressure (13.2 psia), low temperature ( $60^{\circ}\text{F}$ ), low humidity (15%) case was determined to be bounding for evaluation of the pressurizer enclosure and containment response. Sensitivity studies were performed to evaluate the effect of varying the ice condenser temperature on the peak differential pressure. The analysis for the pressurizer enclosure was performed using an ice condenser temperature of  $30^{\circ}\text{F}$ . Using an ice condenser temperature of  $10^{\circ}\text{F}$  will increase the resulting peak differential pressure acting across the wall between the inside of the enclosure and the upper compartment. This increase is bounded by the margin currently applied to the pressurizer enclosure analysis.

The loop subcompartment model (without the nodalization for the steam generator enclosures) was used as a base model for the pressurizer enclosure. The loop subcompartment model was modified to include Nodes 46-49 which represent the pressurizer enclosure in the model.

The pressurizer enclosure TMD nodalization network is similar to the models for the loop subcompartment and the steam generator enclosure for the first 45 nodes. Nodes 46-49 represents the pressurizer enclosure in the model. The nodalization network for the pressurizer enclosure is illustrated in Figures 14.3.4-18 through 14.3.4-21 and Figure 14.3.4-27. Figure 14.3.4-18 illustrates the TMD model plan view at the equipment room elevation. Figure 14.3.4-19 provides the TMD model containment section view. Figure 14.3.4-20 is the plan view at the ice condenser compartments. Figure 14.3.4-21 contains the layout of the containment shell for the TMD model. Figure 14.3.4-26 illustrates the nodalization specific to the pressurizer enclosure and Figure 14.3.4-

# UFSAR Revision 30.0

 An AEP Company	<b>INDIANA MICHIGAN POWER</b> <b>D. C. COOK NUCLEAR PLANT</b> <b>UPDATED FINAL SAFETY ANALYSIS REPORT</b>	Revised: 29.0 Section: 14.3.4.2 Page: 8 of 21
---	---	---

27 illustrates the nodalization network and flow paths. The spray line break was postulated to occur at the top of the pressurizer enclosure in Node 46.

The TMD input flow path characteristics are based upon incompressible flow modeling. The TMD program adjusts the incompressible flow equations with the area ratios ( $A_T/A$ ) to account for compressible effects in the high subsonic flow regime. The TMD flow path input data for the pressurizer enclosure is contained in Table 14.3.4-28. Refer to Section 14.3.4.2.3.1 for definition of table terms.

The net free volume and the vent area for the pressurizer enclosure is presented in Table 14.3.4-32. The vent area represents the minimum flow path area leaving the pressurizer enclosure. The vent area for the pressurizer enclosure is determined by summing the minimum flow path areas from Nodes 47-4, 48-4 and 49-4.


Figures 14.3.4-71 through 14.3.4-75 illustrate the pressure time histories for the upper compartment and the pressurizer enclosure. The maximum calculated differential pressure is 8.82 psid. The maximum calculated differential pressure across the vessel is 0.45 psid. An additional 10% margin is included in the results to bound the results and provide conservatism.

## **14.3.4.2.6 Fan Accumulator Room Evaluation**

The fan accumulator room enclosure is designed for a double-ended break in the 30 inch steam line (inside area of 4.27 ft<sup>2</sup>) downstream of the steam line flow restrictor. This is the inline flow venturi downstream of the steam generator nozzle. The break occurs in the longest line with an orifice of 1.4 ft<sup>2</sup> in the cross connection with the steam dump header. This orifice in the turbine building restricts backflow so that the entrained flow from the other three steam generators will not reach the break before the main steam isolation valves close at ten seconds, reducing the pressure peak. The mass and energy release rates for this case are presented in Table 14.3.4-17.

The mass and energy releases consist of both the initial steam blowdown from the steam generator side of the break (forward flow) with choking conditions reached in the inline flow venturi and the reverse flow (steam flow coming out of the turbine end of the break). The blowdown consists of steam at 1192 BTU/lb, which corresponds to the saturation enthalpy at 1020 psia. The TMD computer code assuming unaugmented critical flow was used to calculate the pressurization

## UFSAR Revision 30.0

 An AEP Company	<b>INDIANA MICHIGAN POWER</b> <b>D. C. COOK NUCLEAR PLANT</b> <b>UPDATED FINAL SAFETY ANALYSIS REPORT</b>	Revised: 29.0 Section: 14.3.4.2 Page: 9 of 21
---	---	---

response inside the fan accumulator room to the postulated break in the main steam line. The range of initial containment conditions considered for the analysis are as follows:

- Temperature range of 60-120°F
- Pressure range of 13.2-15.0 psia
- Humidity range of 15-100 percent
- Ice Condenser Temperature range of 10-30°F

The low pressure (13.2 psia), low temperature (60°F), low humidity (15%), low ice condenser temperature (10°F) case was determined to be bounding for determination of the peak differential pressure. High pressure (15.0 psia), low temperature (60°F), low humidity (15%), high ice condenser temperature (30°F) case was determined to be bounding for the determination of the peak pressure in the fan accumulator room.


The nodalization network for the fan accumulator room is illustrated in Figures 14.3.4-19, 14.3.4-20 and 14.3.4-28 through 14.3.4-30. Figure 14.3.4-28 illustrates the TMD model plan view at the equipment room elevation. Figure 14.3.4-19 provides the TMD model containment section view. Figure 14.3.4-20 is the plan view at the ice condenser compartments. Figure 14.3.4-29 contains the layout of the containment shell for the TMD model. Figures 14.3.4-22 illustrate the noding, flow paths and TMD network for the fan accumulator room subcompartment. Nodes 27, 31 and 54-57, as shown on Figure 14.3.4-28, represent the fan accumulator rooms in the TMD model. The steam line break was postulated to occur in the fan room in Node 55.

The TMD input flow path characteristics are based upon incompressible flow modeling. The TMD program adjusts the incompressible flow equations with the area ratios ( $A_T/A$ ) to account for compressible effects in the high subsonic flow regime. The TMD flow path input data for the fan accumulator room is contained in Table 14.3.4-29.

The fan accumulator room free volume and vent area are presented in Table 14.3.4-32. The vent area is determined by summing the flow areas leaving the fan accumulator room subcompartment (Nodes 27-3, 28, 29, 54-3, 28, 55-2, 26, 28, 56-1, 26 and 57-1, 26).

Figures 14.3.4-76 through 14.3.4-97 illustrate the pressure time histories for the peak differential pressure across the key internal structures and walls of the fan accumulator room. Figures 14.3.4-98 through 14.3.4-102 illustrate the pressure time histories for the peak pressure in the fan accumulator room. The calculated peak pressure in the fan accumulator room is 15.40 psig. The peak calculated differential pressure between the fan accumulator room and the ice condenser

# UFSAR Revision 30.0

 An AEP Company	<b>INDIANA MICHIGAN POWER</b> <b>D. C. COOK NUCLEAR PLANT</b> <b>UPDATED FINAL SAFETY ANALYSIS REPORT</b>	Revised: 29.0 Section:14.3.4.2 Page: 10 of 21
---	---	---

lower plenum is 15.69 psid, between the adjoining instrument room is 15.20 psid and between the upper compartment is 13.00 psid.

## **14.3.4.2.7 Loop Subcompartments Evaluation**

### **14.3.4.2.7.1 Base Model Analysis**

As part of the  $T_{hot}$  Reduction Program in the late 1980's, the mass and energy releases for the DEHL and DECL breaks were recalculated. Results showed that the peak rates increased by approximately 10% and 20% for the DECL and DEHL cases respectively when compared to the original analysis. The results of this analysis are shown in the following table:

	<b>Peak Differential Pressure</b>			
Item	DP [1-25] DP [6-25]	DP [2-25] DP [5-25]	DP (7,8,9 TO 25)	Shell Peak Pressure (40, 45)
1988 Base <sup>1</sup>	16.8 psid	12.2 psid	10.7 psid	13.1 psig
1988 Total <sup>2</sup>	18.7 psid	13.0 psid.	11.2 psid	14.0 psig


Figures 14.3.4-103 through 14.3.4-110 present the pressure time histories for the lower compartment elements (1-6), the upper compartment (25) and element 40 on the shell for the DEHL break in compartment 1 case. Figures 14.3.4-111 and 14.3.4-112 present the pressure time histories for element 2 and element 25 for the DEHL in compartment 2 case. Figure 14.3.4-113 present the pressure time history for element 40 on the shell for the DECL case.

---

<sup>1</sup> 1988 Base refers to the TMD analysis conducted in 1988 that formed the basis for the  $T_{hot}$  Reduction Program results in 1988. This item is called “base” because these are the raw results from the TMD computer runs. This information does not include effects of 15% flow blockage, variation in initial subcompartment pressure and temperature, and uncertainty.

<sup>2</sup> 1988 Total refers to the total pressure results that were generated for the  $T_{hot}$  Reduction Program in 1988. This item includes the raw results from the TMD computer runs (1988 Base), and the effects of 15% flow blockage, variation in initial subcompartment pressure and temperature, and uncertainty.

## UFSAR Revision 30.0

 An <b>AEP</b> Company	<b>INDIANA MICHIGAN POWER</b> <b>D. C. COOK NUCLEAR PLANT</b> <b>UPDATED FINAL SAFETY ANALYSIS REPORT</b>	Revised: 29.0 Section: 14.3.4.2 Page: 11 of 21
--	---	--

These results were used as a starting point for the current analysis. The current analysis for the loop sub compartment utilizes adders and scaling factors to account for changes in initial RCS conditions and uncertainties and as-built data for the compartment.

### **14.3.4.2.7.2 Current Analysis**

The current methodology is an evaluation that includes a representative TMD run that is used to determine the impact of geometric changes associated with as-built plant subcompartment information on past loop sub compartment analysis results. The results from the TMD run was used to scale prior results to include as-built effects.

The loop sub compartment, including the lower crane wall, upper crane wall, containment shell and operating deck are designed to withstand the pressures which are due to a postulated double-ended primary loop break in the loop sub compartments. The TMD computer code assuming unaugmented critical flow was used to calculate the pressurization response inside the loop sub compartments. Both the DEHL and DECL breaks were evaluated for development of differential pressures. The double-ended cold leg break (DECL) results from previous analysis is augmented by the results of the DEHL break to account for changes in TMD input due to as-built plant data.


Mass and energy releases were developed for a double-ended hot leg break (DEHL) and are presented in Table 14.3.4-18. SATAN-V models, consistent with the methodology of reference (21), were developed utilizing the appropriate RCS data, such as enthalpies, pressures and flows. The RCS data utilized for the analysis is as follows:

- |                                      |               |
|--------------------------------------|---------------|
| • NSSS Power (MWt)                   | 3600          |
| • RCS Pressure (psia)                | 2250          |
| • Core Average Temperature (°F)      | 549.9 - 584.9 |
| • Vessel Outlet Temperature (°F)     | 582.2 - 615.2 |
| • Vessel/Core Inlet Temperature (°F) | 511.7 - 547.6 |

Measurement uncertainties of +67 psi for system pressure and +/-5.1°F for temperature are applied to the RCS data. For the short term mass and energy releases, low RCS temperatures and high pressure are bounding. The bounding RCS initial conditions are as noted below.

- Vessel/Core Inlet Temperature of 506.6°F
- RCS Pressure of 2317 psia

## UFSAR Revision 30.0

 An <b>AEP</b> Company	<b>INDIANA MICHIGAN POWER</b> <b>D. C. COOK NUCLEAR PLANT</b> <b>UPDATED FINAL SAFETY ANALYSIS REPORT</b>	Revised: 29.0 Section:14.3.4.2 Page: 12 of 21
--	---	---

The initial containment conditions bounded by the TMD analysis includes the following:

- Temperature range of 60-120°F
- Pressure range of 13.2-15.0 psia
- Humidity range of 15-100 percent
- Ice Condenser Temperature range of 10-30°F


The bounding initial conditions utilized in the analysis for the loop subcompartment are as follows:

- Initial pressure of 15.0 psia
- Lower compartment temperature of 110°F
- Ice condenser temperature of 30°F
- Upper compartment temperature of 75°F
- Fan accumulator/pipe trench temperature of 98°F
- Upper reactor cavity temperature of 110°F
- Steam generator enclosure temperature of 110°F
- Humidity of 15%

Sensitivity studies were performed to evaluate the effect of varying the ice condenser temperature on the peak differential pressure. The analysis for the loop subcompartment was performed using an ice condenser temperature of 30°F. Using an ice condenser temperature of 10°F will increase the resulting peak differential pressures. These increases are bounded by the margins currently applied to the loop subcompartment analysis. Additionally, included in the evaluation of the loop subcompartment is consideration of 15% ice condenser flow blockage and the effects of both DEHL and DECL break locations.

The loop subcompartment TMD nodalization network is similar to the models for the pressurizer enclosure and the steam generator enclosure for the first 45 nodes. Nodes 46-53, which are specific for the loop subcompartment model, represent the steam generator enclosures. The nodalization network for the loop subcompartment is illustrated in Figures 14.3.4-18 through 14.3.4-21 and Figure 14.3.4-31. Figure 14.3.4-18 illustrates the TMD model plan view at the equipment room elevation. Figure 14.3.4-19 provides the TMD model containment section view. Figure 14.3.4-20 is the plan view at the ice condenser compartments. Figure 14.3.4-21 contains the layout of the containment shell for the TMD model. Figure 14.3.4-31 illustrates the specific nodalization

## UFSAR Revision 30.0

 <b>INDIANA MICHIGAN POWER</b> <small>An AEP Company</small>	<b>INDIANA MICHIGAN POWER D. C. COOK NUCLEAR PLANT UPDATED FINAL SAFETY ANALYSIS REPORT</b>	Revised: 29.0 Section:14.3.4.2 Page: 13 of 21
--	---	---


network for the loop subcompartment. Contained within this figure are the flow paths from the loop subcompartment.

The TMD input flow path characteristics are based upon incompressible flow modeling. The TMD program adjusts the incompressible flow equations with the area ratios ( $A_T/A$ ) to account for compressible effects in the high subsonic flow regime. The TMD flow path input data for the loop subcompartment is contained in Table 14.3.4-30. Refer to Section 14.3.4.2.3.1 for definition of table terms.

The DEHL in Node 1 was determined to be the limiting break for determination of peak differential pressure across the operating deck, across the lower and upper crane wall, the ice condenser ice basket uplift force and lattice frame forces and the intermediate and top deck drag forces. The DECL break in Node 1 was determined to be limiting for the differential pressure across the containment shell. Pressure time history plots are included as Figures 14.3.4-114 through 14.3.4-122 for the loop subcompartment analysis.



## UFSAR Revision 30.0

 An <b>AEP</b> Company	<b>INDIANA MICHIGAN POWER</b> <b>D. C. COOK NUCLEAR PLANT</b> <b>UPDATED FINAL SAFETY ANALYSIS REPORT</b>	Revised: 29.0 Section:14.3.4.2 Page: 14 of 21
--	---	---

The following tables provide the peak differential across the operating deck, upper and lower crane wall, containment shell and the peak differential pressure between the steam generator enclosure and the ice condenser.

<b><u>Peak Differential Pressure</u></b>				
Item	DP [1-25] DP [6-25]	DP [2-25] DP [5-25]	DP (7,8,9 TO 25)	Shell Peak Pressure (40, 45)
Original base <sup>3</sup>	14.1 psid	10.6 psid	8.2 psid	10.8 psig
2001 Base <sup>4</sup>	18.2 psid	12.2 psid	10.7 psid	13.1 psig
2001 Total <sup>5</sup>	20.2 psid	14.0 psid	11.8 psid	14.8 psig


---

<sup>3</sup> Original Base refers to the TMD analysis conducted in 1974. This item is called “base” because these are the raw results from the TMD computer runs. This information does not include effects of 15% flow blockage, variation in initial subcompartment pressure and temperature, and uncertainty.

<sup>4</sup> 2001 Base refers to the TMD analysis & evaluation conducted in 2001 that formed the basis for the results. This item is called “base” because these are the raw results from the base TMD run. This information does not include effects of 15% flow blockage, variation in initial subcompartment pressure and temperature, and uncertainty.

<sup>5</sup> 2001 Total refers to the total pressure results that were generated for the analysis and evaluation program in conducted 2001. This item includes the raw results from the TMD computer runs (2001 Base), and the effects of 15% flow blockage, variation in initial subcompartment pressure and temperature, and uncertainty.

## UFSAR Revision 30.0


 An AEP Company	<b>INDIANA MICHIGAN POWER</b> <b>D. C. COOK NUCLEAR PLANT</b> <b>UPDATED FINAL SAFETY ANALYSIS REPORT</b>	Revised: 29.0 Section:14.3.4.2 Page: 15 of 21
---	---	---

<b><u>Peak Differential Pressure Between the Steam Generator Enclosure and the Ice Condenser</u></b>				
Item	DP [46-41]	Time	DP [50-10,11,12]	Time
2001 Base <sup>4</sup>	9.42 psid	0.0621 s	10.03 psid	0.3624 s
2001Total <sup>5</sup>	11.36 psid	0.0621 s	11.97 psid	0.3624 s

In addition to the results provided above, the vertical distribution of peak differential pressure for the ice condenser end wall for the lower plenum is 14.8 psid and 11.8 / 9.2 / 7.4 psid for the bottom/middle/top 16 feet of the ice bed region, respectively. The azimuthal distribution of peak differential pressure for the ice condenser is presented in Table 14.3.4-35. The loop subcompartment analysis also generates the peak blowdown differential pressure across the ice condenser lower plenum floor and horizontal seal acting downward. The peak differential pressure was calculated to be 10.4 psid. Pressure time history plots which can be used for the ice condenser lower plenum and for the fan accumulator room are contained in Figures 14.3.4-121 and 14.3.4-122, respectively.

Early sensitivity studies, illustrated in Table 14.3.4-36 (see Section 14.3.4.5.3.4, "Early Sensitivity Studies"), demonstrated the effects of changes in certain variables on the operating deck differential pressure and the shell pressure. The purpose of that study was to illustrate the sensitivity of the TMD code results to different input and assumption conditions and to illustrate the inherent analysis conservatism. The purpose of the tables was not to supply an extrapolation tool for all subcompartments since the work was done for a specific subcompartment and trends may be different for other compartments. For example, the effect of initial compartment pressure on the peak differential pressure can be either a benefit or a penalty depending upon the flow regime before and during the peak. Additionally, if the peak occurs later in time the trend will be geometry dependent. That is, the pertinent downstream element would pressurize differently based upon specific key variables, such as flow areas and resistance into and out of the element. A combination of both sonic and subsonic flow regime periods could occur over the total transient. Since the new analysis is sufficiently different when compared to the original sensitivity basis, Table 14.3.4-36 should only be used for guidance.

# UFSAR Revision 30.0

 <b>INDIANA MICHIGAN POWER</b> <small>An AEP Company</small>	<b>INDIANA MICHIGAN POWER D. C. COOK NUCLEAR PLANT UPDATED FINAL SAFETY ANALYSIS REPORT</b>	Revised: 29.0 Section:14.3.4.2 Page: 16 of 21
--	---	---

## **14.3.4.2.8 Reactor Cavity Evaluation**

The reactor cavity is designed for a single ended break of an RCS loop at its connection to the reactor vessel nozzle. The break is considered to be a longitudinal split in the loop piping at the primary shield wall of an area equivalent to the cross sectional area of a reactor coolant pipe, i.e. 4.12 ft<sup>2</sup>. A circumferential failure of the pipe at this location would result in a much smaller flow discharge area because the vessel, pipe and sleeve arrangement is such that no significant relative movement can take place.

The purpose of this analysis is to calculate the initial pressure response in the reactor cavity to a loss of coolant accident. The reactor cavity pressure analysis was performed for the upper and lower reactor cavities, the reactor vessel annulus and the reactor pipe annulus. The mass and energy releases for the analysis is presented in Table 14.3.4-19 for the single-ended cold leg break (SECL) and Table 14.3.4-20 for the single-ended hot leg break (SEHL). The RCS data utilized for the analysis is as follows:

- |                                      |               |
|--------------------------------------|---------------|
| • NSSS Power (MWt)                   | 3600          |
| • RCS Pressure (psia)                | 2250          |
| • Core Average Temperature (°F)      | 549.9 - 584.9 |
| • Vessel Outlet Temperature (°F)     | 582.2 - 615.2 |
| • Vessel/Core Inlet Temperature (°F) | 511.7 - 547.6 |


Measurement uncertainties of +67 psi for system pressure and +/-5.1°F for temperature are applied to the RCS data. The mass and energy releases were determined utilizing the following bounding RCS initial conditions.

- Vessel/Core Inlet Temperature of 506.6°F
- RCS Pressure of 2317 psia

In this evaluation, the effect of the following initial containment conditions was also assessed:

- Temperature range of 60-160°F in the loop subcompartments.
- Temperature range of 60-120°F in the upper and lower reactor cavities.
- Pressure range of 13.2-15.0 psia.
- Humidity range of 15-100 percent.

## UFSAR Revision 30.0

 An <b>AEP</b> Company	<b>INDIANA MICHIGAN POWER</b> <b>D. C. COOK NUCLEAR PLANT</b> <b>UPDATED FINAL SAFETY ANALYSIS REPORT</b>	Revised: 29.0 Section: 14.3.4.2 Page: 17 of 21
--	---	--

The effects of the ice condenser are conservatively neglected in this analysis. Various assumptions concerning reactor cavity insulation and HVAC ductwork are included in the analysis for the reactor cavity. Due to the blowdown forces associated with the break, the insulation on the broken loop pipe was assumed to be displaced outward through the penetration in the primary shield wall. The insulation on the reactor vessel wall will either be crushed or displaced from the reactor vessel region. The HVAC ductwork in the upper reactor cavity is assumed to collapse and the HVAC ductwork in the windows at the top of the biological shield will be crushed and displaced into the loop compartment. In addition, three inspection hatch covers furthest from the break location are assumed to be held closed. This is represented by the flow paths from Nodes 41, 42 and 43 to Node 38.

As described previously, the reactor cavity TMD model is significantly different than the TMD model for the other containment subcompartments. The reactor cavity TMD model nodalization is illustrated in Figures 14.3.4-32, 14.3.4-33 and 14.3.4-34. Figure 14.3.4-32 shows the reactor cavity TMD model containment section view. Figure 14.3.4-33 illustrates the reactor cavity TMD model layout of reactor vessel annulus elements and Figure 14.3.4-34 illustrates the reactor cavity TMD model nodalization network. The break is postulated to occur in Node 1.


The TMD input flow path characteristics are based upon incompressible flow modeling. The TMD program adjusts the incompressible flow equations with the area ratios ( $A_T/A$ ) to account for compressible effects in the high subsonic flow regime. The TMD flow path input data for the reactor cavity is contained in Table 14.3.4-31.

The Steam Generator Tube Plugging Program, SGTP, parameters affect the Reactor Cavity Pressure Analysis through the mass and energy releases provided as input into the analysis. There is no direct impact of SGTP level on short-term mass and energy release rate calculations. The major impact results from changes to RCS temperature. For short-term effects, higher release rates typically result from cooler RCS conditions. The mass and energy releases used as input for the Reactor Cavity Pressure Analysis reflected limiting conditions and therefore, the NSSS performance parameters for the SGTP Program did not impact the results.

Based upon a review of Reference 34, it was concluded that the analysis assumptions used to perform the Reactor Cavity Pressure Analysis remain bounding. The assumptions and design inputs that are changed in Reference 34 relate to systems and components that do not affect the Reactor Cavity Pressure Analysis.

The net free volume and vent area from the upper and lower reactor cavities is documented in Table 14.3.4-32. The vent area represents the available flow path area leaving the reactor cavities

## UFSAR Revision 30.0

 An AEP Company	<b>INDIANA MICHIGAN POWER</b> <b>D. C. COOK NUCLEAR PLANT</b> <b>UPDATED FINAL SAFETY ANALYSIS REPORT</b>	Revised: 29.0 Section: 14.3.4.2 Page: 18 of 21
---	---	--

and entering the loop subcompartment. The upper cavity vent area is determined by summing the available flow path areas from Nodes 38-51 and 38-52. The lower cavity vent area is determined by summing the available flow path areas from Nodes 46-51, 47-51, 48-51, 50-51, 41-52, 42-52, 43-52, 49-52, and the limiting area from Nodes 2-60-58-51. As shown in Table 14.3.4-32, vent areas from the upper and lower reactor cavities were 165 and 172 square feet, respectively.

Figures 14.3.4-123 through 14.3.4-129 present pressure time histories for the break compartment (TMD node 1), the lower reactor cavity (TMD node 2), the reactor vessel annulus near the break (TMD node 3), the upper reactor cavity (TMD node 38), the broken loop pipe sleeve (TMD node 46), the loop subcompartments (TMD node 51) and the broken loop inspection port (TMD node 53).

Figures 14.3.4-130 through 14.3.4-132 present the differential pressure time histories for the lower reactor cavity wall, the upper reactor cavity wall, and the missile shield.


### **14.3.4.2.8.1 Upper Reactor Cavity**

The limiting break for the upper reactor cavity is a single-ended break of the primary cold leg. As shown in Table 14.3.4-19, mass and energy releases were developed for this break using SATAN-V models. High initial temperature (120°F), low initial pressure (13.2 psia) and low humidity (15%) are limiting for this analysis for both peak pressure and peak differential pressure. Upper reactor cavity pressurization effects were calculated with the TMD code assuming unaugmented critical flow.

The following results are summarized:

	<b>Peak Upper Cavity Pressure</b>	<b>Peak Missile Shield Differential Pressure</b>	<b>Peak Cavity Wall Differential Pressure</b>
Calculation current	48.5 psig	50.84 psid	50.0 psid
Original calculation	47.0 psig	44.1 psid	44.1 psid

## UFSAR Revision 30.0

 An AEP Company	<b>INDIANA MICHIGAN POWER</b> <b>D. C. COOK NUCLEAR PLANT</b> <b>UPDATED FINAL SAFETY ANALYSIS REPORT</b>	Revised: 29.0 Section: 14.3.4.2 Page: 19 of 21
---	---	--

### **14.3.4.2.8.2 Lower Reactor Cavity**

As in the upper reactor cavity analysis, the limiting break for the lower reactor cavity is a single-ended break of the primary cold leg. Low initial temperature (60°F), low initial pressure (13.2 psia) and low humidity (15%) are limiting for this analysis for peak differential pressure. Low initial temperature (60°F), high initial pressure (15.0 psia) and low humidity (15%) are limiting for this analysis for peak pressure.


The results are summarized below:

	<b>Peak Lower Cavity Pressure</b>	<b>Peak Differential Pressure Between Lower Cavity And Lp Subcompartments</b>
Current calculation	17.12 psig	18.22 psid
Original calculation	13.8 psig	12.3 psid

### **14.3.4.2.8.3 Reactor Vessel Annulus and Reactor Pipe Annulus**

The reactor vessel annulus and pipe annuli peak pressures were evaluated using a homogeneous, unaugmented critical flow model. The peak break flow rates for the single-ended cold leg (SECL) and single-ended hot leg (SEHL) breaks were considered. The limiting break was found to be the SEHL break because, even though the peak break flow rate was higher for the SECL, the enthalpy was higher for the SEHL. High initial temperature (120°F), low initial pressure (13.2 psia) and

## UFSAR Revision 30.0

 An AEP Company	<b>INDIANA MICHIGAN POWER</b> <b>D. C. COOK NUCLEAR PLANT</b> <b>UPDATED FINAL SAFETY ANALYSIS REPORT</b>	Revised: 29.0 Section:14.3.4.2 Page: 20 of 21
---	---	---

low humidity (15%) are limiting for this analysis for peak pressure. The results are summarized below:

	<b>Peak Pipe Annulus Pressure (SEHL)</b>	<b>Peak Reactor Vessel Annulus Pressure (SEHL)</b>
Revised calculation <sup>6</sup>	630 psig	160 psig
TMD Analysis Peak Values	665 psig <sup>7</sup>	675 psig <sup>8</sup>
Original calculation <sup>9</sup>	735 psig	95 psig

The revised calculation results are based upon a manual calculation method consistent with the original licensing methodology. This evaluation was then compared to the TMD analysis results. For the peak pipe annulus pressure, the original manual calculation bounds both the revised calculation and the TMD analysis results. For the peak reactor vessel annulus pressure, the TMD analysis results are considerably higher than the results from the manual calculation. However, this TMD pressure is highly localized near the break. The peak reactor vessel annulus pressure on the opposite side of the vessel is less than 50 psig.

#### **14.3.4.2.8.4 Reactor Vessel Nozzle Inspection Hatch Cover**

The above analyses were performed with the replacement inspection hatch covers. Theoretically, the inspection hatch covers could either remain closed or be fully opened. In the subcompartment analyses the most limiting action is assumed. To maximize the resulting pressure in the

---

<sup>6</sup> These values represent the average hand calculated values for the two annuli utilizing the M&E release data and volume/flow path data.


<sup>7</sup> This is the broken loop pipe annulus (Node 46).

<sup>8</sup> This is the vessel annulus area directly below the break location (Node 3).

<sup>9</sup> Original calculation refers to the values determined during initial licensing (1973).



## UFSAR Revision 30.0


 An <b>AEP</b> Company	<b>INDIANA MICHIGAN POWER</b> <b>D. C. COOK NUCLEAR PLANT</b> <b>UPDATED FINAL SAFETY ANALYSIS REPORT</b>	Revised: 29.0 Section:14.3.4.2 Page: 21 of 21
--	---	---

subcompartment, three inspection hatch covers were assumed to remain closed in the analysis. The selected covers were the three furthest from the break location represented by the flow paths from Nodes 41, 42 and 43 to Node 38. The individual flow paths for each reactor vessel nozzle inspection hatch covers vary . To determine the resulting flow areas, refer to Table 14.3.4-31. In the event of a primary leg break, the hinged door is designed to open. Based on the pressure time histories, it can be determined that all hatch covers would open. This would result in a decreased peak upper cavity pressure.


### **14.3.4.2.9 Short Term Containment Analysis Conclusions**

The results of the short-term containment analyses and evaluations for the Cook Nuclear Power Plants demonstrate that, for the steam generator enclosure, the pressurizer enclosure, the fan accumulator room, the loop subcompartment and the reactor cavity area, the resulting peak pressures/differential pressures remain below the allowable design peak pressures/differential pressures. Refer to Table 5.2-8 for a listing of the equivalent design pressure capabilities. The structural adequacy was confirmed through evaluations using Section 5.2.2.3 of the UFSAR as acceptance criteria.

# UFSAR Revision 30.0

 An <b>AEP</b> Company	<b>INDIANA MICHIGAN POWER</b> <b>D. C. COOK NUCLEAR PLANT</b> <b>UPDATED FINAL SAFETY ANALYSIS REPORT</b>	Revised: 29.0 Section:14.3.4.3 Page: i of i
--	---	---

<b>14.3 REACTOR COOLANT SYSTEM PIPE RUPTURE (LOSS OF COOLANT ACCIDENT) .....</b>	<b>1</b>
<b>14.3.4 Containment Integrity Analysis .....</b>	<b>1</b>
14.3.4.3 Mass And Energy Release Analysis For Postulated Loss-Of-Coolant Accidents .....	1
14.3.4.3.1 Mass and Energy Release Data.....	2
14.3.4.3.1.1 Short Term Mass and Energy Release Data .....	2
14.3.4.3.1.1.1 Early Design Analyses (Historical).....	2
14.3.4.3.1.1.2 Current Design Basis Analyses .....	5
14.3.4.3.1.2 Long Term Mass and Energy Release Data.....	5
14.3.4.3.1.2.1 Application of Single Failure Analysis .....	5
14.3.4.3.1.2.2 Mass and Energy Release Data .....	6
14.3.4.3.1.2.3 (deleted).....	8
14.3.4.3.1.2.4 (deleted).....	8
14.3.4.3.1.2.5 Sources of Mass and Energy.....	8
14.3.4.3.1.2.6 Significant Modeling Assumptions .....	10

 An AEP Company	INDIANA MICHIGAN POWER D. C. COOK NUCLEAR PLANT <b>UPDATED FINAL SAFETY ANALYSIS REPORT</b>	Revised: 29.0 Section: 14.3.4.3 Page: 1 of 10
---	---	---

## **14.3 REACTOR COOLANT SYSTEM PIPE RUPTURE (LOSS OF COOLANT ACCIDENT)**

### **14.3.4 Containment Integrity Analysis**


#### **14.3.4.3 Mass And Energy Release Analysis For Postulated Loss-Of-Coolant Accidents**

This analysis presents the mass and energy releases to the containment subsequent to a hypothetical loss-of-coolant accident (LOCA). The following results for long-term LOCA mass and energy releases and subsequent containment response have been validated for Unit 1 with the reactor internals converted to an upflow configuration.

The containment system receives mass and energy releases following a postulated rupture in the RCS. These releases continue over a time period, which, for the LOCA mass and energy analysis, is typically divided into four phases:

1. **Blowdown:**  
The period of time from accident initiation (when the reactor is at steady state operation) to the time that the lower plenum begins to re-pressurize after initial coolant evacuation.
2. **Refill:**  
The period of time when the reactor vessel lower plenum is being filled by accumulator and ECCS water. The WCOBRA/TRAC code mechanistically calculates this phase.
3. **Refld :**  
The period of time that begins when the water from the reactor vessel lower plenum enters the core and ends when the core is completely quenched.
4. **Post-Refld :**  
The period of time following the reflood phase. It is during this portion of the transient that (for the DECL and DEPS breaks) a two phase mixture exiting the core enters the steam generators, resulting in reverse heat transfer from the secondary side to the primary side. Heat transfer from the steam generator secondary metal to the fluid, and then from the fluid to the tubes, is accounted for in a mechanistic fashion.

# UFSAR Revision 30.0

 An AEP Company	<b>INDIANA MICHIGAN POWER</b> <b>D. C. COOK NUCLEAR PLANT</b> <b>UPDATED FINAL SAFETY ANALYSIS REPORT</b>	Revised: 29.0 Section:14.3.4.3 Page: 2 of 10
---	---	--

The WCAP-17721-P [23] methodology uses a single code for all phases of the LOCA transient through the time of peak containment pressure.

Three distinct locations in the reactor coolant system loop can be postulated for pipe rupture.

1. Hot leg (between vessel and steam generator)
2. Cold leg (between pump and vessel)
3. Pump suction (between steam generator and pump)

Using the WCAP-17721-P WCOBRA/TRAC methodology [23], full double ended ruptures were analyzed in the cold leg and the pump suction leg, each with 1 and 2 trains of safety injection, to cover the spectrum of possible limiting break locations for D. C. Cook Unit 1 in the context of the new methodology.

Full double ended ruptures of the cold leg and pump suction leg behave similarly, or more specifically, both behave dissimilarly from a double ended rupture of the hot leg. This is because the hot leg break provides a direct vent path to containment for the core exit flow during the post-blowdown phases. This has the effect of allowing the two phase mixture to bypass the steam generators, yielding significantly reduced integrated energy release in the long term. While the blowdown has the potential to be more severe for the hot leg break, ice condenser plants are inherently limited by the long term mass and energy releases after the ice bed is depleted. Therefore, the hot leg break has been excluded from the spectrum of runs. The double ended pump suction and double ended cold leg breaks both provide a mechanism to transport a two phase mixture to both the intact and broken steam generators, and so both have been analyzed with WCOBRA/TRAC.


#### **14.3.4.3.1 Mass and Energy Release Data**

##### **14.3.4.3.1.1 Short Term Mass and Energy Release Data**

###### **14.3.4.3.1.1.1 Early Design Analyses (Historical)**

The mass and energy release rate transients for all the design cases are given in Figures 14.3.4-133 through 14.3.4-140. All cases are generated with the SATAN-V break model consisting of Moody-Modified Zaloudek critical flow correlations applied at the break element. Since no mechanistic constraints have been established for full guillotine rupture, an instantaneous pipe severance and disconnection is assumed for all transients. Assumptions specific to the early design transients are as follows:

## UFSAR Revision 30.0

 <b>INDIANA MICHIGAN POWER</b> An AEP Company	<b>INDIANA MICHIGAN POWER</b> <b>D. C. COOK NUCLEAR PLANT</b> <b>UPDATED FINAL SAFETY ANALYSIS REPORT</b>	Revised: 29.0 Section: 14.3.4.3 Page: 3 of 10
---	---	---

For the hot leg mass and energy release rate transient to loop subcompartments:

Figures 14.3.4-133, -134


1. A double ended guillotine type break.
2. A break located just outside the biological shield.
3. A break located in the worst loop.
4. A six node upper plenum model.
5. A 16 node broken hot leg pipe model.
6. A discharge coefficient ( $C_D$ ) equal to 1.
7. A 100% power condition with  $T_{hot} = 606.4^{\circ}\text{F}$  and  $T_{cold} = 540.4^{\circ}\text{F}$ .

For the cold leg mass and energy release rate transient to loop subcompartments:

Figures 14.3.4-135, -136

1. A double ended guillotine type break.
2. A break located just outside the biological shield.
3. A break located in the worst loop.
4. A seven node downcomer model.
5. A 16 node broken hot leg pipe model.
6. A discharge coefficient ( $C_D$ ) equal to 1.
7. A full power condition with  $T_{hot} = 606.4^{\circ}\text{F}$  and  $T_{cold} = 540.4^{\circ}\text{F}$ .

## UFSAR Revision 30.0

 An <b>AEP</b> Company	<b>INDIANA MICHIGAN POWER</b> <b>D. C. COOK NUCLEAR PLANT</b> <b>UPDATED FINAL SAFETY ANALYSIS REPORT</b>	Revised: 29.0 Section: 14.3.4.3 Page: 4 of 10
--	---	---

For hot leg mass and energy release rate transients to subcompartments:

Figures 14.3.4-137, -138


1. A single ended split type break.
2. A break just outside the hot leg nozzle.
3. A break in the pressurizer loop.
4. A six node upper plenum model.
5. A 16 node broken hot leg pipe model.
6. A discharge coefficient ( $C_D$ ) equal to 1.
7. Full power condition  $T_{hot} = 606.4^{\circ}\text{F}$  and  $T_{cold} = 540.4^{\circ}\text{F}$ .

For the cold leg mass and energy release rate transient to subcompartments:

Figures 14.3.4-139, -140

1. A single ended split type break.
2. A break just outside the cold leg nozzle.
3. A break in the pressurizer loop.
4. A seven node downcomer model.
5. A 16 node broken hot leg pipe model.
6. A discharge coefficient ( $C_D$ ) equal to 1.
7. A full power condition  $T_{hot} = 606.4^{\circ}\text{F}$  and  $T_{cold} = 540.4^{\circ}\text{F}$ .

## UFSAR Revision 30.0

 An AEP Company	<p style="text-align: center;"><b>INDIANA MICHIGAN POWER</b> <b>D. C. COOK NUCLEAR PLANT</b> <b>UPDATED FINAL SAFETY ANALYSIS REPORT</b></p>	<p>Revised: 29.0 Section: 14.3.4.3 Page: 5 of 10</p>
---	--	--

For the mass and energy release rate transient to the pressurizer enclosure, a 6 inch spray line pipe break was considered (Figures 14.3.4-141, -142):

1. A guillotine type break modeled as a 0.147 ft<sup>2</sup> split in the cold leg at the pump discharge (area of the six inch pressurizer spray feed line) and a 0.087 ft<sup>2</sup> split in the top of the pressurizer (area of 4 inch spray nozzle).
2. Valves in spray lines are assumed to be open.
3. No pipe resistance for the feed line considered.
4. A full power condition  $T_{\text{hot}} = 606.4^{\circ}\text{F}$  and  $T_{\text{cold}} = 540.4^{\circ}\text{F}$ .
5. A discharge coefficient ( $C_D$ ) equal to 1.

The mass and energy release rate transients for all the generated cases are supported by an extensive investigation of short term phenomena. Section 14.3.4.5 includes detailed discussion of the phenomena and the results.

### **14.3.4.3.1.1.2 Current Design Basis Analyses**

Analyses were conducted to support changes in Reactor Power and revised RCS parameters, such as enthalpy, on the mass and energy releases. Details of the subcompartment evaluation are presented in Section 14.3.4.2.5 for the Pressurizer Enclosure Evaluation, Section 14.3.4.2.7 for the Loop Subcompartments Evaluation and, Section 14.3.4.2.8, for the Reactor Cavity Evaluation.

### **14.3.4.3.1.2 Long Term Mass and Energy Release Data**


#### **14.3.4.3.1.2.1 Application of Single Failure Analysis**

An analysis of the effects of the single failure criteria has been performed on the mass and energy release rates for the DECL break. An inherent assumption in the generation of the mass and energy release is that offsite power is lost. This results in the actuation of the emergency diesel generators, required to power the safety injection system. This is not an issue for the blowdown period, which is limited by the compression peak pressure.

The limiting minimum safety injection case has been analyzed for the effects of a single failure. In the case of minimum safeguards, the single failure postulated to occur is the loss of an emergency diesel generator. This results in the loss of one pumped safety injection train, thereby minimizing the safety injection flow. The analysis further considers the RHR and SI pump head curves to be degraded by 15% and the charging pump head curve to be degraded by 10%. This results in the greatest SI flow reduction for the minimum safeguards case.



# UFSAR Revision 30.0

 An AEP Company	<p style="text-align: center;"><b>INDIANA MICHIGAN POWER</b> <b>D. C. COOK NUCLEAR PLANT</b> <b>UPDATED FINAL SAFETY ANALYSIS REPORT</b></p>	<p>Revised: 29.0 Section: 14.3.4.3 Page: 6 of 10</p>
---	--	--

## **14.3.4.3.1.2.2      *Mass and Energy Release Data***


WCOBRA/TRAC consists of two primary source codes, COBRA-TF and TRAC-PD2. COBRA-TF is a three dimensional thermal hydraulic code that is used to model the vessel in detail, and TRACPD2 is a one dimensional code that is used to model loop piping, pumps, steam generators, and various boundary conditions. The WCOBRA/TRAC computer code is currently used as the PWR ECCS evaluation model by Westinghouse; it is fully capable of calculating the thermal/hydraulic RCS response to a large pipe rupture. The use of WCOBRA/TRAC for this application has been qualified by comparison with scalable test data covering the expected range of conditions and important phenomena. Modifications to WCOBRA/TRAC were required to model the specifics of importance to the LOCA M&E analysis, and these updates are discussed below.

The WCOBRA/TRAC steam generator, modeled in accordance with the ECCS evaluation model, was shown to over predict the reverse heat transfer from the steam generators. Updates were made to more accurately calculate the steam generator cool down. These updates were validated by comparison to FLECHT-SEASET steam generator separate effects tests. The result is a computer code capable of modeling phenomena associated with the large break LOCA conditions that provides significant margin relative to the current WCAP-10325-P-A [22] methodology because the stored RCS and SG energy is released at a mechanistically calculated rate instead of forced out over a conservatively short duration.

Beginning with the peak clad temperature (PCT) D. C. Cook Unit 1 model, specific updates were made to the model to bias it for containment integrity purposes. These key updates included:

1. Updated the PCT nodding structure to include safety injection and accumulator injection in all loops
2. Maximized the RWST temperature (105°F, technical specification maximum)
3. Applied accumulator upper limit pressure (672.7 psia), lower limit liquid volume (921 ft<sup>3</sup>), and maximum temperature (120°F)
4. RCS volume was increased by 3% for thermal expansion and measurement uncertainty
5. SG tube plugging level was reduced to 0% (assumption maximizes RCS volume and flow/heat transfer area of SG tubes)

## UFSAR Revision 30.0

 An <b>AEP</b> Company	<b>INDIANA MICHIGAN POWER</b> <b>D. C. COOK NUCLEAR PLANT</b> <b>UPDATED FINAL SAFETY ANALYSIS REPORT</b>	Revised: 29.0 Section: 14.3.4.3 Page: 7 of 10
--	---	---

6. Increased the RCS temperatures to the high end of the operating range band and included uncertainty for a target  $T_{avg}$  of 580.5°F
7. Increased the RCS initial pressure to 2317 psia (including uncertainties)
8. Increased the pressurizer liquid level, targeting maximum water volume of 1215 ft<sup>3</sup>
9. Increased core power to account for uncertainty at full power, targeting 3317 MWt
10. Applied ANS 1979 + 2 $\sigma$  decay heat
11. Turned off fuel rod swelling model
12. Used Baker-Just correlation for metal/water reaction
13. Updated the steam generator nodding structure per WCOBRA/TRAC M&E methodology
14. Biased the steam generator secondary side volumes high by 3% to account for uncertainty


The resulting model was used to calculate the mass and energy releases for the limiting break scenario, a double ended cold leg break with minimum safeguards. The WCOBRA/TRAC tool calculates all phases of the peak pressure LOCA transient, including blowdown, refill, reflood, and post reflood long term. The resulting blowdown and post blowdown mass and energy releases are found in Table 14.3.4-41 and Table 14.3.4-42, respectively.

After containment depressurization, the mass and energy release available to containment is generated directly from core boiloff / decay heat.

The mass and energy release from decay heat is based on the 1979 ANSI/ANS Standard, shown in Reference 24 and the following input:

1. The highest decay heat release rates come from the fission of U-238 nuclei. Thus, to maximize the decay heat rate a maximum value (8%) has been assumed for the U-238 fission fraction.
2. The second highest decay heat release rate comes from the fission of U-235 nuclei. Therefore, the remaining fission fraction (92%) has been assumed for U-235.

## UFSAR Revision 30.0

 An AEP Company	<p style="text-align: center;"><b>INDIANA MICHIGAN POWER</b> <b>D. C. COOK NUCLEAR PLANT</b> <b>UPDATED FINAL SAFETY ANALYSIS REPORT</b></p>	<p>Revised: 29.0 Section: 14.3.4.3 Page: 8 of 10</p>
---	--	--

3. The factor which accounts for neutron capture in fission products has been taken directly from Table 10 of the standard.
4. The number of atoms of Pu-239 produced per second has been assumed to be 70% of the fission rate.
5. The total recoverable energy associated with one fission has been assumed to be 200 MeV/fission.
6. The fuel has been assumed to be at full power for 108 seconds.
7.  $2\sigma$  uncertainty has been applied to the fission product decay. This accounts for a 98% confidence level.

### **14.3.4.3.1.2.3 (deleted)**

### **14.3.4.3.1.2.4 (deleted)**

### **14.3.4.3.1.2.5 Sources of Mass and Energy**


The sources of mass and energy considered in the LOCA mass and energy release analysis are provided below for the double-ended cold legbreak with minimum safety injection.

The mass sources are the reactor coolant system, accumulators, and pumped safety injection. The energy sources include:

1. Reactor coolant system water
2. Accumulator water
3. Pumped injection water
4. Decay Heat
5. Core stored energy
6. Reactor coolant system metal (including the steam generator tube metal)
7. Steam generator metal (including the shell, wrapper, and internals)
8. Steam generator secondary fluid energy (liquid and steam)

All sources of mass and energy listed above are considered in the WCOBRA/TRAC portion of the analysis. The water in the RCS, accumulators, safety injection boundary conditions, and SG secondary is explicitly modeled. Core decay heat (including feedback effects during blowdown) is included in the WCOBRA/TRAC fuel rod model. The fuel rod model also includes an energy term to represent core stored energy. The reactor coolant system (RCS) and steam generator

## UFSAR Revision 30.0

 <small>An AEP Company</small>	<p style="text-align: center;"><b>INDIANA MICHIGAN POWER</b> <b>D. C. COOK NUCLEAR PLANT</b> <b>UPDATED FINAL SAFETY ANALYSIS REPORT</b></p>	<p>Revised: 29.0 Section: 14.3.4.3 Page: 9 of 10</p>
--	--	--


(SG) metal, and the associated heat transfer from these sources, is modeled in the WCOBRA/TRAC analysis.

In the mass and energy release data presented, no zirconium-water reaction heat was considered because the clad temperature did not rise high enough for the rate of the zirconium-water reaction heat to be of any significance.

The consideration of the various energy sources in the mass and energy release analysis provides assurance that all available sources of energy have been included in the analysis. Although Cook Nuclear Plant Unit 1 is not a Standard Review Plan Plant, the review guidelines presented in Standard Review Plan Section 6.2.1.3 have been satisfied.

The methods and assumptions used to release the various energy sources are given in Reference 22, which has been approved as a valid evaluation model by the Nuclear Regulatory Commission.

# UFSAR Revision 30.0


 An AEP Company	<b>INDIANA MICHIGAN POWER</b> <b>D. C. COOK NUCLEAR PLANT</b> <b>UPDATED FINAL SAFETY ANALYSIS REPORT</b>	Revised: 29.0 Section: 14.3.4.3 Page: 10 of 10
---	---	--

## **14.3.4.3.1.2.6 Significant Modeling Assumptions**


The following assumptions were employed to ensure that the mass and energy releases are conservatively calculated, thereby maximizing energy release to containment:

1. Maximum expected operating temperatures of the reactor coolant system (100% full power conditions)
2. An allowance in temperature for instrument error and dead band (+5.1°F)
3. The RCS volume was increased by 3% (composed of a 1.6% allowance for thermal expansion and a 1.4% allowance for uncertainty).
4. Core rate thermal power of 3317 MWt (100.34% of 3306 MWt - conservative compared to licensed power of 3304 MWt).
5. Steam generator secondary side mass was biased conservatively high.
6. Initial fuel temperatures, and thus the core stored energy, were based on late in life conditions that included the effects of fuel pellet thermal conductivity degradation.
7. A maximum containment backpressure equal to design pressure.
8. An allowance for RCS initial pressure uncertainty (+67 psi)
9. Steam generator tube plugging leveling (0% uniform)
  - a. Maximizes reactor coolant volume and fluid release
  - b. Maximizes heat transfer area across the SG tubes
  - c. Reduces coolant loop resistance, which reduces delta-p upstream of the break, and increases break flow

# UFSAR Revision 30.0

 An <b>AEP</b> Company	<b>INDIANA MICHIGAN POWER</b> <b>D. C. COOK NUCLEAR PLANT</b> <b>UPDATED FINAL SAFETY ANALYSIS REPORT</b>	Revised: 27.0 Section:14.3.4.4 Page: i of i
--	---	---

<b>14.3 REACTOR COOLANT SYSTEM PIPE RUPTURE (LOSS OF COOLANT ACCIDENT) .....</b>	<b>1</b>
<b>14.3.4 Containment Integrity Analysis .....</b>	<b>1</b>
14.3.4.4 Mass and Energy Release Analysis for Postulated Secondary System Pipe Ruptures Inside Containment .....	1
14.3.4.4.1 Short Term Mass and Energy Releases.....	1
14.3.4.4.1.1 <i>Steam Generator Doghouse</i> .....	2
14.3.4.4.1.2 <i>Fan Accumulator Room</i> .....	3
14.3.4.4.2 Long Term Mass and Energy Release Data.....	3
14.3.4.4.2.1 <i>Pipe Break Blowdowns Spectra and Assumptions</i> .....	3
14.3.4.4.2.2 <i>Break Flow Calculations</i> .....	6
14.3.4.4.2.3 <i>Single Failure Effects</i> .....	7

 An AEP Company	<p>INDIANA MICHIGAN POWER D. C. COOK NUCLEAR PLANT UPDATED FINAL SAFETY ANALYSIS REPORT</p>	<p>Revised: 27.0 Section: 14.3.4.4 Page: 1 of 7</p>
---	---	---

## **14.3 REACTOR COOLANT SYSTEM PIPE RUPTURE (LOSS OF COOLANT ACCIDENT)**

### **14.3.4 Containment Integrity Analysis**

#### **14.3.4.4 Mass and Energy Release Analysis for Postulated Secondary System Pipe Ruptures Inside Containment**

A series of steamline breaks were analyzed to determine the most severe break condition for the containment temperature and pressure response. The assumptions on the initial conditions are taken to maximize the mass and energy released. The range of possible operating conditions for Unit 1 is presented in Table 14.1-1. The subsections that follow describe the short-term mass and energy releases, which address steamline break effects in the steam generator enclosure and the fan accumulator room, and a feedwater line break in the steam generator enclosure, followed by the long-term mass and energy releases.


##### **14.3.4.4.1 Short Term Mass and Energy Releases**

The short term mass and energy releases are broken down into steamline break locations in the fan accumulator room and steam line and feedwater line breaks in the steam generator doghouses. The details of each of these break locations are discussed below. The limiting plant condition in terms of both steam generator mass inventory and initial secondary system pressure are obtained when the plant is at hot shutdown. Since the no-load conditions are identical for both Unit 1 and Unit 2, one group of short term mass and energy release analyses will be applicable for both units.

Initial blowdown from the steam generator will be dry steam as a result of the approximately 5000 lbm. of steam in the upper head. This accentuates the initial peak compartment pressure. For the doghouse break, the flow rate was based on the Moody correlation for an initial reservoir pressure of 1106 psia, and included the steam generator exit nozzle loss. This was the value originally used for Unit 2 at the time of initial licensing. This is conservative to the licensing basis no-load pressure of 1020 psia. Depressurization of the steam generator causes an initial decrease in steam flow.



## UFSAR Revision 30.0

 An AEP Company	<p style="text-align: center;"><b>INDIANA MICHIGAN POWER</b> <b>D. C. COOK NUCLEAR PLANT</b> <b>UPDATED FINAL SAFETY ANALYSIS REPORT</b></p>	<p>Revised: 27.0 Section: 14.3.4.4 Page: 2 of 7</p>
---	--	---

The following assumptions were made for calculating steam generator blowdown with entrainment. Note that these assumptions are in the conservative direction for maximum water entrainment.


1. No credit was taken for the separation capability of the steam generator internals (swirl vanes and dryers).
2. Flow between regions of the steam generator was assumed as homogeneous with no slip or separation. Regions of the steam generator are the downcomer, bundle, swirl vane cylinders, and dryers.
3. Flow resistance between the steam generator regions was considered.
4. No credit was taken for flow resistance in the piping between the steam generator and the break.
5. Break flow was determined by the Moody (Reference 25 of Section 14.3.4.7) correlation with the discharge coefficient conservatively assumed as unity.

The mass and energy releases were also calculated for a postulated break in the main feedwater piping. For the feedwater line break event, the no-load steam generator pressure is 1020 psia and the full-power feedwater temperature is 449°F. Both the steam generator and the main feedwater system are assumed at saturation conditions for purposes of determining the liquid enthalpy values. The initial mass in the steam generator is 180,400 lb<sub>m</sub>.

### **14.3.4.4.1 Steam Generator Doghouse**

The mass and energy release to the steam generator doghouse from a steamline break and a feedwater line break has been analyzed. One case considers a steam line break between the steam generator shell and the steam line flow restrictor (break at the steam generator nozzle). The postulated break area is 4.60 ft<sup>2</sup> in the forward flow direction (normal direction of the steam flow) based on the inside diameter of the pipe. The break area defined in the reverse flow direction (opposite direction of the normal steam flow) is 4.909 ft<sup>2</sup> based on the inside diameter of the pipe. After the initial blowdown of the steam pipe, the reverse direction flowrate is limited by the area (1.4 ft<sup>2</sup>) defined by the inline flow restrictor (venturi) on the faulted steam line. The inline flow restrictor is located in the turbine bypass header in the turbine building. The second case models a feedwater line break at the nozzle to the steam generator, downstream of the feedwater line check valve. The feedwater line break area is 1.117 ft<sup>2</sup>, which corresponds to a nominal pipe diameter of 16" with an inside diameter of 14.314".

## UFSAR Revision 30.0

 An AEP Company	<p style="text-align: center;"><b>INDIANA MICHIGAN POWER</b> <b>D. C. COOK NUCLEAR PLANT</b> <b>UPDATED FINAL SAFETY ANALYSIS REPORT</b></p>	<p>Revised: 27.0 Section: 14.3.4.4 Page: 3 of 7</p>
---	--	---

The calculated mass and energy release rates into the steam generator doghouse, for both break locations, are presented as Table 14.3.4-15.

### **14.3.4.4.1.2 Fan Accumulator Room**

Blowdown of the steam piping was calculated with the SATAN-4 computer code. The SATAN-4 code does not consider momentum flux. Neglect of this effect is conservative for high velocity steam blowdown since it overpredicts the steam pressure near the break. Since steam pressure and steam density are overpredicted, frictional losses are underpredicted.

Piping blowdown consists of steam at 1192 Btu/lbm (saturation enthalpy at 1020 psia).

Steam piping blowdown consists of reverse flow (steam flow coming out the turbine end of the break), and -- for the break in the fan room -- the initial steam blowdown from the steam generator end until choking conditions are reached in the flow restrictor.

The SATAN model consists of 69 elements simulating the four steam generators and steam lines and the steam dump header. For the fan room analysis, flow restrictors with a throat area of 1.4 ft<sup>2</sup> were assumed in the steam line cross ties near the turbine.

Reverse flow was assumed to be terminated after 10 seconds as a result of steam line isolation. No credit was taken for partial isolation valve closure prior to 10 seconds.

The calculated mass and energy release rates for the fan accumulator room steam line break analyses are presented in Table 14.3.4-17.

### **14.3.4.4.2 Long Term Mass and Energy Release Data**


Steamline break mass and energy releases have been calculated for Unit 1 accounting for the numerous plant changes associated with thimble plug removal (TPR), the measurement uncertainty recapture (MUR) uprate program, and the replacement steam generators (RSGs). The full spectrum of the steamline breaks has been analyzed using the approved methodology in Reference 37 at the licensed NSSS power of 3327 MWt with the BWI-Series 51 RSGs.

#### **14.3.4.4.2.1 Pipe Break Blowdowns Spectra and Assumptions**

The following assumptions have been used in the mass and energy release analysis.


- a. Double-ended pipe ruptures are assumed to occur at the discharge nozzle of one steam generator downstream of the integral flow restrictor. Split-pipe breaks are assumed to occur downstream of the discharge nozzle of one steam generator.

## UFSAR Revision 30.0

 <p><b>INDIANA MICHIGAN POWER</b> <small>An AEP Company</small></p>	<p><b>INDIANA MICHIGAN POWER</b> <b>D. C. COOK NUCLEAR PLANT</b> <b>UPDATED FINAL SAFETY ANALYSIS REPORT</b></p>	<p>Revised: 27.0 Section: 14.3.4.4 Page: 4 of 7</p>
--	--	---

- b. Liquid entrainment in the steam blowdown is modeled for the zero power double-ended rupture. All other double-ended ruptures and the split breaks assume the blowdown is dry saturated steam.
- c. The steamline break protection system design for Unit 1 actuates on a low steam line pressure in 2-out-of-4 loops.
- d. Steamline isolation is assumed complete 11.0 seconds after the setpoint is reached for either low steam line pressure or hi-hi containment pressure. The isolation time allows 3 seconds for electronic delays and signal processing plus 8 seconds for valve closure. The total delay time of 11 seconds for steamline isolation supports the relaxation of the main steam isolation valve (MSIV) closure time.
- e. The break size is limited by the cross-sectional flow area of the BWI Series-51 steam generator integral flow restrictor in the outlet nozzle. 1.4 square-foot double-ended pipe breaks have been evaluated at 100.34 [includes 0.34 percent uncertainty], 70, 30, and zero percent power levels of the MUR uprated 3327 MW NSSS thermal power. Also, at zero percent power, a 1.0 square foot small double-ended pipe break has been evaluated.
- f. Four combinations of steamline ruptures have been evaluated assuming split-pipe ruptures:
  - 1. 0.865 square foot equivalent diameter at 100.34 percent power,
  - 2. 0.857 square foot equivalent diameter at 70 percent power,
  - 3. 0.834 square foot equivalent diameter at 30 percent power,
  - 4. 0.808 square foot equivalent diameter at zero percent power.
- g. Failure of a main steam isolation valve, failure of main feedwater isolation or main feedwater pump trip, and failure of auxiliary feedwater runout control have been considered. Two cases of each break size and power level scenario have been evaluated with one case modeling the MSIV failure and the other case modeling the AFW runout control failure. Each case also assumed continued main feedwater addition to bound the feedwater isolation or main feedwater pump trip failure. Main feedwater isolation via FMO valves is assumed complete 44 seconds after the setpoint is reached for either low steam line pressure or high containment pressure.

## UFSAR Revision 30.0

 <b>INDIANA MICHIGAN POWER</b> <small>An AEP Company</small>	<b>INDIANA MICHIGAN POWER D. C. COOK NUCLEAR PLANT UPDATED FINAL SAFETY ANALYSIS REPORT</b>	Revised: 27.0 Section: 14.3.4.4 Page: 5 of 7
--	---	--


- h. Core residual heat generation is assumed based on the 1979 American Nuclear Society (ANS) decay heat plus 2-sigma model (Reference 24).
- i. The end-of-life shutdown margin is assumed to be 1.3%  $\Delta k/k$  at no load, equilibrium xenon conditions, and the most reactive RCCA stuck in its fully withdrawn position.
- j. An end-of-life moderator density coefficient reflecting the most reactive stuck RCCA conditions is assumed.
- k. Minimum capability for injection of boric acid (2350 ppm) solution corresponding to the most restrictive single failure in the safety injection system is assumed. The emergency core cooling system (ECCS) consists of the following systems:
  - 1. the passive accumulators,
  - 2. the low-head safety injection (residual heat removal) system,
  - 3. the intermediate-head safety injection system, and
  - 4. the high-head safety injection (charging) system.

Only the high-head safety injection (charging) system, the intermediate-head safety injection system, and the passive accumulators are modeled for the steamline break accident analysis.

The safety injection flowrates assumed in the steamline break analysis corresponds to that delivered by one charging pump and one intermediate-head pump delivering full flow to the cold legs. The safety injection flows assumed in this analysis take into account the degradation of the ECCS charging and intermediate-head pump performance. No credit has been taken for the low concentration borated water, which must be swept from the lines downstream of the boron injection tank isolation valves prior to the delivery of boric acid to the reactor coolant loops. For this analysis, a boron concentration of 0 ppm for the boron injection tank is assumed.

After the generation of the safety injection signal (appropriate delays for logic, instrumentation, and signal transport included), the appropriate valves begin to operate and the safety injection charging and intermediate-head pumps start. In 27 seconds, the valves are assumed to be in their final positions and the pumps are

# UFSAR Revision 30.0

 An AEP Company	<p style="text-align: center;"><b>INDIANA MICHIGAN POWER</b> <b>D. C. COOK NUCLEAR PLANT</b> <b>UPDATED FINAL SAFETY ANALYSIS REPORT</b></p>	<p>Revised: 27.0 Section: 14.3.4.4 Page: 6 of 7</p>
---	--	---

assumed to be at full speed and drawing suction from the RWST. The volume containing the low concentration borated water is swept into the core before the 2350 ppm borated water reaches the core. This delay, described above, is inherently included in the steamline break model.

The modeling of the safety injection system in LOFTRAN is described in Reference 26.

- l. For the at-power cases, reactor trip is available via the safety injection signal, overpower protection (high neutron flux signal or OPAT signal), and the low pressurizer pressure signal.
- m. Offsite power is assumed to be available. Continued operation of the reactor coolant pumps maximizes the energy transferred from the reactor coolant system to the steam generators.
- n. No steam generator tube plugging is assumed to maximize the heat transfer characteristics of the RSGs.

## **14.3.4.4.2 Break Flow Calculations**


- **Steam Generator Blowdown**

The LOFTRAN computer code (Reference 26) is used to calculate the break flows and enthalpies of the release through the steamline break. Blowdown mass and energy releases determined using LOFTRAN include the effects of core power generation, main and auxiliary feedwater additions, engineered safeguards systems, reactor coolant thick metal heat storage, and reverse steam generator heat transfer. LOFTRAN has been approved for analysis of steamline break mass and energy releases via Supplement 1 of Reference 37.

- **Steam Plant Piping Blowdown**

The calculated mass and energy releases include the contribution from the secondary steam piping. For all double-ended ruptures, the steam piping blowdown begins at the time of the break and continues at a uniform rate until the entire piping inventory is released. The flowrate is determined using the Moody correlation, the pipe cross-sectional area, and the initial steam pressure. Following the piping blowdown, flow from the intact steam generators continues to simulate the reverse steam generator flow until steamline isolation for all double-ended ruptures and split breaks.

## UFSAR Revision 30.0


 An AEP Company	<p style="text-align: center;"><b>INDIANA MICHIGAN POWER</b> <b>D. C. COOK NUCLEAR PLANT</b> <b>UPDATED FINAL SAFETY ANALYSIS REPORT</b></p>	<p>Revised: 27.0 Section: 14.3.4.4 Page: 7 of 7</p>
---	--	---

### **14.3.4.4.2.3 Single Failure Effects**

- a. Failure of a main steam isolation valve (MSIV) increases the volume of steam piping that is not isolated from the break. When all MSIVs operate, the piping volume capable of blowing down is located between the steam generator and the first isolation valve. If the MSIV fails to close on the affected steam generator, the volume between the break location and the isolation valves in the other steamlines, including the safety and relief valve headers and other connecting lines, will feed the steamline break.
- b. Failure of a diesel generator results in the loss of one containment safeguards train, resulting in minimum heat removal capability.
- c. Failure of the main feedwater regulating valve (MFRV) to close results in additional inventory in the main feedwater line, which would not be isolated from the steam generator. The mass in this volume can flash into steam and exit through the break. All steamline break cases conservatively assumed failure of the MFRV to close, which resulted in the additional inventory available for release through the steamline break as well as a longer duration for the higher than normal main feedwater flows before the backup main feedwater motor-operated isolation valve (MFIV) closes.
- d. Failure of the auxiliary feedwater runout control equipment could result in higher AFW flowrates entering the steam generator prior to the realignment of the auxiliary feedwater system. The auxiliary feedwater flowrates assumed in the steamline break analysis are a function of the steam generator pressure into which the AFW flows. The auxiliary feedwater flowrates into the steam generator at the break location are twice as high with runout control failure than with no failure of the AFW control.


The long-term steamline break calculated mass and energy release rates for both the limiting double-ended rupture and split break are presented in Tables 14.3.4-7 and 14.3.4-8, respectively.

# UFSAR Revision 30.0

 An AEP Company	INDIANA MICHIGAN POWER D. C. COOK NUCLEAR PLANT UPDATED FINAL SAFETY ANALYSIS REPORT	Revised: 29.0 Section:14.3.4.5 Page: i of ii
---	--	--


<b>14.3 REACTOR COOLANT SYSTEM PIPE RUPTURE (LOSS OF COOLANT ACCIDENT) .....</b>	<b>1</b>
<b>14.3.4 Containment Integrity Analysis .....</b>	<b>1</b>
14.3.4.5 Containment Integrity Analysis - Background Information .....	1
14.3.4.5.1 LOCA Mass and Energy Release Data .....	1
14.3.4.5.1.1 Model Description .....	1
14.3.4.5.1.2 Comparison to other Critical Flow Models .....	2
14.3.4.5.1.3 Comparison to Experimental Data .....	3
14.3.4.5.1.4 Application to Transient Conditions .....	4
14.3.4.5.1.5 Parametric Studies .....	5
14.3.4.5.1.6 Break Size, Type and Location .....	5
14.3.4.5.1.7 Hot Leg Nodal Configuration.....	6
14.3.4.5.1.8 Cold Leg Studies .....	6
14.3.4.5.1.9 Nodal Configuration .....	6
14.3.4.5.1.10 Pump Modeling.....	7
14.3.4.5.1.11 Summary .....	7
14.3.4.5.2 Experimental Verification.....	8
14.3.4.5.2.1 Early Tests.....	8
14.3.4.5.2.2 1973 Waltz Mill Tests.....	9
14.3.4.5.2.2.1 Test Purpose .....	9
14.3.4.5.2.2.2 Test Facility.....	9
14.3.4.5.2.2.3 Test Procedure .....	10
14.3.4.5.2.2.4 Results.....	11
14.3.4.5.3 Short Term Containment Response .....	12
14.3.4.5.3.1 Results Based on 1973 Waltz Mill Tests.....	12
14.3.4.5.3.2 Subcritical Flow Model Studies .....	12
14.3.4.5.3.3 Derivation of the Compressibility Multiplier .....	13
14.3.4.5.3.4 Choked Flow Characteristics .....	14
14.3.4.5.3.5 Early Sensitivity Studies.....	15

# UFSAR Revision 30.0

 An <b>AEP</b> Company	<b>INDIANA MICHIGAN POWER</b> <b>D. C. COOK NUCLEAR PLANT</b> <b>UPDATED FINAL SAFETY ANALYSIS REPORT</b>	Revised: 29.0 Section: 14.3.4.5 Page: ii of ii
--	---	--

14.3.4.5.4	Ice Condenser Performance Criteria .....	17
14.3.4.5.4.1	<i>Inlet Door Performance</i> .....	20
14.3.4.5.4.1.1	<i>Introduction</i> .....	20
14.3.4.5.4.1.2	<i>Design Criteria</i> .....	21
14.3.4.5.4.1.3	<i>Performance Capability</i> .....	22
14.3.4.5.4.2	<i>Top and Intermediate Deck Door Performance</i> .....	24
14.3.4.5.4.2.1	<i>Design Criteria</i> .....	25
14.3.4.5.4.2.2	<i>Performance Capability</i> .....	25
14.3.4.5.4.3	<i>Vent Design and Performance</i> .....	26
14.3.4.5.4.3.1	<i>Introduction</i> .....	26
14.3.4.5.4.3.2	<i>Large Break Performance Requirements</i> .....	26
14.3.4.5.4.3.3	<i>Small Break Performance Requirements</i> .....	27
14.3.4.5.4.4	<i>Drain Design and Performance</i> .....	27
14.3.4.5.4.4.1	<i>Introduction</i> .....	27
14.3.4.5.4.4.2	<i>Large Break Performance Requirements</i> .....	28
14.3.4.5.4.4.3	<i>Small Break Performance Requirements</i> .....	28
14.3.4.5.4.4.4	<i>Normal Operational Performance</i> .....	29
14.3.4.6	Changes from Base Containment Analyses: Note Concerning Tables and Figures .....	29
14.3.4.7	References for Section 14.3.4 .....	29



 An AEP Company	INDIANA MICHIGAN POWER D. C. COOK NUCLEAR PLANT UPDATED FINAL SAFETY ANALYSIS REPORT	Revised: 29.0 Section:14.3.4.5 Page: 1 of 33
---	--	--

## **14.3 REACTOR COOLANT SYSTEM PIPE RUPTURE (LOSS OF COOLANT ACCIDENT)**

### **14.3.4 Containment Integrity Analysis**

#### **14.3.4.5 Containment Integrity Analysis - Background Information**

##### **14.3.4.5.1 LOCA Mass and Energy Release Data**

###### **14.3.4.5.1.1 Model Description**


Mass and energy release rate transients generated for the TMD pressure calculation are supported by an extensive investigation of short term blowdown phenomena. The SATAN-V code was used to predict early blowdown transients. The study concerned a verification of the conservatism of the SATAN-V calculated transients. This verification was accomplished through two approaches: a review of the validity of the SATAN-V break model, and a parametric study of significant physical assumptions.

The SATAN-V code uses a control volume approach to model the behavior of the Reactor Coolant System resulting from a large break in a main coolant pipe. Release rate transients are determined by the SATAN-V break model which includes a critical flow calculation and an implicit representation of pressure wave propagation.

The SATAN-V critical flow calculation uses appropriately defined critical flow correlations applied for fluid conditions at the break element. For the early portion of blowdown, subcooled, saturated, and two-phase critical flow regimes are encountered. SATAN-V uses the Moody (Reference 25) correlation for saturated and two-phase fluid conditions and a slight modification of the Zaloudek (Reference 27) correlation for the subcooled blowdown regime.

Since most short term blowdown transients are characterized by a peak mass and energy release rate that occurs during a subcooled condition, the Zaloudek application is particularly significant. The Zaloudek correlation is modified to merge to Moody predicted mass velocities at saturation in the break element. This correlation appears in the critical flow routine of SATAN-V in the form:

## UFSAR Revision 30.0

 An AEP Company	<p style="text-align: center;"><b>INDIANA MICHIGAN POWER</b> <b>D. C. COOK NUCLEAR PLANT</b> <b>UPDATED FINAL SAFETY ANALYSIS REPORT</b></p>	<p>Revised: 29.0 Section: 14.3.4.5 Page: 2 of 33</p>
---	--	--

$$G_{\text{crit}} = CK_1 \sqrt{(5.553 * 10^5)(P - C_1 P_{\text{sat}})}$$

where:

- $G_{\text{crit}}$  = critical flow in lb. mass/sec-ft<sup>2</sup>  
 $P$  = reservoir pressure (psia)  
 $P_{\text{sat}}$  = reservoir saturation pressure (psia)  
 $C_1$  = constant where  $.5 < C_1 < 1$

$$CK_1 = \sqrt{\frac{.1037}{1 - C_1}} = \text{constant adjusted such that when } P = P_{\text{sat}}, G_{\text{crit}} \text{ from Zaloudek matches the}$$

SATAN-V Moody critical flow calculated at zero quality. For the present analysis,  $C_1$  equals 0.9 and  $CK_1$  equals 1.018. The modification also more conservatively accounts for the phenomena of increasing mass velocity with increasing degrees of subcooling. The slope of the subcooled  $G$  vs.  $P$  curve is steeper for the modified correlation. The low quality portion of the SATAN-V critical flow model is presented in Figure 14.3.4-143. The Moody saturation line corresponds to the condition upstream in the break element where quality equals zero and pressure equals saturation pressure. Thus when pressure equals saturation pressure in the break element the Zaloudek and Moody critical flow values are equal. When pressure exceeds saturation pressure in the break element, the modified Zaloudek is used for the critical flow calculation. The steep slope of the Zaloudek  $G$  vs.  $P$  line indicates the over-accounting for the subcooling effect.


### **14.3.4.5.1.2 Comparison to other Critical Flow Models**

The Henry-Fauske critical flow correlation was considered for comparison (References 16, 28, and 29). This correlation models flow nonequilibrium via an approach which includes an empirical parameter. This parameter describes the deviation from equilibrium mass transfer and depends on flow geometry.

The value is selected for a particular configuration based on the range of throat equilibrium qualities. The value for constant area ducts is used in the present analysis. This choice is based on the worst possible double-ended break geometry described below.

For cold leg and hot leg breaks, the majority of the flow, about 65%, comes from the vessel side of the break. For this side, the geometry may be described as an entrance nozzle and a straight pipe of approximately 12 feet in length with a diameter of 29 inches. This length of pipe represents the distance from the reactor vessel to the periphery of the biological shield. No

## UFSAR Revision 30.0

 An AEP Company	<b>INDIANA MICHIGAN POWER</b> <b>D. C. COOK NUCLEAR PLANT</b> <b>UPDATED FINAL SAFETY ANALYSIS REPORT</b>	Revised: 29.0 Section:14.3.4.5 Page: 3 of 33
---	---	--

double-ended break can occur within the biological shield because of the restricted movement within the pipe annulus. Hence the constant area value is appropriate.

Like the SATAN-V model, the Henry-Fauske correlation yields a  $G_{crit}$  in terms of upstream conditions and like the SATAN-V model it also exhibits a steeper slope of the G vs. P line for subcooled conditions. As can be seen in Figure 14.3.4-143, the Henry-Fauske saturated liquid line is below the Moody saturated line (SATAN-V model) for pressures greater than about 1000 psia.


For short term blowdown calculations, the significant pressure region is from 1000 psia to 1800 psia, with increased emphasis on subcooled conditions for the 1000 psia end. Subcooled mass velocity versus pressure is given for the two fluid temperatures corresponding to  $P_{sat} = 1000$  and  $P_{sat} = 1800$ . It is clear from the figure that the slope of the Zaloudek G vs. P line is steeper in both cases. This increased sensitivity coupled with the higher value for Moody at saturation causes the SATAN-V model to predict higher mass velocities. Hence the SATAN-V model is a more conservative treatment of critical flow than the Henry-Fauske model.

In the original FLASH model,(Reference 30) the Moody correlation was extended to subcooled conditions. This treatment is employed in many blowdown codes and thus it is appropriate to compare the SATAN-V model to these values. This is illustrated in Figure 14.3.4-144. Again, the Zaloudek treatment yields higher mass velocities and the SATAN-V model is more conservative.

### **14.3.4.5.1.3 Comparison to Experimental Data**

The margin included in the modified Zaloudek prediction of subcooled critical flow rates is demonstrated by a review of experimental subcooled critical flow data. Figures 14.3.4-145 and -146 present a plot of measured vs. predicted critical flow values for Zaloudek's own data.(References 27 and 31) The figures indicate that when the modified correlation is applied to Zaloudek's data, the predicted critical flow values are significantly higher than measured flow rates.

The margin associated with the SATAN-V critical flow calculation may also be demonstrated by a review of the low quality data presented by Henry in ANL-7740 (Reference 29). Exit plane quality, in terms of the Moody model, is determined as a function of upstream conditions by assuming an isentropic expansion to exit plane (i.e., critical) pressure. The lowest exit plane qualities where the Moody model is applied in the SATAN-V code occur for expansion from saturated liquid conditions; a plot of these are shown in Figure 14.3.4-147. For exit plane

 An AEP Company	<p style="text-align: center;"><b>INDIANA MICHIGAN POWER</b> <b>D. C. COOK NUCLEAR PLANT</b> <b>UPDATED FINAL SAFETY ANALYSIS REPORT</b></p>	<p>Revised: 29.0 Section: 14.3.4.5 Page: 4 of 33</p>
---	--	--

qualities above the line, the Moody model is used in the SATAN-V code. Below the line, the Modified Zaluodek model is used.

Henry's comparison between data and model shows that for the range of exit plane quality greater than 0.02, the Moody model overpredicts the data, hence is conservative.

For the region below 0.02, it is appropriate to compare Henry's results with the Modified Zaluodek model, as used in the SATAN-V code. This is done in Figure 14.3.4-148 for all of Henry's data points. As can be seen, the Zaluodek model overpredicts the flow. A discharge coefficient of 0.6 would be more reasonable than the 1.0 value used in SATAN-V.

#### **14.3.4.5.1.4 Application to Transient Conditions**

The Zaluodek correlation was developed for stagnation (reservoir) pressure and quasi-steady-state critical flow conditions. It is extended to application in the SATAN-V break element and transient flow conditions. This extension is justified because of the following considerations.


The pressure in the break element differs from the value in a nearby large volume because of three effects:

1. Pressure drop due to friction
2. Pressure drop due to spatial acceleration (momentum flux)
3. Pressure drop due to the transient

The friction term in the reactor application is quantifiable; this term is less important than the other two. The sensitivity of the break flow rate to fluid friction was evaluated via a parametric study. For the purposes of this study, an analysis was made wherein the frictional resistance between the vessel and the break was reduced from the design values by a factor of one hundred. Over the period from 0.0 to 60 milliseconds (which includes the peak break flow), the integrated mass flow differed by less than 18 lbm from the design friction case; the total release over this period was about 5000 lbm.

Spatial acceleration is the major source of pressure drop upstream of the break between the reservoir and the pipe, causing steep pressure gradients in the approach region to critical flow. This term is not calculated explicitly in the SATAN-V code. Spatial acceleration is accounted for by the use of critical flow correlations (Zaluodek or Moody) which contain this effect. No credit is taken for pressure drop due to spatial acceleration for elements other than the break element. Hence the pressure calculated by SATAN-V may be interpreted as a stagnation pressure which is the appropriate pressure for the Zaluodek and Moody models.

## UFSAR Revision 30.0

 An AEP Company	<b>INDIANA MICHIGAN POWER</b> <b>D. C. COOK NUCLEAR PLANT</b> <b>UPDATED FINAL SAFETY ANALYSIS REPORT</b>	Revised: 29.0 Section: 14.3.4.5 Page: 5 of 33
---	---	---

Prior to the occurrence of the peak release rate, the break element and upstream reservoir pressures differ as a result of the transient described by pressure wave propagation. The applicability of the SATAN-V break model to this situation is verified by the code's ability to match recorded semi-scale transients. SATAN simulations of LOFT transients support the SATAN-V transient calculation. Figure 14.3.4-149 presents a comparison of LOFT pressure transients recorded near the break to the SATAN-V model of the LOFT break element transient. The graphs demonstrate the ability of the SATAN-V code to track pressure waves in the broken pipe.

Moreover, the critical flow correlation is implemented in the present analysis by combining the correlation with the appropriate momentum equation. This provides a model for predicting break flow acceleration vis-a-vis a quasi-steady simulation. This is found to have little effect on containment pressure but is a more physical representation.

Thus the SATAN-V break model is supported by subcooled critical flow data, by comparison to other correlations, and by ability to simulate short term transients.

### **14.3.4.5.1.5 Parametric Studies**


With confirmation of the conservatism of the SATAN-V break model, a series of parametric studies were undertaken to identify the blowdown transient corresponding to the most severe TMD results. A series of basic sensitivities were first studied to set the scope of the more detailed investigations. The assumptions of break size, break type and break location were considered. The results of this analysis were evaluated using the TMD code.

### **14.3.4.5.1.6 Break Size, Type and Location**

A break of an area corresponding to twice the coolant pipe area was the most severe for mass and energy release. For this size break both double-ended guillotine and double-ended split type breaks were considered. These break types differ in that the split allows full communication between approach regions at each side of the break while the guillotine models a complete severance of two ends of a broken coolant pipe.

SATAN-V transients were generated for both type double-ended breaks with the guillotine break resulting in higher mass and energy release rates. The split type break is less severe because flow is reduced from the loop side of the break. This is because communication makes the break element pressure higher than would occur for the loop end in a guillotine rupture. The higher break element pressure yields a smaller pressure gradient for driving loop side flow. The vessel end is relatively unaffected by break type because a choked condition remains at the nozzle. In particular, the split type break results in a 10,000 lbm/sec reduction in peak mass flow rate.

# UFSAR Revision 30.0

 An AEP Company	<p style="text-align: center;"><b>INDIANA MICHIGAN POWER</b> <b>D. C. COOK NUCLEAR PLANT</b> <b>UPDATED FINAL SAFETY ANALYSIS REPORT</b></p>	<p>Revised: 29.0 Section: 14.3.4.5 Page: 6 of 33</p>
---	--	--

The influence of break location on TMD peak pressure was considered by generating blowdown transients for possible worst break locations. The results indicated that a double-ended break in the pump suction leg was clearly less severe for short term blowdown release rates and that no such clear decision could be made between hot and cold leg breaks.

More detailed parametric studies were continued for the cold leg and the hot leg double-ended guillotine breaks. The two locations produce intrinsically different TMD pressure responses and therefore must be dealt with in separate parametric surveys.

#### **14.3.4.5.1.7 Hot Leg Nodal Configuration**

A study of the SATAN-V nodal configuration has been applied to the hot leg double-ended guillotine break. It was found that for this break the nodal configuration of the broken hot leg and the upper plenum are significant to short term transients. Spatial convergence was achieved for the upper plenum after the addition of four nodes to the standard SATAN-V two node upper plenum model. These nodes are hemispherical shells arranged concentrically from the broken hot leg nozzle and approximate the propagation of the pressure wave in the upper plenum. They are significant in that they specify the inertial response of the upper plenum. Spatial convergence was demonstrated because doubling the number of nodes yielded less than a one percent change in break flow at all times.

Sensitivity to nodal configuration in the broken hot leg pipe was also investigated. Models with from 4 to 16 nodes were used to generate transients. Increasing the number of nodes was found to give a better simulation of pressure wave propagation in the pipe.

#### **14.3.4.5.1.8 Cold Leg Studies**

The cold leg break transient was also reviewed in terms of significant parameters.


The Reactor Coolant System behavior is different for cold leg breaks and the peak containment pressure occurs later for cold leg breaks.

#### **14.3.4.5.1.9 Nodal Configuration**

For the cold leg break the nodal configuration of the broken cold leg and the downcomer is significant to the transient. Spatial convergence was achieved with the addition of three additional nodes to the standard SATAN-V model. These are annular rings arranged concentrically from the broken cold leg nozzle and model propagation of the pressure wave in the downcomer.

As in the hot leg sensitivity, from 4 to 16 pipe node models were tried for the cold leg transient. Again, more nodes gave a better simulation of pressure wave propagation in the broken pipe.

# UFSAR Revision 30.0

 An AEP Company	<p style="text-align: center;"><b>INDIANA MICHIGAN POWER</b> <b>D. C. COOK NUCLEAR PLANT</b> <b>UPDATED FINAL SAFETY ANALYSIS REPORT</b></p>	<p>Revised: 29.0 Section: 14.3.4.5 Page: 7 of 33</p>
---	--	--

## **14.3.4.5.1.10 Pump Modeling**

For the time period of interest, the variation in pump inlet density is small and the variation in pump speed is small. This model was found to have no effect.

## **14.3.4.5.1.11 Summary**

From the hot leg and cold leg studies, the design basis mass and energy release rates have been finalized. The mass and energy release rate transients for all the design cases are given in Figures 14.3.4-133 to -142. All cases are generated from the SATAN-V break model consisting of Moody-Modified Zaloudek critical flow correlations applied at the break element. Since no mechanistic constraints have been established for full guillotine pipe rupture, an instantaneous pipe severance and disconnection is assumed for all transients. Assumptions specific to the presented transients are discussed in section 14.3.4.3.1.1.

Figures 14.3.4-137, -138 -139, and -140 present mass and energy release rate transients for hot leg and cold leg split type breaks of a single ended pipe area. For breaks of this size, the split type break is used as a design basis and this choice is justified by a generic study of the effect of break type on short term release rates. A discussion of this study and of break type influence was given as a response to question 6.71 to the Catawba PSAR (USNRC Docket No's. 50-413 and 50-414). It is sufficient for this discussion to note that for single ended breaks, a split type break results in higher release rates.


Differences in blowdown mass and energy release rates between hot leg and cold leg single ended split breaks result from the influence of the hot water in the upper plenum and hot legs. For a cold leg single ended split, the flashing fluid in the upper plenum and hot legs sustains flow to the break from both the vessel and from the loop through the broken loop pump. This flashing, then, acts to maintain a subcooled blowdown for the cold leg break.

For the hot leg single ended split no such pressurization effect occurs at the break. Flashing fluid in the hot leg and upper plenum, rather, results in an extensive two-phase blowdown condition. The broken leg pump continues to remain effective during the hot leg split transient and thus draws flow away from the break.

The hot leg and cold leg double ended release rate transients presented in the figures discussed above are the result of a guillotine type break. This basis is again justified as a result of the generic break type study referenced above. The study indicated that for breaks of twice the coolant pipe area, a guillotine type break resulted in the highest release rates.



## UFSAR Revision 30.0

 An AEP Company	<p style="text-align: center;"><b>INDIANA MICHIGAN POWER</b> <b>D. C. COOK NUCLEAR PLANT</b> <b>UPDATED FINAL SAFETY ANALYSIS REPORT</b></p>	<p>Revised: 29.0 Section: 14.3.4.5 Page: 8 of 33</p>
---	--	--

An explanation of the differences in the release rate transients presented for hot leg and cold leg double-ended breaks is complicated by the fact that these are guillotine type breaks. Since the guillotine break models a complete separation of the broken pipe, conditions at each end of the break must be considered individually. The total release rate is then the sum of contributions from each end.

Flashing of the fluid in the hot legs again accounts for the higher mass flow rates observed for the cold leg double-ended break in comparison to the hot leg double-ended transient. However, two other influences are significant for breaks of this type and area.

For the cold leg guillotine, the increased break area requires higher flows if a subcooled blowdown condition is to be maintained at the break. A subcooled blowdown occurs at the vessel end of the broken pipe but because of the broken loop pump resistance to increased flow, a two-phase blowdown occurs at the loop end of the break.

Since for both hot leg and cold leg breaks the loop side of the break experiences a two-phase blowdown, the loop layout geometry determines the difference in their release rates. Higher release rates are observed for the loop side of hot leg break because it is fed from the reservoir of water in the inlet plenum of the steam generator. No such supply of water exists at the loop side of the cold leg break. In fact, flow to the cold leg loop side is restricted by the resistance of the broken loop pump.

The differences in release rates for the double-ended break are thus the result of two effects. A higher vessel side mass flow rate for the cold leg break results from a subcooled blowdown maintained by the pressurizing effect of flashing hot leg fluid.

A lower loop side mass flow is observed for the cold leg break because of the differences accountable to loop layout geometry. However, since the subcooled blowdown effect dominates the total release rate, the cold leg double-ended guillotine still results in highest total mass discharge rates.


### **14.3.4.5.2 Experimental Verification**

#### **14.3.4.5.2.1 Early Tests**

The performance of the TMD Code was verified against the 1/24 scale air tests and the 1968 Waltz Mill tests. For the 1/24 scale model the TMD Code was used to calculate flow rates to compare against experimental results. The effect of increased nodalization was also evaluated. The Waltz Mill test comparisons involved a reexamination of test data. In conducting the reanalyses, representation of the 1968 Waltz Mill test was reviewed with regard to parameters



## UFSAR Revision 30.0

 An AEP Company	<b>INDIANA MICHIGAN POWER</b> <b>D. C. COOK NUCLEAR PLANT</b> <b>UPDATED FINAL SAFETY ANALYSIS REPORT</b>	Revised: 29.0 Section: 14.3.4.5 Page: 9 of 33
---	---	---

such as loss coefficients and blowdown time history. The details of this information are given in Reference 14.

### **14.3.4.5.2.2 1973 Waltz Mill Tests**

#### **14.3.4.5.2.2.1 Test Purpose**

The Waltz Mill Ice Condenser Blowdown Test Facility was reactivated in 1973 (Reference 2) to verify the ice condenser performance with the following redesigned plant hardware scaled to the test configuration:

1. Perforated metal ice baskets and new design couplings.
2. Lattice frames sized to provide the correct loss coefficient relative to plant design.
3. Lower support beamed structure and turning vanes sized to provide the correct turning loss relative to the plant design.
4. No ice baskets in the lower ice condenser plenum opposite the inlet doors.


The primary objective of these tests was to determine the transient heat transfer and fluid flow performance of the ice condenser design and to confirm that conclusions derived from previous Waltz Mill tests had not been significantly changed by the redesign of plant hardware. Consequently, the design of the test hardware was configured to provide heat transfer and fluid flow characteristics which were equivalent to those in the plant design. It should be noted that test hardware was not representative of structural characteristics for the plant design since structural response to blowdown was not one of the test objectives. In addition, responses of lower, intermediate, and upper deck doors to blowdown were not included in the test objectives.

#### **14.3.4.5.2.2.2 Test Facility**

The Waltz Mill Ice Condenser Blowdown Facility consists of a boiler, receiver vessel, and instrumentation room, and also ice storage and ice machine rooms which are used in conjunction with the ice technology facility. Figure 14.3.4-150 shows the general arrangement of the facility. The boiler and receiver vessels are connected by a 12" schedule 160 pipe in which is located a rupture disc assembly.

The boiler is 3 feet in diameter and 20 feet long, mounted on a structural frame. It can be heated electrically to pressurize a maximum of 117 cubic feet of water to an allowable maximum of 1586 psig pressure at 600°F. Strip heaters mounted on the outside of the boiler shell provide the heat. The flow rate from the boiler is controlled by an orifice located in the piping between the boiler and receiver vessel.

## UFSAR Revision 30.0

 An AEP Company	<p style="text-align: center;"><b>INDIANA MICHIGAN POWER</b> <b>D. C. COOK NUCLEAR PLANT</b> <b>UPDATED FINAL SAFETY ANALYSIS REPORT</b></p>	<p>Revised: 29.0 Section: 14.3.4.5 Page: 10 of 33</p>
---	--	---

The 12" piping between the boiler and receiver vessel is heated by strip heaters attached to the outside surface of the pipe. Figure 14.3.4-151 shows the piping is arranged into three sections as far as flow and heater capability are concerned. This permits operating the piping and sections of the piping at various subcooled temperatures relative to the boiler.

Figure 14.3.4-152 shows the internal arrangement of the receiver vessel. The ice chest section contains eight ice baskets, 12" diameter by 36 feet high, arranged in a 2 x 4 array. Lattice frames are located at six foot levels of the ice baskets. The baskets set on a lower support structure with flow blockage areas proportional to the plant. Turning vanes are located below the ice baskets and direct the flow entering the lower inlet up through the ice baskets. The vessel is divided into lower and upper compartments. The flow enters the lower compartment from the 12" pipe diffusers, is directed into the ice chest, past the ice baskets and then vents into the upper compartment. The ice chest is wood. All metal surfaces are insulated to limit the heat transfer to these surfaces.


Figure 14.3.4-153 shows the location and typical arrangement for the temperature and pressure measurements that will be made inside the receiver vessel ice chest. The outputs from the transducers are connected to a data acquisition system with scanning rates of 2000 samples per second or 200 samples per second.

### **14.3.4.5.2.2.3 Test Procedure**

The ice baskets are filled in the penthouse at the top of the receiver vessel by a blower system before being lowered into the ice chest. Prior to installing ice baskets, the receiver vessel and building is cooled down by an air recirculation and refrigeration system. A lattice frame is installed after each six foot array of ice baskets and a hold down bar attached through the ice chest walls to prevent basket uplift. After all baskets are installed, the receiver vessel top manhole is closed and the boiler then brought to test conditions.

The boiler is evacuated and filled with demineralized water and the heatup started by energizing the strip heaters. As the water heats in the boiler and expands, it is vented through a letdown heat exchanger. The initial fill of the boiler is measured as well as the water relieved so that the total amount of water in the boiler and piping is always known. Water is circulated between the boiler and downstream piping during heatup by the recirculation system to the various sections of the 12" piping (Figure 14.3.4-151). Subcooled conditions can, thus, be obtained for the water preceding the saturated water in the boiler itself. By using the heaters, recirculating systems, and letdown system, test energy conditions are obtained.

## UFSAR Revision 30.0

 An AEP Company	<p style="text-align: center;"><b>INDIANA MICHIGAN POWER</b> <b>D. C. COOK NUCLEAR PLANT</b> <b>UPDATED FINAL SAFETY ANALYSIS REPORT</b></p>	<p>Revised: 29.0 Section: 14.3.4.5 Page: 11 of 33</p>
---	--	---

The flow from the boiler and subcooled piping to the receiver vessel is controlled by an orifice plate located in front of the rupture disc assembly. By varying the size of orifice, the blowdown rate can be changed in accordance with the test plans. It is calculated that the maximum orifice required is 5.5".

After the boiler has reached test pressure and temperature, the blowdown is initiated by the rupture disc assembly. This is a double disc assembly with the pressure between the discs normally at about half the boiler operating pressure. The rupture disc burst pressure rating is 60 - 75% of the boiler operating pressure. The pressure between the discs is provided by a high pressure gas cylinder of nitrogen. At blowdown, the gas pressure is quickly released from the cavity between the discs by venting it into the downstream side of the rupture disc, causing the discs to rupture and the water upstream of the discs to be released into the receiver vessel.

At the time the pressure is started to vent from between the rupture discs, the data acquisition systems is actuated so that data is recorded throughout the blowdown transient. Data recording continues for ten seconds at high speed and then is reduced to a 1/10 speed for five minutes.


A preliminary set of test conditions is presented in Table 14.3.4-37.

### **14.3.4.5.2.2.4 Results**

Confirmation of the predicted ice condenser pressure performance was determined by comparing test results with TMD code predictions for the appropriate test conditions and configuration. Initially, the TMD code predictions were based on assumptions that provided best agreement with previous Waltz Mill test results (e.g., 30% entrainment).

The TMD Code has, as a result of the 1973 test series, been modified to match ice bed heat transfer performance.

# UFSAR Revision 30.0

 An AEP Company	<p style="text-align: center;">INDIANA MICHIGAN POWER D. C. COOK NUCLEAR PLANT UPDATED FINAL SAFETY ANALYSIS REPORT</p>	<p>Revised: 29.0 Section: 14.3.4.5 Page: 12 of 33</p>
---	---	---

## **14.3.4.5.3 Short Term Containment Response**

### **14.3.4.5.3.1 Results Based on 1973 Waltz Mill Tests**

A number of analyses have been performed to determine the various pressure transients resulting from hot and cold leg reactor coolant pipe breaks in any one of the six lower compartment elements. The analyses were performed using the following assumptions and correlations:

1. Flow was limited by the unaugmented critical flow correlation.
2. The TMD variable volume door model, which accounts for changes in the volumes of TMD elements as the door opens, was implemented.
3. The heat transfer calculation used was based on performance during the 1973-74 Waltz Mill test series. A higher value of the ELJAC parameter has been used and an upper bound on calculated heat transfer coefficients has been imposed (see Reference 3).

### **14.3.4.5.3.2 Subcritical Flow Model Studies**

For high Mach number subsonic flow, the TMD momentum equation incorporates a compressibility multiplier to account for compressibility effects resulting from area changes, and uses an average density along constant area flow paths.


With these modifications, both inertial and density effects are modeled by the TMD computer code.

A description of the compressibility multiplier, its derivation and application, is presented in this section. A brief description of the method by which the polytropic exponent (a necessary parameter in the compressibility multiplier approach) is calculated is also provided.

These effects have been examined for the D. C. Cook plant short term transient analysis by comparing previous analyses where these methods were not used to analyses using these methods.

For the plant the worst case RCS pipe break is a DEHL rupture in the lower compartment element 6. Results are presented also, for comparison purposes, for a DECL rupture in element 6.

The results of the short term pressure analysis are summarized in Table 14.3.4-38. The values given in parentheses are those pressures calculated on the same basis but without using a compressibility multiplier. As can be seen from the table, the effects of the modifications to the TMD code are minimal.

 <p><b>INDIANA MICHIGAN POWER</b> <small>An AEP Company</small></p>	<p align="center"><b>INDIANA MICHIGAN POWER D. C. COOK NUCLEAR PLANT UPDATED FINAL SAFETY ANALYSIS REPORT</b></p>	<p>Revised: 29.0 Section: 14.3.4.5 Page: 13 of 33</p>
--	---	---

Consideration was given to determining the effect of a varying polytropic exponent of the flow mixture across the throat section of a flow path. This was done by lowering the steam-water polytropic exponent calculated by the code by 5, 10 and 20%. The lowered polytropic exponent variance computer runs were made for a DEHL break in lower compartment element #6. The results are presented in Table 14.3.4-39 and it is apparent that the polytropic exponent variance has virtually no effect on the results.

#### **14.3.4.5.3.3 Derivation of the Compressibility Multiplier**

The system under study is shown in Figure 14.3.4-154. The flow assumptions are:

1. Steady flow
2. Zero gravity effects
3. Isentropic conditions
4. Fluid is an ideal gas
5. Channel wall is non-conducting (no heat transfer)

The resulting compressibility multiplier is:

$$y = \left[ r^{2/\gamma} \left( \frac{\gamma}{\gamma-1} \right) \left( \frac{(1-r) \left( \frac{\gamma-1}{\gamma} \right)}{1-r} \right) \right]^{1/2} \left[ \frac{1-B^4}{1-B^4 r^{2/\gamma}} \right]^{1/2}$$

The choked mass flow rate is:

$$\dot{m} = ay \left[ \frac{2g\rho_1(P_1 - P_2)}{1-B^4} \right]^{1/2}$$


where

$$B = (a/A)^{1/2}$$

We next apply the compressibility multiplier to the friction term of the TMD momentum equation written as:

$$\Delta P = \left( \frac{K + f_1/D}{2\rho g} \right) \left( \frac{\dot{m}^2}{a^2} \right) \quad (3)$$

## UFSAR Revision 30.0

 An AEP Company	<b>INDIANA MICHIGAN POWER</b> <b>D. C. COOK NUCLEAR PLANT</b> <b>UPDATED FINAL SAFETY ANALYSIS REPORT</b>	Revised: 29.0 Section: 14.3.4.5 Page: 14 of 33
---	---	--

Incorporating the compressibility multiplier into the TMD momentum equation, eqn. (3) takes on the form:

$$\Delta P = \frac{(K + f_1 / d) \dot{m}^2}{2 \rho g y^2 a^2} \quad (4)$$

Coupling eqn. (4) with the inertia term presently used in TMD, the momentum equation for general flow systems (non-steady state) appears as:

$$\Delta P = \frac{L}{A} \frac{dm}{dt} + \frac{(K + f_1 D) \dot{m}^2}{2 \rho g y^2 a^2} \quad (5)$$

It should be noted that the TMD (Reference 14) computer code also employs a critical flow correlation as a check on sonic flow conditions. This critical flow correlation has not been modified as a result of this present work.

The compressibility multiplier as it is used in eqn. (4) (and in TMD) is calculated by the code; the only information needed as input is the B factor.


The polytropic exponent is also calculated within the code, dependent upon the flow mixture conditions.

### **14.3.4.5.3.4 Choked Flow Characteristics**

The data in Figure 14.3.4-155 illustrate the behavior of mass flow rate as a function of upstream and downstream pressures, including the effects of flow choking. The upper plot shows mass flow rate as a function of upstream pressure for various assumed values of downstream pressure. For zero back pressure ( $P_d = 0$ ), the entire curve represents choked flow conditions with the flow rate approximately proportional to upstream pressure,  $P_u$ . For higher back pressure, the flow rates are lower until the upstream pressure is high enough to provide choked flow. After the increase in upstream pressure is sufficient to provide flow choking, further increases in upstream pressure cause increases in mass flow rate along the curve for  $P_d = 0$ . The key point in this illustration is that flow rate continues to increase with increasing upstream pressure, even after flow choking conditions have been reached. Thus choking does not represent a threshold beyond which dramatically sharper increases in compartment pressures would be expected because of limitations on flow relief to adjacent compartments.

The phenomenon of flow choking is more frequently explained by assuming a fixed upstream pressure and examining the dependence of flow rate with respect to decreasing downstream pressure. This approach is illustrated for an assumed upstream pressure of 30 psia as shown in

## UFSAR Revision 30.0

 An AEP Company	<p style="text-align: center;"><b>INDIANA MICHIGAN POWER</b> <b>D. C. COOK NUCLEAR PLANT</b> <b>UPDATED FINAL SAFETY ANALYSIS REPORT</b></p>	<p>Revised: 29.0 Section: 14.3.4.5 Page: 15 of 33</p>
---	--	---

the upper plot with the results plotted vs. downstream pressure in the lower plot. For fixed upstream conditions, flow choking represents an upper limit flow rate beyond which further decreases in back pressure will not produce any increase in mass flow rate.

The augmented choked flow relationship used in TMD is based on experimental data obtained for choked two-phase flow through long tubes, short tubes, and nozzles. The short tube data was cited by Henry and Fauske in Reference (16). Henry and Fauske conclude that an identical discharge coefficient may be applied to two-phase critical flow through sharp-edged orifices and short tubes to represent the actual critical flow rate through each geometry. On this basis, since the augmented choked flow correlation is based on short-tube data, it is applicable to sharp-edged orifices as well. Figure 14.3.4-156, from Reference (17), presents experimental data for two phase critical flow through several different geometries. The dashed line on the graph represents the augmented homogeneous equilibrium critical flow relationship used in TMD. Below a quality of 0.2 the augmentation correlation is not applicable. 0.62 is the highest quality at which critical flow is calculated by TMD to occur in a major flow path following a DEHL break in the Cook containment. It is apparent that the augmented critical flow calculated by TMD is conservative within the quality range of interest.


Carofano and McManus (18) have published data for the two-phase flow of air-water and steam-water mixtures. Actually, water vapor was present in the gas phase of the so-called air-water test, making it in effect an air-steam-water test. The data presented in Reference (18) demonstrates that the ratio of experimental air-(steam)-water critical flow values to homogeneous equilibrium model predictions is equal to or greater than the ratio of steam-water experimental critical flow values to homogeneous equilibrium model predictions. Therefore augmentation factors derived by comparing steam-water data to the homogeneous equilibrium model may be used in air-steam-water calculations.

### **14.3.4.5.3.5 Early Sensitivity Studies**

The TMD computer code was used to establish peak pressures and peak pressure differentials for double-ended hot and cold leg breaks, double-ended steam line breaks in the steam generator and fan room enclosures, a 6 inch spray line break for the pressurizer enclosure, and a single-ended pipe break in the reactor cavity of the D. C. Cook Plant. These cases were analyzed with and without augmentation of the calculated homogeneous equilibrium critical mass flow rates, to study the sensitivity of compartment pressures to augmentation. The double-ended hot leg break was assumed to occur in node 6, and the double-ended cold leg break was assumed to occur in node 1 of the TMD model network given in Figure 14.3.4-20. These were the worst locations for a hot leg and a cold leg break, respectively.



## UFSAR Revision 30.0

 An AEP Company	<p style="text-align: center;"><b>INDIANA MICHIGAN POWER</b> <b>D. C. COOK NUCLEAR PLANT</b> <b>UPDATED FINAL SAFETY ANALYSIS REPORT</b></p>	<p>Revised: 29.0 Section: 14.3.4.5 Page: 16 of 33</p>
---	--	---

The pressure response to a hot leg break is only slightly affected by augmentation; the cold leg break pressure response exhibits significant sensitivity to augmentation. Since the hot leg break parameters are limiting for the D. C. Cook Plant, omitting augmentation increases the design basis peak operating deck  $\Delta P$  less than 5%.

No change in the compartment peak pressures or pressure differentials occurred when unaugmented critical flow was used in analyzing the D. C. Cook Plant fan room and steam generator enclosure. Removing augmentation increased the peak pressure and the peak differential pressure in the pressurizer enclosure by 27% and 25%, respectively, in the upper reactor cavity by 17.5% and 19.5%, respectively, and in the lower reactor cavity by 13% and 8%, respectively.

The reason that there is no change in the peak pressures in the steam generator enclosure is that both the peak pressure and peak differential pressure are due to inertia. The fan room pressures remain constant because of high resistances in the flow paths from the fan room to the lower compartment which prevent choking.

In the reactor cavities and pressurizer enclosure, peak pressures occur in the transient coincidental with choking, and therefore a significant change in calculated pressures will occur when the critical flow model is changed (see Table 14.3.4-40).


A number of analyses have been performed using 100 percent moisture entrainment to determine the various pressure transients resulting from hot and cold leg reactor coolant pipe breaks in any one of the six lower compartment elements. The maximum peak pressure and differential pressure for all cases have been determined for each compartment element. Figure 14.3.4-157 is representative of the upper and lower compartment pressure transients that result from a hypothetical double ended rupture of a reactor coolant pipe for the worst possible location in the lower compartment of the containment, a hot leg break (DEHL) in element 6.

In addition, a series of TMD runs investigated the sensitivity of peak pressures to variations in individual input parameters for the design basis blowdown rate and 100% entrainment. This analysis used a DEHL break in element 6, and investigated effects from blowdown sensitivity to addition of the compressibility factor in the momentum equation. Table 14.3.4-36 gives these results.

The sensitivity study results demonstrate that variations in the plant geometric parameters and in ice bed loss coefficients, both of which are known with a high degree of accuracy, have little effect on the peak pressure calculated by TMD for DEHL break in element 6. However, variations in blowdown and entrainment, which are not known with great accuracy, greatly affect



# UFSAR Revision 30.0

 An AEP Company	<p style="text-align: center;"><b>INDIANA MICHIGAN POWER</b> <b>D. C. COOK NUCLEAR PLANT</b> <b>UPDATED FINAL SAFETY ANALYSIS REPORT</b></p>	<p>Revised: 29.0 Section: 14.3.4.5 Page: 17 of 33</p>
---	--	---

the pressure calculated. The highly conservative values used in the design basis analysis ensure a conservative prediction of the peak break compartment pressure.

#### **14.3.4.5.4 Ice Condenser Performance Criteria**

The performance of the ice condenser containment is demonstrated by results and analysis of ice condenser tests performed on a full-scale section test at the Westinghouse Waltz Mill Site. These tests confirmed the ability of the ice condenser to perform satisfactorily over a wide range of conditions, exceeding the range of conditions that might be experienced in an accident inside the containment.

The ice condenser containment performance has been evaluated by testing the following important parameters. A partial list of parameters tested include blowdown rate, blowdown energy, deck leakage, compression ratio, drain performance, ice condenser hydraulic diameter, dead-ended volumes and long term performance. Analytic models have been developed to correlate and supplement these test results in the evaluation of the containment design. The results indicate that the analytical models are conservative and that the performance of the ice condenser containment is predictable relative to these variables.

The layout of the reactor containment compartments and ice condenser provides for effective and efficient use of the ice condenser to suppress pressure buildup.

The lower (Reactor Coolant System) compartment is bounded by the divider barrier such that essentially all of the energy released in this compartment is directed through doors at the bottom of the ice condenser.


Seals are provided on the boundary of compartments and hatches in the operating deck to prevent steam from bypassing the ice condenser.

Layout, size, and flow communication among compartments is arranged to minimize the containment volume compression ratio.

The ice bed geometry provides sufficient ice heat transfer area and flow passages so that the magnitude of the pressure transient resulting from an accident does not exceed the containment design pressure for all reactor coolant pipe breaks sizes up to and including the hypothetical double-ended severance of the reactor coolant piping.

The initial containment peak pressure and peak asymmetrical containment pressure loads are determined by analysis. The analytical results are experimentally verified by comparison with the ice condenser tests. This analysis supplements the experimental proof of performance tests and provides pressure transients for application of the plant design.

## UFSAR Revision 30.0

 An AEP Company	<b>INDIANA MICHIGAN POWER</b> <b>D. C. COOK NUCLEAR PLANT</b> <b>UPDATED FINAL SAFETY ANALYSIS REPORT</b>	Revised: 29.0 Section:14.3.4.5 Page: 18 of 33
---	---	---

The final peak pressure occurring at or near the end of blowdown is determined by a containment volume air compression calculation. A method of analysis of the final peak pressure was developed based on the results of full-scale section tests.

Steam bypass of the ice condenser during the postulated RCS blowdown is to be avoided. The divider deck and any other leakage paths between the lower and upper compartments are reasonably sealed to limit bypass steam flow. For the containment, the analysis considered bypass area as composed of two parts: a conservatively assumed leakage area around the various hatches in the deck, and a known leakage area through the deck drainage holes for spray located at the bottom of the refueling cavity.


Flow distribution to the ice condenser for any RCS pipe rupture that opens the ice condenser inlet doors, up to and including the double-ended RCS pipe rupture, is limited such that the maximum energy input into any section of the ice condenser does not exceed its design capability. The door port flow resistance and size provides this flow distribution for breaks that fully open the ice condenser inlet doors. For breaks that partially open the inlet doors, the lower inlet doors proportion flow into the ice bed limiting maldistribution.

For large pipe breaks, the containment final peak pressure is mainly determined by the displacement of air from the lower compartment into the upper compartment. Only a small amount of steam bypasses the ice condenser by passing through the operating deck and into the upper compartment. This steam bypass then adds a small amount to the final peak pressure.

For small pipe breaks, which generate less than the pressure drop required to fully open the spring-hinged, ice condenser inlet doors and result in the door performance being in the flow proportioning range, a larger than normal fraction of the break flow will pass through the deck by way of the divider deck bypass area and into the upper compartment. Unlike a postulated large break, which sweeps all of the air out of the lower compartment, the smaller breaks do not. Below some break size, only a portion of the lower compartment air will be displaced by the break flow. Also, for breaks less than approximately 10,000 gpm, the ice condenser inlet doors will open; however, only a fraction of the air may be displaced from the lower compartment by the incoming steam. For these small energy release rates, operation of the containment spray system eventually is required to limit the containment pressure rise.

Another case has been examined where it is postulated that a small break loss-of-coolant accident precedes a larger break accident which occurs before all of the coolant energy is released by the small break, (i.e., a double accident). During the small break blowdown, some quantity of steam and air will bypass the ice condenser and enter the upper compartment via

## UFSAR Revision 30.0


 An AEP Company	<p style="text-align: center;"><b>INDIANA MICHIGAN POWER</b> <b>D. C. COOK NUCLEAR PLANT</b> <b>UPDATED FINAL SAFETY ANALYSIS REPORT</b></p>	<p>Revised: 29.0 Section: 14.3.4.5 Page: 19 of 33</p>
---	--	---

leakage in the divider deck. The important design requirement for the case of a double accident is that the amount of steam leakage into the upper compartment must be limited during the first part (small break) of the accident so that only a small increase in final peak pressure results for the second part (double-ended break) of the postulated accident. The steam which reaches the upper compartment will then add to the peak pressure for the second part of the accident. Therefore, the containment spray system is used to limit the partial pressure of steam in the upper compartment due to deck bypass. The key elements which determine the double accident performance are the ice condenser lower doors, which open at a low differential pressure to admit steam to the ice condenser and limit the bypass flow of steam and thus the partial pressure of steam in the upper compartment, and the sprays which condense this bypass flow of steam and limit the partial pressure of steam in the upper compartment to a low value, less than 2 psia. The containment spray set point actuation pressure has been set at 3 psig to limit steam partial pressure to less than 2 psia in the upper compartment for the double accident use.

After a LOCA, the ice condenser has sufficient remaining heat absorption capacity such that, together with the containment spray system, subsequent assumed heat loads are absorbed without exceeding the containment design pressure. The subsequent heat loads considered include reactor core and coolant system stored heat, residual heat, substantial margin for an undefined additional energy release, and consideration of steam generators as active heat sources.

The primary purpose of the Containment Spray System is to spray cool water into the containment atmosphere in the event of a loss-of-coolant accident, thereby ensuring that containment pressure cannot exceed the containment design pressure. Protection is afforded for all pipe break sizes up to and including the hypothetical instantaneous circumferential rupture of a reactor coolant pipe. Adequate containment heat removal capability for the Ice Condenser Containment is provided by two separate full capacity containment spray systems. The Containment Spray System is designed based on the conservative assumption that the core residual heat is continuously released to the containment as steam, eventually melting all ice in the ice condenser. The heat removal capability of each spray system is sized to keep the containment pressure below design after all the ice has melted and residual heat generated steam continues to enter the containment. The spray system is designed to keep the pressure below the design pressure with adequate margin.

# UFSAR Revision 30.0

 An AEP Company	<p style="text-align: center;"><b>INDIANA MICHIGAN POWER</b> <b>D. C. COOK NUCLEAR PLANT</b> <b>UPDATED FINAL SAFETY ANALYSIS REPORT</b></p>	<p>Revised: 29.0 Section: 14.3.4.5 Page: 20 of 33</p>
---	--	---

## **14.3.4.5.4.1 Inlet Door Performance**

### **14.3.4.5.4.1.1 Introduction**

The ice condenser inlet doors form the barrier to air flow through the inlet ports of the ice condenser for normal plant operation. They also provide the continuation of thermal insulation around the lower section of the crane wall to minimize heat input that would promote sublimation and mass transfer of ice in the ice condenser compartment. In the event of a loss-of-coolant incident that would cause a pressure increase in the lower compartment, the doors open, venting air and steam relatively evenly into all sections of the ice condenser.


The inlet doors are essentially pairs of insulated composite panels vertically hinged to a rectangular shaped angle section frame that has a center post. This assembly is fastened to the crane wall support columns which frame the ports through the crane wall from the containment lower compartment to the ice condenser compartment.

The door panels are made of composite steel sheets and urethane foam construction, comprising a total thickness of 7 inches to provide proper insulating characteristics. Each door is mounted to the frame with ball bearing hinges. The door panels are normally held shut against a bulb type gasket seal by the differential pressure produced by the higher density cold air of the ice condenser, sealing against loss of the ice condenser air to the lower compartment.

The door panels are provided with tension spring mechanisms that produce a small closing torque on the door panels as they open. The magnitude of the closing torque is equivalent to providing a one pound per square foot pressure drop through the inlet ports with the door panels open to a position that develops full port flow area.

The zero load position of each spring mechanism is set so that with zero differential pressure across the door panels the gasket seal holds the door slightly open. This provides assurance that all doors will be open slightly and relatively uniformly, prior to development of sufficient lower compartment pressure to cause flow into the ice condenser, therefore eliminating significant inlet maldistribution for very small incidents. For larger incidents the doors open fully and flow distribution is controlled by the inlet ports.

# UFSAR Revision 30.0

 An AEP Company	<p style="text-align: center;"><b>INDIANA MICHIGAN POWER</b> <b>D. C. COOK NUCLEAR PLANT</b> <b>UPDATED FINAL SAFETY ANALYSIS REPORT</b></p>	<p>Revised: 29.0 Section: 14.3.4.5 Page: 21 of 33</p>
---	--	---

## **14.3.4.5.4.1.2 Design Criteria**


### Normal Operation

- a. Doors shall be instrumented to allow remote monitoring of their closed position.
- b. Doors shall be capable of being inspected to determine that they are functioning properly.
- c. The inlet doors shall limit the leakage of air out of the ice condenser to the minimum practical limit.
- d. The inlet doors shall restrict the heat input into the ice condenser to the minimum practical limit.
- e. Normal maintenance and inspection must be performed in a manner that does not hinder the ice condenser performance or availability.

### Accident Conditions

- a. All doors shall open to allow venting of energy to the ice condenser for any leak rate which results in a divider deck differential pressure in excess of the ice condenser cold head.  
  
The force required to open the doors of the ice condenser is sufficiently low such that the energy from any leakage of steam through the divider barrier can be readily absorbed by the containment spray system without exceeding containment design pressure.
- b. Doors and door ports shall limit maldistribution to 150% maximum, peak to average mass input for the accident transient which provides adequate margin in the design ice bed loadings. This is used for any reactor coolant system energy release of sufficient magnitude to cause the doors to open. The inlet doors of the ice condenser are designed to open and distribute steam to the ice condenser in accordance with design basis above, for any postulated loss-of-coolant accident.
- c. The doors are designed to eliminate the possibility of doors remaining closed, even for small break conditions. In particular, two degrees of freedom of rotation are incorporated in the hinges and the sealing gasket is designed to pull out for a postulated condition of sticking. The gasket material is itself selected to prevent sticking.

## UFSAR Revision 30.0

 An AEP Company	<p style="text-align: center;"><b>INDIANA MICHIGAN POWER</b> <b>D. C. COOK NUCLEAR PLANT</b> <b>UPDATED FINAL SAFETY ANALYSIS REPORT</b></p>	<p>Revised: 29.0 Section: 14.3.4.5 Page: 22 of 33</p>
---	--	---

- d. The basic performance requirement for lower inlet doors for design basis accident conditions is to open rapidly and fully, to ensure proper venting of released energy into the ice condenser. The opening rate of the inlet doors is important to ensure minimizing the pressure buildup in the lower compartment due to the rapid release of energy to that compartment.
- e. Ice condenser doors shall be protected from direct steam jet following a postulated steam line break.

### **14.3.4.5.4.1.3 Performance Capability**

#### Normal Operation

The normal operation mode for the ice condenser inlet doors is to serve as an insulated barrier to natural convection heat and air flow through the ice bed, providing a sufficient insulating value to limit heat input into the ice bed. In addition the design and performance of the doors must be consistent with ensuring continuous availability of the ice condenser function.

The importance of normal operation criteria is the establishment of design parameters that provide for long term ice bed life, and for constant ice condenser availability for plant protection. In this context two inlet door design parameters affect these factors. They are heat conductivity and leak tightness.


Heat input is the parameter of prime concern, as it is the major factor influencing ice bed sublimation. Leakage out of the ice bed has been reduced to an insignificant amount. The heat input is a calculated value using a two dimensional heat conductance computer program that has been verified by tests.

The inlet door leakage is predicted by tests to be significantly less than the 50 CFM total used for the ice condenser design. This predicted leakage value has negligible effect on reinforcing the convective flow developed in the ice bed, therefore not affecting sublimation rates significantly. The effect of the make-up air entering the ice condenser due to this leakage is also negligible on refrigeration load or ice condenser air handling unit coil defrost frequency.

Seismic analyses associated with response data for the Cook Nuclear Plant shows that the ice condenser inlet doors will not be opened by the maximum seismic forces. This is due to the very low frequency of the rotational or opening mode, at which the response is negligible, and the ice condenser cold head pressure holds the doors closed.

Figure 14.3.4-158 shows the door opening characteristics as a function of door differential pressure based on a linear spring constant. Notably, there is no special significance to be

## UFSAR Revision 30.0

 An AEP Company	<b>INDIANA MICHIGAN POWER</b> <b>D. C. COOK NUCLEAR PLANT</b> <b>UPDATED FINAL SAFETY ANALYSIS REPORT</b>	Revised: 29.0 Section: 14.3.4.5 Page: 23 of 33
---	---	--

attached to a linear spring constant, and detail design of the door and spring system indicated that non-linear spring characteristics changed the release rate at which maximum maldistribution would occur, but did not change the maximum maldistribution value. The performance characteristics to be expected from the inlet doors would be typical of those shown in Figure 14.3.4-158.

The effect of maximum variation of door proportioning characteristics indicates significantly less maldistribution than the 150% limit.

Importantly, and as discussed in other reports, the ratio of maximum to average flow of steam into the ice condenser for pipe break sizes large enough to fully open the doors is limited by the door ports themselves to a reasonably low value, about 116 percent of the average.

The equilibrium position of the inlet door panels with zero differential pressure is slightly open (about 3/8 inch), which provides a small flow area at each door for uniform inlet flow into each segment of the ice bed. The doors are designed to eliminate the possibility of doors remaining closed, even for small break conditions. In particular two degrees of freedom of rotation are incorporated in the hinges, and the sealing gasket is designed to pull out for a postulated condition of sticking. The gasket material is itself selected to prevent sticking.

Consideration is, however, given in the analysis of ice condenser performance to a hypothetical case of stuck doors at which the most severe of the above postulated malfunctions is overcome by the force on the door. Even in this hypothetical case the door panels would rupture, providing a sufficient flow path into the ice condenser to permit the ice condenser to function to limit containment pressure below design limits.


It is recognized that the springs are an important part of the lower ice condenser doors. These spring assemblies are designed such that the failure of any spring will not significantly change the operating characteristics of the ice condenser doors. This objective has been achieved in a practical manner by the use of four separate tension springs per door, which provides redundancy and assures adequate opening characteristics.

### Accident Conditions

The basic lower inlet door performance requirement for design basis accident conditions is to open rapidly and fully, to insure proper venting of released energy into the ice condenser. The opening rate of the inlet doors is important to insure minimizing the pressure buildup in the lower compartment due to the rapid release of energy to that compartment. The rate of pressure rise and the magnitude of the peak pressure in any lower compartment region is related to the



## UFSAR Revision 30.0

 An AEP Company	<p style="text-align: center;"><b>INDIANA MICHIGAN POWER</b> <b>D. C. COOK NUCLEAR PLANT</b> <b>UPDATED FINAL SAFETY ANALYSIS REPORT</b></p>	<p>Revised: 29.0 Section: 14.3.4.5 Page: 24 of 33</p>
---	--	---

confinement of that compartment, and in particular the active volume and flow restrictions out of that compartment. The time period to reach peak lower compartment pressure due to the design basis accident is a fraction of a second. It is dependent upon flow restrictions and proximity to the break location. The opening rate of the inlet doors is wholly dependent upon the inertia of the door and the magnitude of the forcing function, which is the pressure buildup in the lower compartment due to the energy release. The ice condenser inlet door inertia is slightly less than the doors tested in the ice condenser full scale section tests. These tests demonstrate that door inertia has essentially no effect on the initial peak pressure.

The maximum inlet door structural loading is due to the design basis accident for the doors adjacent to the lower compartment in which the release occurs. Structural analysis for maximum loaded conditions shows that all door members remain well below allowable stress levels. Further verification of the structural adequacy of the door is provided by the proof load testing carried out on the full prototype doors.

The necessary performance of the ice condenser is further ensured by the door design incorporating a low pressure fail open characteristic. Even if it is postulated that the doors were held rigidly along the bottom edge, they would fail open at a differential pressure sufficiently low to allow venting from the lower compartment well within the limits of pressure capability of the structures.

#### **14.3.4.5.4.2 Top and Intermediate Deck Door Performance**


The doors enclosing the top of the ice condenser and forming the roof of the upper plenum are of a non-rigid design lighter than the intermediate deck doors. These top doors are supported by the ice condenser bridge crane support structure. The crane support structure consists of radial beams spanning the ice condenser annulus at the top of the crane wall.

The intermediate deck doors enclose the ice compartment and forming the floor of the upper plenum. These doors are supported by the lattice frame support columns.

The intermediate deck door panels are a 2 1/2 inch foam plastic core with bonded sheet metal facings. These doors are hinged horizontally and are normally closed. The top deck doors are flexible foam bonded to high strength foil steel. These doors are hinged (clamped) on the crane wall side of the top deck and are normally closed. On an increase in pressure in the ice condenser compartment, these doors will open as required, allowing air to flow into the upper containment volume.



## UFSAR Revision 30.0

 An AEP Company	<p style="text-align: center;">INDIANA MICHIGAN POWER D. C. COOK NUCLEAR PLANT UPDATED FINAL SAFETY ANALYSIS REPORT</p>	<p>Revised: 29.0 Section: 14.3.4.5 Page: 25 of 33</p>
---	---	---

### **14.3.4.5.4.2.1 Design Criteria**

#### Normal Operations

1. The top deck will be provided with a total vent area of approximately 20 ft<sup>2</sup>.
2. Doors will limit heat input within their immediate vicinity to the minimum practical limit.
3. Doors will be capable of being inspected during plant shutdown to determine that they are functioning properly.

#### Accident Conditions


1. All doors will open fully for a low differential pressure loading.
2. All doors will be light-weight to have a minimum effect on the initial peak pressure.
3. Doors will be of simple mechanical design to minimize the possibility of malfunction.
4. Doors will not be required to remain either open or closed following an accident.

### **14.3.4.5.4.2.2 Performance Capability**

On an increase in pressure in the ice condenser compartment, these doors will open as required to allow air to flow into the upper compartment. The primary design criterion for these doors is their insulating capability to limit heat flow. The flow area provided by the open doors is that area available in the compartment, considering area reduction by support structures. Both the inertia of the door with the desired insulation capability and the available flow area have been modeled in the ice condenser door tests.

The mean heat input to the plenum through the top deck is about 4.5 Btu/hr-ft<sup>2</sup>. This heat input is removed from the plenum ambient by the ice condenser air handling units and does not affect ice bed sublimation. The effect of this heat load on refrigeration heat load and plenum ambient conditions has been investigated and provides for operation well within the ice condenser design operating parameters.

Incorporation of the vents imposes no operational problem to the ice condenser. The lower doors will effectively seal the ice condenser compartment and limit any flow of air through the compartment to a negligible value. Therefore tight seals are not necessary at the intermediate

 An AEP Company	<p style="text-align: center;"><b>INDIANA MICHIGAN POWER</b> <b>D. C. COOK NUCLEAR PLANT</b> <b>UPDATED FINAL SAFETY ANALYSIS REPORT</b></p>	<p>Revised: 29.0 Section: 14.3.4.5 Page: 26 of 33</p>
---	--	---

deck doors. A balanced flapper is provided to minimize migration of moisture into the ice condenser through the vents.

The open flow area through each deck for air flow due to an incident is slightly larger than the ice condenser test ratio equivalent, providing slightly less resistance to air flow. The slightly larger flow area does not produce any significant change in ice condenser performance, other than to assure flow resistances slightly less restrictive than the reference design.

The top and intermediate deck and doors have been analyzed for all loading combinations. This structural analysis shows that all members remain below allowable stress levels.

#### **14.3.4.5.4.3 Vent Design and Performance**


##### **14.3.4.5.4.3.1 Introduction**

The upper and intermediate doors are not required to remain open following the reactor coolant system blowdown and also are not required to open for small breaks. For these situations, a vent was provided through both the top and intermediate deck to allow air to flow into or from the ice condenser compartment as required. This vent air first passes into the fan cooler plenum at the top of the ice condenser compartment where it mixes with the cooling air. The temperature and humidity of the vent air that passes from this plenum into the ice condenser compartment are therefore about the same as the average temperature and humidity of the air in the condenser compartment.

Accordingly, sublimation or frosting in the ice bed due to this vent flow of air will be limited to a negligible value. Specific performance requirements are given below both for large breaks and for small breaks.

##### **14.3.4.5.4.3.2 Large Break Performance Requirements**

Following the reactor coolant system blowdown, the vents were designed to allow air to return from the upper compartment into the ice condenser without imposing an excessive pressure drop across the upper and intermediate doors. The maximum pressure decay rate and therefore the maximum reverse flow rate of air results from the case where reactor residual heat is not released to the containment following the reactor coolant system blowdown. The pressure decay for this case was measured in a full-scale section test. In this test, the pressure decayed from 6.2 psig to 4.5 psig during the one minute period immediately following the reactor coolant system blowdown. From this pressure decay rate, the plant equivalent flow rate of air was calculated to be 98 lbm/sec. This flow rate developed a pressure drop across each of the upper doors of 0.28 psi, which was well within the structural capability of the upper and intermediate doors and

 An AEP Company	<p style="text-align: center;"><b>INDIANA MICHIGAN POWER</b> <b>D. C. COOK NUCLEAR PLANT</b> <b>UPDATED FINAL SAFETY ANALYSIS REPORT</b></p>	<p>Revised: 29.0 Section: 14.3.4.5 Page: 27 of 33</p>
---	--	---

support structures. Further, in this calculation it was conservatively assumed that no air flowed through the deck or through the containment air recirculation fan duct.

#### **14.3.4.5.4.3 Small Break Performance Requirements**

For small breaks which generate less than the required opening pressure of the upper and intermediate doors, the vent was designed to limit the flow of steam through the deck to an acceptable level during the period of air flow through the condenser and into the upper compartment. For breaks less than approximately 5000 gpm, the full-scale section tests have shown that only a fraction of air is displaced from the lower compartment. The 20 sq. ft. vent area in both the top and intermediate deck provides a low resistance air flow path through the ice condenser to the containment upper compartment for these small break conditions.

#### **14.3.4.5.4.4 Drain Design and Performance**


##### **14.3.4.5.4.4.1 Introduction**

Drains are provided at the bottom of the ice condenser compartment to allow the melt-condensate water to flow out of the compartment during a loss-of-coolant accident. These drains are provided with check valves that are counter-weighted to seal the ice condenser during normal plant operation and to prevent steam flow through the drains into the ice condenser during a loss-of-coolant accident. These check valves will remain closed against the cold air head (1 psf) of the ice condenser and open before the water level rises to the point where it can interfere with the operation of the lower inlet doors, as described in Chapter 5.3.

For a small pipe break, the water inventory in the ice condenser will be produced at a rate proportional to the rate of energy addition from the accident. The water collecting on the floor of the condenser compartment will then flow out through the drains and through the doors, which are open during the blowdown.

For a large pipe break, a short time (on the order of seconds) will be required for the water to fall from the ice condenser to the floor of the compartment. Therefore, it is possible that some water will accumulate at the bottom of the condenser compartment at the completion of the blowdown. Such water accumulation could exert a back pressure on the inlet doors, requiring an additional pressure rise in the lower compartment to open the doors and admit steam to the ice condenser. However, results of full-scale section tests indicated that, even for the design blowdown accident, a major fraction of the water drained from the ice condenser, and no increase in containment pressure was indicated even for the severe case with no drains.

## UFSAR Revision 30.0

 An AEP Company	<p style="text-align: center;"><b>INDIANA MICHIGAN POWER</b> <b>D. C. COOK NUCLEAR PLANT</b> <b>UPDATED FINAL SAFETY ANALYSIS REPORT</b></p>	<p>Revised: 29.0 Section: 14.3.4.5 Page: 28 of 33</p>
---	--	---

### **14.3.4.5.4.4.2 Large Break Performance Requirements**

A number of tests were performed with the reference flow proportional-type door installed at the inlet to the ice condenser, the reference-type hinged door installed at the top of the condenser. Tests were conducted with and without the reference water drain area, equivalent to 15 ft<sup>2</sup> for the plant,<sup>1</sup> at the bottom of the condenser compartment.

Tests were conducted with various assumed blowdown conditions. These tests were performed with the maximum reference blowdown rate, with an initial low blowdown rate followed by the reference rate, with a low blowdown rate alone, and with the maximum reference blowdown rate followed by the simulated core residual heat rate.

The results of all of these tests showed satisfactory condenser performance with the reference type doors, vent, and drain for a wide range of blow-down rates. Also, these tests demonstrate the insensitivity of the final peak pressure to the water drain area. In particular, the results of these full-scale section tests indicated that, even for the reference blowdown rate, and with no drain area provided, the drain water did not exert a significant back pressure on the ice condenser lower doors. This showed that a major fraction of the water had drained from the ice condenser compartment by the end of the initial blowdown. The effect of this test result is that containment final peak pressure is not affected by drain performance.

Although drains are not necessary for the large break performance, approximately 13 ft<sup>2</sup> of drain area are required for small breaks.

### **14.3.4.5.4.4.3 Small Break Performance Requirements**


For small breaks, water will flow through the drains at the same rate that it is produced in the ice condenser. Therefore, the water on the floor of the compartment will reach a steady height which is dependent only on the energy input rate.

To determine that the 12.63 ft<sup>2</sup> drain area met these requirements, the water height was calculated for various small break sizes up to a 30,000 gpm break. Above 30,000 gpm the ice condenser doors would be open to provide additional drainage. The maximum height of water required was calculated to be 2.2 ft above the drain check valve. Since this height resulted in a water level which was more than 1 ft below the bottom elevation of the inlet doors, it was

---

<sup>1</sup> As noted in Chapter 5.3.5.1.6., the D.C. Cook ice condenser floor drains have a flow area of approximately 18 ft<sup>2</sup>. Since the reference tests were performed at Waltz Mill both with and without the reference plant drain area of 15 ft<sup>2</sup>, the D.C. Cook ice condenser drain configuration is bounded by the reference tests.

## UFSAR Revision 30.0

 An AEP Company	<p style="text-align: center;"><b>INDIANA MICHIGAN POWER</b> <b>D. C. COOK NUCLEAR PLANT</b> <b>UPDATED FINAL SAFETY ANALYSIS REPORT</b></p>	<p>Revised: 29.0 Section: 14.3.4.5 Page: 29 of 33</p>
---	--	---

concluded that water will not accumulate in the ice condenser for this condition and that a 12.63 ft<sup>2</sup> drain will give satisfactory performance.

#### **14.3.4.5.4.4 Normal Operational Performance**

During normal plant operation, the sole function of the valve is to remain in a closed position, minimizing air leakage across the seat. To avoid unnecessary contamination of the valve seat, a 1 ½ -inch drain line is connected to the 12 inch line immediately ahead of the valve. Any spillage or defrost water will drain off without causing the valve to be opened.

Special consideration has been given in the design to prevent freezing of the check valves and to minimize check valve leakage.

To minimize the potential for valve freezing, a low conductivity (transite) section of pipe is inserted vertically below the seal slab, while the horizontal run of pipe (steel) is embedded in a warm concrete wall before it reaches the valve. The valve itself is in the upper region of the lower compartment, where ambient temperature is generally above the freezing temperature.

The valve is held in a closed position by virtue of its design as an almost vertical flapper with a hinge at the top. The slight (10°) angle from the vertical holds the flap in place by gravity.

To reduce valve leakage to an acceptable value, a sealant was applied to the seating surface after installation of the valves. Tests show that this will reduce leakage to practically zero. Maximum allowable leakage rate would be approached as a limit only if all the sealant were to disappear completely from all the valves, which is unlikely. Sealant is replaced as necessary.


#### **14.3.4.6 Changes from Base Containment Analyses: Note Concerning Tables and Figures**

If an evaluation or partial re-analysis is needed for some change from one of the base containment analyses of record, and this results in changes to information appearing in the UFSAR, a text description of the new work is provided here in Section 14.3.4. However, unless specifically indicated otherwise, the associated tables and figures for Section 14.3.4 are taken from the base analysis of record, and not any subsequent specific evaluation or partial re-analysis.

#### **14.3.4.7 References for Section 14.3.4**


1. Grimm, N.P. and Colenbrander, H. G. C., "Long Term Ice Condenser, Containment Code - LOTIC Code," WCAP-8354-P-A, September, 2017 (Proprietary) and WCAP-8355-A, September, 2017 (Non-Proprietary).

## UFSAR Revision 30.0

 <b>INDIANA MICHIGAN POWER</b> <small>An AEP Company</small>	<b>INDIANA MICHIGAN POWER D. C. COOK NUCLEAR PLANT UPDATED FINAL SAFETY ANALYSIS REPORT</b>	Revised: 29.0 Section:14.3.4.5 Page: 30 of 33
--	---	---

2. "Final Report Ice Condenser Full Scale Section Test at the Waltz Mill Facility," WCAP-8282, February, 1974 (Proprietary) and WCAP-8110, Supplement 6, May, 1974 (Non-Proprietary).
3. Letter from D. B. Black to B. A. Svensson, August 3, 1988, "Operation at Essential Service Water Temperatures Above 81°F."
4. Hsieh, T. and Raymond, M., "Long Term Ice Condenser Containment Code - LOTIC Code," WCAP-8354-P-A, Supplement 1, April, 1976 (Proprietary) and WCAP-8355, Supplement 1, April, 1976 (Non-Proprietary).
5. Deleted
6. NS-CE-1250, 10/22/76, C. Eicheldinger Letter to J. F. Stolz, NRC, Supplemental Information on LOTIC3 questions.
7. NS-CE-1453, 6/14/77, C. Eicheldinger letter to J. F. Stolz, NRC, Responses to LOTIC3 questions.
8. NS-CE-1626, 12/7/77, C. Eicheldinger letter to J. F. Stolz, NRC, Responses to LOTIC3 questions.
9. Hsieh, T. and Liparulo, N. J., "Westinghouse Long Term Ice Condenser Containment Code -LOTIC3 Code", WCAP-8354-P-A, Supplement 2, February 1979.
10. J. F. Stolz, NRC, to C. Eicheldinger, 5/3/78, "Evaluation of Supplement to WCAP-8354 (LOTIC3)."
11. J. F. Stolz, NRC, to C. Eicheldinger, 5/10/78, "Staff Approval of LOTIC3 Code."
12. Letter No. AEP-80-525, March 10, 1980 (F. Noon of Westinghouse to D. V. Shaller of AEPSC).
13. Letter, G. P. Maloney (AEP) to H. R. Denton (NRC), dated April 1, 1980 (Letter No. AEP:NRC:0131).
14. Salvatori, R. (approved), "Ice Condenser Containment Pressure Transient Analysis Methods," WCAP-8077, March, 1973 (Proprietary) and WCAP-8078, March, 1973 (Non-Proprietary).
15. Salvatori, R. (approved), "Ice Condenser Full Scale Section Test at the Waltz Mill Facility," WCAP-8110, Supplement 6, May, 1974.


## UFSAR Revision 30.0

 <b>INDIANA MICHIGAN POWER</b> <small>An AEP Company</small>	<b>INDIANA MICHIGAN POWER D. C. COOK NUCLEAR PLANT UPDATED FINAL SAFETY ANALYSIS REPORT</b>	Revised: 29.0 Section:14.3.4.5 Page: 31 of 33
--	---	---

16. Henry, R. E., and H.K. Fauske, "Two-Phase Critical Flow of One-Component Mixtures in Nozzles, Orifices, and Short Tubes," Journal of Heat Transfer, May, 1971, pp. 179-187.
17. Smith, R.V., USA Natl. Bur. of Standards Tech. Note No. 179, 1963.
18. Carofano, G.C. and H.N. McManus, "An Analytical And Experimental Study of the Flow of Air-Water and Steam-Water Mixtures in a Converging-Diverging Nozzle," Progress in Heat & Mass Transfer, Vol. 2, pp. 395-417.
19. Letter from John Tillinghast, Indiana & Michigan Power Co., to Edson G. Case, U.S. Nuclear Regulatory Commission, dated January 23, 1978.
20. Letter from G.P. Maloney, Indiana & Michigan Power Co., to Edson G. Case, U.S. Nuclear Regulatory Commission, dated February 27, 1978.
21. WCAP-8264-P-A, Rev. 1, "Westinghouse Mass and Energy Release Data for Containment Design," August 1975
22. "Westinghouse LOCA Mass and Energy Release Model for Containment Design - March 1979 Version," WCAP-10325-P-A, May 1983 (Proprietary), WCAP-10326-A (Non-Proprietary).
23. "Westinghouse Containment Analysis Methodology – PWR LOCA Mass and Energy Release Calculation Methodology," WCAP-17721-P, April 2013 (Proprietary), WCAP-17721-NP, April 2013 (Non-Proprietary).
24. ANSI/ANS-5.1-1979, "American National Standard for Decay Heat Power in Light Water Reactors," August 1979.
25. Moody, F.J., "Maximum flow Rate of Single Component, Two-Phase Mixture," ASME publication, Paper NO. 64-HT-35.
26. Burnett, T. W. T., et al., "LOFTRAN Code Description", WCAP-7907-A, April 1, 1984.
27. Zaloudek, F.R., "Steam-Water Critical Flow From High Pressure Systems," Interim Report, HW-68936, Hanford Works, 1964.
28. Henry, R.E., "A Study of One- and Two-Component, Two-Phase Critical Flows at Low Qualities," ANL-7430.




# UFSAR Revision 30.0

 <p><b>INDIANA MICHIGAN POWER</b> <small>An AEP Company</small></p>	<p align="center"><b>INDIANA MICHIGAN POWER D. C. COOK NUCLEAR PLANT UPDATED FINAL SAFETY ANALYSIS REPORT</b></p>	<p>Revised: 29.0 Section:14.3.4.5 Page: 32 of 33</p>
--	---	--


29. Henry, R.E., "An Experimental Study of Low-Quality, Steam-Water Critical Flow at Moderate Pressures," ANL-7740.
30. Kramer, F.W., "FLASH: A Program for Digital Simulation of the Loss-of-Coolant Accident," Westinghouse Atomic Power Division, WCAP-1678, January, 1961.
31. Zaloudek, F.R., "The Critical Flow of Hot Water Through Short Tubes," HW-77594, Hanford Works, 1963.
32. Deleted
33. Deleted
34. "Donald C. Cook Nuclear Plant Units 1 and 2, Modifications to the Containment Systems, Westinghouse Safety Evaluation, (SECL 99-076, Revision 3)", WCAP-15302, September, 1999 (Westinghouse Non-Proprietary Class 3)
35. AEP-99-329, September 29,1999; Ed Dzenis (Westinghouse Electric Company LLC) to Jim Hawley (American Electric Power), "Reconciliation of Design Information Transmittal DIT No. B-00003-06".
36. AEP-99-417, November 11,1999: E. Dzenis (Westinghouse Electric Company LLC) to G. Hill (American Electric Power), "Response to AEP Questions/Comments on Chapter 14.3.4 Mark-ups".
37. Land R. E., "Mass and Energy Releases Following a Steam Line Rupture" WCAP-8822 (Proprietary) and WCAP-8860 (Nonproprietary), September 1976; Osborne, M. P. and Love, D. S., "Mass and Energy Releases Following a Steam Line Rupture, Supplement 1 - Calculations of Steam Superheat in Mass/Energy Releases Following a Steamline Rupture," WCAP-8822-S 1-P-A (Proprietary) and WCAP-8860-S I-A (Nonproprietary), September 1986.
38. AEP-00-0142, May 9, 2000, W.R. Rice (Westinghouse Electric Company LLC) to Mr. Don Hafer (American Electric Power), "D.C. Cook Units 1 and 2: Containment Integrity Analysis Evaluation for Restart".
39. MD-1-SGRP-017-N "DC Cook Unit 1 RSG Safety Evaluation – Large Break LOCA B&W Replacement Steam Generators (Framatome Calculation No. 51-1266354 rev.1).




## UFSAR Revision 30.0

 An <b>AEP</b> Company	<b>INDIANA MICHIGAN POWER</b> <b>D. C. COOK NUCLEAR PLANT</b> <b>UPDATED FINAL SAFETY ANALYSIS REPORT</b>	Revised: 29.0 Section:14.3.4.5 Page: 33 of 33
--	---	---

40. NED-2001-004-REP, Rev. 0, "American Electric Power Donald C. Cook Nuclear Plant Unit 1 and Unit 2 Loop Subcompartment Analysis", May 2001
41. NED-2001-005-REP, Rev. 0, "American Electric Power Donald C. Cook Nuclear Plant Unit1 and Unit 2 Pressurizer Enclosure Subcompartment Analysis", April 2001
42. NED-2001-018-REP, Rev. 0, "American Electric Power Donald C. Cook Nuclear Plant Unit 1 and Unit 2 Fan/Accumulator Room Subcompartment Analysis", May 2001
43. NED-2001-012-REP, Rev. 0, "American Electric Power Donald C. Cook Nuclear Plant Unit 1 and Unit 2 Steam Generator Enclosure Subcompartment Analysis", May 2001
44. NED-2001-013-REP, Rev. 2, "American Electric Power Donald C. Cook Nuclear Plant Unit 1 and Unit 2 Reactor Cavity Subcompartment Analysis", Feb 28, 2008
45. AEP-04-52, "D. C. Cook Units 1 and 2 – TMD Steam Generator Enclosure Reanalysis", dated September 13, 2004.

 <small>An AEP Company</small>	<b>INDIANA MICHIGAN POWER</b> <b>D. C. COOK NUCLEAR PLANT</b> <b>UPDATED FINAL SAFETY ANALYSIS REPORT</b>	Revised: 28.0 Section: 14.3.5 Page: i of i
--	---	--

<b>14.3 REACTOR COOLANT SYSTEM PIPE RUPTURE (LOSS OF COOLANT ACCIDENT) .....</b>	<b>1</b>
<b>14.3.5 Environmental Consequences of a Loss-Of-Coolant-Accident .....</b>	<b>1</b>
14.3.5.1 Basic Radioactivity Removal Features.....	1
14.3.5.2 Basic Events and Release Fractions .....	2
14.3.5.3 Containment Iodine Removal Capabilities .....	3
14.3.5.3.1 Elemental Iodine Spray Removal Coefficients.....	3
14.3.5.3.2 Maximum Elemental Iodine Decontamination Factor .....	4
14.3.5.3.3 Particulate Iodine Spray Removal Coefficients.....	5
14.3.5.4 Containment Model .....	5
14.3.5.5 Engineered Safety Feature Leakage Outside Containment Model.	6
14.3.5.6 Containment Purge Model.....	8
14.3.5.7 Control Room Model .....	8
14.3.5.8 Atmospheric Dispersion Factors .....	8
14.3.5.9 Radiological Consequence Analysis Results .....	8
14.3.5.10 Population Center Considerations.....	9
14.3.5.11 References for Section 14.3.5.....	9
<b>14.3.6 Deleted .....</b>	<b>10</b>
<b>14.3.7 Long Term Cooling.....</b>	<b>10</b>
<i>Effect of the Replacement Steam Generators on Unit 1 .....</i>	<i>10</i>
<b>14.3.8 Nitrogen Blanketing .....</b>	<b>10</b>
<i>Effect of the Replacement Steam Generators on Unit 1 .....</i>	<i>10</i>

 An AEP Company	<p style="text-align: center;"><b>INDIANA MICHIGAN POWER</b> <b>D. C. COOK NUCLEAR PLANT</b> <b>UPDATED FINAL SAFETY ANALYSIS REPORT</b></p>	<p>Revised: 28.0 Section: 14.3.5 Page: 1 of 10</p>
---	--	--

## **14.3 REACTOR COOLANT SYSTEM PIPE RUPTURE (LOSS OF COOLANT ACCIDENT)**

### **14.3.5 Environmental Consequences of a Loss-Of-Coolant-Accident**

The radiological consequence analysis is performed based on Regulatory Guide 1.183 for the alternative source term. Parameters used in this analysis are listed in Table 14.3.5-1.

The results of analyses presented in this section demonstrate that the amounts of radioactivity released to the environment in the event of a loss-of-coolant accident do not result in radiation exposures that exceed the offsite and control room limits specified in Regulatory Guide 1.183 and 10 CFR 50.67.


Chapters 5 and 6 describe the protective systems and features of the unit which are specifically designed to limit the consequences of a major loss-of-coolant accident. The capability of the Emergency Core Cooling System for preventing melting of the fuel clad and the ability of the passive Ice Condenser Containment to absorb the blowdown resulting from a major loss of coolant are discussed in Sections 14.3.2 and 14.3.4, respectively. The capability of the engineered safety features in meeting the appropriate regulatory dose limits is demonstrated in this section.

#### **14.3.5.1 Basic Radioactivity Removal Features**

Removal of iodine from the Donald C. Cook Nuclear Plant containment atmosphere following a loss-of-coolant accident is affected by the containment spray system, the ice condenser, and several natural processes.

The effectiveness of a spray system in quickly and efficiently removing radioactive iodine has been repeatedly demonstrated in tests conducted at Oak Ridge National Laboratory (ORNL), Containment Systems Experiment (CSE), and by reactor manufacturers. For Cook Nuclear Plant, American Electric Power Service Corporation (AEPSC) has performed jointly with Battelle-Columbus Laboratories a detailed analysis to further study the removal of gaseous elemental iodine by sprays and to calculate the efficiency when certain non-ideal factors are considered. From this work we can state that the spray system in Cook Nuclear Plant will by itself reduce the radioactive iodine leakage from the containment to values which result in doses below the appropriate regulatory limits before taking credit for the ice condenser removing any gaseous elemental iodine.

## UFSAR Revision 30.0

 An AEP Company	<b>INDIANA MICHIGAN POWER</b> <b>D. C. COOK NUCLEAR PLANT</b> <b>UPDATED FINAL SAFETY ANALYSIS REPORT</b>	Revised: 28.0 Section: 14.3.5 Page: 2 of 10
---	---	---


Westinghouse has demonstrated the removal of gaseous elemental iodine through the process of steam condensation in an ice column, and they have evaluated the efficiency of this iodine removal. This work is reported in WCAP-7426 Topical Report Iodine Removal in the Ice Condenser System, dated March 1970 (Reference 1). The borated iced bed in Cook Nuclear Plant has been buffered with sodium hydroxide to assist in removing iodine from the air-steam mixture entering the ice condenser after a loss-of-coolant accident. The data from the Westinghouse tests shows efficient iodine removal from steam and from mixtures of steam and noncondensibles such as air. These tests and the iodine removal model applied to the results show that the ice condenser in a large containment building reduces the gaseous elemental iodine concentration after an accident. The treatment in the Westinghouse report ignored any other iodine removal system (that is, a containment spray system, except for the assumptions implicit in the steam production predictions).

Although the ice condenser is a substantial additional iodine removal feature, since the Cook Nuclear Plant meets the appropriate regulatory dose limits before taking credit for its iodine removal capability, this capability is not credited when evaluating the environmental consequences of a loss of coolant accident.

### **14.3.5.2 Basic Events and Release Fractions**

For the purpose of evaluating the environmental consequences of a loss of coolant accident, a double-ended rupture of a reactor coolant loop is considered with partial engineered safety features operating from the emergency power system. As shown in previous portions of this chapter, the Emergency Core Cooling System, with only diesel-generator power, prevents clad melting and limits zirconium-water reaction to an insignificant extent, assuring that the core remains intact and in place. As a result of the cladding temperature increases and the rapid system depressurization, however, cladding failure may occur in the hotter regions of the core.

The fission product radionuclides used to analyze the radiological consequence of a loss of coolant accident are based on elements given in Regulatory Guide 1.183 for the alternative source term. The core inventory is listed in Table 14.A.1-1. For this analysis, it is assumed that the core inventory is released to the containment atmosphere according to the release fractions and timing of release phases given in Regulatory Guide 1.183 for the gap release and early in-vessel damage phases. Plate-out of elemental iodine on internal surfaces is not credited in the analysis. Of the radioiodine released to the containment in a postulated accident, 95% is assumed to be cesium iodide, 4.85% is assumed to be elemental iodine, and 0.15% is assumed to be organic iodide. With the exception of elemental and organic iodine and noble gases, fission products are assumed to be in particulate form.

 <p><b>INDIANA MICHIGAN POWER</b> <small>An AEP Company</small></p>	<p><b>INDIANA MICHIGAN POWER</b> <b>D. C. COOK NUCLEAR PLANT</b> <b>UPDATED FINAL SAFETY ANALYSIS REPORT</b></p>	<p>Revised: 28.0 Section: 14.3.5 Page: 3 of 10</p>
--	--	--

### **14.3.5.3 Containment Iodine Removal Capabilities**

Fission product cleanup models identified in Regulatory Guide 1.183 and Standard Review Plan 6.5.2 are used to determine iodine removal capabilities by the containment spray system.

For the purpose of evaluating the containment spray system, some of the containment regions are not assumed to be directly sprayed, including the ice condenser bed and inside the steam generator and pressurizer enclosures. The unsprayed volume conservatively represents 313,028 ft<sup>3</sup> of the total 1,087,679 ft<sup>3</sup> free volume. In order to account for unsprayed regions, the removal of iodines takes place only in the sprayed regions, while mass transfer of iodine from unsprayed to sprayed regions accounts for the decrease in the iodine concentration in the unsprayed volumes.

#### **14.3.5.3.1 Elemental Iodine Spray Removal Coefficients**

Elemental iodine removal coefficients for spray in the containment atmosphere are determined using the basic equation below for a well mixed drop model. This gas phase controlling resistance model implicitly assumes that the spray solution is a sodium hydroxide boric acid solution, which is consistent with plant design.


$$\lambda_s = \frac{6k_g tF}{Vd}$$

Where:

- kg is the gas phase mass transfer coefficient
- t is the spray drop fall time
- F is the minimum volumetric spray flow rate
- V is the containment free volume of a given sprayed region
- d is the drop diameter

The containment includes the following three sprayed regions: upper compartment, lower compartment, and fan rooms. Conservatively minimized containment spray volumetric flow rates for the purpose of determining iodine removal capabilities are 1466 gpm in the upper compartment, 660 gpm in the lower compartment, and 201 gpm in the fan rooms. These flow rates are based on an assumed single failure. Conservatively minimized sprayed containment free volumes are 621,968 ft<sup>3</sup> in the upper compartment, 103,770 ft<sup>3</sup> in the lower compartment, and 48,913 ft<sup>3</sup> in the fan rooms.

## UFSAR Revision 30.0

 An AEP Company	<p style="text-align: center;"><b>INDIANA MICHIGAN POWER</b> <b>D. C. COOK NUCLEAR PLANT</b> <b>UPDATED FINAL SAFETY ANALYSIS REPORT</b></p>	<p>Revised: 28.0 Section: 14.3.5 Page: 4 of 10</p>
---	--	--

The spray drop fall time is estimated by the ratio of the average spray fall height to the terminal velocity of the mass mean drop. Conservatively minimized average spray fall heights are 58.6 ft for the upper compartment, 28.5 ft for the lower compartment, and 20.1 ft for the fan rooms. The drop terminal velocity is determined from the dimensionless Reynolds number of the drop. The spray is characterized by the following drop size distribution for Sprayco Model 1713A spray nozzles:

1. log normal distribution with a 282  $\mu\text{m}$  mean diameter and 0.7021 geometric standard deviation,
2. 4000  $\mu\text{m}$  diameter cutoff to the log normal distribution, and
3. 160 drop sizes ranging from 25 to 4000  $\mu\text{m}$  in diameter with 25  $\mu\text{m}$  diameter increments.

The coalescence of spray drops during their fall through the containment atmosphere is assumed to be caused by the overlapping of adjacent spray patterns and the collision of different sizes of drops from the same nozzle falling at different velocities. In order to account for changes in the drop size distribution due to the coalescence of spray drops, conservatively large percentage reductions are applied to total calculated elemental iodine removal coefficients.


The resulting elemental iodine spray removal coefficients are 20.0 per hour in the upper compartment, 20.0 per hour in the lower compartment, and 20.0 per hour in the fan rooms.

### **14.3.5.3.2 Maximum Elemental Iodine Decontamination Factor**

The maximum elemental iodine decontamination factor is defined as the maximum elemental iodine concentration in the containment atmosphere when sprays actuate divided by the elemental iodine concentration in the containment atmosphere at some time after decontamination. The effectiveness of spray in removing elemental iodine is presumed to end when the maximum elemental iodine decontamination factor of 200 is reached. The maximum elemental iodine decontamination factor for the containment atmosphere that is achieved by the spray system is determined using the equation below.

$$DF = \frac{\text{Total Elemental Iodine Curies in the Compartment}}{\text{Elemental Iodine Curies in the Compartment Atmosphere}}$$

## UFSAR Revision 30.0

 An AEP Company	<b>INDIANA MICHIGAN POWER</b> <b>D. C. COOK NUCLEAR PLANT</b> <b>UPDATED FINAL SAFETY ANALYSIS REPORT</b>	Revised: 28.0 Section: 14.3.5 Page: 5 of 10
---	---	---

### **14.3.5.3.3 Particulate Iodine Spray Removal Coefficients**

Particulate iodine removal coefficients for spray in the containment atmosphere are determined using the equation below.

$$\lambda_p = \frac{3h_{fall}FE}{2Vd}$$

where:

E/d is the ratio of a dimensionless collection efficiency E to the average spray drop diameter d

Since the removal of particulate material chiefly depends on the relative sizes of particles and spray drops, it is convenient to combine parameters that cannot be known. It is conservative to assume E/d is 10 per meter initially (i.e., 1% efficiency for spray drops of 1 millimeter in diameter) and then changes abruptly to 1 spray drop per meter after the aerosol mass has been depleted by a factor of 50 (i.e., 98% of the suspended mass is 10 times more readily removed than the remaining 2%).


The resulting particulate iodine spray removal coefficients are 5.06 per hour in the upper compartment, 6.65 per hour in the lower compartment, and 3.03 per hour in the fan rooms—until the particulate iodine decontamination factor reaches 50. After the particulate iodine decontamination factor reaches 50, particulate iodine spray removal coefficients are reduced to 0.506 per hour in the upper compartment, 0.665 per hour in the lower compartment, and 0.303 per hour in the fan rooms. Lastly, because removal mechanisms for particulate iodines are significantly different from and slower than removal mechanisms for elemental iodine, there is no need to limit the decontamination factor for particulate iodines.

### **14.3.5.4 Containment Model**

The containment is divided into the following five containment regions: upper compartment, lower compartment, fan rooms, dead-ended region, and ice condenser. The upper compartment, lower compartment and fan rooms include both sprayed and unsprayed portions. The dead-ended region and ice condenser are unsprayed. The containment free volumes are shown in Table 14.3.5-1.

The containment air recirculation / hydrogen skimmer system circulates air from the upper compartment through the fan rooms to the lower compartment and then from the lower compartment through the ice condenser back to the upper compartment, thus establishing a circulation pattern. Relative to sprayed and unsprayed containment regions, for the containment

## UFSAR Revision 30.0

 An AEP Company	<p style="text-align: center;"><b>INDIANA MICHIGAN POWER</b> <b>D. C. COOK NUCLEAR PLANT</b> <b>UPDATED FINAL SAFETY ANALYSIS REPORT</b></p>	<p>Revised: 28.0 Section: 14.3.5 Page: 6 of 10</p>
---	--	--

equalization function, the suction source for the containment air recirculation fan is the sprayed upper compartment. For the hydrogen skimming function, the suction sources for the containment air recirculation fan are the unsprayed upper compartment and unsprayed lower compartment. The discharge flow from the containment air recirculation fan is assumed to be proportionately distributed by volume between the sprayed lower compartment and unsprayed lower compartment. Similarly, the flow through the ice condenser is assumed to be proportionately distributed by volume between the sprayed upper compartment and unsprayed upper compartment. Conservatively minimized containment air recirculation flow rates are shown in Table 14.3.5-1. These flow rates are based on an assumed single failure.

The mixing rate between sprayed and unsprayed portions of the same containment region, i.e., the upper compartment or lower compartment, is conservatively assumed to reflect natural convection and to be two turnovers of the unsprayed region per hour.

The radioactivity released from the fuel is assumed to mix instantaneously and homogeneously throughout the free volume of the containment as it is released.


### **14.3.5.5 Engineered Safety Feature Leakage Outside Containment Model**

Subsequent to the emptying of the refueling water storage tank during the initial phase of emergency core cooling, water from the containment sump is recirculated by the residual heat removal pumps and spray pumps and cooled via the residual heat exchangers and spray heat exchangers and then returned to the Reactor Coolant System and containment. Because the containment sump water contains the radioactivity of the spilled reactor coolant, the potential off-site and control room exposures due to operation of these external recirculation paths is evaluated.

Engineered safety feature systems that circulate sump water outside containment are assumed to leak during their intended operation. With the exception of noble gases, all fission products released from the fuel to the containment are assumed to be instantaneously and homogeneously mixed in the containment sump water at the time of release from the core. The minimum containment sump volume is conservatively assumed to be 50,995 ft<sup>3</sup>. With the exception of iodine, all radioactive materials in the recirculating liquid are assumed to be retained in the liquid phase. ESF leakage into the auxiliary building is addressed separately from the back leakage into the refueling water storage tank. The radioiodine that is postulated to be available for release to the environment from the auxiliary building is assumed to be 97% elemental and 3% organic. Since the temperature of engineered safety feature leakage outside containment is less than



## UFSAR Revision 30.0

 An AEP Company	<b>INDIANA MICHIGAN POWER</b> <b>D. C. COOK NUCLEAR PLANT</b> <b>UPDATED FINAL SAFETY ANALYSIS REPORT</b>	Revised: 28.0 Section: 14.3.5 Page: 7 of 10
---	---	---

212°F, the amount of iodine that becomes airborne outside containment is assumed to be 10% of the total iodine activity in the leaked fluid.

The effective unfiltered engineered safety feature leakage outside containment is defined as the sum of the unfiltered engineered safety feature leakage in the auxiliary building.


The administratively controlled limit for unfiltered engineered safety feature leakage into the auxiliary building is 0.1 gpm. In the loss of coolant radiological consequence analysis, engineered safety feature leakage outside containment is taken as two times the sum of the simultaneous leakage from all components in the engineered safety feature recirculation systems. Therefore, in the analysis, the effective unfiltered engineered safety feature leakage into the auxiliary building is assumed to be 0.2 gpm.

The evaluation of ESF leakage through pump miniflow isolation valves located on lines that connect to the RWST is based upon the guidance of NUREG/CR-5950. With sump pH controls in place, the iodine in the containment sump is considered to be nonvolatile. However, when introduced into the acidic solution of the RWST, a portion of the particulate iodine is converted to elemental iodine. The methodology of NUREG/CR-5950 accounts for two iodine transport/removal mechanisms. The first is the fraction of the total iodine in the tank that is released in the form elemental iodine, and the second is the partitioning of elemental iodine between the liquid and vapor phases of the tank.

The fraction of the total iodine that becomes elemental is a function of both the RWST pH and the total iodine concentration in the tank. The time-dependent RWST pH increases from an initial value of 4.479 as the sump fluid, with an assumed constant pH of 7.0, mixes with the remaining inventory in the tank following switchover to recirculation. Similarly, the total RWST iodine concentration increases from an initial value of zero as fresh iodine is transported into the tank from the sump. These two parameters combine to produce the elemental iodine fraction, which increases from 0.0 at the beginning of the event to a maximum of 19.14% near the end of the 30 day analysis duration.

The ratio of the elemental iodine concentrations between the liquid and vapor phases of the tank is determined by a partition coefficient that is a function of the RWST liquid temperature. The RWST temperature increases moderately from hot sump fluid introduced into the tank. No credit is taken for heat removal in the piping between the sump and the tank or heat losses through the tank walls. The corresponding time-dependent RWST elemental iodine partition coefficient decreases from 45.41 at the beginning of the event to 31.92 after 30 days. A similar approach is taken with the organic iodine, using a constant release fraction of 0.0015 and a conservative partition coefficient of 1.0.

## UFSAR Revision 30.0

 An AEP Company	<b>INDIANA MICHIGAN POWER</b> <b>D. C. COOK NUCLEAR PLANT</b> <b>UPDATED FINAL SAFETY ANALYSIS REPORT</b>	Revised: 28.0 Section: 14.3.5 Page: 8 of 10
---	---	---

The elemental and organic iodine release fractions and partition coefficients are applied to the leakage flow rate from the sump to the RWST to obtain an adjusted volatile iodine release rate from the tank. An administrative limit of 0.5 gpm is established for back leakage to the RWST. The radiological consequence analysis assumes an ESF leak rate to the RWST of 1.0 gpm, which is two times the administrative limit.

### **14.3.5.6 Containment Purge Model**

Since the containment is purged during power operations, releases from the containment purge system prior to containment isolation are analyzed. The radionuclide inventory in the reactor coolant system liquid is assumed to be released to the containment at the initiation of the loss of coolant accident. This inventory is based on the technical specification reactor coolant system equilibrium activity without iodine spiking, which is listed in Table 14.A.3-3.

### **14.3.5.7 Control Room Model**

The control room is modeled as a discrete volume using the parameters listed in Table 14.3.5-1. The assumed failure of an emergency diesel generator results in one control room ventilation train operating.

### **14.3.5.8 Atmospheric Dispersion Factors**


Release locations used in the dose analysis are listed in Table 14.3.5-1. Corresponding atmospheric dispersion factors are provided in Tables 2.2.-11 and 2.2-12.

### **14.3.5.9 Radiological Consequence Analysis Results**

This dose consequences for this event are shown below:

	<b>EAB (rem TEDE)</b>	<b>LPZ (rem TEDE)</b>	<b>Control Room (rem TEDE)</b>
Loss of Coolant Accident	21.48	8.30	4.56
Acceptance Limit	25	25	5

The control room dose is within the 5 rem TEDE 10 CFR 50.67 limit. The EAB and LPZ doses are below the 25 rem guideline level of Regulatory Guide 1.183. Because of the combination of independent conservative assumptions, the doses actually expected following the occurrence of a loss of coolant accident would be much lower than the values here given.

 <b>INDIANA MICHIGAN POWER</b> <small>An AEP Company</small>	<b>INDIANA MICHIGAN POWER D. C. COOK NUCLEAR PLANT UPDATED FINAL SAFETY ANALYSIS REPORT</b>	Revised: 28.0 Section: 14.3.5 Page: 9 of 10
--	---	---

### **14.3.5.10 Population Center Considerations**

The preceding discussion shows that engineered safety features adequately protect persons at the site exclusion radius and at the low population zone radius from accidental exposure in excess of the limits for these distances set forth in Regulatory Guide 1.183. This regulation also requires that the reactor be so situated that there is no population center (defined as a city of 25,000) having its nearest boundary closer than 1-1/3 times the low population zone radius.


The nearest boundary of the population center lies at a minimum distance of 8 miles (12,872 meters) from the reactor containment which is considerably more than the required 1-1/3 times the low population zone.

The above evaluations show that the ice condenser reactor containment provides a passive means for both rapidly absorbing the energy from a postulated loss-of-coolant accident and reducing the off-site consequences to below the allowable limits.

### **14.3.5.11 References for Section 14.3.5**

1. WCAP-7426 Westinghouse Topical Report. "Iodine Removal in the Ice Condenser System", March 1970.
2. TID-14844: Calculation of Distance Factors for Power and Test Reactor Sites, March, 1962, Division of Licensing and Regulation, AEC.
3. NUREG/CR-2900, Predicted Rates of Formation of Iodine Hydrolysis Species at pH Levels, Concentrations, and Temperatures Anticipated in LWR Accidents, October 1982.

# UFSAR Revision 30.0

 An AEP Company	<p style="text-align: center;"><b>INDIANA MICHIGAN POWER</b> <b>D. C. COOK NUCLEAR PLANT</b> <b>UPDATED FINAL SAFETY ANALYSIS REPORT</b></p>	<p>Revised: 28.0 Section: 14.3.5 Page: 10 of 10</p>
---	--	---

## **14.3.6 Deleted<sup>1</sup>**

## **14.3.7 Long Term Cooling**

Specific analyses on this subject have not been performed for Unit 1. Discussions on this subject in the Unit 2 FSAR are, in general, applicable to Unit 1 as well.

### **Effect of the Replacement Steam Generators on Unit 1**

The effect of the RSGs on long term cooling has been evaluated. A calculation performed for the RSGs demonstrates that the sensible heat of the original steam generators (OSGs) is slightly larger than that of the RSGs at nominal conditions when considering primary, secondary, and metal mass. Consequently, the cooling requirements for systems such as the residual heat removal system and the auxiliary feedwater system are reduced slightly with the RSGs. Therefore long term core cooling is not adversely affected by steam generator replacement.

## **14.3.8 Nitrogen Blanketing**

Specific analyses on this subject have not been performed for Unit 1. Discussions on this subject in the Unit 2 FSAR are, in general, applicable to Unit 1 as well.


### **Effect of the Replacement Steam Generators on Unit 1**

The effect of the RSGs on nitrogen blanketing has been evaluated. This section of the UFSAR originally was a portion of the response to a question addressing the issue of nitrogen blanketing from the accumulators during a small break LOCA. Extensive analyses have since been performed to study the general behavior of small break LOCA. Accumulator nitrogen was not identified as a potential source of non-condensable gas in the RCS. The small break LOCA evaluation for the RSGs concludes that small break LOCA acceptance criteria continue to be met at Unit 1 with the installation of RSGs. Therefore, use of the RSGs does not affect the nitrogen blanketing information reported in the UFSAR.

---


<sup>1</sup> Section 14.3.6 deleted by UCR-1997 Rev 0 with the following exceptions:

- Section 14.3.6.6 relocated is to new Section 5.8;
- Section 14.3.6.6.1 relocated to new Section 5.8.1;
- Section 14.3.6.6.2 relocated to new Section 5.8.2;
- Section 14.3.6.6.3 relocated to new Section 5.8.3;
- Section 14.3.6.7 relocated to new Section 5.8.4

 An AEP Company	INDIANA MICHIGAN POWER D. C. COOK NUCLEAR PLANT <b>UPDATED FINAL SAFETY ANALYSIS REPORT</b>	Revised: 27.0 Section: 14.3.9 Page: i of iii
---	---	--


<b>14.3 REACTOR COOLANT SYSTEM PIPE RUPTURE (LOSS OF COOLANT ACCIDENT) .....</b>	<b>1</b>
<b>14.3.9 Containment and Recirculation Sump Analyses .....</b>	<b>1</b>
<i>Plant Configuration .....</i>	<i>2</i>
<i>General Analyses Considerations .....</i>	<i>3</i>
14.3.9.1 Accidents Leading to Sump Recirculation.....	4
14.3.9.2 Accident Description – General System Performance .....	5
14.3.9.3 Containment Sump Inventory Analysis .....	9
14.3.9.3.1 Method of Analysis .....	9
14.3.9.3.1.1 Computer Code Utilized.....	9
14.3.9.3.1.2 Assumptions .....	10
14.3.9.3.1.3 Acceptance Criteria .....	12
14.3.9.3.2 Results .....	13
14.3.9.3.3 Conclusions.....	15
14.3.9.4 Recirculation Sump Analyses.....	15
14.3.9.4.1 Debris Generation .....	16
14.3.9.4.1.1 Break Selection.....	16
14.3.9.4.1.2 Debris Sources .....	19
14.3.9.4.1.3 Results.....	20
14.3.9.4.2 Debris Transport.....	20
14.3.9.4.2.1 Computer Code Utilized.....	21
14.3.9.4.2.2 Method of Analysis .....	21
<i>Blowdown Transport.....</i>	<i>22</i>
<i>Washdown Transport .....</i>	<i>23</i>
<i>Pool Fill and Recirculation Transport.....</i>	<i>23</i>
14.3.9.4.2.3 Results.....	24
14.3.9.4.3 Recirculation Sump Hydraulic Analysis .....	24
14.3.9.4.3.1 Computer Code Utilized.....	26

# UFSAR Revision 30.0


 An <b>AEP</b> Company	<b>INDIANA MICHIGAN POWER</b> <b>D. C. COOK NUCLEAR PLANT</b> <b>UPDATED FINAL SAFETY ANALYSIS REPORT</b>	Revised: 27.0 Section: 14.3.9 Page: ii of iii
--	---	---

14.3.9.4.3.2	Method of Analysis .....	26
	Design Input Parameters .....	26
	Forward Flow Cases .....	26
	Reverse Flow Case .....	27
	Vortex Evaluation .....	27
14.3.9.4.3.3	Results .....	28
	Forward Flow Cases .....	28
	Reverse Flow Case .....	29
	Vortex Evaluation .....	29
14.3.9.5	Recirculation Sump Strainer Head Loss .....	29
14.3.9.5.1	Recirculation Sump Strainer Debris Only Testing .....	29
14.3.9.5.2	Recirculation Sump Strainer Chemical Effects Testing .....	31
	MFTL Testing .....	31
	Vuez Testing .....	32
14.3.9.5.3	System Head Loss Determination .....	32
14.3.9.5.3.1	Method of Analysis .....	33
14.3.9.5.3.2	System Head Loss Results .....	34
14.3.9.6	Design Considerations for Upstream and Downstream Effects ....	36
14.3.9.6.1	Upstream Effects .....	36
14.3.9.6.2	Downstream Effects .....	38
14.3.9.6.2.1	Method of Analysis .....	38
	Ex-Vessel Recirculation Flow Path Blockage .....	39
	Ex-Vessel Recirculation Flow Path Wear .....	39
	In-Vessel Flow Path Blockage .....	39
	In-Vessel Fuel Rod Debris Deposition .....	39
14.3.9.6.2.2	Assumptions .....	40
14.3.9.6.2.3	Acceptance Criteria .....	40
14.3.9.6.2.4	Results .....	41
14.3.9.6.2.5	Conclusions .....	42

UFSAR Revision 30.0

 An <b>AEP</b> Company	<p>INDIANA MICHIGAN POWER D. C. COOK NUCLEAR PLANT UPDATED FINAL SAFETY ANALYSIS REPORT</p>	<p>Revised: 27.0 Section: 14.3.9 Page: iii of iii</p>
--	---	---

14.3.9.7 References for Sections 14.3.9 ..... 42

 An AEP Company	<p>INDIANA MICHIGAN POWER D. C. COOK NUCLEAR PLANT UPDATED FINAL SAFETY ANALYSIS REPORT</p>	<p>Revised: 27.0 Section: 14.3.9 Page: 1 of 44</p>
---	---	--

## **14.3 REACTOR COOLANT SYSTEM PIPE RUPTURE (LOSS OF COOLANT ACCIDENT)**


### **14.3.9 Containment and Recirculation Sump Analyses**

Section 14.3.9 provides a description of the containment configuration, equipment design, and integrated analyses which were performed to demonstrate that the long-term core and containment cooling design functions specified in Section 6.2 and 6.3 are maintained following postulated accidents leading to sump recirculation. Long-term functionality during these scenarios depends on containment configuration and equipment that supports the transport of blowdown mass and ice melt to the recirculation sump (Upstream Effects), acceptable performance of the recirculation sump in the presence of debris-laden water including chemical effects (Strainer Head Loss), and operability of the ECCS and CTS while drawing filtered water from the recirculation sump (Downstream Effects). To address these issues, the containment and recirculation sump analyses include consideration of post-accident mass and energy release inside containment, fluid transport of blowdown and ice melt mass within the upper and lower containment and their subcompartments, debris generation, debris transport within the loop and annulus subcompartments of lower containment, and the performance of systems designed to support core and containment cooling functions by preventing/minimizing potential component blockage or wear due to operation with debris-laden fluid. Assessments of plant-specific containment debris sources and containment design features and their impacts on ECCS and containment spray performance conform to the requirements of Generic Letter 2004-02 (Reference 7).

To facilitate an understanding of the analyses scope and accident progression, a description of the plant layout and equipment involved in the containment and recirculation sump modeling is included below.



## UFSAR Revision 30.0

 <b>INDIANA MICHIGAN POWER</b> <small>An AEP Company</small>	<b>INDIANA MICHIGAN POWER D. C. COOK NUCLEAR PLANT UPDATED FINAL SAFETY ANALYSIS REPORT</b>	Revised: 27.0 Section: 14.3.9 Page: 2 of 44
--	---	---

### **Plant Configuration**

The Cook Nuclear Plant ice condenser containment consists of four uniquely defined and separated volumes:


1. upper containment,
2. ice condenser,
3. reactor cavity, and
4. lower containment.

The upper containment area, which does not contain any high energy piping, is physically separated from lower containment and the reactor cavity by the divider barrier and the ice condenser. The ice condenser forms an approximate 300 degree arc around containment between the containment wall and the crane wall. The ice condenser has 24 paired lower inlet doors in the loop compartment which open following a pipe break, allowing suppression of the initial pressure surge in containment. The intermediate deck doors are located just above the ice bed and at the top of the ice condenser section are the top deck doors which allow steam and non-condensable gases to vent to upper containment. The reactor cavity is the volume surrounding the reactor vessel. The physical communication path between the reactor cavity and the lower containment is through openings in the primary shield wall and above the flood-up overflow wall.

The lower containment consists of two subcompartments, the area inside the crane wall (loop compartment) and the area outside the crane wall (annulus). Post-accident blowdown and ice melt inventory initially accumulates in the loop compartment. The water inventory in the lower containment is referred to as the containment sump. The recirculation sump, on the other hand, refers to the enclosed area that accumulates water for direct suction by the RHR and containment spray pumps. The recirculation sump is made up of:

1. a main strainer module fit into the face of an enclosed compartment in front of the crane wall that deposits water into a sump that extends below the 598' 9 3/8" containment floor, under the crane wall extension, and to the RHR and containment spray pump suction lines, and
2. a remote strainer module located in the annulus that empties into a waterway that directs filtered water through a penetration in the crane wall into the front section of the recirculation sump (See Figure 14.3.9-13).

## UFSAR Revision 30.0

 An AEP Company	<b>INDIANA MICHIGAN POWER</b> <b>D. C. COOK NUCLEAR PLANT</b> <b>UPDATED FINAL SAFETY ANALYSIS REPORT</b>	Revised: 27.0 Section: 14.3.9 Page: 3 of 44
---	---	---

The main strainer has an effective surface area of 900 ft<sup>2</sup> and the remote strainer has an effective area of 1,072 ft<sup>2</sup>. The recirculation sump strainers are designed to:

1. provide adequate filtration of expected debris generated by postulated accidents, thereby preventing adverse effects on systems and equipment from water drawn from the recirculation sump by RHR or CTS pumps, and
2. ensure minimal head loss so the necessary water level inside the recirculation sump is maintained.

### **General Analyses Considerations**


The containment sump analysis, described in Section 14.3.9.3, verifies the minimum sump water level for a spectrum of LBLOCA, SBLOCA and MSLLB pipe breaks to ensure that calculated water levels support the possible transition to the recirculation mode of operation. The amount of water required in the containment sump for the various pipe break scenarios is based on satisfying NPSH requirements for RHR and containment spray pumps, and to prohibit excessive air entrainment and the formation of a vortex when transferring to the recirculation mode of operation. The acceptability of the minimum containment sump water level design requirements was demonstrated through empirical testing.

The containment sump inventory analysis does not specifically consider the effects of debris in the water during the injection phase. Rather, it implicitly relies on physical plant equipment in containment to allow free water flow between the loop compartment and annulus, and to the main and remote strainers. The recirculation sump inventory analyses, described in Section 14.3.9.4, does not consider plant specific debris effects, which include the resulting differences in water level between the containment and recirculation sumps as debris is deposited on the main and remote strainers.

The general approach for recirculation sump performance, described in Section 14.3.9.4, begins with an analysis of the containment sump's dynamic inventory as a result of ice melt, mass blowdown and movement of water inside lower containment before sump recirculation begins.

Results from the containment sump inventory analysis are used as an input for recirculation sump analyses. The recirculation sump analysis assumes bounding flow rates through the ECCS and CTS to maximize the transport of debris to the strainers and corresponding head loss across the strainers. Physical plant changes installed to address sump debris issues ensured that component design functions would continue to be met despite the presence of debris-laden water and do not impact the conclusion from the containment sump inventory analysis. The

## UFSAR Revision 30.0

 An AEP Company	<p style="text-align: center;"><b>INDIANA MICHIGAN POWER</b> <b>D. C. COOK NUCLEAR PLANT</b> <b>UPDATED FINAL SAFETY ANALYSIS REPORT</b></p>	<p>Revised: 27.0 Section: 14.3.9 Page: 4 of 44</p>
---	--	--

recirculation sump analyses were generally performed in accordance with the guidance provided in NEI-04-07 (Reference 9).


Successful outcomes of recirculation sump performance occur when the containment sump inventory and the recirculation sump inventory analyses meet designated acceptance criteria.

The sections which follow:

1. identify the set of postulated high energy line breaks at Cook Nuclear Plant which can lead to the recirculation mode of post-accident operation,
2. provide accident progression from a sump inventory perspective for each identified accident,
3. describe methods of analyses for component performance affecting recirculation sump operation,
4. present analysis results for containment sump inventory,
5. describe the results of recirculation sump strainer debris loading analyses and testing including consideration of chemical effects, and
6. present analyses results and conclusions for recirculation sump performance.

### **14.3.9.1 Accidents Leading to Sump Recirculation**

Specific accidents evaluated for sump recirculation in Section 14.3.9 are identified in Sections 14.3.9.3 and 14.3.9.4. The first set of accidents in Section 14.3.9.3 represents the broadest range of events that can lead to the entry conditions for sump recirculation, regardless of the need for sump recirculation for accident mitigation. This analysis determines the availability of a minimum containment sump inventory for each potential accident at the transition point when the shift from injection to recirculation cooling is to commence and during long-term sump recirculation. The second set of analyses in Section 14.3.9.4 constitutes that subset of the first set where worst case debris generation and transport is expected to occur and the need for long-term recirculation for accident mitigation is required. Since each set of analyses in Sections 14.3.9.3 and 14.3.9.4 represents a distinct group possible accident scenarios, the selected bounding accidents in each group are different. Taken together, however, successful outcomes in Sections 14.3.9.3 and 14.3.9.4 indicate that long-term core and containment recirculation cooling functions will be satisfied.

 An AEP Company	<p style="text-align: center;"><b>INDIANA MICHIGAN POWER</b> <b>D. C. COOK NUCLEAR PLANT</b> <b>UPDATED FINAL SAFETY ANALYSIS REPORT</b></p>	<p>Revised: 27.0 Section: 14.3.9 Page: 5 of 44</p>
---	--	--

## **14.3.9.2 Accident Description – General System Performance**

The D. C. Cook plant design includes passive and active design features to provide core cooling and containment pressure suppression in the event of a Loss of Coolant Accident (LOCA) or Main Steam Line Break (MSLB) inside containment. The passive features include the ice condenser inside containment which provides containment pressure suppression and mass for containment sump inventory, and safety injection (SI) system accumulators which automatically discharge into the RCS when the RCS pressure drops below the accumulator pressure. The active features include the ECCS trains for coolant injection and the containment spray system. Refer to Sections 14.3.9.3 and 14.3.9.4 for further discussion of the postulated accidents for which these systems are required to respond.


The physical arrangement of the containment structures and equipment is such that steam discharged from postulated pipe breaks in lower containment will be forced through the ice condenser to reach the upper containment. Pipe breaks postulated to occur in the annulus will also exhibit this behavior. However, the arrangement of the containment will not allow the steam discharge from such a break to directly enter the ice condenser. The steam will flow through openings in the crane wall into the loop compartment and then into the ice condenser.

After a postulated pipe break, the containment pressure will increase (at a rate dependent on the break size) as the steam discharges into containment. At very low containment pressures, the ice condenser lower inlet doors will open sufficiently for steam to enter the ice condenser. The steam entering the ice condenser will be condensed and the condensate and melted ice will drain into the loop compartment and, consequently, the containment and the recirculation sumps.

When a low pressurizer pressure or high containment pressure signal is received, the safeguards systems will initiate an SI signal. The SI signal will initiate several automatic actions, including: reactor trip, emergency diesel generator (EDG) start, opening the boron injection tank (BIT) isolation valves and charging pump suction valves from the RWST, and starting the centrifugal charging (CC) pumps, SI pumps, and residual heat removal (RHR) pumps. The high containment pressure input to the SI signal will also start the containment air recirculation (CEQ) fans. The effect of these actions will produce the following plant conditions:

- The CC pumps will be operating, delivering borated water from the RWST to the four RCS cold legs. The CC pumps are low flow, high pressure pumps and will provide injection for any postulated break size including very small break LOCAs. At a pre-determined RCS pressure, with an SI signal present, the minimum flow valves will open, returning pump discharge flow to the pump

## UFSAR Revision 30.0

 An <b>AEP</b> Company	<b>INDIANA MICHIGAN POWER</b> <b>D. C. COOK NUCLEAR PLANT</b> <b>UPDATED FINAL SAFETY ANALYSIS REPORT</b>	Revised: 27.0 Section: 14.3.9 Page: 6 of 44
--	---	---


suction to prevent deadheading the pump. If the RCS pressure drops below the reset setpoint, the minimum flow valves will close.

- The SI pumps will be operating, attempting to deliver borated water from the RWST to the four RCS cold legs. The SI injection into the cold legs will be through the accumulator injection lines. This piping is separate from the CC injection location. The SI pumps are low flow, moderately high pressure pumps that will provide injection at pressures typical of certain small break LOCAs. During the injection phase, the minimum flow valves will be open, returning a portion of the discharge flow to the RWST through a pressure reducing orifice.
- The RHR pumps will be operating, attempting to deliver borated water from the RWST to the four RCS cold legs. The RHR pumps also inject through the accumulator discharge lines. The RHR pumps are high flow, low pressure pumps that will provide injection at pressures typical of large break LOCAs. At a pre-determined minimum flow rate, minimum flow line isolation valves will open, returning pump discharge flow to the pump suction to prevent deadheading. In addition, the RHR system has the capability to be re-aligned to discharge a portion of the RHR flow through separate containment spray ring headers in a containment spray mode of operation.
- The CEQ fans will begin operating after a delay of approximately five minutes (U1) and two minutes (U2) following a high containment pressure signal. The CEQ fans provide forced air circulation between the lower and upper containment through the ice condenser.

There are two redundant trains of Emergency Core Cooling System (ECCS) which include two CC pumps, two SI pumps, and two RHR pumps. Assuming no equipment failures, all six pumps will be operating. The EDGs will start and automatically load in the event that the LOCA is coincident with a loss of off-site power (LOOP). The system alignment described above is considered the injection phase of the accident.

Following receipt of a hi-hi containment pressure signal, the containment spray system (CTS) will actuate. The injection phase alignment of the CTS system draws suction from the RWST and discharges through upper and lower containment spray ring headers. The CTS flow in the upper containment drains to the refueling canal and to the CEQ Fan rooms. Water entering the refueling canal is returned to the loop compartment through two 12 inch and one 10 inch drain pipes at the bottom of the canal. For Unit 1, the water collected in the CEQ Fan Room Stairwell

## UFSAR Revision 30.0

 An AEP Company	<b>INDIANA MICHIGAN POWER</b> <b>D. C. COOK NUCLEAR PLANT</b> <b>UPDATED FINAL SAFETY ANALYSIS REPORT</b>	Revised: 27.0 Section: 14.3.9 Page: 7 of 44
---	---	---


and Ventwell drains to the pipe tunnel sump in the annulus. In Unit 2, the CEQ Fan Room Stairwell and Ventwell lines drain to the lower containment sump in the loop compartment. The check valve internals were removed from the check valves for the Stairwell and Ventwell drains for both units to address the single failure and flooding concerns. Holes in the flood-up overflow wall allow water to flow freely between the annulus and loop compartment. (Reference 6)

The SI accumulators are vessels filled with borated water and pressurized with nitrogen gas. While the majority of the equipment associated with the injection mode is initiated by a safety injection signal, the accumulators require no power source or initiation signal. When the RCS pressure falls below the minimum value required by Technical Specifications, mechanically operated check valves normally isolating the accumulators from the RCS will open, injecting borated water into the four RCS cold legs. There are four accumulators, with one accumulator supplying each cold leg.

The main objectives of the injection phase are to provide immediate core cooling, replenish lost primary coolant, and suppress containment pressure. At the end of the injection phase, the usable contents of the RWST will have been transferred to the containment sump and RCS, and depending on the break size and RCS response, the SI accumulators may have also been discharged.

When the RWST low level alarm is received following the postulated LOCA, the switchover to recirculation mode can begin once sufficient water level is verified to be present in the containment sump. Successful completion of this objective assumes that the water sources supplied to the RCS and containment return to the containment sump. The validity of this assumption is addressed in Section 14.3.9.6.1, Upstream Effects. Operators will initiate the recirculation mode by securing the suctions of the RHR and CTS pumps, one train at a time. The CC and SI pumps will continue to inject into the RCS from the RWST until the low-low level alarm is reached. During this time period, the suction of each RHR and CTS pump will be aligned to the recirculation sump inside containment, one train at a time. This pump alignment will allow the spilled coolant, injected water, and melted ice that have collected in the containment and recirculation sumps during the injection phase to be recirculated through the RCS and containment atmosphere and back to the containment sump. In the recirculation mode, the CC and SI pumps will take suction from the RHR pump discharge. One CC pump and one SI pump will take suction from each RHR pump discharge. The switchover to recirculation mode will be complete when the suctions of all the operating CC and SI pumps are being supplied by RHR flow from the recirculation sump.

## UFSAR Revision 30.0

 An <b>AEP</b> Company	<b>INDIANA MICHIGAN POWER</b> <b>D. C. COOK NUCLEAR PLANT</b> <b>UPDATED FINAL SAFETY ANALYSIS REPORT</b>	Revised: 27.0 Section: 14.3.9 Page: 8 of 44
--	---	---

There are several other plant systems that will operate along with the ECCS and CTS to accomplish system functional objectives while in the recirculation mode. The RHR pump discharge will be routed through the RHR heat exchangers prior to injection back into the RCS. The RHR heat exchangers are cooled by the Component Cooling Water (CCW) system. The RHR heat exchangers are located between the RHR pumps and the CC and SI pump suction points, so the CC and SI pump injection water will also be cooled. The CTS pump discharge will be routed through the containment spray heat exchangers prior to discharge back into containment. The containment spray heat exchangers are cooled by the Essential Service Water (ESW) system. Thus, the containment is cooled by these two sets of heat exchangers.


The main objectives of the recirculation mode are to keep the core flooded, suppress containment pressure, and provide long-term core and containment cooling. Successful execution of these objectives assumes an ability of the ECCS and CTS to function while drawing filtered water from the recirculation sump. The validity of this assumption is described in Section 14.3.9.6.2, Downstream Effects. As the RCS and containment cool and de-pressurize, the operators will manually stop (or start) ECCS and CTS components as necessary to maintain the RCS/containment in the desired condition.

During a main steam line break event, a low pressurizer pressure, low steam line pressure, or high steam line differential pressure signal will initiate an SI signal. The sequence of events described above for a LOCA would be similar for a MSLB inside containment, except that transfer to the recirculation mode is not expected to occur. Refer to Section 14.3.9.4.1.1 for additional information. Additionally, main steam line isolation would occur and limit the secondary-side inventory discharged to containment. The ECCS pumps would start as described, but would only be providing makeup flow to the RCS system, since there would be no loss of reactor coolant.

Given successful Upstream Effects, which ensure that blowdown and injected RWST water reach the front of the recirculation sump, and Downstream Effects, which demonstrate tolerance for the quality of filtered water in the recirculation sump, satisfactory core and containment long-term cooling will depend on adequate containment and recirculation sump inventory at the time of recirculation switchover and thereafter. Further, there are unique features of the Cook Nuclear Plant ice condenser containment design that lead to directions of conservatism for accident parameters that are different than for peak containment pressure and peak clad temperature analyses. For these reasons, it is important to perform stand-alone analyses of sump inventory



# UFSAR Revision 30.0

 An AEP Company	<p style="text-align: center;"><b>INDIANA MICHIGAN POWER</b> <b>D. C. COOK NUCLEAR PLANT</b> <b>UPDATED FINAL SAFETY ANALYSIS REPORT</b></p>	<p>Revised: 27.0 Section: 14.3.9 Page: 9 of 44</p>
---	--	--

using worst-case assumptions for the range of scenarios in which recirculation cooling may be required.

## **14.3.9.3 Containment Sump Inventory Analysis**

### **14.3.9.3.1 Method of Analysis**

#### **14.3.9.3.1.1 Computer Code Utilized**


The containment sump inventory analysis (Reference 1) was performed using the MAAP4 code version 4.0.4.1 (FAI, 1999). (Note: the last digit in the code designation indicates an enhancement to the official internationally distributed version of 4.0.4. Version 4.0.4.1 was created to support this analysis and allows separate temperatures to be supplied on the cooling side of the containment spray heat exchangers and the RHR heat exchangers.) The MAAP4 code calculates the behavior of and interactions between the ECCS, RCS and containment following a postulated accident. It does not calculate debris-related effects on plant equipment or recirculation sump performance. These effects are addressed in Section 14.3.9.4. Consequently, the predicted containment sump inventory reflects time-dependent mass and energy inputs from ECCS/containment spray injection and recirculation, ice melt, RCS holdup, accumulator injection, and water flow between containment compartments.

The Cook Nuclear Plant reactor coolant system is represented as a typical Westinghouse 4-loop design available in MAAP4. Two RCS loops are included in the standard MAAP4 model, with one loop including a single steam generator and associated piping, and the other loop including the composite behavior of the remaining three steam generators and associated piping. The spectrum of RCS break sizes evaluated include a Double-Ended Cold Leg (DECL) and a variety of smaller breaks, including breaks on the reactor vessel itself. The MAAP4 primary system break flow model determines mass and energy releases for steam and water flows leaving the reactor coolant system by assuming they are in thermodynamic equilibrium. This characterization of the break flows maximizes water enthalpy, and minimizes steam release to containment atmosphere that is available to melt ice. For main steam line break cases, the MAAP4 break flow model assumes that saturated steam was released into the lower containment.

The physical arrangement of the D.C. Cook containment is modeled in MAAP4 by 14 nodes with 44 flow junctions coupling the various nodes. Typically, a simple free volume versus height table is used to represent each node, although a detailed volume versus height table is used for the reactor cavity. The flow junctions account for both forced and natural convection flows. Two junctions are included to represent holes in the primary shield wall between the loop



## UFSAR Revision 30.0

 An AEP Company	<p style="text-align: center;"><b>INDIANA MICHIGAN POWER</b> <b>D. C. COOK NUCLEAR PLANT</b> <b>UPDATED FINAL SAFETY ANALYSIS REPORT</b></p>	<p>Revised: 27.0 Section: 14.3.9 Page: 10 of 44</p>
---	--	---

compartment and the reactor cavity that accommodate Nuclear Instrumentation System (NIS) reach rods. Tables 14.3.9-1 and 14.3.9-2 list the 14 containment nodes and the 44 flow junctions, respectively, included in the Cook Nuclear Plant containment model. In addition to the physical arrangement of the Cook Nuclear Plant containment, the ice condenser lower inlet doors were determined to have a major effect on the containment response. The lower inlet doors control the flow of steam entering the ice condenser, and consequently the amounts of condensate and melted ice flowing back to the loop compartment. MAAP4 models the lower inlet door response (degree of opening) as a function of the imposed flow rate consistently with the lower inlet door characteristic shown in Figure 14.3.4-93. The MAAP4 ice melt model was extensively benchmarked against data from Westinghouse Waltz Mill tests (Reference 2) and Pacific Northwest Laboratories tests (Reference 3).


### **14.3.9.3.1.2 Assumptions**

The objective of the MAAP4 analyses of containment sump inventory was to determine if there was a sufficient amount of water in the containment sump to support recirculation without considering the effects of debris-laden fluid and recirculation sump strainer blockage.

The directions of conservatism for key parameters in the containment sump inventory analysis were evaluated and validated by a formal Failure Modes and Effects Analysis that was performed to identify the key parameters and appropriate directions of conservatism. These key parameter values were determined to either minimize the amount of water available to collect in the containment sump or to affect the rate that water accumulated in the containment sump. For example, an assumption that increases the rate of RCS cooldown would increase the amount of water held-up in the RCS and would affect both the rate that water accumulates in containment and the total amount of water available to containment. An assumption that increases heat removal from the lower containment atmosphere would reduce the amount of energy reaching the ice condenser; this would reduce the rate of ice melting and, consequently, the rate that water from ice melt accumulates in the containment. The following major input assumptions are used in the MAAP4 analysis for containment sump inventory.

1. Two sets of initial conditions are analyzed:
  - a. Mode 1: The plant is initially operating at a core power level of 3250 MWt plus reactor coolant pump heat, which remains conservative and bounding for the Measurement Uncertainty Recapture (MUR) power uprate. Effective break size diameters ranging from a full Double-Ended Cold Leg Guillotine (DECLG) to 0.5 inches were assumed. Both the loop


## UFSAR Revision 30.0

 <p><b>INDIANA MICHIGAN POWER</b> An <b>AEP</b> Company</p>	<p><b>INDIANA MICHIGAN POWER</b> <b>D. C. COOK NUCLEAR PLANT</b> <b>UPDATED FINAL SAFETY ANALYSIS REPORT</b></p>	<p>Revised: 27.0 Section: 14.3.9 Page: 11 of 44</p>
--	--	---

compartment and the reactor cavity were considered as potential break locations.

- b. Mode 3: The plant is at the lower temperature bound of Mode 3 (350°F & 1000 psig). A maximum effective break size diameter of 6 inches was assumed. Both the loop compartment and the reactor cavity were considered as potential break locations.
2. A best-estimate core residual heat generation based upon the ANS 1979 decay heat model without uncertainty was assumed.
3. Maximum safeguards are employed for ECCS/CTS pumps, e.g., two CTS pumps and two containment spray heat exchangers; two residual heat removal pumps and two residual heat removal heat exchangers; two safety injection pumps; and two centrifugal charging pumps.
4. Minimum containment air recirculation, i.e., one of two CEQ fans operating at conservatively low flow (consistent with the peak containment pressure analysis). Note that the FMEA determined that the most limiting single failure was a failure of one CEQ fan.
5. A conservatively low value for ice mass is assumed in the ice condenser at accident initiation. The ice temperature is also set to a conservatively low value. This temperature maximizes heat absorption by the ice before melting, which tends to decrease ice mass melt rate.
6. ESW cooling water supplied to the CTS heat exchangers at minimum temperature and conservatively high flow rate.
7. CCW cooling water supplied to the RHR heat exchangers at minimum temperature and conservatively high flow rate.
8. Maximum RHR and CTS heat exchanger performance (i.e., UA).
9. Uncertainties are applied to the high containment pressure ESF signals' setpoints to cause CTS actuation at the lowest containment pressure possible (i.e., cause CTS to initiate as early as possible). The uncertainties are applied consistently so the CEQ fan also starts at the lowest containment pressure possible.
10. Maximum ice condenser bypass flow area as documented in Reference 1.

## UFSAR Revision 30.0

 An AEP Company	<p style="text-align: center;"><b>INDIANA MICHIGAN POWER</b> <b>D. C. COOK NUCLEAR PLANT</b> <b>UPDATED FINAL SAFETY ANALYSIS REPORT</b></p>	<p>Revised: 27.0 Section: 14.3.9 Page: 12 of 44</p>
---	--	---


11. Minimum delivered RWST inventory at the minimum water temperature allowed by Technical Specifications.
12. Minimum accumulator inventory allowed by Technical Specifications at the minimum pressure allowed by Technical Specifications and at the minimum containment temperature allowed by Technical Specifications.
13. Maximum allowable ECCS leakage outside containment following switchover to recirculation.
14. Maximum initial containment pressure allowed by Technical Specifications.
15. Minimum initial containment gas temperatures allowed by Technical Specifications.
16. Maximum RCS cooldown rate allowed by the Emergency Operating Procedures.

### **14.3.9.3.1.3 Acceptance Criteria**

The purpose of the analysis is to demonstrate that there is sufficient water inventory available to the containment sump to preclude vortex formation in the recirculation sump. High levels of air ingested into the suction of the ECCS/CTS pumps can potentially result in damage to those pumps. Thus, air ingress is typically limited to values between 2% and 5% by equipment manufacturers. If vortex formation is precluded in the water pool used as the suction source to the pumps, then air is prevented from entering the pumps.

As demonstrated in Reference 1, the minimum containment sump water level required to preclude pump vortexing is not the same fixed elevation value for all conditions. The minimum containment sump water level to preclude vortexing is a function of the total amount of water being drawn from the recirculation sump once the plant initiates recirculation. The recirculation sump flow demand is determined by the number of CTS pumps operating and the combination of the number of ECCS pumps operating, RCS pressure, and head loss across the recirculation sump strainers. As will be seen, small break LOCA events typically do not depressurize similarly to a large break LOCA event. Even though all six ECCS pumps may be in operation for some smaller breaks, only the CC pumps and potentially the SI pumps are actually providing positive flow to the RCS. As long as RCS pressure remains above the shutoff head of the RHR pumps, the RHR pumps will not be drawing additional water from the recirculation sump inventory.

## UFSAR Revision 30.0

 An AEP Company	<p style="text-align: center;"><b>INDIANA MICHIGAN POWER</b> <b>D. C. COOK NUCLEAR PLANT</b> <b>UPDATED FINAL SAFETY ANALYSIS REPORT</b></p>	<p>Revised: 27.0 Section: 14.3.9 Page: 13 of 44</p>
---	--	---

For this analysis the criterion for acceptable containment sump water level performance was established as follows. A minimum containment recirculation sump level greater than or equal to 602'-10" was required for Mode 1 events. This containment sump water level elevation was determined to preclude vortex formation in the ECCS pump suction flow for all ECCS/CTS flow demand by scale recirculation sump testing. As noted above and as documented in Reference 1, this criterion includes margin for smaller break sizes in Mode 1 as the typical recirculation sump flow demand decreases with decreasing break size. This margin was not explicitly credited in the assessment of the acceptability of the recirculation sump in Mode 1.


Certain Mode 3 LOCA events were determined to achieve minimum containment sump levels slightly less than 602'-10" for short periods of time following switchover to recirculation. This is due to the lower mass and energy release from the RCS experienced during a Mode 3 LOCA and the resultant decrease in ice condenser ice melt rate. However, overall ECCS and CTS flow required for mitigation of a Mode 3 LOCA is less than the maximum flow used in the original containment sump demonstration tests. As shown in Reference 1, the analysis demonstrates that minimum containment sump levels below 602'-10" are acceptable to prevent vortexing in the recirculation sump, at flows less than the maximum flows used in the original containment sump demonstration tests. For Mode 3 LOCA events, the analysis demonstrated that minimum containment sump levels less than 602'-10" was still sufficient to prevent vortexing at the reduced ECCS and CTS flow rates expected.

### **14.3.9.3.2 Results**

The results of three transients are presented. Time profiles of ice bed mass, reactor cavity water level, containment sump water level, and RCS pressure are presented for each case. Figures 14.3.9-1 through 14.3.9-4 show the relevant parameters following a DECLG LOCA in Mode 1. Figures 14.3.9-5 through 14.3.9-8 show the same parameters for the limiting water level case in Mode 1 (a 1 inch break on the cold leg nozzle that partially feeds the reactor cavity). Figures 14.3.9-9 through 14.3.9-12 show parameters for the limiting water level case in Mode 3 (a 6 inch break on the cold leg nozzle that partially feeds the reactor).

The most limiting case for the minimum containment sump level during recirculation is that break size in which the containment sprays are initiated but there is minimal ice melting when the sprays are operating. These are situations in which the steam partial pressure in the loop compartment is minimized (small break LOCA) and the potential for condensation is maximized (the coldest spray temperature).

## UFSAR Revision 30.0

 An AEP Company	<b>INDIANA MICHIGAN POWER</b> <b>D. C. COOK NUCLEAR PLANT</b> <b>UPDATED FINAL SAFETY ANALYSIS REPORT</b>	Revised: 27.0 Section: 14.3.9 Page: 14 of 44
---	---	--

For the DECL break case, the initial discharge of steam and energy is sufficient to melt enough of the ice bed such that the minimum containment water level at any given time is at least several feet above the applicable vortex limit for Mode 1 at all times (Figures 14.3.9-1 through 4). Thus, the large DECL break does not result in conditions that challenge the Mode 1 acceptance criterion.


For the spectrum of LOCA conditions evaluated in the loop compartment for Mode 1, a break with an effective diameter of 1" represents the minimum condition where sprays would be initiated and the steam partial pressure in the loop compartment would be the lowest. This condition represents the most limiting case for a break directly into the loop compartment. The minimum level in the containment sump for this most limiting transient is 9 inches above the appropriate limit for vortexing of 602'10".

For postulated breaks in the cold leg inside the primary shield wall (referred to as reactor cavity breaks), the water discharge from the break is represented as having a 50/50 split between the reactor cavity and the loop compartment based on jet impingement analyses of the two-phase discharge. For these types of breaks, the most limiting case of a 1 inch effective break diameter results in a minimum level in the containment sump of 603'1-1/2" which is 3-1/2 inches above the Mode 1 acceptance criterion of 602'10" (Figures 14.3.9.5 through 8).

Possible break locations were also considered for the RPV lower and upper heads. The maximum break size in the lower head is a rupture (severing) of an in-core instrument penetration tube which provides a break diameter of 0.61 inches with a discharge coefficient of less than 0.6. This is not sufficient to actuate the containment sprays. Thus, the containment sump water level is well above the 602'10" at the time of recirculation which is in excess of 36 hours. A review of possible upper head breaks concludes that two size ruptures should be considered: a failure of a CRDM and the severing of the 0.6 inch diameter reactor head vent. The former initiates the containment sprays and has a minimum level above that of the 1" break in the reactor cavity. The latter case, like the instrument line break, does not result in the sprays being actuated. Therefore, the Mode 1 LOCA cases assuming breaks on the reactor pressure vessel into the reactor cavity result in containment sump water levels during recirculation which are greater than the appropriate design basis limit for vortexing.

Several Mode 3 cases were examined ranging from a 6 inch break to a 2 inch break. The 6 inch break into the loop compartment results in a water level above the acceptance criterion (Figures 14.3.9-9 through 12). The 2 inch break does not actuate the sprays, and the containment sump water level is always above the vortex criterion. This break size spectrum was examined for

## UFSAR Revision 30.0

 An AEP Company	<b>INDIANA MICHIGAN POWER</b> <b>D. C. COOK NUCLEAR PLANT</b> <b>UPDATED FINAL SAFETY ANALYSIS REPORT</b>	Revised: 27.0 Section: 14.3.9 Page: 15 of 44
---	---	--

breaks into the loop compartment as well as the reactor cavity (split flow conditions). While some of these resulted in minimum levels below the Mode 1 acceptance criterion, given the consideration that the reduced sump demand flows for these LOCAs which are smaller than the design basis DECL, there is a sufficient water level to prevent vortexing based on the Cook Nuclear Plant specific sump tests (Reference 1).

The assessment of main steam line breaks into the containment for two different size breaks results in a water level in the containment sump that is above the Mode 1 acceptance criterion to preclude vortex formation. Furthermore, since there is no break in the RCS, there is no long term need for the containment sprays and the injection to the RCS is only that needed to maintain the pressurizer level as the RCS cools down. In addition, the contents of the faulted steam generator are added to the containment sump increasing the amount of water available. Hence, the minimum containment sump water level in these sequences is always above the appropriate criterion for vortexing.

### **14.3.9.3.3 Conclusions**


The analysis demonstrates that RWST delivered inventory, ice melt, and RCS and safety injection accumulator water inventory released to containment, are sufficient to ensure that the minimum containment sump level is sufficient to preclude vortex formation in the suction flow to the RHR/CTS pumps. The containment sump inventory analysis includes consideration of limiting single failures of ECCS and CTS components, determination of the limiting break size and locations, and envelope the range of potential plant operation.

### **14.3.9.4 Recirculation Sump Analyses**

The recirculation sump analyses were performed in accordance with Generic Letter 2004-02 requirements (Reference 7). The recirculation sump analyses include

1. design modifications to significantly reduce the potential effects of post-accident debris and latent material on the functions of the ECCS and CTS during sump recirculation,
2. testing and/or analysis to determine break locations, identity and quantity of debris sources, determination of debris transport fractions, determination of upstream and downstream effects, and confirmation of the recirculation function,
3. implementation of Technical Specifications to reflect the plant modifications and the change to a mechanistic recirculation sump strainer blockage evaluation,

# UFSAR Revision 30.0

 An AEP Company	<p style="text-align: center;"><b>INDIANA MICHIGAN POWER</b> <b>D. C. COOK NUCLEAR PLANT</b> <b>UPDATED FINAL SAFETY ANALYSIS REPORT</b></p>	<p>Revised: 27.0 Section: 14.3.9 Page: 16 of 44</p>
---	--	---

4. use of an Alternate Evaluation methodology that includes operator actions to reduce recirculation flow if the containment recirculation sump water level instruments indicate an increased head loss across the recirculation sump strainers that threatens vortex limits for RHR and CTS pumps,
5. changes to programs, processes, and procedures to limit the introduction of materials into containment that could adversely impact the recirculation function,
6. monitoring programs to ensure containment conditions continue to support the recirculation function, and
7. application of conservative measures to assure adequate margins in actions taken to address Generic Letter 2004-02.

The analytical and testing aspects of the response to Generic Letter 2004-02 requirements are provided below.

#### **14.3.9.4.1 Debris Generation**


##### **14.3.9.4.1.1 Break Selection**

Break selection for recirculation sump inventory analyses was based on determining the size and location of High Energy Line Breaks (HELBs) which produce debris and potentially present the greatest challenge to recirculation sump performance. Only those breaks requiring recirculation for Cook Nuclear Plant accident mitigation were to be considered, in accordance with References 9 and 12. These potentially include LBLOCA's, certain SBLOCA's, and MSLB's.

Resolution of Large Break Loss of Coolant Accidents (LBLOCAs) in Generic Letter 2004-02 for recirculation sump inventory analyses can be addressed through either a classical evaluation of the largest RCS Double Ended Guillotine Break (DEGB), i.e., those with a total cross sectional break area  $\geq 1.0 \text{ ft}^2$ , and its effects or by use of an Alternate Evaluation approach defined in Section 6 of References 9 and 12. Cook Nuclear Plant has selected the Alternate Evaluation approach. This approach requires evaluation of two distinct pipe break scenarios for the large break LOCA, each with their own set of allowed assumptions and methodologies. The first scenario requires a 10 CFR 50.46 design basis, long-term cooling evaluation of all LOCA break sizes up to a defined Debris Generation Break Size (DGBS) that is smaller than a Double Ended Guillotine Break (DEGB) of the largest RCS pipe. This regime of break sizes is referred to as Region I and is defined as either a complete guillotine break of the largest diameter pipe connected to the main RCS coolant loop piping or an area equivalent to a guillotine break of a 14 inch schedule 160 line, which equates to an effective break area of 196.6 square inches assuming



## UFSAR Revision 30.0

 An <b>AEP</b> Company	<b>INDIANA MICHIGAN POWER</b> <b>D. C. COOK NUCLEAR PLANT</b> <b>UPDATED FINAL SAFETY ANALYSIS REPORT</b>	Revised: 27.0 Section: 14.3.9 Page: 17 of 44
--	---	--


both sides of the break are pressurized. The second scenario (Region II breaks) requires that long-term cooling requirements be demonstrated for break sizes above the DGBS and up to the DEGB of the largest RCS pipe. Due to the reduced likelihood of occurrence; however, References 9 and 12 provide guidance that can be used to justify more realistic evaluation techniques and inputs for the DEGB, and they allow the use of operator actions to mitigate the consequences of sump blockage, when specified justification can be provided.

A rupture of the RCS pressure boundary less than 1.0 ft<sup>2</sup> total cross sectional area is classified as a SBLOCA. The minimum size break required to be analyzed for debris generation and transport is 2 inches per Section 3.3.4.1 of Reference 9. The evaluation determined that there are no SBLOCA's outside the crane wall that result in sump recirculation. Further, from a debris generation and transport standpoint, SBLOCAs are bounded by the results of LBLOCAs. As a result, SBLOCA's were not analyzed for recirculation sump inventory.

While LOCAs are considered the most likely type of debris generating HELBs that could lead to sump recirculation, other break scenarios were examined to determine if they resulted in debris generation and the need for ECCS recirculation as a means of long-term cooling. WCAP-15302 (Reference 10) defines the MSLB as a short-term event compared to a LOCA event and states that containment recirculation is not assumed to occur within the duration for which the transient is analyzed. An evaluation was performed to determine if a MSLB needed to be evaluated per the GL 2004-02 requirements. This evaluation determined that the licensing basis analysis for the MSLB mass and energy releases into containment does not include the availability of long-term recirculation water for event mitigation. For Cook Nuclear Plant, the MSLB bounds the feedwater line break for mass and energy release within containment. As a result, secondary system breaks were not analyzed for recirculation sump inventory.



## UFSAR Revision 30.0

 An AEP Company	<p style="text-align: center;"><b>INDIANA MICHIGAN POWER</b> <b>D. C. COOK NUCLEAR PLANT</b> <b>UPDATED FINAL SAFETY ANALYSIS REPORT</b></p>	<p>Revised: 27.0 Section: 14.3.9 Page: 18 of 44</p>
---	--	---

Ultimately, the following general break locations were considered in the recirculation sump inventory analyses because they represented bounding variations in debris generation by size, quantity, and type of debris:

1. Breaks in the RCS with the largest potential for debris
2. Large breaks with two or more different types of debris
3. Breaks in the most direct path to the recirculation sump
4. Large breaks with the largest potential particulate debris to insulation ratio by weight
5. Breaks that generate a "thin bed" – high particulate with 1/8" fiber bed


Several break locations within the RCS have the potential to generate the largest quantity of debris. These include a break in the crossover leg piping on each of the four loops, a reactor nozzle break in the reactor cavity, an alternate break in the pressurizer surge line, and an alternate break in each of the four RCS loops. The alternate breaks are those considered as DGBS breaks.

For each of the above break locations, the corresponding zone of influence (ZOI) was established to determine the amount of material destroyed by the break. The ZOI is defined as the spherical volume centered at the break location in which the jet pressure is greater than or equal to the destruction damage pressure of the insulation, coatings, and other materials impacted by the break jet. The radius of the sphere is determined by the pipe diameter and the destruction pressures of the potential target debris material. The break with the largest potential for debris generation is the Reactor Coolant System (RCS) crossover line.

The debris generated by the most limiting cases in Break No. 1 will bound Break No. 2 because each of the breaks for Break No. 1 create at least two different types of debris. Break No. 1 at the RCS Loop 2 crossover leg will provide the greatest potential for debris transport to the recirculation sump. Break No. 1 also envelopes Break No. 3 since the RCS Loop 2 piping has the most direct path to the recirculation sump. Break No. 4 is included to generate the largest insulation particulate debris combination of calcium silicate, Min-K and Marinite. Therefore, only Break types 1, 4 and 5 are applicable for debris generation analysis.

For the DGBS, the ZOI was established using a hemispherical volume oriented such that the maximum quantity of debris would be generated from the break. The use of the hemispherical volume was performed per Section 6.3.4 of References 9 and 12.

## UFSAR Revision 30.0

 An AEP Company	<p style="text-align: center;"><b>INDIANA MICHIGAN POWER</b> <b>D. C. COOK NUCLEAR PLANT</b> <b>UPDATED FINAL SAFETY ANALYSIS REPORT</b></p>	<p>Revised: 27.0 Section: 14.3.9 Page: 19 of 44</p>
---	--	---

### **14.3.9.4.1.2 Debris Sources**

In order to evaluate recirculation sump strainer blockage, debris sources inside containment with the potential to be transported to the recirculation sump strainers were identified. The following general debris sources exist in containment:


- a. Insulation Debris
- b. Coatings Debris
- c. Latent Debris
- d. Containment Materials

The insulation debris sources which were evaluated for recirculation sump blockage are reflective metallic insulation (RMI), fibrous insulation, calcium silicate (Cal-Sil), Marinite and Min-K. Table 14.3.9-3 contains the location and quantities of the bounding insulation debris sources assumed in the analyses. The quantity of insulation materials from Unit 2 were used since they bound the quantities in Unit 1.

Closed-cell foam insulation is installed on various service water piping lines inside lower containment. All closed-cell foam insulation installed in the loop compartment up to the 650 ft elevation has been installed with two layers of stainless steel jacketing. Testing was performed on this jacketing configuration and it was demonstrated that the closed-cell foam insulation remains encapsulated following the break. Therefore, closed-cell foam insulation is not considered a debris source for recirculation sump blockage.

There are two types of coatings in use at D.C. Cook, qualified and unqualified coatings. The qualified coatings are epoxy coating systems and the unqualified coatings consist of epoxy, alkyd and cold galvanizing coating systems. Qualified and unqualified coatings within a break ZOI are postulated to fail as a result of direct impingement. The break ZOI for qualified coatings is a distance of five pipe diameters from the break, or 5D, and the break ZOI for unqualified coatings is 10D. Qualified coatings outside of a break ZOI will remain intact whereas unqualified coatings outside of a break ZOI are postulated to fail as a result of the post-accident environmental conditions. The size distribution of the unqualified coating debris changes depending on whether the unqualified coating is within or outside of the break ZOI. Table 14.3.9-4 presents the coatings debris source for the DEGB within the ZOI and Table 14.3.9-5 presents the coatings debris source for the DGBS within the ZOI. Table 14.3.9-6 presents the unqualified coatings debris source outside of the ZOI, for either break size.

## UFSAR Revision 30.0

 An AEP Company	<b>INDIANA MICHIGAN POWER</b> <b>D. C. COOK NUCLEAR PLANT</b> <b>UPDATED FINAL SAFETY ANALYSIS REPORT</b>	Revised: 27.0 Section: 14.3.9 Page: 20 of 44
---	---	--

Latent debris is defined as dirt, dust, paint chips, fibers, pieces of paper, plastic, tape, adhesive labels or other materials that are present inside the containment building prior to a LOCA. Electromark labels are used inside the containment building. These labels represent latent debris if they are located in a break ZOI, applied to a painted surface, or if they are submerged. All unqualified labels are assumed to fail inside containment during a LOCA. Fire barrier tape is installed on conduits inside containment for the purpose of electrical separation. This fire barrier tape is classified as latent debris within a break ZOI. Outside a break ZOI, the fire barrier tape does not fail as it is secured at each end by stainless steel fasteners. Flexible conduit PVC jacketing located in the loop compartment is postulated to fail during a LOCA and therefore represents a latent debris source. Small amounts of foreign material are present in the ice condenser. This ice condenser foreign material constitutes a latent debris source. Table 14.3.9-7 documents the bounding quantity of latent debris evaluated inside the containment building by location. Tables 14.3.9-22 and 14.3.9-23 provide the bounding quantity of debris for sacrificial strainer area consideration for the main and remote strainers for the DEGB and DGBS.


Containment materials may also be considered a debris source if they produce a chemical precipitate when the material is either submerged or subjected to containment spray. Table 14.3.9-8 identifies the containment materials considered as chemical effects debris sources, the amount of the material, and whether the material is submerged or non-submerged.

### **14.3.9.4.1.3 Results**

Two break locations have been identified as bounding for this analysis. These bounding breaks are a double ended guillotine break (DEGB) of the crossover leg in loop 4 and the alternate break in the loop 4 crossover leg which produces the maximum debris load for the debris generation break size (DGBS) break.

### **14.3.9.4.2 Debris Transport**

Debris transport predicts the blowdown, washdown, pool fill, and recirculation transport of the debris that would be generated from a high energy line break requiring recirculation. The transport analysis includes computational fluid dynamics (CFD) modeling of the containment pool during both the pool fill and recirculation phases. Debris transport was determined for each type/size of debris at each of the break locations postulated in the Cook Nuclear Plant debris generation analysis. The debris generation analysis determined that 10 cases should be analyzed for debris transport. These cases are for a break in the crossover leg piping on each of the four loops, a reactor nozzle break in the reactor cavity, an alternate break in the pressurizer surge line and an alternate break in each of the four primary loops.

 An AEP Company	<p>INDIANA MICHIGAN POWER D. C. COOK NUCLEAR PLANT UPDATED FINAL SAFETY ANALYSIS REPORT</p>	<p>Revised: 27.0 Section: 14.3.9 Page: 21 of 44</p>
---	---	---

#### **14.3.9.4.2.1 Computer Code Utilized**

The Computation Fluid Dynamics (CFD) calculation for pool fill and recirculation flow in the Cook Nuclear Plant containment pool was performed using Flow-3D Version 9.0. Flow-3D is a general-purpose computer code for modeling the dynamic behavior of liquids and gases influenced by a wide variety of physical processes. The program is based on the fundamental laws of mass, momentum, and energy conservation for the treatment of time-dependent multi-dimensional problems.

A three-dimensional CAD model of the Cook Nuclear Plant containment building was constructed based on structural drawings of the containment building. The CAD model was built from a point below the floor of the containment building (elevation 598.78') to the top of the dog houses (elevation 695.00').


#### **14.3.9.4.2.2 Method of Analysis**

Debris transport is the estimation of the fraction of debris that is transported from the break location to the recirculation sump strainers. The four major debris transport modes are:

- *Blowdown transport* – the vertical and horizontal transport of debris to all areas of containment by the break jet.
- *Washdown transport* – the vertical (downward) transport of debris by the containment sprays and break flow.
- *Pool fill transport* – the transport of debris by break and containment spray flows from the refueling water storage tank (RWST) to regions that may be active or inactive during recirculation.
- *Recirculation transport* – the horizontal transport of debris from the active portions of the recirculation pool to the recirculation sump strainers by the flow through the emergency core cooling system (ECCS).

The methodology used in this analysis is based on NEI 04-07 (Reference 9). The specific effect of each mode of transport was analyzed for each type of debris generated, and a logic tree was developed to determine the total transport to the recirculation sump strainers.

# UFSAR Revision 30.0

 <b>INDIANA MICHIGAN POWER</b> <small>An AEP Company</small>	<b>INDIANA MICHIGAN POWER D. C. COOK NUCLEAR PLANT UPDATED FINAL SAFETY ANALYSIS REPORT</b>	Revised: 27.0 Section: 14.3.9 Page: 22 of 44
--	---	--


The general methodology for the transport analysis includes:

1. Creation of a three-dimensional model of the containment building and determine transport flow paths.
2. Evaluation of the debris types, size distributions and transport fractions.
3. Inclusion of the ice melt and containment spray flows in the CFD calculation to model the effects on the containment pool. Bounding containment spray flow rates of 4,556 gpm for upper containment, 1,638 gpm for the loop compartment and 606 gpm for the annulus were used.
4. Development and use of transporting metrics to evaluate the potential for debris transport in the Cook Nuclear Plant containment pool. Metrics for predicting debris transport have been adopted or derived from data. The transport mechanisms involved are:
  - a. Carrying of suspended debris by bulk flow to the sump
  - b. Tumbling/sliding of sunken debris to the sump
  - c. Lifting of sunken debris over a curb
5. Determination of the fraction of debris in the loop compartment that would be transported to the main strainer and annulus during pool fill-up.
6. Determination of the fraction of debris that would be transported to the main strainer and to the remote strainer during recirculation.
7. Determination of the overall transport fraction for each type of debris.

## **Blowdown Transport**

The blowdown following a LOCA would impact the debris sources in the vicinity of the break location. Steam from the blowdown, carrying debris with it, would be relieved through openings in the crane wall to the annulus, through the ice condenser lower inlet doors, and through openings to the reactor cavity. Based on the Transient Mass Distribution (TMD) analysis (Section 14.3.4.2.7), seventy percent of the mass and energy release is directed to the ice condenser, twenty-two percent is directed to the annulus and the remaining eight percent is directed towards the reactor cavity. Fine debris is easily transported with the blowdown flow so the fraction of fine debris blown into the ice condenser, annulus and reactor cavity was assumed to be proportional to the TMD flow split.

## UFSAR Revision 30.0

 An AEP Company	<p style="text-align: center;"><b>INDIANA MICHIGAN POWER</b> <b>D. C. COOK NUCLEAR PLANT</b> <b>UPDATED FINAL SAFETY ANALYSIS REPORT</b></p>	<p>Revised: 27.0 Section: 14.3.9 Page: 23 of 44</p>
---	--	---

Pieces of RMI, Cal-Sil, Marinite, Electromark labels and fire barrier tape would also be blown toward the same locations. For conservatism, it was assumed that neither small nor large pieces of debris would be blown into and remain within the ice condenser or the reactor cavity. Some of the small pieces could be blown over the top of the overflow wall and through the crane wall openings in the overflow wall to the annulus.

### **Washdown Transport**

During the washdown phase, debris in upper containment, which includes failed unqualified coatings, is washed down to the loop compartment by the Containment Spray System via the refueling canal drains. Any debris resident in the ice condenser as a result of the blowdown will be washed down to the loop compartment by the ice melt via the ice condenser drains. Washdown may also occur from the CEQ fan rooms through the floor drain lines. Although the floor drain lines are protected from transporting large debris sources due to the installed debris interceptors, small debris sources will pass through the drain lines into lower containment. In Unit 1, the water from the CEQ fan room will drain to the pipe tunnel sump in the annulus. In Unit 2, the CEQ fan room will drain to the lower containment sump in the loop compartment.


### **Pool Fill and Recirculation Transport**

During pool fill, the flow of water would transport insulation debris from the break location and other containment debris sources to all areas of the containment sump. As water enters the containment sump, it initially flows in shallow, high velocity sheets. As the water level rises, debris would be transported to the main strainer and the debris interceptor located in front of the holes in the flood-up overflow wall.

During pool fill, the temperature ranges from a maximum of 190 °F during blowdown to 160 °F at the beginning of recirculation. During the pool fill debris transport analysis, the flow through the main strainer was calculated to be approximately 7100 gpm. This flow rate was determined using a combined resistance factor for the strainer system. The pool fill and recirculation CFD analysis used a water temperature of 160 °F. In terms of debris transport, a large change in water temperature does not make a significant difference in the CFD calculation since it was determined that a hot pool develops approximately the same velocity and turbulence as a cooler pool. The total injection and recirculation flow rate for this analysis, using maximum ECCS and CTS pump flow is 15,500 gpm and 14,400 gpm, respectively.

The pool fill and recirculation debris transport fractions were determined using CFD modeling. The result of this modeling was a three-dimensional model showing the turbulence and fluid velocities within the pool. By comparing the direction of pool flow, the magnitude of the

## UFSAR Revision 30.0

 An AEP Company	<b>INDIANA MICHIGAN POWER</b> <b>D. C. COOK NUCLEAR PLANT</b> <b>UPDATED FINAL SAFETY ANALYSIS REPORT</b>	Revised: 27.0 Section: 14.3.9 Page: 24 of 44
---	---	--

turbulence and velocity, the initial location of debris, and the specific debris transport metrics, the transport of each type/size of debris was determined.

### **14.3.9.4.2.3 Results**

Blowdown following a LOCA in the loop compartment will carry a large fraction of fine debris into the ice condenser, as well as some debris to the annulus and to the reactor cavity. Due to the large ice melt and spray flows, the majority of transportable debris located in these flow paths will be washed to lower containment. During the pool fill phase of the accident, a large fraction of the debris will be transported to the main strainer. The transport analysis determined that most of the fine debris will be transported to either the main or the remote strainers. Small and large pieces of debris will not be transported to the remote strainer since there are no breaks located in the annulus and due to the location of the debris interceptors installed in the loop compartment. Following determination of the debris transport for each of the break locations associated with the RCS loop piping, an evaluation was performed to determine the bounding breaks for both the DEGB and DGBS. These break locations were determined to be the RCS Loop 4 crossover leg for the DEGB and the alternate break in RCS Loop 4 for the DGBS. Table 14.3.9-10 shows the debris transported to the main strainer at the end of the pool fill phase, overall transport to the main strainer, and overall transport to the remote strainer for the DEGB. Table 14.3.9-11 shows the debris transported to the main strainer at the end of the pool fill phase, overall transport to the main strainer, and overall transport to the remote strainer for the DGBS. The breaks in the reactor cavity and pressurizer surge line were determined to be bounded by the DEGB in the RCS piping and the DGBS break in the RCS piping, respectively.


### **14.3.9.4.3 Recirculation Sump Hydraulic Analysis**

Postulated LOCAs for which sump recirculation is required are in the loop compartment or reactor cavity. For a LBLOCA, once water level in the loop compartment exceeds the height of the main strainer curb during the injection phase, debris-laden water would begin to flow through the main strainer into the recirculation sump. When level in the recirculation sump reaches slightly above floor level, strained water from the recirculation sump would begin to flow through the waterway toward the remote strainer. Initially, this would only fill the waterway until the water level reaches the height of the lowest set of strainer elements in the remote strainer. When the loop compartment water level exceeds this height, strained water would begin back-flowing out of the remote strainer into the annulus.

Additionally, when water level in the loop compartment exceeds approximately 5 inches, debris-laden water will begin flowing through the openings in the flood-up overflow wall, filling the



## UFSAR Revision 30.0

 <b>INDIANA MICHIGAN POWER</b> <small>An AEP Company</small>	<b>INDIANA MICHIGAN POWER D. C. COOK NUCLEAR PLANT UPDATED FINAL SAFETY ANALYSIS REPORT</b>	Revised: 27.0 Section: 14.3.9 Page: 25 of 44
--	---	--

space between the flood-up overflow wall and the curb at the crane wall opening. Once water level in this area exceeds approximately 12 inches, debris-laden water will begin flowing into the annulus through this flow path.

Once recirculation flow is established, reverse flow through the remote strainer will cease. Water will then flow into the recirculation sump through both the main strainer and the remote strainer and waterway. Since a pipe break requiring recirculation is not postulated to occur in the annulus, debris at the remote strainer would have been transported from the loop compartment to the annulus during the initial blowdown, or transported to the annulus through the overflow wall flow holes during pool fill-up, or it would have consisted of latent debris resident in the annulus prior to the event. As a result, the remote strainer would be essentially debris free at the beginning of recirculation. Due to the waterway head loss, the preferential flow path for recirculation flow would be through the main strainer, until the main strainer becomes substantially blocked by debris. The division of flow between the main and remote strainers is a function of the head loss through the associated strainer and the waterway.


A recirculation sump hydraulics analysis was performed to analyze the above flow characteristics of the main and remote strainer system under various bounding strainer loading conditions. The purpose of the analysis was to ensure that the required sump recirculation flow rate could be achieved for all postulated conditions. The analysis used Computational Fluid Dynamics (CFD) calculations of flow through the main and remote strainers for the following cases to determine the flow split between the main strainer and the remote strainer and their associated head loss.

1. Forward Flow – Clean Main and Remote Strainers
2. Forward Flow – Main Strainer 90% Blocked, Remote Strainer Clean
3. Forward Flow – Main Strainer 100% Blocked, Remote Strainer Clean
4. Reverse Flow – Flow Enters into Main Strainer and Out of Remote Strainer during Pool Fill

The recirculation sump hydraulic analysis also evaluated the potential for vortex formation in the recirculation sump during RHR and CTS operation, as a function of water level inside the recirculation sump. This analysis, performed with the same methodology that was used for the original Alden Laboratories analysis (Froude number correlation), concluded that an air entraining vortex would not occur with a water level inside the recirculation sump of 601'-6".



## UFSAR Revision 30.0

 An AEP Company	<p style="text-align: center;"><b>INDIANA MICHIGAN POWER</b> <b>D. C. COOK NUCLEAR PLANT</b> <b>UPDATED FINAL SAFETY ANALYSIS REPORT</b></p>	<p>Revised: 27.0 Section: 14.3.9 Page: 26 of 44</p>
---	--	---

This analysis also assumed that the column height of water being considered was directly above the recirculation sump suction piping openings.

Finally, the analysis included a calculation of the maximum pressure load on the waterway considering both forward and reverse flow to ensure an acceptable structural design (Reference Section 6.2.2).

### **14.3.9.4.3.1 Computer Code Utilized**

The CFD calculation for sump flow through the recirculation sump strainers and waterway was performed using Flow-3D Version 9.0. The CFD analysis of the flow through the strainers is based on the CAD model, as discussed in Section 14.3.9.4.2.1, which represents the physical construction of the containment building and flow domain. The CFD model was developed to simulate fluid flow in the recirculation sump to predict flow patterns which would occur during the recirculation phase of a LOCA.

### **14.3.9.4.3.2 Method of Analysis**


#### **Design Input Parameters**

1. The maximum ECCS flow rate during recirculation is 14,400 gpm.
2. Water level: 5.9 ft above the containment sump floor, or elevation 604.7 ft, was used as the minimum water level during recirculation for the analyzed accidents. This is conservative since the lowest water level produces the highest flow velocities and turbulence levels, thus resulting in the highest transport fractions.
3. Water temperature: The water temperature was 190°F for the forward flow case, and the water temperature for the reverse flow case was 200°F.
4. Total recirculation sump strainer area is 1,938 ft<sup>2</sup>, with the main strainer having 900 ft<sup>2</sup> and the remote strainer 1,038 ft<sup>2</sup>. (Analyzed recirculation sump strainer size is conservatively smaller than the installed recirculation sump strainer.)

### **Forward Flow Cases**

The objective of the flow analyses was to determine the flow distribution through the main strainer and the remote strainer and associated waterway. As discussed in Section 14.3.9.4.3, three forward flow hydraulic flow cases were analyzed. For the clean case, both the main and remote strainers were completely open and unrestricted by debris. This case provides the minimum pressure drop through the system. This established the recirculation sump hydraulic conditions for various stages of main strainer loading to determine the bounding cases for flow

# UFSAR Revision 30.0

 An AEP Company	<p style="text-align: center;"><b>INDIANA MICHIGAN POWER</b> <b>D. C. COOK NUCLEAR PLANT</b> <b>UPDATED FINAL SAFETY ANALYSIS REPORT</b></p>	<p>Revised: 27.0 Section: 14.3.9 Page: 27 of 44</p>
---	--	---

to/from the remote strainer. For the 100% blocked main strainer case, the main strainer area was assumed to be completely blocked by debris and the remote strainer was debris free. In this case, the remote strainer had to pass the full recirculation flow. This established the worst case head loss across the remote strainer and the highest pressure load for the waterway.

## **Reverse Flow Case**

The hydrostatic pressure in the containment sump is greater than the annulus hydrostatic pressure during the pool fill phase. This hydrostatic pressure difference drives flow from the containment sump to the annulus through the remote strainer waterway and remote strainer. This is defined as the reverse flow case. The reverse flow case was evaluated to determine the pressure load on the wall surfaces of the remote strainer waterway during the pool fill phase. The maximum reverse flow rate for this analysis is 6,400 gpm. This flow rate was determined by establishing flow resistance values for each of the components within the flow path.


## **Vortex Evaluation**

The adequacy of the original recirculation sump design with respect to prevention of significant air entrainment following a LOCA was tested using a 1:2.5 scale model of the Cook Nuclear Plant design in 1978. This testing, which was performed by Alden Laboratories and documented in Reference 5, demonstrated that neither vortex formation nor air ingestion by the ECCS or CTS pumps would likely occur if the water outside the recirculation sump was at or above elevation 602'-3", with 50% of the screen area blocked. The basis for the 602'-3" limit was to ensure there was a sufficient height of water to provide the necessary flow over the curb and blocked portions of the screen. This limit was found to be acceptable in Reference 5 since it was less than the minimum water level of 602'-10" expected in the containment sump.

The original Alden testing evaluated vortex formation considering the water level in the containment sump with 50% of the screen area not blocked. This allowed for visual evaluation of the development of surface swirls and vortices since the water level inside the recirculation sump was essentially at the same level as the containment sump.

Since the original Alden testing did not evaluate a condition under which a head loss could develop due to debris loading across the entire surface of the strainer, resulting in a water level difference between the containment sump and recirculation sump, an additional vortex analysis was performed using the Alden test cases. This analysis, performed with the same methodology that was used for the original Alden Laboratories analysis (Froude number correlation), concluded that an air entraining vortex would not occur with a water level inside the recirculation sump of 601'-6". This analysis also assumed that the column height of water being

## UFSAR Revision 30.0

 An AEP Company	<b>INDIANA MICHIGAN POWER</b> <b>D. C. COOK NUCLEAR PLANT</b> <b>UPDATED FINAL SAFETY ANALYSIS REPORT</b>	Revised: 27.0 Section: 14.3.9 Page: 28 of 44
---	---	--

considered was directly above the recirculation sump suction piping openings. This water level defined the acceptance criterion for minimum recirculation sump water level against which the analyses of the bounding forward flow cases identified in Section 14.3.9.4.3 were judged. In addition, the minimum water level was used in establishing the alarm setpoint for Containment Recirculation Sump Water Level instruments, installed inside the recirculation sump. These instruments, qualified to RG 1.97 requirements, annunciate if water level during sump recirculation drops inside the recirculation sump to a value that is indicative of a significant head loss across the recirculation sump strainers.


An additional concern associated with vortexing is the potential for air to be ingested from the surface of the containment sump pool, through the strainer, and into the recirculation sump. This is of particular concern when conditions of minimum submergence exist. As a result, testing was performed at the recirculation sump strainer vendor's facilities. Water level was intentionally lowered during this testing to approximately 2 inches above the strainer pockets at maximum head loss conditions to determine if any vortices would form on the surface of the containment sump. The testing determined that no vortices would form.

### **14.3.9.4.3.3 Results**

#### **Forward Flow Cases**

Analyses of bounding flow scenarios through the main and remote strainer/waterway system were performed to estimate the flow split between the remote strainer and the main strainer and to determine the associated head loss through the strainer system, the latter being indicated by the resulting water level inside the recirculation sump. Results indicated that the flow split and head loss change rapidly when the main strainer blockage was changed from fully blocked to 10% open. Figure 14.3.9-14 provides the performance curve for the recirculation sump strainer system, indicating the variance in flow split for the main and remote strainers as a function of blockage of the main strainer, and the strainer system head loss as a function of blockage of the main strainer. The predicted maximum head loss across the recirculation sump strainer was 2.8 ft-H<sub>2</sub>O for the main strainer fully blocked case. This head loss is approximately the same as the available hydrostatic head from water in the containment sump.

Review of the forward flow cases indicates that the largest pressure load through the remote strainer/waterway system occurs when the main strainer is completely blocked and all recirculation flow is entering the remote strainer. The estimated pressure load for this case is bounding for all forward and reverse flow cases at 4.5 ft-H<sub>2</sub>O. This maximum pressure load was found to be acceptable.

 An AEP Company	<p style="text-align: center;"><b>INDIANA MICHIGAN POWER</b> <b>D. C. COOK NUCLEAR PLANT</b> <b>UPDATED FINAL SAFETY ANALYSIS REPORT</b></p>	<p>Revised: 27.0 Section: 14.3.9 Page: 29 of 44</p>
---	--	---

## **Reverse Flow Case**

A Reverse Flow Case was evaluated to determine the pressure load on wall surfaces of the remote strainer waterway during the pool fill phase. During pool fill, the hydrostatic pressure in the loop compartment pool is greater than the hydrostatic pressure in the annulus. This hydrostatic pressure difference drives flow from the containment sump to the annulus through the main strainer, remote strainer waterway, and remote strainer. The maximum reverse flow rate through the remote waterway and remote strainer corresponds to the maximum head loss through the remote strainer system. The head loss through the remote strainer system, for the reverse flow case is 1.85 ft-H<sub>2</sub>O. The maximum pressure load on the remote strainer waterway is 1.75 ft-H<sub>2</sub>O. This maximum pressure load was found to be acceptable.

## **Vortex Evaluation**

The vortex evaluation determined that air entraining vortex formation in the recirculation sump will not occur if the minimum recirculation sump water level is above 601'-6". Containment Recirculation Sump Water Level instruments are installed inside the recirculation sump with control room indication and alarm to warn the operators of excessive recirculation sump strainer blockage during sump recirculation. (See Table 7.8-1)

### **14.3.9.5 Recirculation Sump Strainer Head Loss**

Plant-specific impacts on the recirculation sump strainer system due to postulated debris buildup and chemical effects on the main and remote strainers were determined through a series of scaled tests. Three different test loop configurations were used for head loss testing of the recirculation sump strainers. These included:


- Large Scale Test Loop
- Multi Functional Test Loop (MFTL)
- Vuez Facility Tank Test Loop

The Large Scale Test Loop was used for debris only testing and the MFTL and Vuez Facility Test Loop were used for chemical effects testing. Clean strainer head loss testing was performed on all three loops to establish the baseline head loss before debris or chemical addition. Details of the tests are provided below.

#### **14.3.9.5.1 Recirculation Sump Strainer Debris Only Testing**

The Large Scale Test Loop utilized a strainer assembly with segregated approach areas for main and remote strainer sections that allowed separate debris additions to either strainer section.

## UFSAR Revision 30.0

 An AEP Company	<b>INDIANA MICHIGAN POWER</b> <b>D. C. COOK NUCLEAR PLANT</b> <b>UPDATED FINAL SAFETY ANALYSIS REPORT</b>	Revised: 27.0 Section: 14.3.9 Page: 30 of 44
---	---	--

Approximate flow distribution between the main and remote strainer sections was collected during testing. The test configuration differed from the Cook Nuclear Plant installation in that there was no waterway in the test facility and no vent pipe for the modeled sump. These divergences were addressed during evaluations of the test results.

A scaling factor of 41 was used for the Large Scale Test Loop, based on test loop flow rate capability. This scaling factor resulted in the use of 15 strainer pockets for the main strainer side and 18 strainer pockets for the remote strainer side. This number of pockets represents the equivalent of 824 ft<sup>2</sup> for the main strainer and 989 ft<sup>2</sup> for the remote strainer. The remaining recirculation sump strainer area, 76 ft<sup>2</sup> for the main strainer and 83 ft<sup>2</sup> for the remote strainer, represents sacrificial strainer area. Sacrificial strainer area is used for debris sources, such as tags, labels, tape, and other similar materials. Refer to Section 14.3.9.4.1.2 for information pertaining to quantities of debris sources in containment.


Debris only strainer head loss testing was performed on the Large Scale Test Loop for both the DEGB and the DGBS scenarios. The tests were the standard head loss tests consisting of stepped flow rates and stepped homogeneous debris additions, debris sequence tests, event sequence tests, and flow reduction sequences.

Debris sequence testing was designed to pre-load the test strainer with purely fibrous debris prior to addition of debris with both fiber and particulate, followed by other particulate, and then RMI. This test was performed to determine if the debris quantities could form a thin bed that would result in higher head losses than a homogeneously mixed debris test sequence.

Event sequence testing was performed to simulate, to the extent practical, a conservatively calculated, homogeneous mixed delivery of debris to the main strainer during pool fill, with its corresponding flow rate, followed by an increase to a similarly conservative quantity of homogeneously mixed debris to both the main and remote strainer with a stepped increase in flow to the 100% recirculation flow rate.

Flow reduction sequence tests were performed during the standard homogeneous debris addition tests to determine the impact the flow reduction would have on the system head loss. These tests were performed by reducing flow equivalent to removal of a CTS pump, followed by reducing flow equivalent to removal of another CTS pump, reducing flow equivalent to removal of an RHR pump, and then securing all flow followed by restoring flow equivalent to restarting an RHR pump, followed by sequential restoration of flow equivalent to restarting the remaining RHR and CTS pumps.

## UFSAR Revision 30.0

 An AEP Company	<b>INDIANA MICHIGAN POWER</b> <b>D. C. COOK NUCLEAR PLANT</b> <b>UPDATED FINAL SAFETY ANALYSIS REPORT</b>	Revised: 27.0 Section: 14.3.9 Page: 31 of 44
---	---	--

Debris quantities used for the DEGB and the DGBS tests for the main strainer are provided in Table 14.3.9-12. Debris quantities used for the DEGB and the DGBS tests for the remote strainer are provided in Table 14.3.9-13.

The head loss results from the DEGB tests are shown in Figures 14.3.9-15 through 14.3.9-17. The head loss results from the DGBS tests are shown in Figures 14.3.9-18 through 14.3.9-20. Based on the analysis of this testing, the testing performed in the Large Scale Test Loop was determined to provide the data necessary to establish system head loss values. The results from this testing were used as an input to a calculation that establishes the overall system clean strainer head loss that considers the series-parallel configuration of the installed strainer system. The system head loss analysis is described in Section 14.3.9.5.3.

### **14.3.9.5.2 Recirculation Sump Strainer Chemical Effects Testing**


#### **MFTL Testing**

The MFTL utilized a strainer assembly representative of a non-vented main strainer only. This was due to the limitation of the MFTL to model the physically separate strainers at Cook Nuclear Plant, but was adequate for testing to determine the increase in strainer head loss above the debris only cases as a result of chemical effects.

Testing on the MFTL included testing of both the DEGB and DGBS scenarios. A scaling factor of 19.2 was used for this testing based on the available test strainer area. To establish the effects of chemical precipitates on the debris only head loss, extended tests were performed to establish a baseline debris only head loss. Chemicals were then added to the test loop to generate the expected chemical precipitates, based on bench top testing that considered the expected quantities of precipitates that would be formed, as established by WCAP-16530-NP, Evaluation of Post-Accident Chemical Effects in Containment Sump Fluids to Support GSI-191 (Reference 8). For both the DEGB and DGBS tests, sodium aluminate solution was added to achieve 40%, 70%, 100%, 120%, and 140% of the predicted total quantity. For the DEGB test, calcium chloride and sodium silicate solutions were added to the test loop in the same percentages as the sodium aluminate solution. For the DGBS test, the calcium chloride and sodium silicate solutions were added in three separate additions with a final percentage of the predicted quantity of 287% and 298%, respectively.

The debris quantities used for the DEGB and DGBS tests are provided in Table 14.3.9-14. The chemical quantities used for the DEGB and DGBS are provided in Tables 14.3.9-15 and 14.3.9-16.

## UFSAR Revision 30.0

 An AEP Company	<b>INDIANA MICHIGAN POWER</b> <b>D. C. COOK NUCLEAR PLANT</b> <b>UPDATED FINAL SAFETY ANALYSIS REPORT</b>	Revised: 27.0 Section: 14.3.9 Page: 32 of 44
---	---	--

The head loss result from the DEGB test is shown in Figure 14.3.9-21. The head loss result from the DGBS test is shown in Figure 14.3.9-22. The application of the limiting head loss from these tests is described in Section 14.3.9.5.3.2.

### **Vuez Testing**

The Vuez facility tank test loop was used for longer term integrated chemical effects testing. It utilized a four-pocket strainer assembly that was representative of the main strainer only. The Vuez test loop determined the impact of chemical precipitates formed through the interaction of expected chemicals and materials in containment following a LOCA. Testing on this loop was performed for a 30-day duration and considered DEGB debris quantities except for RMI. The testing was initiated at the expected maximum sump temperature of 190°F and then gradually reduced over the test duration to 80°F, the conservatively minimum temperature expected to be achieved following an accident. Testing accommodated the expected pH changes during the initial stages of the accident in both the containment sump pool and CTS spray. Materials that exist in containment, or equivalent surrogates, were included in the test tank, either submerged or in the region where spray would interact with the materials. For this testing, spray was maintained for 48 hours to maximize the interaction of the spray with exposed materials that would not be submerged in the containment sump pool. Application of the limiting head loss from this test is described in Section 14.3.9.5.3.2.

The debris quantities used for this test are provided in Table 14.3.9-17. The containment materials and their quantities considered for these tests are provided in Tables 14.3.9-18 and 14.3.9-19.


The time history response of this test is shown in Figure 14.3.9-23.

### **14.3.9.5.3 System Head Loss Determination**

As described in Sections 14.3.9.5.1 and 14.3.9.5.2, the testing that was performed did not model the installed plant configuration of a main strainer in parallel with the remote strainer and associated waterway. The debris only head loss testing performed in the Large Scale Test Loop provided a combined head loss across the in-parallel main and remote strainers, without consideration of the head loss across the waterway. The testing performed in the MFTL and Vuez test loops provided the head loss across an equivalent main strainer only. Nevertheless, the testing performed in these loops provided the data needed to determine the expected increase in debris only head loss due to the additional impact of chemical precipitate interaction with the debris bed. Methods used to extrapolate the test data to an appropriate debris only and chemical effects head loss factors are addressed below.



## UFSAR Revision 30.0

 An AEP Company	<p style="text-align: center;"><b>INDIANA MICHIGAN POWER</b> <b>D. C. COOK NUCLEAR PLANT</b> <b>UPDATED FINAL SAFETY ANALYSIS REPORT</b></p>	<p>Revised: 27.0 Section: 14.3.9 Page: 33 of 44</p>
---	--	---

### **14.3.9.5.3.1 Method of Analysis**

To establish a system head loss for the installed recirculation sump strainer system, utilizing the data obtained from the testing described in Section 14.3.9.5.1, a mathematical model was developed. The model was designed to correlate the test data with the calculated hydraulic analysis described in Section 14.3.9.4.3.3. To address test data collected at different temperatures, the model normalized the data to a common temperature input value.


The selected method for determining system head loss identified an appropriate K-factor for the strainer system, based on the hydraulic analysis (CFD) described in Section 14.3.9.4.3 and the clean strainer head loss testing performed in the Large Scale Test Loop. This was accomplished by determining the flow split between the main and remote strainer sections with the data obtained, correlating the scaled strainer test areas to the installed plant configuration, and then including the head loss of the waterway in series with the remote strainer. This approach was used for the standard homogeneous debris test results and the event sequence test results from the large scale test loop cases described in Section 14.3.9.5.1. To account for uncertainties, an additional conservatism was applied to the results of the debris only system head loss analysis. The calculated head loss was increased by 50%.

To account for the increase in system head loss resulting from chemical precipitate interaction with the strainer debris bed (chemical effects), the percentage increase in head loss from MFTL and Vuez testing, described in Section 14.3.9.5.2, was determined. MFTL test results indicated a worst case increase in debris only head loss for the DEGB and DGBS of approximately 43% and 53% respectively, while the Vuez testing determined an increase of approximately 40%. To account for uncertainties with the testing, an additional margin was added to bound the test results. The selected value for the increase in debris only head loss as a result of chemical effects is 70%. Similar to the method used to address uncertainties in the debris only test results, the 70% chemical effects increase is applied to the measured system head loss. This provides additional conservatism in that the chemical effects testing was performed on an equivalent main strainer only, the strainer section that will be most heavily loaded with debris resulting in a higher debris only head loss than the remote strainer. The resulting composite multiplication factor for overall recirculation sump strainer system head loss from the debris only test results is  $1.5 \times 1.7 = 2.55$ . Application of this head loss increase factor provides margin for uncertainties in analysis and testing for debris and chemical effects.

Allowable head loss across the recirculation sump strainers is a function of the height of water in the containment sump pool since Cook Nuclear Plant has a fully vented recirculation sump. The



## UFSAR Revision 30.0

 An AEP Company	<b>INDIANA MICHIGAN POWER</b> <b>D. C. COOK NUCLEAR PLANT</b> <b>UPDATED FINAL SAFETY ANALYSIS REPORT</b>	Revised: 27.0 Section: 14.3.9 Page: 34 of 44
---	---	--


allowable head loss design limit is based on the available driving head of water at the fully vented recirculation sump, subject to the stipulations contained in NUREG/CR-6808, "Knowledge Base for the Effect of Debris on Pressurized Water Reactor Emergency Core Cooling Sump Performance," dated February 2003, Section 1.3.2 (Reference 11). As noted therein, the effective maximum hydrostatic head loss allowed across a debris bed for a partially submerged sump screen (for which a fully vented sump is considered) is approximately equal to one half the height of the sump pool. If the head loss across a sump strainer due to debris accumulation exceeds this hydrostatic head, the volumetric flow to the pumps drawing on the sump will decrease below the required flow. This will result in decreasing level inside the recirculation sump. For Cook Nuclear Plant, the design maximum head loss for DEGB, DGBS, and 2" SBLOCA were determined by taking one half the available pool height (minus 0.3 ft for the curb height). Table 14.3.9-20 provides the water level at the initiation of recirculation, the minimum water level during recirculation, the time from event initiation until the minimum water level is reached, and the minimum submergence (height of water over the strainer) for the main and remote strainers for the DEGB, the DGBS and the SBLOCA scenarios. The resulting strainer design maximum head loss at minimum recirculation water level for a DEGB is 2.8 ft H<sub>2</sub>O. The strainer design maximum head loss at minimum recirculation water level for a DGBS is 2.65 ft H<sub>2</sub>O. The strainer design maximum head loss at minimum recirculation water level for a 2" SBLOCA is 2.4 ft H<sub>2</sub>O. These head loss limits protect the calculated vortex limit of 601'-6" described in Section 14.3.9.4. As discussed in Section 6.1, the elevation associated with the required NPSH for the pumps taking suction from the recirculation sump is substantially below the elevation associated with the assumed maximum head loss.

### **14.3.9.5.3.2 System Head Loss Results**

The following discussion utilized the results of testing that were provided in millibar and subsequently converted to inches of water to provide a relationship between the head loss and water level inside the recirculation sump.

The limiting debris only head loss test case for the DEGB was determined to be an all debris case, designated as Test Case T2121-3, and run on the Large Scale Test Loop described in Section 14.3.9.5.1. After achieving 100% debris and 100% flow, this test was allowed to run for 24 hours. The highest head loss achieved during the 24-hour run was 11.3 inches H<sub>2</sub>O at approximately 16 hours after 100% debris, 100% flow was achieved. The head loss at the end of 24 hours from the 100% debris, 100% flow point was approximately 9.5 inches H<sub>2</sub>O and slowly decreasing. The head loss values provided are at a conservatively low normalized temperature value. The time history response of this test is shown in Figure 14.3.9-15.

## UFSAR Revision 30.0

 An AEP Company	<b>INDIANA MICHIGAN POWER</b> <b>D. C. COOK NUCLEAR PLANT</b> <b>UPDATED FINAL SAFETY ANALYSIS REPORT</b>	Revised: 27.0 Section: 14.3.9 Page: 35 of 44
---	---	--


For the DEGB, the maximum, temperature-normalized strainer head loss of 11.3 inches H<sub>2</sub>O resulted in a calculated system head loss for the installed system of approximately 1.046 ft H<sub>2</sub>O. Applying the uncertainty factor of 2.55, described in Section 14.3.9.5.3.1, results in a maximum head loss across the recirculation sump strainer system of 2.67 ft H<sub>2</sub>O. This head loss is slightly below the maximum allowed head loss of 2.8 ft H<sub>2</sub>O, thus confirming that the recirculation strainers will pass sufficient flow to protect the 601' 6" vortex limit. The margin between the minimum expected water level inside the recirculation sump and the vortex limit, for the DEGB, is approximately 0.5 ft H<sub>2</sub>O. In the event that the strainer system head loss does exceed the maximum allowable head loss of 2.8 ft H<sub>2</sub>O, water level inside the recirculation sump will decrease to the level where the recirculation sump level switches will alarm in the control room, prompting flow reduction in accordance with emergency procedures.

The limiting debris head loss case for the DGBS was determined to be an event sequence test, designated as Test T2121-6, and run on the Large Scale Test Loop described in Section 14.3.9.5.1. The highest head loss achieved during this test was 7.2 inches H<sub>2</sub>O approximately 3 3/4 hours after reaching 100% flow. At the end of the test, the head loss was approximately 7.0 inches H<sub>2</sub>O and decreasing slowly. The head loss values are at the normalized temperature value. The time history response of this test is shown in Figure 14.3.9-19.

For the DGBS, the maximum, temperature-normalized strainer head loss of 7.2 inches H<sub>2</sub>O resulted in a calculated system head loss for the installed system of approximately 0.819 ft H<sub>2</sub>O. Applying the uncertainty factor of 2.55, described in Section 14.3.9.5.3.1, results in a maximum head loss across the recirculation sump strainer system of 2.09 ft H<sub>2</sub>O. This head loss is substantially below the maximum allowed head loss of 2.65 ft H<sub>2</sub>O and is bounded by the results of the DEGB. The margin between the minimum expected water level inside the recirculation sump and the vortex limit, for the DGBS, is approximately 0.8 ft H<sub>2</sub>O.

Specific strainer head loss testing was not performed for the 2" SBLOCA. Conservatively applying the strainer system head loss results from the DGBS analysis results in a head loss of 2.09 ft H<sub>2</sub>O. This head loss is below the maximum allowed head loss of 2.4 ft H<sub>2</sub>O. This is also conservative in that the expected flow rate for the ESF systems would be below the full flow value assumed for the larger breaks, thus decreasing the head loss across the strainer system. The margin between the minimum expected water level inside the recirculation sump and the vortex limit for the full flow rate applied to the SBLOCA, is approximately 0.3 ft H<sub>2</sub>O.

Given the Alternate Evaluation approach used for recirculation sump inventory analyses, as described in Section 14.3.9.4.1.1, it is acceptable to rely on operator actions to mitigate the

 An AEP Company	<p style="text-align: center;"><b>INDIANA MICHIGAN POWER</b> <b>D. C. COOK NUCLEAR PLANT</b> <b>UPDATED FINAL SAFETY ANALYSIS REPORT</b></p>	<p>Revised: 27.0 Section: 14.3.9 Page: 36 of 44</p>
---	--	---

consequences of debris loading in excess of allowable design limits. To determine the effects of reducing ECCS and/or CTS pump flow in this eventuality, the DEGB testing on the Large Scale Test Loop included a flow reduction sequence to simulate the removal of one pump from service at a time until flow was stopped, followed by returning flow to the equivalent 100% value. The head loss following the first flow reduction step (equivalent to removal of a CTS pump) was approximately 5.9 inches H<sub>2</sub>O (non-normalized). Following the second flow reduction, the head loss was approximately 3.2 inches H<sub>2</sub>O (non-normalized). The head loss following restoration of flow to 100% was approximately 5.4 inches H<sub>2</sub>O (non-normalized). These test results demonstrated the positive effects of flow reduction on head loss across the main recirculation strainer and provided evidence that operator actions in response to Emergency Operating Procedures for recirculation sump level instrument alarms in the control room could reduce flow across the strainers and restore water level inside the recirculation sump. This ensures air entraining vortices do not occur.


### **14.3.9.6 Design Considerations for Upstream and Downstream Effects**

#### **14.3.9.6.1 Upstream Effects**

An Upstream Effects assessment was performed in concert with the incorporation of Generic Letter 2004-02 into Cook Nuclear Plant's licensing basis. The assessment evaluated flow paths associated with the recirculation function of the containment sump to ensure they would not hold up inventory that should flow to the containment and recirculation sumps and possibly impact the RHR and CTS pumps ability to provide the necessary flow for core and containment cooling. Potential choke points identified in the Upstream Effects evaluation of the flow paths are identified and described below.

The lower containment is made up of two compartments—the area inside the crane wall (loop compartment) and the area outside the crane wall (annulus). These two areas are primarily connected by five 10-inch holes drilled through the flood-up overflow wall and two approximately 4-ft by 10-ft openings in the crane wall. A debris interceptor protects the flood-up overflow wall holes on the loop compartment side of the overflow wall. This debris interceptor consists of vertical perforated plates with a solid top cover plate, with an approximate 6-inch gap between the top and the sides. Analytically, it is assumed that the perforated plate section becomes blocked by debris and all water flow passes through the gap. The top plate is solid to prevent debris generated from the accident from falling into the area between the flood-up overflow wall hole and the perforated plate section of debris interceptor. To properly address the functionality of the debris interceptor installed at the flood-up overflow, its flow characteristics

## UFSAR Revision 30.0

 An AEP Company	<b>INDIANA MICHIGAN POWER</b> <b>D. C. COOK NUCLEAR PLANT</b> <b>UPDATED FINAL SAFETY ANALYSIS REPORT</b>	Revised: 27.0 Section: 14.3.9 Page: 37 of 44
---	---	--

were included in the CFD model for both pool fill and recirculation (Section 14.3.9.4.2). Further information regarding the construction of this debris interceptor is provided in Section 6.2.2.


The overflow wall holes are protected on the annulus side of the flood-up overflow wall by a set of 2-foot tall radiation shields that are set back from the holes by approximately 16-inches with gaps at the bottom of the shields of approximately 2-inches. Openings exist at the ends of the shields which further promote flow through this region. The two larger openings in the crane wall have installed trash racks designed to block the transport of large pieces of debris. No credit has been taken in the debris transport analysis for the crane wall opening trash racks to block debris from transporting between the loop compartment and the annulus. The design of the flood-up overflow wall debris interceptor ensures that it will not become a choke point which will adversely affect the recirculation sump inventory analyses.

Other potential upstream blockage points include the ice condenser drain lines, the refueling canal spray drain lines, and the CEQ fan room drain lines.

There are twenty-one 12-inch ice condenser drain lines for draining the melting ice into the loop compartment. If one of these drains were to become blocked, the water would simply flow to the other drains or the melted ice flow would spill over to the loop compartment through the ice condenser lower inlet doors. As a result, this flow path is not considered a choke point which will adversely affect the recirculation sump inventory analyses.

The plant is designed so that the majority of the upper containment spray water flows to lower containment through the three drain lines in the bottom of the refueling canal. The drains include two 12-inch drain lines and one 10-inch drain line, which discharge directly below the refueling canal. By design, the refueling canal drains are separated by sufficient distance to ensure that any credible missile generated in upper containment will not block more than half the total flow area. If one of these lines was to become blocked with debris, the other two lines are sufficiently sized to drain the upper containment spray flow, resulting in overall pool flow patterns that are essentially the same. As a result, refueling canal drains are not considered a choke point which will adversely affect the recirculation sump inventory analyses.

The fraction of upper containment spray that sprays or drains down into the CEQ fan rooms is drained to the pipe tunnel sump for Unit 1 and to the lower containment sump for Unit 2 through a set of 3-inch floor drains. The CEQ fan room drains consist of one drain in the east CEQ fan room and two drains in the west CEQ fan room. Debris blockage of these drain lines would result in decreasing containment sump inventory over time and decreasing the available head for flow through the main and remote strainers. Debris interceptors are installed at the openings to

 An AEP Company	<p style="text-align: center;"><b>INDIANA MICHIGAN POWER</b> <b>D. C. COOK NUCLEAR PLANT</b> <b>UPDATED FINAL SAFETY ANALYSIS REPORT</b></p>	<p>Revised: 27.0 Section: 14.3.9 Page: 38 of 44</p>
---	--	---

the CEQ fan room drains to prevent them from being blocked by debris. Openings exist at both the Unit 1 pipe tunnel sump and the Unit 2 lower containment sump to allow the water entering the sumps from the CEQ fan rooms to enter the containment sump pool. As a result, the CEQ fan room drains are not considered choke points which will adversely affect the recirculation sump inventory analyses.

#### **14.3.9.6.2 Downstream Effects**

Achieving long-term core and containment cooling functions pursuant to Generic Letter 2004-02 requires proper performance of the ECCS and CTS while drawing filtered water from the recirculation sump. The execution of these functions is documented in the Downstream Effects evaluations. These evaluations determined the post-LOCA impact of debris-laden fluid drawn from inside the recirculation sump on successful functioning of downstream equipment in the recirculation flow path during the component's mission time. Downstream Effects evaluations included potential debris effects on ECCS and CTS pumps, throttle valves in the injection flow paths, orifices, spray nozzles, process instruments, heat exchangers, reactor vessel flow path components, and reactor core fuel flow path components. Considerations included potential blockage of equipment flowpaths, wear and abrasion of surfaces, blockage of flow clearances through fuel assemblies, and debris deposition on the fuel clad surface.

The scope of the Downstream Effects evaluations included:


1. Ex-Vessel Recirculation Flow Path Blockage
2. Ex-Vessel Recirculation Flow Path Component Wear
3. In-Vessel Flow Path Blockage
4. In-Vessel Fuel Rod Debris Deposition

The recirculation flow paths for the ECCS and CTS are shown on Figures 14.3.9-24 and 14.3.9-25 respectively.

#### **14.3.9.6.2.1 Method of Analysis**

Downstream Effects evaluations were performed in accordance with WCAP-16406-P, "Evaluation of Downstream Sump Debris Effects in Support of GSI-191" (References 13 and 14) and WCAP-16793-NP, "Evaluation of Long-Term Cooling Considering Particulate, Fibrous and Chemical Debris in the Recirculating Fluid" (Reference 15). The debris materials in the recirculation fluid were taken from those debris sources described in Section 14.3.9.4.1.2.

## UFSAR Revision 30.0

 An AEP Company	<b>INDIANA MICHIGAN POWER</b> <b>D. C. COOK NUCLEAR PLANT</b> <b>UPDATED FINAL SAFETY ANALYSIS REPORT</b>	Revised: 27.0 Section: 14.3.9 Page: 39 of 44
---	---	--

Downstream Effects evaluations include consideration of long and short-term ECCS and CTS operating lineups, conditions of operation, and mission times for LOCA mitigation. Mission times for the systems were determined through review of UFSAR LOCA accident analyses and in consideration of the need to demonstrate that bulk and local temperatures are stable or continuously decreasing and that there is no credible mechanism for debris entrained in the recirculating water to unacceptably affect the stable heat removal mechanism.

### **Ex-Vessel Recirculation Flow Path Blockage**

The ex-vessel recirculation flow path blockage evaluation was performed in accordance with Reference 13 and 14. This evaluation determined the openings and expected flow rates which exist for the components in the recirculation flow path ensures that debris would not block the required flow paths.

### **Ex-Vessel Recirculation Flow Path Wear**

The ex-vessel recirculation flow path wear evaluation was performed in accordance with References 13 and 14. This evaluation determined the clearances and material thicknesses for components and sub-components in the recirculation flow path to ensure debris-laden fluid would not result in component failure that would challenge the ability to provide the necessary core and containment cooling for the required mission time. The types of sub-components evaluated include pump seals, impellers, wear rings, bushings, and bearings, heat exchanger tubes, valve plugs and seats, and orifice edge openings. An evaluation was also performed to establish that the system flow characteristics remained within an acceptable operating range to ensure continued core and containment cooling via the recirculation function.

### **In-Vessel Flow Path Blockage**


The in-vessel blockage evaluation was performed in accordance with References 13 and 15. This evaluation determined the thickness of the fiber bed that could form on the fuel assembly bottom nozzles as a function of the fibrous debris that could bypass the recirculation sump strainers. Estimates of the fibrous debris bypassing the strainer were based on testing performed at the strainer vendor test facility with additional consideration for fibrous material contained in other insulation and fire barrier materials, as described in Section 14.3.9.4.1.2.

### **In-Vessel Fuel Rod Debris Deposition**

The in-vessel fuel rod deposition evaluation was performed in accordance with Reference 15 using the LOCADM code, Version 1.0. The evaluation considered both Unit 1 and Unit 2 using core thermal power values of 3315 MWt and 3482 MWt, respectively, and minimum and



## UFSAR Revision 30.0

 An AEP Company	<p style="text-align: center;"><b>INDIANA MICHIGAN POWER</b> <b>D. C. COOK NUCLEAR PLANT</b> <b>UPDATED FINAL SAFETY ANALYSIS REPORT</b></p>	<p>Revised: 27.0 Section: 14.3.9 Page: 40 of 44</p>
---	--	---

maximum containment sump volumes. The debris source term used for the evaluation is described in Section 14.3.4.9.1.2.

### **14.3.9.6.2.2 Assumptions**

The ex-vessel recirculation flow path blockage evaluation conservatively assumed a nominal strainer opening of 1/8 inch diameter. This opening size results in an assumed maximum debris size of 1/4 inch passing through the recirculation sump strainers. This assumption is consistent with the guidance provided in Reference 13.

The ex-vessel recirculation flow path wear evaluation conservatively assumed debris sizes and quantities which resulted in maximum wear of the affected components. This evaluation also conservatively neglected the filtration of particulate debris by the recirculation sump strainers, the fuel assembly bottom nozzles, and the fuel assembly spacer grids. This evaluation did assume the only particulate debris reduction mechanism to be settling in the reactor vessel lower plenum and that particulate debris would not be reduced in size during transport through the recirculation flow path. For all pumps within the recirculation flow path, it was assumed that the pumps were at their minimum operability limits for performing the hydraulic analysis verification at the beginning of recirculation, and multi-stage pumps were within their In-Service Testing flow limits for determination of mechanical verification (vibration) due to pumping debris-laden water for the required mission time.

The in-vessel flow path blockage evaluation conservatively used values of fibrous debris available for filtration by the recirculation sump strainers in excess of those values assumed to be generated during a LOCA.

The in-vessel fuel rod debris deposition analysis conservatively assumed that all deposition within the recirculation flow path occurs on fuel heat transfer surfaces, no carryover of debris from core boil-off, impurity deposition on the fuel clad surface is directly related to core power distribution, and deposits will not be thinned by flow attrition or by dissolution.


### **14.3.9.6.2.3 Acceptance Criteria**

The acceptance criteria for the ex-vessel recirculation flow path blockage evaluation are that no required component in the recirculation flow path will be blocked by debris with particle sizes less than or equal to 1/4 inch, and that debris will not accumulate within the systems or components resulting in blockage of the flow path.

Acceptance criteria for the ex-vessel recirculation flow path wear evaluation are that the required core and containment cooling functions will be provided for the necessary mission time while



## UFSAR Revision 30.0

 An AEP Company	<b>INDIANA MICHIGAN POWER</b> <b>D. C. COOK NUCLEAR PLANT</b> <b>UPDATED FINAL SAFETY ANALYSIS REPORT</b>	Revised: 27.0 Section: 14.3.9 Page: 41 of 44
---	---	--

satisfying accident analysis inputs and assumptions described elsewhere in Chapter 14 (Unit 1 and Unit 2). This includes criteria which demonstrate that ECCS and CTS pumps, in the presence of system and component debris-related degradation, continue to provide minimum flowrates to meet cold and hot leg recirculation needs and not exceed pump runout limits. Relative to mission times, reviews of post-LOCA accident analyses and related Emergency Operating Procedures indicate that no Safety Injection pump flow requirements are needed beyond 30 hours. Given the potential need for RHR, CCP and CTS operations beyond 30 hours, the associated Downstream Effects were evaluated for a 30 day operating duration for these systems. This extended duration is reasonable given the conservative nature of the methodology used to develop inputs to head loss testing and the LOCA analyses timelines contained in UFSAR Chapter 14. It is also consistent with Section 2.3 of Reference 17.

The acceptance criterion for the in-vessel flow blockage evaluation is that the thickness of the fibrous debris bed formed on the fuel assembly bottom nozzles is less than 0.125 inches thick. (Reference 13)


The first acceptance criterion for the in-vessel fuel rod debris deposition analysis is that the maximum fuel cladding temperature maintained during periods when the core is covered will not exceed a core average clad temperature of 800°F. This acceptance criterion is applied after the initial quench of the core (Reference 15) and is consistent with the long-term core cooling requirements stated in 10 CFR 50.46(b)(4) and 10 CFR 50.46(b)(5). The second acceptance criterion is that the total debris deposition on the fuel rods (oxide + crud + precipitate) is less than 50 mils. This criterion ensures that bridging of debris between adjacent fuel rods will not occur. (References 15 and 16)

#### **14.3.9.6.2.4 Results**

Results of the ex-vessel recirculation flow path blockage evaluation determined that there were no required systems or components within the recirculation flow path that would become blocked by debris.

Results of the ex-vessel recirculation flow path wear evaluation determined that the systems would provide the required flow for core and containment cooling for the assigned mission times. This evaluation also determined that the intermediate head injection pumps (SI) were susceptible to excessive vibration due to increased clearances within the pump from debris-laden fluid wear after approximately 15 days. Specifically, the SI pumps were found to be capable of operating for at least 15 days, the CTS pumps for at least 30 days, and the RHR and CCP pumps in excess of 30 days. Considering the wear in the systems and the pumps, an evaluation was

## UFSAR Revision 30.0

 An AEP Company	<p style="text-align: center;"><b>INDIANA MICHIGAN POWER</b> <b>D. C. COOK NUCLEAR PLANT</b> <b>UPDATED FINAL SAFETY ANALYSIS REPORT</b></p>	<p>Revised: 27.0 Section: 14.3.9 Page: 42 of 44</p>
---	--	---

performed that determined the system minimum flow requirements would continue to be met. Additionally, this evaluation determined that none of the pumps would reach run-out flow conditions.

Results from the in-vessel flow blockage evaluation determined that the maximum filter bed thickness on fuel assembly bottom nozzles is 0.028 inches. This result is acceptable because it satisfies the maximum thickness criterion of 0.125 inches.

Results from the in-vessel fuel rod debris deposition analysis determined that the maximum average fuel cladding temperature for Unit 1 is 365.71°F, and for Unit 2 is 358.10°F. The maximum debris deposition thickness on the fuel rods for Unit 1 is 17 mils and is 16 mils for Unit 2. These results are acceptable because they meet the acceptance criteria for the maximum cladding temperature and maximum debris deposition thickness of 800°F and 50 mils, respectively. Table 14.3.9-21 provides the results of all cases analyzed for both Unit 1 and Unit 2.


#### **14.3.9.6.2.5 Conclusions**

Downstream Effects evaluations found that debris-related degradation of ECCS and CTS did not prevent these systems from performing their core and containment cooling functions in mitigating the consequences of a LOCA.

#### **14.3.9.7 References for Sections 14.3.9**


1. I&M to NRC letter C1099-08, "Technical Specification Change Request – Containment Recirculation Sump Water Inventory," Attachment 7, FAI-99-77, "Containment Sump Level Evaluation for the D.C. Cook Plant," dated October 1, 1999.
2. Salvatori, R., 1974, - Final Report: Ice Condenser Full-Scale Section Test at the Waltz Mill Facility, Westinghouse Proprietary Class 2 Report, WCAP-8282.
3. Ligothke, M. W. et al., 1991, - Ice-Condenser Aerosol Test, NUREG/CR-5768, PNL-7765.
4. MPR Associates, Inc., - Containment Sump Level Design Condition and Failure Effects Analysis for Potential Draindown Scenarios, September 1999.
5. Padmanabhan, M., - Hydraulic Model Investigation of Vortexing and Swirl Within a Reactor Containment Recirculation Sump, Donald C. Cook Nuclear Power Station, Alden Research Laboratory Report 108-78/M178PF, 1978.

## UFSAR Revision 30.0

 <b>INDIANA MICHIGAN POWER</b> <small>An AEP Company</small>	<b>INDIANA MICHIGAN POWER D. C. COOK NUCLEAR PLANT UPDATED FINAL SAFETY ANALYSIS REPORT</b>	Revised: 27.0 Section: 14.3.9 Page: 43 of 44
--	---	--

6. SER N99124 dated 12/13/1999, Amendments 234 & 217: Containment Recirculation Sump Water Inventory.
7. NRC Generic Letter 2004-02, "Potential Impact of Debris Blockage on Emergency Recirculation During Design Basis Accidents at Pressurized-Water Reactors," dated September 13, 2004, including associated I&M to NRC letters.
8. WCAP-16530-NP, "Evaluation of Post-Accident Chemical Effects in Containment Sump Fluids to Support GSI-191", dated June 2005.
9. NEI-04-07, "Pressurized Water Reactor Sump Performance Methodology," dated December 2004, ML041550332.
10. I&M to NRC letter C1099-08, "Technical Specification Change Request – Containment Recirculation Sump Water Inventory," Attachment 10, WCAP-15302, "Modifications to the Containment Systems, Westinghouse Safety Evaluation (SECL 99-076, Revision 3)," dated September 1999.
11. NUREG/CR-6808, "Knowledge Base for the Effect of Debris on Pressurized Water Reactor Emergency Core Cooling Sump Performance," dated February 2003.
12. NRC Letter, "Pressurized Water Reactor Containment Sump Evaluation Methodology," of December 6, 2004 with attached NRC Staff Safety Evaluation on NEI 04-07, ML043280007 and ML043280631
13. Westinghouse WCAP-16406-P, "Evaluation of Downstream Sump Debris Effects in Support of GSI-191," Rev. 1 of August 2007
14. NRC Document, "Safety Evaluation by the Office of Nuclear Reactor Regulation Topical Report (TR) WCAP-16406-P, Revision 1, Evaluation of Downstream Sump Debris Effects in Support of GSI-191, Pressurized Water Reactor Owners Group, Project No. 694," of December 20, 2007, ML073480324 and ML073520295.
15. Westinghouse WCAP-16793, "Evaluation of Long-Term Cooling Considering Particulate, Fibrous and Chemical Debris in the Recirculating Fluid," Rev. 0 of May 2007
16. PWROG Letter OG-08-18, Responses to the NRC Request for Clarification to Request for Additional Information (RAI) on WCAP-16793-NP, 'Evaluation of

## UFSAR Revision 30.0

 An <b>AEP</b> Company	<b>INDIANA MICHIGAN POWER</b> <b>D. C. COOK NUCLEAR PLANT</b> <b>UPDATED FINAL SAFETY ANALYSIS REPORT</b>	Revised: 27.0 Section: 14.3.9 Page: 44 of 44
--	---	--

Long-Term Cooling Considering Particulate, Fibrous and Chemical Debris in the Recirculating Fluid' (PA-SEE-0312),” of January 17, 2008.

17. NRC Letter, “Revised Guidance for Review of Final Licensee Responses to Generic Letter 2004-02, ‘Potential Impact of Debris Blockage on Emergency Recirculation during Design Basis Accidents at Pressurized-Water Reactors’,” William H Ruland to Anthony R. Pietrangelo, of March 28, 2008